Super$B$
Technical Design Reports

The Physics

May 31, 2011

Abstract

Super$B$ is a high luminosity e^+e^- collider that will be able to indirectly probe new physics at energy scales far beyond the reach of any man made accelerator planned or in existence. Just as detailed understanding of the Standard Model of particle physics was developed from stringent constraints imposed by flavour changing processes between quarks, the detailed structure of any new physics is severely constrained by flavour processes as a result of either the Standard Model or any new physics effects. In order to elucidate this strucutre it is necessary to perform a number of complementary studies of a set of golden channels. With these measurements in hand, the pattern of deviations from the Standard Model behaviour can be used as a test of the structure of new physics. If new physics is found at the LHC, then the many golden measurements from Super$B$ will help decode the subtle nature of the new physics. However if no new particles are found at the LHC, Super$B$ will be able to search for new physics at energy scales up to $10 - 100$TeV. In either scenario, flavour physics measurements that can be made at Super$B$ play a pivotal role in understanding the nature of physics beyond the Standard Model. A strategy for using the interplay between measurements to understand physics beyond the Standard Model is discussed in detail in this document.

This report details the Physics case of the Super$B$ Project, updating the work previously discussed in all previous reports.

Contents

1. Executive summary

This is a 2 page executive summary of the document.

2. Introduction

This introduction is intended to provide a more in-depth summary of the TDR than given in the executive summary.

A. What is Super$B$?

B. Physics beyond the Standard Model

C. Standard Model measurements

D. Outline of the physics TDR

E. Golden channels studied with Fast and Full simulation

This section is intended to provide a record of which studies included in the document have used Super$B$ simulation (Fast or FullSim) in order to derive the quoted sensitivities.

3. Tau physics

Searching for lepton-flavor-violating (LFV) τ decays constitutes one of the most clean and powerful tools to discover and characterize NP scenarios. Although the SM when complemented with the experimentally observed neutrino-mixing phenomenology does include LFV τ decays, the rates are extremely low and experimentally unobservable, making the discovery of LFV an unambiguous signal for physics beyond the SM.

Experimental investigations on *CP* violation in τ decay and on the τ EDM and $g-2$ provide Super$B$ with additional experimentally clean tools to advance our knowledge on unexplored territories, with the ability to test some specific NP scenarios.

With an integrated luminosity of $75\,\mathrm{ab}^{-1}$, Super$B$ will be able to explore a significant portion of the parameter space of most New Physics scenarios by searching for LFV in τ decays. While the MEG experiment will search for $\mu \to e\gamma$ with great sensitivity, Super$B$ will uniquely explore transitions between the third and first or second generations, providing crucial information to determine the specific New Physics model that produces LFV. The LHC experiments are, in general, not competitive in LFV searches. Furthermore, Super$B$ includes features that make it superior to Belle II for LFV searches: a larger planned luminosity and a polarized electron beam, which is equivalent to a substantial boost in effective luminosity, and smaller beam currents, leading to smaller machine backgrounds. Super$B$ can have a 80% longitudinally polarized electron beam, which will provide means to improve the selection of LFV final states, given a specific LFV interaction, or to better determine the features of the LFV interaction, once they are found.

Experimental studies on *CP* violation in τ decay and on the τ EDM and $g-2$ are especially clean tools, because they rely on measurement of asymmetries with relatively small systematic uncertainties from the experiment. The beam polarization also improves the experimental sensitivity for τ EDM and $g-2$ determinations, by allowing measurements of the polarization of a single τ, rather than measurements of correlations between two τ leptons produced in the same event. With this technique, Super$B$ can test whether supersymmetry is a viable explanation for the present discrepancy on the muon $g-2$. Although the most plausible NP models constrained with the available experimental results predict *CP* violation in τ decay and the τ EDM in a range that is not measurable, Super$B$ can test specific models that enhance those effects to measurable levels.

A. Lepton Flavour Violation

Predictions from New Physics models

LFV in the MSSM

In the following, we discuss the size of τ LFV effects on decays and correlations that are expected in supersymmetric extensions of the SM and, in particular, in the so-called constrained MSSM, The flavor-conserving phenomenology of this framework is characterized by five parameters: $M_{1/2}$, M_0, A_0, $\tan\beta$, sgn μ. We will discuss a subset of the "Snowmass Points and Slopes" (SPS) [1], which we consider adequate to illustrate the variety of predictions and the features of the model on lepton flavor violation processes (see Table I).

TABLE I: Values of $M_{1/2}$, M_0, A_0, $\tan\beta$, and sign of μ for the SPS points considered in the analysis.

SPS	$M_{1/2}$ (GeV)	M_0 (GeV)	A_0 (GeV)	$\tan\beta$	μ
1 a	250	100	-100	10	> 0
1 b	400	200	0	30	> 0
2	300	1450	0	10	> 0
3	400	90	0	10	> 0
4	300	400	0	50	> 0
5	300	150	-1000	5	> 0

At all the SPS points, LFV decays are dominated by the contribution of dipole-type effective operators of the form $(\bar{l}_i \sigma_{\mu\nu} l_j F^{\mu\nu})$. Defining $\mathcal{R}^{(a)}_{(b)} = \mathcal{B}(\tau \to a)/\mathcal{B}(\tau \to b)$, The dipole dominance allows us to establish the following relations:

$$\mathcal{R}^{(\mu ee)}_{(\mu\gamma)} \approx 1.0 \times 10^{-2} \;\to\; \mathcal{B}(\tau \to \mu e^+ e^-) < 5 \times 10^{-10},$$
$$\mathcal{R}^{(\mu \rho^0)}_{(\mu\gamma)} \approx 2.5 \times 10^{-3} \;\to\; \mathcal{B}(\tau \to \mu \rho^0) < 10^{-10},$$
$$\mathcal{R}^{(3\mu)}_{(\mu\gamma)} \approx 2.2 \times 10^{-3} \;\to\; \mathcal{B}(\tau \to 3\mu) < 10^{-10},$$
$$\mathcal{R}^{(\mu\eta)}_{(\mu\gamma)} < 10^{-3} \;\to\; \mathcal{B}(\tau \to \mu\eta) < 5 \times 10^{-11},$$

where the bounds correspond to the present limit $\mathcal{B}(\tau \to \mu\gamma) < 4.5 \times 10^{-8}$. Similar relations hold for $\tau \to e$ transitions. Assuming an experimental reach at Super$B$ at the level of 10^{-9} only $\tau \to \mu\gamma$ and $\tau \to e\gamma$ decays would be within experimental reach in this list. However, it is interesting to notice that some processes as $\tau \to \mu\rho$ ($\rho \to \pi^+\pi^-$) can reach branching ratios of 10^{-10} for special values of the parameters [2]. Taking into account that these modes are cleaner from the experimental point of view, they could still be interesting processes in a Super$B$.

To estimate the overall scale of $\tau \to (\mu, e)\gamma$ rates, we must specify the value of the LFV couplings, since they are not determined by the SPS conditions. In

the mass-insertion and leading-log approximation, assuming that the leading LFV couplings appear in the left-handed slepton sector, we can write:

$$\frac{\mathcal{B}(l_j \to l_i\gamma)}{\mathcal{B}(l_j \to l_i\bar{\nu}_i\nu_j)} \approx \frac{\alpha^3}{G_F^2}\frac{\left|\left(m^2_{\tilde{L}}\right)_{ji}\right|^2}{M_S^8}\tan^2\beta,$$

where, to a good approximation, $M_S^8 \simeq 0.5 M_0^2 M_{1/2}^2 \times (M_0^2 + 0.6 M_{1/2}^2)^2$. In a Grand Unified Theory (GUT) with heavy right-handed neutrinos, the off-diagonal entries of the slepton mass matrix $m^2_{\tilde{L}}$ are likely to be dominated by the flavor mixing in the (s)neutrino sector. These terms can be expressed as:

$$\left(m^2_{\tilde{L}}\right)_{ji} \approx -\frac{6M_0^2 + 2A_0^2}{16\pi^2}\,\delta_{ij}, \qquad (1)$$

where $\delta_{ij} = \left(Y_\nu^\dagger Y_\nu\right)_{ji}\log(M_{GUT}/M_R)$ in terms of the neutrino Yukawa couplings (Y_ν), the average heavy right-handed neutrino mass (M_R) and the GUT scale ($M_{GUT} \sim 10^{15}$–10^{16} GeV). The experimental information on neutrino masses and mixings is not sufficient to fix completely the structure in the neutrino Yukawa matrix, even assuming some kind of quark-lepton unification. We can take two limiting situations that are called "CKM-like" and "PMNS-like" [3]. Taking the "PMNS-like" case and given the large phenomenological value of the 2–3 mixing in the neutrino sector (and the corresponding suppression of the 1–3 mixing) we expect $|\delta_{32}| \gg |\delta_{31}|$ hence $\mathcal{B}(\tau \to \mu\gamma) \gg \mathcal{B}(\tau \to e\gamma)$. For sufficiently heavy right-handed neutrinos, the normalization of Y_ν is such that $\mathcal{B}(\tau \to \mu\gamma)$ can reach values in the 10^{-9} range. In particular, $\mathcal{B}(\tau \to \mu\gamma) \gtrsim 10^{-9}$ if at least one heavy right-handed neutrino has a mass around or above 10^{13} GeV (in SPS 4) or 10^{14} GeV (in SPS 1a,1b,2,3,5).

A key issue that must be addressed is the role of $\mathcal{B}(\mu \to e\gamma)$ in constraining the LFV couplings and, more generally, the correlations between $\mathcal{B}(\tau \to (\mu, e)\gamma)$ and $\mathcal{B}(\mu \to e\gamma)$ in this framework. An extensive analysis of such questions has been presented in Ref. [4, 5], under the hypothesis of a hierarchical spectrum for the heavy right-handed neutrinos.

The overall structure of the $\mathcal{B}(\tau \to \mu\gamma)$ vs. $\mathcal{B}(\mu \to e\gamma)$ correlation in SPS 1a is shown in Fig. 1. As anticipated, $\mathcal{B}(\tau \to \mu\gamma) \sim 10^{-9}$ requires a heavy right-handed neutrino around or above 10^{14} GeV. This possibility is not excluded by $\mathcal{B}(\mu \to e\gamma)$ only if the 1–3 mixing in the lepton sector (the θ_{13} angle of the neutrino mixing matrix) is sufficiently small. This is a general feature, valid at all SPS points, as illustrated in Fig. 2. In Table II we show the predictions for $\mathcal{B}(\tau \to \mu\gamma)$ and $\mathcal{B}(\tau \to \mu\mu\mu)$ corresponding to the neutrino mass parameters chosen in Fig. 2 (in particular $M_{N_3} = 10^{14}$ GeV), for the various SPS points. Note that this case contains points that are within the Super$B$ sensitivity range, yet are not excluded by $\mathcal{B}(\mu \to e\gamma)$ (as illustrated in Fig. 2). It is also interesting to notice the possible correlations with other processes. For instance, in $SU(5)$ GUT models a large CP phase in the B_s system would imply a large $\mathcal{B}(\tau \to \mu\gamma)$ due to the unification of the squark and slepton mass matrices at $M_{\rm GUT}$ [6–9].

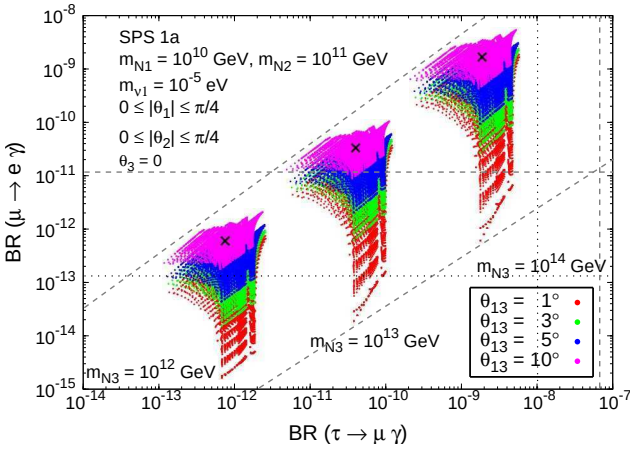

FIG. 1: $\mathcal{B}(\tau \to \mu\gamma)$ vs. $\mathcal{B}(\mu \to e\gamma)$ in SPS 1a, for three reference values of the heavy right-handed neutrino mass and several values of θ_{13}. The horizontal dashed (dotted) line denotes the present experimental bound (future sensitivity) on $\mathcal{B}(\mu \to e\gamma)$. All other relevant parameters are set to the values specified in Ref. [4].

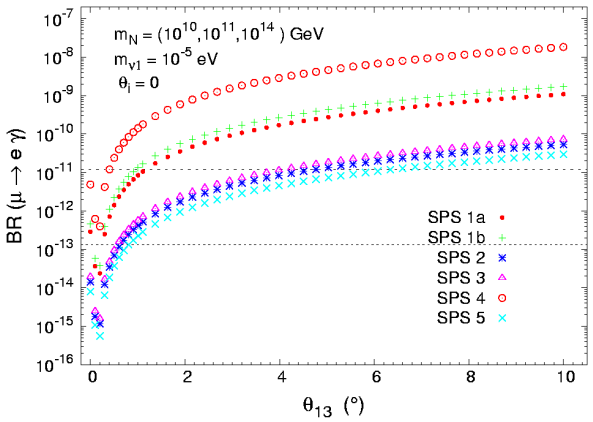

FIG. 2: $\mathcal{B}(\mu \to e\,\gamma)$ as a function of θ_{13} (in degrees) for various SPS points. The dashed (dotted) horizontal line denotes the present experimental bound (future sensitivity). All other relevant parameters are set to the values specified in Ref. [4].

It is unlikely that MSSM would be realised in nature with an entirely flavor blind soft sector while the Yukawa sector presents a highly nontrivial structure. Thus, we must explore other "flavored MSSM" realizations to be able to analyze the host of new results

TABLE II: Predictions for $\mathcal{B}(\tau \to \mu\gamma)$ and $\mathcal{B}(\tau \to \mu\mu\mu)$ corresponding to the SPS points. The values of m_{N_i} and m_{ν_1} are as specified in Fig. 2 [4].

SPS	1 a	1 b	2	3	4	5
$\mathcal{B}(\tau \to \mu\gamma) \times 10^{-9}$	4.2	7.9	0.18	0.26	97	0.019
$\mathcal{B}(\tau \to \mu\mu\mu) \times 10^{-12}$	9.4	18	0.41	0.59	220	0.043

that will arrive from Super$B$ and LHC experiments. The use of flavor symmetries can explain the complicated Yukawa structures and at the same time predict a non-trivial structure in the soft-breaking terms. In such flavor models, we can have a large variety of predictions with different flavor symmetries. However, LFV processes are always the most interesting observables in these models and it is relatively easy to obtain $\mathcal{B}(\tau \to \mu\gamma) \sim 10^{-9}$ as shown in Ref. [10, 11] for an $SU(3)$ flavor symmetry. We have to emphasize here that this process can even compete in sizable regions of the parameter space with the future bound at MEG for the process $\mu \to e\gamma$.

LFV in other scenarios

At large $\tan\beta$ and not too heavy Higgs masses, another class of LFV interactions is relevant, the effective coupling between a μ–τ pair and the heavy (scalar and pseudoscalar) Higgs bosons. This coupling can overcome the constraints on $\mathcal{B}(\tau \to \mu\mu\mu)$ and $\mathcal{B}(\tau \to \mu\eta)$ dictated by $\mathcal{B}(\tau \to \mu\gamma)$ in the dipole-dominance scenario. Such a configuration cannot be realized in the CMSSM, but it could be realized in the so-called Non Universal Higgs Masses (NUHM) SUSY scenario. In such a framework, there are specific regions of the parameter space in which processes like $\tau \to \mu\eta$ and $\tau \to \mu f_1(980)$, $f_1(980) \to \pi^+\pi^-$ could have a branching ratio in the range 10^{-9} to 10^{-10}, comparable or even slightly larger than $\mathcal{B}(\tau \to \mu\gamma)$ [2, 12, 13].

Another interesting set of possibilities is MSSM with R-parity violation (RPV) [14]. In these models several of the bounds on RPV couplings are obtained from B and τ processes. Super$B$ can improve the bounds on couplings or might even discover a signal for RPV MSSM. The processes $\tau \to \mu\eta$ and $\tau \to \mu\mu\mu$ are especially interesting and can be used at Super$B$ to improve existing bounds by more than an order of magnitude.

Finally, in some non-SUSY NP frameworks, such as Little Higgs Models with T parity (LHT) or $Z^{'}$ models with non-vanishing LFV couplings ($Z^{'}\ell_i\ell_j$), the $\tau \to \mu\mu\mu$ rate could be significantly enhanced to a level that matches or exceeds the rate of $\tau \to \mu\gamma$ (see *e.g.* [15]). In this respect, a measurement of $\mathcal{B}(\tau \to \mu\mu\mu)$ to the level of 10^{-10} would be interesting test of NP even for $\mathcal{B}(\tau \to \mu\gamma) \lesssim 10^{-9}$.

Super$B$ experimental reach

The vast experience accumulated on the B-factories offers a reliable base for estimating the reach of Super$B$ on τ LFV searches. To a first approximation, the Super$B$ detector is expected to have performances comparable to or better than *BABAR* for electron identification and for electromagnetic energy resolution and hermiticity. The Super$B$ project on the other hand has an improved momentum resolution, thanks to silicon layers closer to the beams, and improved muon identification.

The typical τ LFV decay search consists in counting candidate events and measuring if there is an excess against the expected background. By running a *BABAR* analysis unchanged on a larger statistical sample, all expected upper limits scale with at least as the square root of the luminosity increase ($\propto 1/\sqrt{\mathcal{L}}$). This extrapolation poses a lower limit for the Super$B$ reach, which will be ameliorated by detector improvements and only moderately worsened by a small expected increase of beam backgrounds. If it is possible to maintain the B factory efficiencies while keeping the expected amount of background events negligible, then Super$B$ will deliver upper limits that will scale linearly with the integrated luminosity ($\propto 1/\mathcal{L}$). In the first approximation, scaling by $1/\mathcal{L}$ is possible for τ LFV decays into three leptons, or into a lepton and two hadrons in the final state (where the two hadrons may come through a hadron resonance). On the other hand, searches for $\tau \to \ell\gamma$ suffer higher backgrounds and tend to scale more like $\propto 1/\sqrt{\mathcal{L}}$.

BABAR τ LFV searches are optimized for the best expected upper limits, which typically corresponds to maximizing the signal efficiency while keeping the expected background events of the order one or less, when the analysis is not background dominated. Since the analysis optimization depends on the size of the analyzed sample and on the amount of expected backgrounds, one must re-optimize the B-factory analyses for the Super$B$ luminosity, especially for the low background searches. In the following, we extrapolate from the most recent results from *BABAR* by re-optimizing the analysis for $\tau \to \ell\ell\ell$, and assuming a conservative $1/\sqrt{\mathcal{L}}$ scaling for $\tau \to \ell\gamma$.

The experimental reach is expressed in terms of "the expected 90% CL upper limit" assuming no signal, as well as in terms of a "3σ evidence branching fraction" in the presence of projected backgrounds; furthermore a minimum of 5 expected signal events is required to establish evidence for a signal. In the absence of signal, for large numbers of expected back-

ground events $N_{\rm bkg}$, the expected 90% CL upper limit for the number of signal events can be approximated as $N_{90}^{UL} \sim 1.28(1/2+\sqrt{1/2+N_{\rm bkg}})$[1] whereas for small $N_{\rm bkg}$ a value for N_{90}^{UL} is obtained using the method described in [16], which gives, for $N_{\rm bkg} \sim 0$, $N_{90}^{UL} \sim 2.4$. If a signal is determined from counting events within a signal region, the 90% CL branching ratio upper limit is:

$$B_{90}^{UL} = \frac{N_{90}^{UL}}{2N_{\tau\tau}\epsilon} = \frac{N_{90}^{UL}}{2\mathcal{L}\sigma_{\tau\tau}\epsilon}\,, \qquad (2)$$

where $N_{\tau\tau} = \mathcal{L}\sigma_{\tau\tau}$ is the number of τ-pairs produced in e^+e^- collisions; $\mathcal{L}$ is the integrated luminosity, $\sigma_{\tau\tau}$=0.919 nb [17] is the τ-pair production cross section, and ϵ is the signal efficiency.

The $\tau \to \mu\gamma$ projected sensitivity is based on the most recent *BABAR* result [18]. Some Super$B$ improvements with respect to *BABAR* are taken into account:

- The smaller beam size and (to a minor extent) the improved momentum resolution will improve the invariant mass and energy resolution of the τ candidates and are expected to reduce the signal region area by 35%.
- The improved coverage for photons is expected to increase the acceptance by 20%.

Further gains are possible by re-optimizing the analysis for the Super$B$ detector and exploiting beam polarization effects. The high energy electrons beam at Super$B$ can be ∼80% longitudinally polarized, influencing the angular distribution of the τ decay products in a way that depends on the interaction that causes LFV. Figure 3 shows that with beam polarization the helicity angles of the τ pair decay products can be used to significantly suppress the background when one τ decays to $\mu\gamma$ and the other one to $\pi\nu$. Similar background suppressions are also obtained with $\rho\nu$ and $e\nu\overline{\nu}$ decays on the other side.

While further investigations are ongoing to quantify analysis improvements, we provide here a more conservative estimate of the Super$B$ reach on τ LFV, which does not consider beam polarization and other possible improvements on the analysis. For $\tau \to \mu\gamma$,

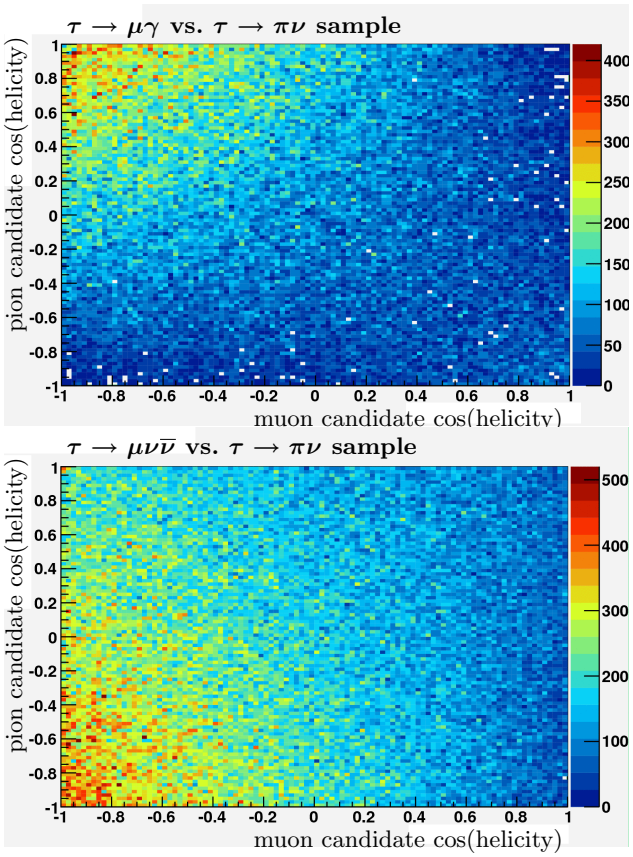

FIG. 3: Distribution of the cosine of the helicity angle of the muon and pion candidates when selecting τ pairs events decaying to $\tau \to \mu\gamma$ and $\tau \to \pi\nu$. The top plot shows simulated signal events, the bottom plot shows simulated $\tau \to \mu\nu\overline{\nu}$ background events. In both cases, the electron beam is 80% longitudinally polarized.

we expect the final efficiency to be ∼ 7.3% and the final background to be ∼ 260 events. This leads to an expected 90%CL upper limit of 2.4×10^{-9} and a 3σ evidence reach of 5.4×10^{-9}. One additional benefit of beam polarization is the possibility to determine the helicity structure of the LFV coupling from the final state momenta distributions (see for instance Ref. [19] for the $\tau \to \mu\mu\mu$ process). The extrapolation of the $\tau \to e\gamma$ search receives benefits from similar improvements, and has a projected 90% CL upper limit of 3.0×10^{-9} and a 3σ evidence reach of 6.8×10^{-9}.

By re-optimizing the *BABAR* analyses for 75 fb^{-1} of data, we obtained refined projected upper limits for LFV searches for τ into three leptons [20], which lie between the $\propto 1/\mathcal{L}$ and the $\propto 1/\sqrt{\mathcal{L}}$ extrapolations (see Fig. 4). Super$B$ detector improvements are expected to have a minor impact for these channels, and they are conservatively neglected. After optimization the expected backgrounds are small so beam polarization has a minor impact (which we neglect here) on the

[1] This formula has been obtained by approximating the Poisson distributed number of background and signal events with Gaussian distributions and the value 1.28 satisfies the relation

$$90\% \approx \int_{-\infty}^{\mu+1.28\sigma} G(\mu,\sigma),$$

where $G(\mu,\sigma)$ is a Gaussian with mean μ and variance σ^2. For order 100 expected background events, the formula approximates toy Monte Carlo simulations within better than 5%.

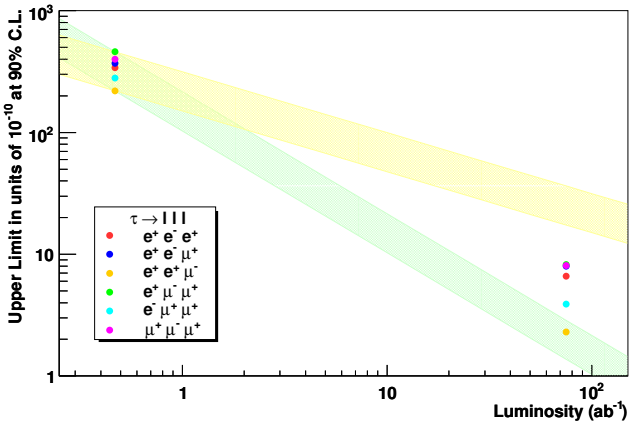

FIG. 4: Expected Super$B$ 90% CL upper limits for $\tau \to \ell\ell\ell$ LFV decays compared with the most recent *BABAR* expected upper limits. The upper and lower bands indicate the $1/\sqrt{\mathcal{L}}$ and $1/\mathcal{L}$ extrapolations, respectively.

expected reach of the search. The re-optimization has been performed by using the *BABAR* data and the simulation of the *BABAR* detector. The expected 90% confidence upper limits are in the range 2.3×10^{-10} to 8.2×10^{-10}, depending on the channel, and the 3σ evidence branching fractions are 1.2×10^{-9} to 4.0×10^{-9}. For technical reasons, the amount of simulated data that has been used (equivalent to about twice the *BABAR* collected luminosity) permits only a crude estimate of some specific backgrounds that have exactly the same particle content of the signal as a result of rare and accidental combination of SM processes. For instance, the *BABAR* simulated samples only contain a few events where a $\tau \to \mu\nu\bar{\nu}$ decay combines with an e^+e^- pair from an ISR photon to accidentally match the τ mass and energy, therefore the extrapolation to the Super$B$ integrated luminosity has some uncertainty. To improve these extrapolations, one needs to simulate large samples of generic background that can be used to study the Super$B$ environment. Work is ongoing within Super$B$ to this end.

We consider the projected results for $\tau \to \ell\ell\ell$ as indicative of the Super$B$ sensitivity for hadronic LFV final states containing a lepton (either a muon or electron) and a hadronic system such as a pseudoscalar or vector meson (π^0, η, η', K^0_S, ω, ϕ, K^*, f_1, *etc.*) or a non-resonant two body system comprising a combination of pions or kaons.

The LFV searches $\tau \to \ell\pi^0$ and $\tau \to \ell\eta\,(\eta \to \gamma\gamma)$, will suffer from accidental backgrounds similar to $\tau \to \ell\gamma$. These backgrounds arise when combinations of two hard photons from an initial state radiation (ISR) event accidentally are reconstruct with an invariant mass $m_{\gamma\gamma}$ compatible with the π^0 or η mass. However the rate for two hard-photon ISR emission will be about 100 times lower than that of single hard photon emission. By requiring $m_{\gamma\gamma}$ to be consistent with that of a π^0 or η we are able to suppress much of this background. Consequently background from ISR events are not expected to be an issue at Super$B$ luminosities.

Compared with Belle II, the Super$B$ project is expected to have a significantly better reach on τ LFV as a result of: (i) a larger design instantaneous and integrated luminosity and (ii) the availability of a highly polarized electron beam in the baseline design of the collider. Table III summarizes the expected sensitivities at Super$B$ for golden LFV decays, which do not yet include possible analysis optimization and the full exploitation of beam polarization effects.

TABLE III: Expected 90% CL upper limits and 3σ evidence reach on LFV decays with 75 ab^{-1} with a polarized electron beam.

Process	Expected 90% CL upper limit	3σ evidence reach
$\mathcal{B}(\tau \to \mu\gamma)$	2.4×10^{-9}	5.4×10^{-9}
$\mathcal{B}(\tau \to e\gamma)$	3.0×10^{-9}	6.8×10^{-9}
$\mathcal{B}(\tau \to \ell\ell\ell)$	2.3–8.2×10^{-10}	1.2–4.0×10^{-9}

B. Measurement of the τ $g-2$

be accommodated if $\tan\beta \gtrsim 10$ and $\mu > 0$.

A measurement of the τ anomalous magnetic moment could be used to confirm or disprove the possibility that the discrepancy in Δa_μ is the result of NP. The natural scaling of heavy-particle effects on lepton magnetic dipole moments, implies $\Delta a_\tau / \Delta a_\mu \sim m^2_\tau / m^2_\mu$. Thus, if we interpret the present muon discrepancy as a signal of NP we would expect $\Delta a_\tau \approx 10^{-6}$.

In the supersymmetric case, such an estimate holds for all the SPS points (see Table IV) and, more generally, in the limit of almost degenerate slepton masses. If $m^2_{\tilde{\nu}_\tau} \ll m^2_{\tilde{\nu}_\mu}$ (as happens, for instance, in the so-called effective-SUSY scenario), Δa_τ could be enhanced up to the 10^{-5} level.

TABLE IV: Values of Δa_μ and Δa_τ for various SPS points.

SPS	1 a	1 b	2	3	4	5
$\Delta a_\mu \times 10^{-9}$	3.1	3.2	1.6	1.4	4.8	1.1
$\Delta a_\tau \times 10^{-6}$	0.9	0.9	0.5	0.4	1.4	0.3

In a manner similar to an EDM, the τ anomalous moment $(g-2)$ influences both the angular distribution and the polarization of the τ produced in e^+e^- annihilation. Polarized beams allow the measurement of the real part of the $g-2$ form factor by measuring the

τ polarization with just the τ polar angle distribution, i.e. without looking at the angular distribution of the τ decay products in the τ rest frame. Bernabéu *et al.* [21] estimate that Super$B$ with $75\,\mathrm{ab}^{-1}$ will measure the real and imaginary part of the $g-2$ form factor at the $\Upsilon(4S)$ with a resolution in the range $[0.75-1.7]\times10^{-6}$. Two measurements of the real part of $g-2$ are proposed: one fitting just the polar angle distribution of the τ leptons, and one based on the measurement of the transverse and longitudinal polarization of the τ from the angular distribution of its decay products. All events with τ leptons decaying either in $\pi\nu$ or $\rho\nu$ are considered, but no detector effects are accounted for. For the τ polarization measurements, electron beams with 100% polarization are assumed. Studies simulating more realistic experimental conditions are ongoing. While the polar angle distribution measurement will conceivably suffer from uncertainties in the τ direction reconstruction, the preliminary results on the τ EDM measurement mentioned above indicate that reconstruction systematic effects are small for asymmetries using the τ polarization. Using the estimated precision on the τ EDM measurement, we expect that Super$B$ can measure the real part of the $g-2$ form factor with a statistical error of 2.4×10^{-6}. With such resolution, Super$B$ will be able to measure the SM-predicted τ magnetic anomaly at the percent level.

C. τ electric dipole moment

In minimal SUSY frameworks with flavor-independent *CP*-violating phases, like the constrained MSSM, lepton EDMs (d_ℓ) scale linearly with the lepton mass. As a result, the existing limits on the electron EDM generally preclude any visible effect in the τ and μ cases. In more general MSSM models, however, the strength of *CP* violation may be different for different flavors and this simple linear scaling does not apply [10]. A very simple example is given by models where the *CP*-violation phases are associated with the third generation, in our case, to the stau trilinear coupling, A_τ [22]. In this case the τ EDM will be large and EDMs for the first two generations will be suppressed by small mixings. Unfortunately, there are also situations where the additional flavor dependence can generate a further suppression in the τ EDM [10]. Thus, it is necessary to measure all three lepton EDMs independently in order to determine the flavor dependence of *CP* phases. Furthermore in multi-Higgs models the EDMs scale with the cube of the lepton mass [23], thus d_τ can be enhanced significantly. However, in this case the e and μ EDMs receive sizeable two-loop contributions from Barr-Zee diagrams. Again these scale linearly with the lepton masses. As a result, one can derive an approximate bound $d_\tau \lesssim 0.1\times(m_\tau/m_\mu)^3(m_\mu/m_e)d_e$ which is still very strong. From the present experimental upper bound on the electron EDM, $d_e \lesssim 10^{-27}e\,\mathrm{cm}$ it follows that $d_\tau \lesssim 10^{-22}e\,\mathrm{cm}$.

The τ EDM influences both the angular distributions and the polarization of the τ produced in e^+e^- annihilation. With a polarized electron beam it is possible to reconstruct observables from the angular distribution of the products of a single τ decay that unambiguously discriminates between the contribution due to the τ EDM and other effects [24, 25]. Recent studies have provided an estimate of the Super$B$ upper limit sensitivity for the real part of the τ EDM $|\mathrm{Re}\{d_\tau^\gamma\}| \leq 7.2\times10^{-20}\,e\,\mathrm{cm}$ with $75\,\mathrm{ab}^{-1}$ [24]. The result assumes a 100% polarized electron beam colliding with unpolarized positrons at the $\Upsilon(4S)$ resonance. Uncertainty on the polarization is neglected, and a perfect reconstruction of the decay $\tau\to\pi\nu$ is assumed. Studies have been done assuming more realistic conditions:

- An electron beam with a linear polarization of $80\%\pm1\%$.
- 80% geometric acceptance.
- Track reconstruction efficiency $97.5\%\pm0.1\%$ (similarly to that achieved in LEP analyses [26] and *BABAR* ISR analyses [27].

The process $e^+e^-\to\tau^+\tau^-$ is simulated with the KK generator [28] and the Tauola package for τ decay [28]; the simulation includes the complete spin correlation density matrix of the initial-state beams and the final state τ leptons. τ EDM effects are simulated by weighting the τ decay product angular distributions. These studies are not complete, and do not yet include uncertainties in reconstructing the τ direction. Preliminary indications are that the τ EDM experimental resolution is $\approx10\times10^{-20}e\,\mathrm{cm}$, corresponding to an angular asymmetry of 3×10^{-5}. Uncertainties in track reconstruction give a systematic contribution of $\approx1\times10^{-20}\,e\,\mathrm{cm}$. Asymmetries proportional to the τ EDM depend on events that go into the same detector regions but arise from τ leptons produced at different angles, minimizing the impact of efficiency uncertainties. It must be noted that all the hadronic τ channels theoretically have the same statistical power as the $\tau\to\pi\nu$ mode in measuring the τ polarization [29], and can therefore be used to improve the experimental resolution.

A search for the τ EDM using unpolarized beams has been completed at Belle [30]. In this case, one must measure correlations of the angular distributions of both τ leptons in the same events thereby losing both reconstruction efficiency and statistical precision. The analysis shows the impact of inefficiency and uncertainties in the τ direction reconstruction, and also

demonstrates that all τ decays, including leptonic decays with two neutrinos, provide statistically useful information for measurement of the τ EDM. With $29.5\,\mathrm{fb}^{-1}$ of data, the experimental resolution on the real and imaginary parts of the τ EDM is between $0.9 \times 10^{-17}\,e\,\mathrm{cm}$ and $1.7 \times 10^{-17}\,e\,\mathrm{cm}$, including systematic effects. An extrapolation to Super$B$ with a data sample of $75\,\mathrm{ab}^{-1}$ (assuming systematic effects can be reduced according to statistics) corresponds to an experimental sensitivity of between $17 \times 10^{-20}\,e\,\mathrm{cm}$ and $34 \times 10^{-20}\,e\,\mathrm{cm}$.

D. *CP* Violation in τ decays

CP violation in the quark sector has been observed both in the K and in the B systems. All experimental results thus far can be explained by the complex phase of the CKM matrix. On the contrary *CP* violation in the lepton sector has not been observed yet. *CP*-violating effects in charged-lepton decays within the SM are predicted to be vanishingly small. For instance, the *CP* asymmetry rate of $\tau^{\pm} \to K^{\pm}\pi^0\nu$ is estimated to be of order $\mathcal{O}(10^{-12})$ [31]. For the decay $\tau^{\pm} \to K_S\pi^{\pm}\nu$ a small *CP* asymmetry of 3.3×10^{-3} is induced by the known *CP*-violating phase of the $K^0\overline{K}^0$ mixing amplitude [32]. This asymmetry is known to a precision of 2%. Hence the *CP* violating asymmetry in this mode can serve as a calibration measurement for searches for effects in other τ decays. Any observed deviation from expected asymmetries in τ decays would be a clear sign of NP.

Most of the known NP models cannot generate observable *CP*-violating effects in τ decays (see *e.g.*, [15]). The only known exceptions are RPV SUSY [14, 33] or specific non-supersymmetric multi-Higgs models [34–36]. In such frameworks NP contributes at tree level, and if the sfermions or charged Higgs particles are relatively light with sizable couplings to the light quarks, then the NP contributions can be significant. In some cases the *CP* asymmetries of various τ decay channels or T-odd *CP*-violating asymmetries in the angular distribution can be enhanced up to the level of 10^{-1}. Such enhancements from NP are compatible with limits from other observables, and saturate at the experimental limits obtained by CLEO [35–37]. In particular, these models have been shown to be able to produce sizable asymmetries in the decays $\tau \to K\pi\nu_\tau$, $\tau \to K\eta^{(\prime)}\nu_\tau$, and $\tau \to K\pi\pi\nu_\tau$ [33–36].

A first search for *CP* violation in τ decay has been conducted by the CLEO collaboration [37], looking for a tau-charge-dependent asymmetry of the angular distribution of the hadronic system produced in $\tau \to K_S\pi\nu$. In multi-Higgs doublet NP scenarios the *CP*-violating asymmetry arises from the Higgs coupling and the interference between S wave scalar exchange and P wave vector exchange. The Cabibbo-suppressed decay mode into $K_S\pi\nu$ has a larger mass-dependent Higgs coupling. Furthermore, events in the sidebands of the K_S mass distributions can be used to calibrate the detector response. Using a data sample of $13.3\,\mathrm{fb}^{-1}$ (12.2×10^6 τ pairs) CLEO obtains the mean of the optimal asymmetry observable $\langle\xi\rangle = (-2.0 \pm 1.8) \times 10^{-3}$. As this measurement relies on detector calibration using data side-band events it is conceivable that Super$B$ with $75\,\mathrm{ab}^{-1}$ would not be limited by systematics and could reach an experimental sensitivity of $\sigma_{\langle\xi\rangle} \approx 2.4 \times 10^{-5}$.

E. Precision measurements of τ decays

1. $|V_{us}|$

TO COMPLETE ...

2. *Charged current universality*

Tree-level Higgs exchanges in supersymmetric new physics models can induce modifications of lepton universality of order 0.1% [38], smaller but close to the present experimental accuracy of $\approx 0.2\%$ [39]. As discussed in Ref. [40], Super$B$ can probably measure lepton universality to 0.1% or better. However the measurement is limited by experimental systematic uncertainties on the measurement of the τ leptonic branching fractions and the τ lifetime, as the modest progress provided by the existing B Factories also confirms [41]. Therefore it cannot be advocated that the Super$B$ advantages in terms of luminosity are crucial and necessary for the advancement of this particular sector, although large statistical samples will be an advantage to reduce experimental systematic uncertainties.

3. *Hadronic spectral functions and muonic* $g-2$

4. *Lorentz structure*

The Standard Model prediction for the muon anomalous magnetic moment is not in perfect agreement with recent experimental results. In particular, $\Delta a_\mu = a_\mu^{\mathrm{exp}} - a_\mu^{\mathrm{SM}} \approx (3 \pm 1) \times 10^{-9}$. Within the MSSM, this discrepancy can naturally

F. Search for second-class currents

In the SM, approximate conservation of isospin symmetry implies that hadronic currents corresponding to $J^{PG} = 0^{+-}, 0^{-+}, 1^{++}, 1^{--}$, known as second-class

currents (SCC) [42], are suppressed by the difference between the down- and up-quark masses. This suppression makes the search for decays mediated by SCC a test of the SM, a way to shed light on hadronic states, and a way to search for new physics contributions to SM-suppressed decays.

For example, the SM branching fraction of the SCC decay $\tau^- \to \eta\pi^-\nu_\tau$ is predicted to be in the range $(2-4) \times 10^{-6}$[43], assuming, as commonly believed, that the $a_0^-(980)$ is a four-quark state. A measured branching fraction around 10^{-5} would mean that $a_0^-(980)$ is actually a $d\bar{u}$ meson, and a value greater than about 3×10^{-5} could indicate the possible existence of a new-physics scalar component in the weak interaction.

There is no published search for $\tau^- \to \eta\pi^-\nu_\tau$, but BaBar has searched for the related decay $\tau^- \to \eta'(958)\pi^-\nu_\tau$ using 384 fb^{-1}, and has determined its branching fraction to be smaller than 7.2×10^{-6} [44]. With the full data set of 75 ab^{-1}, SuperB could push the limit to about a third of the theoretical upper limit of 1.4×10^{-6} [45]. Similarly, the experimental reach for $\tau^- \to \eta\pi^-\nu_\tau$ is expected to place limits on scalar new-physics contributions and may be sensitive enough to elucidate the nature of the $a_0^-(980)$. BaBar has also studied $\tau^- \to \omega\pi^-\nu_\tau$ and has set a 0.69% upper limit on the SCC fraction in this decay [46].

G. Precision measurements of τ properties

1. *τ lifetime measurements*

2. *τ mass measurements*

H. Section summary

The section summary should provide a succinct recap of the main points discussed within the section, including (if relevant) summary tables of sensitivitites.

4. B Physics at the $\Upsilon(4S)$

This section contains highlights of the B physics programme from Super$B$. The focus of much of the material presented here is the search for physics beyond the standard model. The following sub-sections discuss time-dependent CP measurements, theoretical and experimental aspects of a number of rare decay golden channels including $B \to K^{(*)}\nu\overline{\nu}$, $B \to X_{s,d}\gamma$, $B \to X_{s,d}\ell^+\ell^-$, $B \to \ell\nu(\gamma)$, measurements of $|V_{ub}|$ and $|V_{cb}|$, Δm_d and CPT tests. In addition to these processes that can shed light on new physics there are standard model control measurements comprising precision CKM determination. One area of B decays that is a rich test bed for theoretical understanding and testing of new tools is that of charmless hadronic decays. This area will remain interesting in the era of Super$B$.

A. Rare decays with missing energy

1. $B \to \ell\nu$

One of the most important applications of the recoil technique (tag reconstruction method) described in the previous section is in the search for $B^+ \to \tau^+\nu$, where the presence of two or more neutrinos in the final state effectively eliminates any meaningful kinematic information that can be used to identify the signal decay [2]. Searches performed to date have therefore utilized the tag reconstruction method (both hadronic and semi-leptonic tags), relying on signal topology for the selection, exploiting the low particle multiplicity of the signal decays compared with background events. After a cleanly-reconstructed tag B has been selected, the event is required to possess either one or three additional charged tracks, particle ID requirements are imposed to distinguish between hadronic and leptonic τ decay candidates, then mode-specific constraints are imposed on the presence of neutral energy in the calorimeter. The limitation on this technique is ultimately imposed by systematic uncertainties on the background resulting from knowledge of the background track multiplicity and calorimeter "extra energy" distributions. The extra energy distribution is particularly problematic, since it relies on excellent understanding of low energy clusters resulting from diverse sources including beam backgrounds, hadronic cluster "split-offs", neutral hadrons etc. One advantage that Super$B$ has over the existing B Factories in this respect is the ability to validate the MC modeling of the extra energy using "signal-like" exclusive decay control samples, *e.g.* by plotting the extra energy distribution for events in which a clean $B \to K^*\gamma$ or similar event has been reconstructed in addition to the tag B. With the existing B factory data sets, this technique does not yield sufficient statistics for meaningful studies. However at Super$B$ this ability is expected to permit $B^+ \to \tau^+\nu$ branching fraction measurements to remain statistically limited even with the full Super$B$ data statistics.

One can find a brief theoretical overview of the $B \to \ell\nu$ channels in Ref. [40]. Both in the SM and in the generic 2HDM, the ratios of leptonic branching fractions is given simply by the ratio of final state lepton masses squared. It is therefore extremely useful to have a good measurement of not only $B^+ \to \tau^+\nu$, but also $B^+ \to \mu^+\nu$ in order to provide an internal consistency check of these measurements. This is particularly important given the current $\sim 2\sigma$ discrepancy between V_{ub} measurements, the CKM fit excluding V_{ub} and $B^+ \to \tau^+\nu$. $B^+ \to \mu^+\nu$ results have been reported by both *BABAR* and Belle (using untagged analyses) with resulting branching fraction limits which are within about a factor of two of SM expectations. In addition a first study has been published by *BABAR* using the hadronic tag reconstruction method. The tagged and untagged approaches are complementary and both are expected to yield clear observations of $B^+ \to \mu^+\nu$ with Super$B$ luminosity. Due to the cleaner signal signature in this mode, it is likely that the ultimate precision on $B^+ \to \mu^+\nu$ will be similar to $B^+ \to \tau^+\nu$. *BABAR* has recently extended the $B^+ \to \ell^+\nu$ ($\ell = e, \mu$) to include the radiative decay $B^+ \to \ell^+\nu\gamma$ using a hadronic tag method. Although this analysis suffers from limited statistics with the *BABAR* dataset, the additional kinematic constraints which are available with this method (as well as improved over continuum backgrounds) permit an almost background free signal selection, although at the cost of signal efficiency. This method is expected to have sensitivity to the SM rate well within the nominal Super$B$ luminosity range, and it will be important contribution toward a precision determination of $B^+ \to \ell^+\nu$ as in the limit of small photon energy this radiative mode becomes an important component of the $B^+ \to \ell^+\nu$ signal.

[2] This is actually not quite true. Leptonic τ decays from $B^+ \to \tau^+\nu$ preferentially produce low momentum electrons and muons, while $\tau^+ \to \pi^+\nu_\tau$ produces high momentum pions. To date, neither *BABAR* nor Belle has explicitly incorporated this feature into their studies.

TABLE V: SM predictions and experimental 90% C.L. upper bounds for the four $b \to s\nu\bar{\nu}$ observables.

Observable	SM prediction	Experiment
$\mathcal{B}(B^0 \to K^{*0}\nu\bar{\nu})$	$(6.8^{+1.0}_{-1.1}) \times 10^{-6}$ [47]	$< 80 \times 10^{-6}$ [49]
$\mathcal{B}(B^+ \to K^+\nu\bar{\nu})$	$(3.6 \pm 0.5) \times 10^{-6}$ [50]	$< 14 \times 10^{-6}$ [51]
	$(4.5 \pm 0.7) \times 10^{-6}$ [47]	
$\mathcal{B}(\bar{B} \to X_s\nu\bar{\nu})$	$(2.7 \pm 0.2) \times 10^{-5}$ [47]	$< 64 \times 10^{-5}$ [52]
$\langle F_L(B \to K^*\nu\bar{\nu})\rangle$	0.54 ± 0.01 [47]	–

2. $B \to K\nu\bar{\nu}$

3. New physics in $B \to K^{(*)}\nu\bar{\nu}$ decays

Rare B decays with a $\nu\bar{\nu}$ pair in the final state are interesting probes of new physics, since they allow one to transparently study Z penguin and other electroweak penguin effects in the absence of dipole operator and Higgs penguin contributions, which are often more important than Z contributions in $b \to s\ell^+\ell^-$ decays. Moreover, since the neutrinos escape the detector unmeasured, the $B \to K^{(*)} + E_{\rm miss}$ channel can also contain contributions from other light SM-singlet particles substituting the neutrinos in the decay.

The inclusive decay $\bar{B} \to X_s\nu\bar{\nu}$ is the theoretically cleanest $b \to s\nu\bar{\nu}$ decay due to the absence of form factor uncertainties, but is experimentally very challenging to measure. The exclusive decay $B \to K\nu\bar{\nu}$ currently provides most stringent constraints on NP with an experimental upper bound only a factor of three above the SM prediction. The $B \to K^*\nu\bar{\nu}$ decay has the advantage that, in addition to its differential decay rate, it in principle provides access to an additional observable via the angular distribution of the K^* decay products $K^\pm\pi^\mp$: the K^* longitudinal polarization fraction $F_L(q^2)$, which is theoretically very clean since form factor uncertainties cancel to a large extent [47].

The SM predictions and current experimental upper bounds are summarized in table V. However, for the modes involving a charged B in the initial state, it should be noted that the bounds in the rightmost column do not take into account an important background from $B \to \tau\nu$ decays with the τ subsequently decaying to a K or K^* and a (anti-)neutrino, which has been recently pointed out in [48]. This contribution is expected to be small at Super$B$ (roughly 15–30% of the SM value for $B^+ \to K^+\nu\bar{\nu}$). With data available at Super$B$ it will be possible to accurately determine the background contribution from $\mathcal{B}(B \to \tau\nu)$ decays and on doing so increase the precision with which we can extract the signal. The sensitivities quoted in the table are conservative for this reason.

The $b \to s\nu\bar{\nu}$ transition is governed by the effective Hamiltonian

$$\mathcal{H}_{\rm eff} = -\frac{4\,G_F}{\sqrt{2}} V_{tb}V_{ts}^* \left(C_L^\nu \mathcal{O}_L^\nu + C_R^\nu \mathcal{O}_R^\nu\right) \;+\; \text{h.c.}\,, \quad (3)$$

where the operators are $\mathcal{O}^\nu_{L,R} = \frac{e^2}{8\pi^2}(\bar{s}\gamma_\mu P_{L,R} b)(\bar{\nu}P_L\nu)$, and the $C^\nu_{L,R}$ are the corresponding Wilson coefficients. In the SM, $C_L^\nu \approx -6.38$ and the right-handed Wilson coefficient vanishes. In models beyond the SM, both C_L^ν and C_R^ν can be non-zero and complex; however, the two exclusive and the inclusive decay rates as well as F_L only depend on two independent combinations of these Wilson coefficients, which can be written as

$$\epsilon = \frac{\sqrt{|C_L^\nu|^2 + |C_R^\nu|^2}}{|(C_L^\nu)^{\rm SM}|}\,, \qquad \eta = \frac{-\text{Re}\,(C_L^\nu C_R^{\nu *})}{|C_L^\nu|^2 + |C_R^\nu|^2}\,, \quad (4)$$

implying $(\epsilon, \eta)_{\rm SM} = (1, 0)$. This allows one to express the observables of $b \to s\nu\bar{\nu}$ decays in a general NP model as

$$R(B \to K^*\nu\bar{\nu}) \;=\; (1 + 1.31\,\eta)\epsilon^2, \quad (5)$$

$$R(B \to K\nu\bar{\nu}) \;=\; (1 - 2\,\eta)\epsilon^2, \quad (6)$$

$$R(\bar{B} \to X_s\nu\bar{\nu}) \;=\; (1 + 0.09\,\eta)\epsilon^2, \quad (7)$$

$$\langle F_L\rangle/\langle F_L\rangle_{\rm SM} \;=\; \frac{(1 + 2\,\eta)}{(1 + 1.31\,\eta)}, \quad (8)$$

where $R(X) = \mathcal{B}(X)/\mathcal{B}(X)_{\rm SM}$ and $\langle F_L\rangle$ refers to F_L appropriately integrated over the neutrino invariant mass [47]. Eq. (8) highlights an important feature of the observable F_L: it only depends on η and not on ϵ. Any experimentally observed deviation from the SM prediction of F_L would unambiguously imply the presence of right-handed currents.

In Fig. 5, the existing constraints on the ϵ-η plane are shown in combination with the hypothetical constraints arising from a measurement of all four observables with infinite precision. It is self-evident that the complementarity between the different modes allows us to over-constrain the point (ϵ, η).

Concerning the size of possible NP effects in $b \to s\nu\bar{\nu}$ decays, it is instructive to parameterize the dominance of Z penguin contributions in many models by a modified bsZ coupling [53]. In this way, the NP contributions to $b \to s\nu\bar{\nu}$ transitions are automatically correlated to other $b \to s$ transitions sensitive to this coupling. A particularly stringent constraint in this respect turns out to be the branching ratio of the inclusive decay $\bar{B} \to X_s\ell^+\ell^-$. Assuming no NP contributions apart from the modified bsZ couplings, the measurement of this branching ratio implies that the $b \to s\nu\bar{\nu}$ branching ratios cannot be enhanced by more than a factor of two above the SM. However, this bound can be weakened substantially by assuming other NP contributions to $\bar{B} \to X_s\ell^+\ell^-$, such as photon penguins.

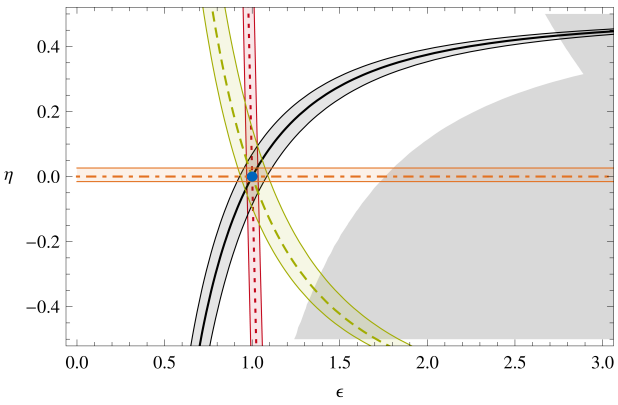

FIG. 5: Hypothetical constraints on the ϵ-η-plane, assuming all four observables have been measured with infinite precision. The error bands refer to theory uncertainties only. The green band (dashed line) represents $\mathcal{B}(B \to K^*\nu\bar{\nu})$, the black band (solid line) $\mathcal{B}(B \to K\nu\bar{\nu})$, the red band (dotted line) $\mathcal{B}(B \to X_s\nu\bar{\nu})$ and the orange band (dot-dashed line) $\langle F_L \rangle$. The shaded area is ruled out experimentally at the 90% confidence level.

Very large effects can in principle be obtained in family non-universal Z' models. If the Z' couples more strongly to neutrinos than to charged leptons, the constraints on the flavour-changing couplings from $\bar{B} \to X_s\ell^+\ell^-$ and $B_s \to \mu^+\mu^-$ can be weakened or entirely absent.

In the Minimal Supersymmetric Standard Model (MSSM), NP effects in the $b \to s\nu\bar{\nu}$ observables turn out to be quite limited, even in the general, non-minimal flavour violating case [47, 54]. While gluino contributions to $C^{\nu}_{L,R}$ are strongly constrained by the $b \to s\gamma$ decay, $\tan\beta$-enhanced Higgs-mediated contributions to C^{ν}_{R} are also negligible once the stringent bound from $B_s \to \mu^+\mu^-$ is taken into account. Visible effects can thus only be generated in presence of a sizable $(\delta_u^{RL})_{32}$ mass insertion by means of up-squark-chargino loops. Consequently, while C^{ν}_{R} (and thus F_L) is SM-like, the branching ratios can be enhanced or suppressed by at most 35% [47].

Spectacular NP effects can be obtained in models with light invisible particles produced in the $b \to s$ transition, even if the $b \to s\nu\bar{\nu}$ amplitude is unaffected by NP, since experiments actually measure the process $b \to s + E_{\rm miss}$. This can happen *e.g.*in models with light scalar dark matter [55], light neutralinos [56, 57], light Next to Minimal Supersymmetric Standard Model (NMSSM) pseudoscalar Higgs [58] or light radions [59]. A crucial point in this case is that the invariant mass distributions of the $b \to s + E_{\rm miss}$ decays can be strongly modified, which has to be taken into account in the experimental searches. In addition, the parameterization in Eqns. (5)–(8) do not apply in this case. Therefore, a contribution from particles other than neutrinos to the $b \to s + E_{\rm miss}$ observables would be signaled by a failure of the individual constraints on the ϵ-η plane meeting at a single point.

Summing up, $b \to s\nu\bar{\nu}$ transitions are interesting probes of NP, as one can perform a theoretically clean study of non-standard Z penguin effects. The experimentally accessible observables are the differential branching ratios of $B \to X_s\nu\bar{\nu}$, $B \to K\nu\bar{\nu}$ and $B \to K^*\nu\bar{\nu}$ and the K^* longitudinal polarization fraction $F_L(q^2)$ in $B \to K^*\nu\bar{\nu}$. In a general NP model, these observables depend on two real parameters, ϵ and η, which can be over-constrained by the four measurements.

While the effects in models with minimal flavour violation (MFV) are quite limited and in the non-MFV MSSM can reach at most 35%, well-motivated models exist where much larger effects are possible, *e.g.*Z' models with family non-universal couplings.

Since the neutrinos in the final state cannot be detected, the actual measurements probe the process $b \to s + E_{\rm miss}$, which can receive contributions from particles other than neutrinos in models with new light invisible particles. In this case, spectacular effects and strong modifications of the invariant mass spectra can be obtained.

The recoil technique has been developed in CLEO, and subsequently adopted by both *BABAR* and Belle, in order to search for rare B decays with undetected particles, like neutrinos, in the final states. This technique consists of the reconstruction of one of the two B mesons (the B_{tag}) in a hadronic or semi-leptonic final state, and the search for the signal decay of the other B (the B_{sig}) in the rest of the event. The reconstruction of the B_{tag} allows one to select a pure $B\overline{B}$ sample. Having identified the B_{tag}, everything in the rest of the event by default is the B_{sig} candidate, and so this technique provides a clean environment to search for rare decays.

Since the typical efficiency of the B_{tag} reconstruction is below 1%, the use of this technique at the present B-Factories is almost limited to the search for rare decays with undetected particles like neutrinos in the final state, where strong kinematic constraints are missing. On the other hand, the larger statistics available at Super$B$ would make this technique convenient also for the search of other rare decays, where the high purity of the $B\overline{B}$ sample selected with the recoil method would provide a high level of background suppression.

We have investigated the potential of using the recoil technique at Super$B$ and studied in particular the $B \to K^{(*)}\nu\bar{\nu}$ decays. This channel is an interesting probe for NP in Z^0 penguins [53], such as chargino-up-squark contributions in a generic supersymmetric model. Moreover, due to the presence of undetected neutrinos in the final state, the experimental signature of these decays is $B \to K^{(*)}+$ missing energy, so that

the measured decay rate is sensitive to exotic sources of missing energy, such as light dark matter [55] or "unparticles" [60, 61].

In this analysis, the B_{tag} is reconstructed in the hadronic modes $B \to D^{(*)}X$, where $X = n\pi + mK + pK_s + q\pi^0$ and $n + m + r + q < 6$, or semi-leptonic modes $B \to D^{(*)}\ell\nu$, where $\ell = e, \mu$. In the search for $B \to K\nu\overline{\nu}$, the signal is given by a single track identified as a kaon. In the search for $B \to K^*\nu\overline{\nu}$, we look for a K^* in the $K^{*0} \to K^+\pi^-$, $K^{*\pm} \to K^0_S\pi^\pm$ and $K^{*\pm} \to K^\pm\pi^0$ modes.

The Super$B$ fast simulation has been used to simulate signal events in the Super$B$ and *BABAR* setup. This test showed a 20 to 30% increase in the efficiency at Super$B$ relative to *BABAR*, depending on the final state, mainly provided by the larger acceptance due to the lower $\Upsilon(4S)$ boost. The simulation of $B\overline{B}$ events, where one of the two B mesons decays semi-leptonically and the other generically, showed that a 10% reduction in this important background source is also possible in the semi-leptonic recoil analysis. Based on these observations, we estimate a 20 to 30% increase in the $S/\sqrt{(}B)$ ratio, where S and B are the signal and background yields, respectively.

The results in Table V have been used to update the study presented in [62]. The expected sensitivity to $B \to K^{(*)}\nu\overline{\nu}$ is shown in Fig. 6. The 3σ observation of the $B \to K\nu\overline{\nu}$ decay is expected with a data sample of $10\,ab^{-1}$, while $50\,ab^{-1}$ will be needed to observe $B \to K^*\nu\overline{\nu}$ decays, assuming the branching fraction occurs at a rate consistent with SM-based calculations (See Table V).

We also investigated the feasibility of an angular analysis of the $B \to K^*\nu\overline{\nu}$ decay. Along with the measurement of the Branching Fractions, this analysis would provide a constraint for the two parameters ϵ and ρ given in Eq. 4.

In the angular analysis, the distribution of the cosine of the angle θ between the K^* flight direction in the B_{sig} rest frame and the K flight direction in the $K\pi$ rest frame has to be studied. At least in the hadronic analysis, the B_{sig} rest frame can be deduced from the fully reconstructed B_{tag}, and θ can be easily determined. From toy MC studies, neglecting $\cos(\theta)$ resolution effects and assuming a flat background on $\cos(\theta)$, we estimated that the $B^0 \to K^{*0}\nu\overline{\nu}$ channel in the hadronic recoil could provide an error of about 0.3 on the parameter $< F_L >$ with $75\,\mathrm{ab}^{-1}$ of data. The combination of this information with the measurement of the branching ratios would provide a constraint in the plane (ϵ, η), as shown in Fig. 7, where NP would show up as a deviation from the SM values $(1, 0)$.

In summary, in the search for rare B decays at Super$B$, the high $B\overline{B}$ statistics would enable one to consider using the recoil technique, consisting of the full reconstruction of one of the two B mesons in a hadronic or semi-leptonic mode, and the subsequent search for a signal in the rest of the event. By using the recoil technique one will loose signal efficiency, but in return be able to identify and reconstruct signal and a very clean environment. We have investigated the reach of Super$B$ in the search for the $B \to K^{(*)}\nu\overline{\nu}$ decays in both semi-leptonic and hadronic recoil samples. Preliminary results based on the Super$B$ fast simulation have shown that a 10 to 30% improvement in the sensitivity with respect to the *BABAR* setup is possible, allowing for a 3σ observation of the $B^{0,\pm} \to K^{(*)0,\pm}\nu\overline{\nu}$ decays. An angular analysis of the decay will also be feasible.

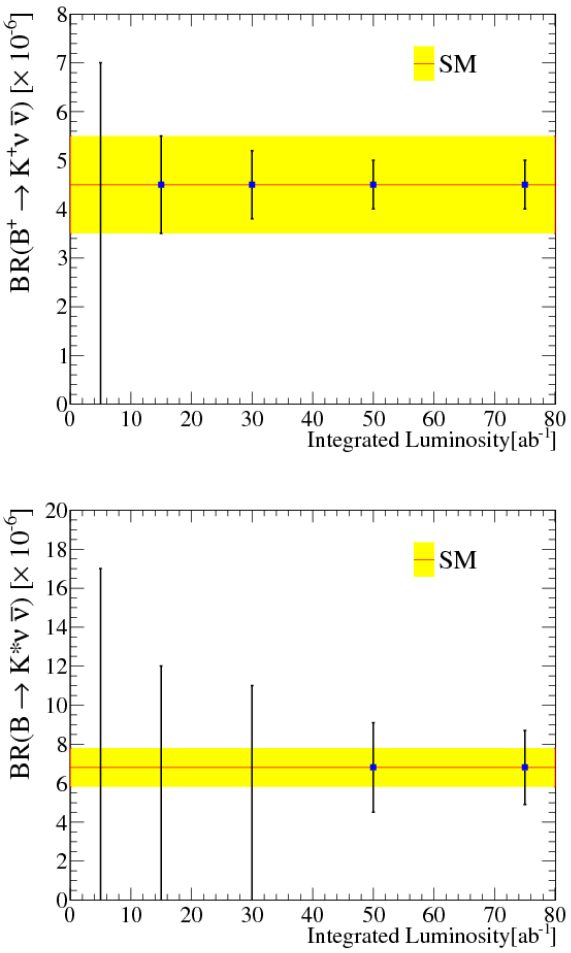

FIG. 6: Expected precision of the measurements of the branching fractions of (top) $B^+ \to K^+\nu\overline{\nu}$ and (bottom) $B^* \to K^*\nu\overline{\nu}$ evaluated as a function of the integrated luminosity. The central values correspond to the calculations found in Ref. [47].

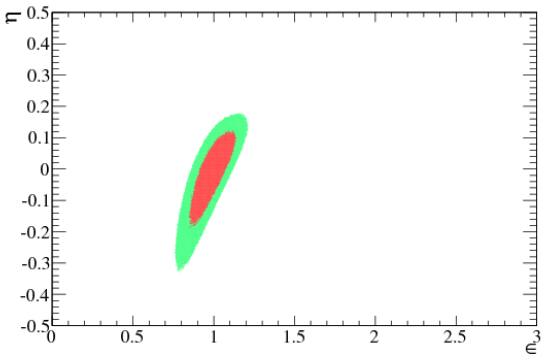

FIG. 7: Expected constraint on the (ϵ, η) plane discussed in Section 4 A 3, from the measurement of the Branching Ratios of $B \to K^{(*)}\nu\overline{\nu}$ and the angular analysis of $B^0 \to K^{*0}\nu\overline{\nu}$ at $75\,ab^{-1}$ (See Figure 6).

B. Leptonic penguins

1. *Inclusive $b \to s\ell^+\ell^-$ decays*

The two inclusive rare decays $\bar{B} \to X_s\gamma$ and $\bar{B} \to X_s\ell^+\ell^-$ are both dominated by perturbative contributions. The relevant Lagrangian density can be found in Refs. [63] and [64]. The SM prediction of $\mathcal{B}(\bar{B} \to X_s\gamma)$ for $E_\gamma > 1.6$ GeV is

$$\mathcal{B}(\bar{B} \to X_s\gamma)|_{E_\gamma > 1.6\ \mathrm{GeV}} = \Big\{ (3.15 \pm 0.23) \times 10^{-4} \quad [63].$$

The overall uncertainty consists of non-perturbative (5%), parametric (3%), higher-order (3%) and m_c-interpolation (3%), which have been added in quadrature. Ref. [65] found a different (but compatible) result using resummation techniques, which however has been strongly questioned in Ref. [66].

This result is based on a global effort to calculate the perturbative corrections to the NNLL level [67–76]. There are other perturbative NNLL corrections that are not yet included in the present NNLL estimate, but are expected to be smaller than the current uncertainty, producing a shift of the central value of about 1.6% at maximum [66].

While the uncertainties due to the input parameters and due to the m_c interpolation could be further reduced, the perturbative error of 3% will remain unless a new major effort to compute the NNNLO is carried out. However, the theoretical prediction has now reached the non-perturbative boundaries. The largest uncertainty is presently due to non-perturbative corrections that scale with $\alpha_s\Lambda_{\rm QCD}/m_b$. A local expansion is not possible for these contributions. A specific piece of these additional non-perturbative corrections has been estimated [77], and found to be consistent with the dimensional estimate of 5%. More recently, a systematic analysis found an overall uncertainty of $4-5\%$ due to all power corrections of this kind [78].

Two explicit examples demonstrate the stringent constraints that can, with these uncertainties, be derived from the measurement of the $\bar{B} \to X_s\gamma$ branching fractions.

Fig. 8 shows the dependence of $\mathcal{B}(\bar{B} \to X_s\gamma)$ on the charged Higgs mass in the 2-Higgs-doublet model (2HDM-II) [63]. The bound on $M_{H^+} = 295$ GeV at

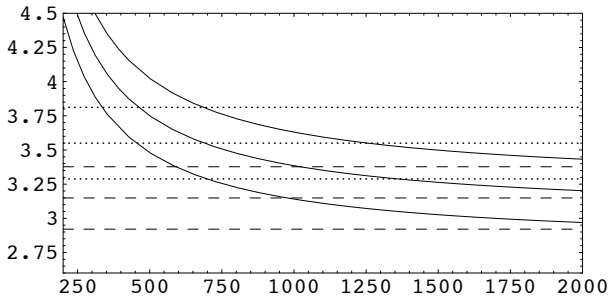

FIG. 8: $\mathcal{B}(\bar{B} \to X_s\gamma) \times 10^{-4}$ as a function of the charged Higgs boson mass M_{H^+} (GeV) in the 2HDM II for $\tan\beta = 2$ (solid lines). Dashed and dotted lines show the SM and experimental results, respectively. The central line for each of the cases corresponds to the central value, and the other lines have been obtained by combining errors in quadrature.

95% CL, shown in Fig. 8, is currently the strongest available lower limit on the charged Higgs mass.

Similarly, the bound on the inverse compactification radius of the minimal universal extra dimension model (mUED) derived from $\mathcal{B}(\bar{B} \to X_s\gamma)$ [79] is $1/R > 600$ GeV at 95% confidence level, as shown in Fig. 9.

The angular decomposition of the $\bar{B} \to X_s\,\ell^+\ell^-$ decay rate provides three independent observables, H_T, H_A, H_L from which one can extract the short-distance electroweak Wilson coefficients that test for NP [80]:

$$\begin{aligned}\frac{d^3\Gamma}{dq^2\,dz} &= \frac{3}{8}\big[(1+z^2)H_T(q^2) \\ &\quad +2(1-z^2)H_L(q^2) \\ &\quad +2zH_A(q^2)\big]\,. \end{aligned} \qquad (9)$$

Here, $z = \cos\theta$, where θ is the angle between the $\ell^\pm$ and B meson three momenta in the di-lepton rest frame, H_A is equivalent to the forward-backward asymmetry, and the q^2 spectrum is given by $H_T + H_L$. The observables depend on the Wilson coefficients C_7^{eff}, C_9^{eff}, and C_{10}^{eff} in the SM.

In the $\bar{B} \to X_s\ell^+\ell^-$ system, one has to remove contributions from $c\bar{c}$ resonances that appear as large peaks in the dilepton invariant mass spectrum, using appropriate kinematic cuts. It is conventional to define "perturbative windows" with $s = q^2/m_b^2$ away from

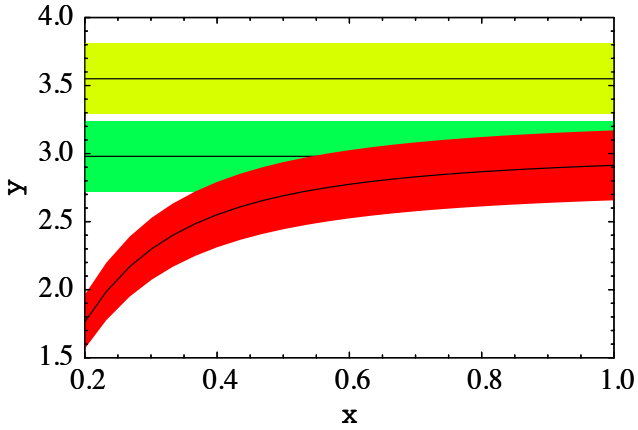

FIG. 9: Branching fraction for $E_0 = 1.6\,GeV$ as a function of $1/R$. The red (dark gray) band corresponds to the LO mUED result. The 68% CL range and central value of the experimental/SM result is indicated by the yellow/green (light/medium gray) band underlying the straight solid line.

charmonium resonances, namely the low dilepton-mass region 1 GeV $< q^2 <$ 6 GeV and the high dilepton-mass region with $q^2 >$ 14.4 GeV. In these windows theoretical predictions for the invariant mass spectrum are dominated by the perturbative contributions; in principle a theoretical precision of order 10% is possible.

The calculations in $\bar{B} \to X_s\ell^+\ell^-$ have achieved a very sophisticated level. The recently calculated NNLL QCD contributions [68, 81–89] have significantly improved the sensitivity of the inclusive $\bar{B} \to X_s\ell^+\ell^-$ decay in testing extensions of the SM in the flavour dynamics sector. In particular, the value of the dilepton invariant mass q_0^2, for which the differential forward-backward asymmetries (FBA) vanishes is one of the most precise predictions in flavour physics with a theoretical uncertainty of order 5%. This corresponds well to the expected experimental sensitivity of $4-6\%$ at Super$B$.

Also non-perturbative corrections scaling with $1/m_b^2$, $1/m_b^3$, or $1/m_c^2$ have to be taken into account. Moreover, factorizable long-distance contributions away from the resonance peaks are important; here using the Krüger-Sehgal (KS) approach [90] one avoids the problem of double-counting.

In the high-q^2 region, one encounters the breakdown of the heavy-mass expansion at the endpoint; while the partonic contribution vanishes in the end-point, the $1/m_b^2$ and $1/m_b^3$ corrections tend towards a non-zero value. However, for an integrated high-q^2 spectrum an effective expansion is found in inverse powers of $m_b^{\rm eff} = m_b \times (1 - \sqrt{\hat{s}_{\rm min}})$ rather than m_b.

Recently, further refinements were presented such as the NLO QED two-loop corrections to the Wilson coefficients whose size is of order 2% [91]. Furthermore, it was shown that in the QED one-loop corrections to matrix elements large collinear logarithms of the form $\log(m_b^2/m_{\rm lepton}^2)$ survive integration if only a restricted part of the dilepton mass spectrum is considered. This adds another +2% contribution in the low-q^2 region for $\mathcal{B}(\bar{B} \to X_s\mu^+\mu^-)$ [92]. This results in the following predictions

$$\mathcal{B}(\bar{B} \to X_s\ell^+\ell^-)_{low} = \begin{cases} (1.59 \pm 0.11) \times 10^{-6} & \ell = \mu \\ (1.64 \pm 0.11) \times 10^{-6} & \ell = e\,. \end{cases} \tag{10}$$

In Ref. [64] the results for the high-q^2 region and for the FBA were derived. The result for the branching ratio (BR) in the high-q^2 region reads

$$\mathcal{B}(\bar{B} \to X_s\ell^+\ell^-)_{high} = \begin{cases} 2.40 \times 10^{-7}\ (1^{+0.29}_{-0.26}) & \ell = \mu \\ 2.09 \times 10^{-7}\ (1^{+0.32}_{-0.30}) & \ell = e\,. \end{cases} \tag{11}$$

In this case the relative impact of the collinear QED logarithm is about -8% (-20%) for muons (electrons) and therefore much larger than in the low-q^2 region due to the steep decrease of the differential decay width at large q^2. The large error in Eq. (11) is mainly due to the sizable uncertainties in the parameters that enter the $O(1/m_b^3)$ non-perturbative corrections. As was pointed out in Ref. [93] the error can be significantly decreased by normalizing the $\bar{B} \to X_s\ell^+\ell^-$ decay rate to the semi-leptonic $\bar{B} \to X_u\ell\bar{\nu}$ decay rate *with the same q^2 cut*. This will only be possible in the future at a Super Flavour Factory. For a lower cut of $q_0^2 = 14.4$ GeV^2 this leads to [64]

$$\mathcal{R}^{\ell\ell}(\hat{s}_0) = \begin{cases} 2.29 \times 10^{-3}(1 \pm 0.13) & \ell = \mu \\ 1.94 \times 10^{-3}(1 \pm 0.16) & \ell = e\,, \end{cases} \tag{12}$$

where $\hat{s} = q^2/m_b^2$. The uncertainties from poorly known $O(1/m_b^3)$ power corrections are now under control and the largest source of error is V_{ub}.

The zero of the FBA is found to be at

$$(q_0^2)_{\ell\ell} = \begin{cases} (3.50 \pm 0.12)\,{\rm GeV}^2 & \ell = \mu \\ (3.38 \pm 0.11)\,{\rm GeV}^2 & \ell = e\,. \end{cases} \tag{13}$$

The error is about 3% but includes parametric and perturbative uncertainties only. This 3% error is applicable only in the absence of cuts on m_X. However, unknown subleading non-perturbative corrections of order $O(\alpha_s\Lambda/m_b)$, which are estimated to give an additional uncertainty of order 5%. It is often argued that especially the small μ dependence at the zero is an accident and should be increased by hand. However, by comparing the NLO-QCD with the NNLO-QCD result one can clearly show that the μ dependence is a reasonable reflection of the perturbative error. Moreover, the zero is stable under change of the b quark mass

scheme; the variation is below 2% when switching from 1S to $\overline{\rm MS}$ or pole scheme. There are also predictions for the FBA integrated over bins in the low-q^2 region, which are usually chosen to be $q^2 \in [1, 3.5]$ GeV^2 and $q^2 \in [3.5, 6]$ GeV^2 [64]:

$$\bar{\mathcal{A}}_{\ell\ell}^{(1,3.5)} = \begin{cases} (-9.09 \pm 0.91)\% & \ell = \mu \\ (-8.14 \pm 0.87)\% & \ell = e \end{cases}, \quad (14)$$

$$\bar{\mathcal{A}}_{\ell\ell}^{(3.5,6)} = \begin{cases} (7.80 \pm 0.76)\% & \ell = \mu \\ (8.27 \pm 0.69)\% & \ell = e \end{cases}, \quad (15)$$

These quantities already allow us to discriminate between different NP scenarios [80, 91, 94]. Moreover, by also including the third independent variable in the double differential decay, (see Eq. (9)) in integrated form, one can fix both the magnitude and sign of all relevant Wilson coefficients in the SM and to put constraints on the parameter space of NP models [80]. NP might also affect the high-scale Wilson Coefficients in such a way that they acquire additional phases. In Refs. [64, 92], the results for the branching ratio and FBA in terms of generic high-scale Wilson Coefficients are given.

Two issues need further comments: (1) After including the NLO QED matrix elements, the electron and muon channels receive different contributions due to terms involving $\ln(m_b^2/m_\ell^2)$. This is the only source of the difference between these two channels. The results presented in Eqns. (10)–(14) correspond to the process $\bar{B} \to X_s \ell^+ \ell^-$ in which QED photons are included in the X_s system and the di-lepton invariant mass does not contain any photon, i.e. $q^2 = (p_{\ell^+} + p_{\ell^-})^2$. This would be exactly the case in a fully inclusive analysis using the recoil technique possible at Super$B$. (How photons are treated in the present B-factory studies is discussed in Ref. [95].)

(2) There is another important source of non-perturbative contributions: Measurements in the low q^2 region require an experimental cut on the hadronic invariant mass, $m_X < m_X^{\rm cut}$, to suppress the huge background from $b \to c(\to s\ell^+\nu)\ell^-\bar{\nu}$ transitions. The latest *BABAR* [96] and Belle [97] analyses use $m_X^{\rm cut} = 1.8\,{\rm GeV}$ and $m_X^{\rm cut} = 2.0\,{\rm GeV}$, respectively. The situation is completely analogous to the inclusive determination of $|V_{ub}|$. The m_X cut causes the rates to be sensitive to the B meson shape functions [98, 99], introducing hadronic uncertainties that can easily spoil the sensitivity to NP in this decay. (The large q^2 region is unaffected by the m_X cut.)

At present, the m_X cut is taken into account by extrapolating the measurements to the full m_X range using MC based on a Fermi motion model. This extrapolation is not reliable and can give at best a rough estimate of the effect of the m_X cut. At Super$B$, measurements of $\bar{B} \to X_s \ell^+ \ell^-$ will reach comparable precision as the current $\bar{B} \to X_s\gamma$ and $\bar{B} \to X_u \ell \bar{\nu}$ measurements and will thus require the same level of rigor in dealing with hadronic shape function effects.

At leading order in $\Lambda_{\rm QCD}/m_b$, the cut on m_X leads to a $10\% - 30\%$ reduction in the rate, which to a good approximation is universal among the different short distance contributions [98, 99]. An accurate calculation of the cut rate requires good knowledge of m_b and the shape function, which will become available from measurements of $B \to X_s\gamma$ and $B \to X_u \ell \bar{\nu}$, as explained in Section. 4 D 1.

At subleading order in $\Lambda_{\rm QCD}/m_b$ additional corrections due subleading shape functions arise [100]. Very little is known about the subleading shape functions, which at present causes an irreducible hadronic uncertainty. Their effects were estimated in Ref. [100] by scanning over a range of models (so the estimates should be taken with caution). Depending on the observable and the value of the m_X cut, the subleading shape functions induce corrections in the rates relative to the leading-order result anywhere between -10% to $+10\%$ with equally large uncertainties. They also break the universality in the different short distance contributions, causing a shift of about $-0.05\,{\rm GeV}^2$ to $-0.1\,{\rm GeV}^2$ in the zero of the forward-backward uncertainty with an equally large uncertainty.

Hence, the current theory uncertainties from non-perturbative corrections in the low q^2 range are above 10%. They can be decreased by raising $m_X^{\rm cut}$, which however will cause an increase in the experimental uncertainties. With the full Super$B$ data set, it may be possible to push the non-perturbative uncertainties well below the 10% level by constraining both the leading and subleading shape functions using the combined $\bar{B} \to X_s\gamma$, $\bar{B} \to X_u \ell \bar{\nu}$, and $\bar{B} \to X_s \ell^+ \ell^-$ data.

More details on the subjects of this section can be found for example in Ref. [101].

2. *Exclusive $B \to K^{(*)} \ell^+ \ell^-$ decays*

Few modes are able to provide such a wealth of information as the decay mode of $B \to K^* l^+ l^-$, ranging from FBA [102], isospin asymmetries [103] to angular observables [104–107]. Each of these observables constructed can provide information on a different type of NP, isospin breaking, right-handed currents, etc. In this sense exploring this mode at a Super$B$ machine is a worthy effort. One of the most interesting observables are those coming from the angular distribution.

One can analyze in full detail the 4- body decay distribution of the $B \to K^*(\to K\pi) l^+ l^-$ in the context of QCD Factorization [108] designing a new method to construct observables based on three steps. First, use the spin amplitudes of the K^* as the key ingredient. Second, construct a quantity with these spin ampli-

tudes that maximizes the sensitivity to a certain type of NP (right-handed currents for example), canceling at the same time, the dependence on the poorly known soft form factors at LO. This later point is inspired in a way in the idea of the zero of the FBA. This particular point of the A_{FB} has attracted a lot of interest due to its cleanliness given the cancellation of form factor dependence at LO. The angular observables A_T^2, A_T^3 and A_T^4 and defined by [104, 106]:

$$A_T^{(2)} = \frac{|A_\perp|^2 - |A_\parallel|^2}{|A_\perp|^2 + |A_\parallel|^2}, \qquad A_T^{(3)} = \frac{|A_{0L}A_{\parallel L}^* + A_{0R}^* A_{\parallel R}|}{\sqrt{|A_0|^2|A_\perp|^2}},$$

$$A_T^{(4)} = \frac{|A_{0L}A_{\perp L}^* - A_{0R}^* A_{\perp R}|}{|A_{0L}^* A_{\parallel L} + A_{0R}A_{\parallel R}^*|},$$

exhibit this quality in the full q^2 region and not just at a single point. Finally, the third step for the constructed quantity to be considered an observable (in this context an observable is a quantity that can be extracted from the angular distribution), is that this quantity fulfills all the symmetries of the distribution.

This last point is one of new fundamental ingredients in this procedure [107]. This requires the identification of all four symmetries [107] of the 4-body decay distribution in the massless case. And those are precisely the symmetries that the quantities constructed should respect. The identification of the symmetries [107] allows one to explicitly solve the spin amplitudes in terms of the coefficients of the distribution. An interesting byproduct of this is a highly non trivial constraint between the coefficients of the 4-body distribution, considered before as independent parameters, that should be fulfilled in the SM when leptons are taken to be massless.

It is important to remark that the new observables that can be easily obtained from a full angular distribution analysis at Super$B$ have a huge sensitivity to right-handed currents driven by the operator O_7', to which A_{FB} is blind, and they all have only a mild dependence on soft form factors. In particular, A_T^2 contains all the information of the FBA and more. The zero of the A_{FB} occurs also in A_T^2 at the LO in the same position and the absence of a zero affects both observables in the same way. Moreover, A_T^2 exhibits a maximal deviation from the SM prediction that is approximately zero, for certain types of models in the region between 1 and 2 GeV^2.

Theoretical uncertainties in those exclusive modes are always larger than in the corresponding inclusive modes due to the well-known problem that Λ/m_b cannot be calculated within QCD factorization. This obviously restricts the new-physics sensitivity of those exclusive modes compared to the corresponding inclusive ones [106].

3. $b \to d\ell^+\ell^-$ decays

The rare decay modes $b \to d\gamma$ and $b \to d\,\ell^+\ell^-$ offer an interesting phenomenology which is complementary to the corresponding $b \to s$ transitions. The corresponding effective Hamiltonian is

$$\begin{aligned} H_{\rm eff}(b \to q) &= -\frac{4G_F}{\sqrt{2}} V_{tb}V_{tq}^* \Bigg[\sum_{i=1}^{8} C_i(\mu)\, O_i(\mu) \\ &\quad + \epsilon_q \sum_{i=1}^{2} C_i(\mu)(O_i(\mu) - O_i^u(\mu)) \Bigg], \end{aligned} \tag{16}$$

where the relevant operators are

$$\begin{aligned} O_1 &= (\bar{q}_L\gamma_\mu T^a c_L)(\bar{c}_L\gamma^\mu T^a b_L) \\ O_1^u &= (\bar{q}_L\gamma_\mu T^a u_L)(\bar{u}_L\gamma^\mu T^a b_L) \\ O_2 &= (\bar{q}_L\gamma_\mu c_L)(\bar{c}_L\gamma^\mu b_L) \\ O_2^u &= (\bar{q}_L\gamma_\mu u_L)(\bar{u}_L\gamma^\mu b_L) \\ O_7 &= e/(16\pi^2)\, m_b(\mu)\, (\bar{q}_L\sigma_{\mu\nu} b_R)F^{\mu\nu} \\ O_8 &= g_s/(16\pi^2)\, m_b(\mu)\, (\bar{q}_L T^a \sigma_{\mu\nu} b_R)G^{a\mu\nu}, \end{aligned} \tag{17}$$

and once again the C_i are Wilson Coefficients. The decisive difference between $b \to d$ and $b \to s$ decays is the size of the respective $\epsilon_q = (V_{ub}V_{uq}^*)/(V_{tb}V_{tq}^*)$, which are

$$\begin{aligned} \epsilon_s &= \tfrac{V_{ub}V_{us}^*}{V_{tb}V_{ts}^*} = -\lambda^2(\bar\rho - i\bar\eta) \simeq -0.01 + 0.02\,i, \\ \epsilon_d &= \tfrac{V_{ub}V_{ud}^*}{V_{tb}V_{td}^*} = \frac{\bar\rho - i\bar\eta}{1 - \bar\rho - i\bar\eta} \simeq -0.02 + 0.42\,i. \end{aligned} \tag{18}$$

As a consequence CP asymmetries are tiny in $b \to s$, but sizable in $b \to d$ transitions, as we will see below. Moreover, due to the democratic pattern of the CKM elements, up-quark loops play an important rôle in $b \to d$ transitions. Their QCD corrections are known at two loops [109, 110]. But also non-perturbative power-corrections have to be taken into account. The $1/m_c^2$ corrections are known and well under control, whereas the contributions to the u quark loops have been shown to be order $\mathcal{O}(\Lambda_{\rm QCD}/m_b)$ [111]. However, a recent systematic analysis of power corrections [78] has found that the contribution due to the operator O_1^u in interference with the operator O_7 vanishes in the total rate; thus, there is no additional uncertainty due to the u quark loops any longer, and the decay rate of $\bar{B} \to X_d\gamma$ is as theoretically clean as the decay rate $\bar{B} \to X_s\gamma$. The complete effect of power corrections on CP asymmetries is not estimated yet. For this purpose the systematic analysis in Ref. [78] has to be extended.

The inclusive decay $\bar{B} \to X_d\gamma$ has been studied at various places in the Literature. The theoretical pre-

dictions for the branching ratio $\mathcal{B}[\bar{B} \to X_d\gamma]$ for photon energies $E_\gamma > 1.6$ GeV are [112, 113]

$$\begin{aligned}
\mathcal{B}[\bar{B} \to X_d\gamma] &= \Big[1.38\,{}^{+0.14}_{-0.21}\big|_{\frac{m_c}{m_b}} \pm 0.15_{\rm CKM} \\
&\quad \pm 0.09_{\rm param.} \pm 0.05_{\rm scale}\Big] \cdot 10^{-5}, \\
\frac{\mathcal{B}[\bar{B} \to X_d\gamma]}{\mathcal{B}[\bar{B} \to X_s\gamma]} &= \Big[3.82\,{}^{+0.11}_{-0.18}\big|_{\frac{m_c}{m_b}} \pm 0.42_{\rm CKM} \\
&\quad \pm 0.08_{\rm param.} \pm 0.15_{\rm scale}\Big] \cdot 10^{-2},
\end{aligned} \tag{19}$$

where the errors in the ratio in Eq. (19) are dominated by CKM uncertainties. Similar numbers are found by a second analysis [114, 115]

$$\begin{aligned}
\langle \mathcal{B}(\bar{B} \to X_d\gamma)\rangle &\simeq 1.3 \cdot 10^{-5}, \\
\frac{\langle \mathcal{B}(\bar{B} \to X_d\gamma)\rangle}{\langle \mathcal{B}(\bar{B} \to X_s\gamma)\rangle} &= \frac{|\xi_t|^2}{|\lambda_t|^2} + \frac{D_u}{D_t}\,\frac{|\xi_u|^2}{|\lambda_t|^2} + \frac{D_r}{D_t}\,\frac{{\rm Re}(\xi_t^*\xi_u)}{|\lambda_t|^2}, \\
&\simeq 3.6 \cdot 10^{-2}\,.
\end{aligned} \tag{20}$$

Here $\langle \mathcal{B}(\bar{B} \to X_d\gamma)\rangle$ always denotes the charge-conjugate averaged branching ratio, $\lambda_i = V_{ib}V_{is}^*$ and $\xi_i = V_{ib}V_{id}^*$ are combinations of CKM elements, and the D_i are functions of m_t, m_b, m_c, μ_b, and α_s.

The SM predictions for the direct CP asymmetries

$$A_{\rm CP}^{b\to q\gamma} \equiv \frac{\Gamma[\bar{B} \to X_q\gamma] - \Gamma[B \to X_{\bar{q}}\gamma]}{\Gamma[\bar{B} \to X_q\gamma] + \Gamma[B \to X_{\bar{q}}\gamma]}$$

are [112, 113]

$$\begin{aligned}
A_{\rm CP}^{b\to s\gamma} &= \Big[0.44\,{}^{+0.15}_{-0.10}\big|_{\frac{m_c}{m_b}} \pm 0.03_{\rm CKM}\,{}^{+0.19}_{-0.09}\big|_{\rm scale}\Big], \% \\
A_{\rm CP}^{b\to d\gamma} &= \Big[-10.2\,{}^{+2.4}_{-3.7}\big|_{\frac{m_c}{m_b}} \pm 1.0_{\rm CKM}\,{}^{+2.1}_{-4.4}\big|_{\rm scale}\Big]\% \,.
\end{aligned}$$

The additional parametric uncertainties are subdominant. Again, a second analysis finds similar results [114, 115]

$$\begin{aligned}
A_{\rm CP}^{b\to s\gamma} &\simeq \frac{{\rm Im}(\lambda_t^*\lambda_u)\,D_i}{|\lambda_t|^2\,D_t} \sim 0.5\%, \\
A_{\rm CP}^{b\to d\gamma} &\simeq \frac{{\rm Im}(\xi_t^*\xi_u)\,D_i}{|\xi_t|^2\,D_t} \sim -13\%\,.
\end{aligned} \tag{21}$$

The radiative FCNC processes exhibit yet another interesting quantity, which can serve as a Null test of the SM, namely the unnormalized, untagged $\bar{B} \to X_{s+d}\,\gamma$ CP asymmetry. This quantity vanishes in the U-spin limit $m_s = m_d$ [116], and hence in this limit and for real Wilson coefficients one has

$$\begin{aligned}
&\big[\Gamma(\bar{B} \to X_s\,\gamma) - \Gamma(B \to X_{\bar{s}}\,\gamma)\big] \;+ \\
&\big[\Gamma(\bar{B} \to X_d\,\gamma) - \Gamma(B \to X_{\bar{d}}\,\gamma)\big] \;=\; 0.
\end{aligned} \tag{22}$$

The size of the untagged $\bar{B} \to X_{s+d}\,\gamma$ CP asymmetry is a measure of U-spin breaking. In the SM within the partonic contribution one finds [117, 118]

$$|\Delta\mathcal{B}(B \to X_s\gamma) + \Delta\mathcal{B}(B \to X_d\gamma)| \sim 1 \cdot 10^{-9}\,. \tag{23}$$

Power corrections beyond the leading partonic contribution are expected to be small, since U-spin breaking in $1/m_{b,c}^2$ corrections bring up a factor of m_s^2/m_b^2. This is also shown for the non-perturbative corrections to the u quark loops which scale like $\Lambda_{\rm QCD}/m_b$ [118]. We therefore conclude that any sizable value of the untagged $\bar{B} \to X_{s+d}\,\gamma$ *CP* asymmetry is a direct signal for NP.

The untagged $\bar{B} \to X_{s+d}\,\gamma$ *CP* asymmetry also offers the possibility for interesting analyses in NP models. For example, the experimental accuracy of the untagged CP asymmetry at the current B-factories is $\pm 3\%$, which allows one to distinguish between MFV and more general flavour models, where the untagged *CP* asymmetry can reach $\sim 10\%$ [113]. However, a distinction between MFV with and without flavour-blind phases not possible at existing B-factories, but within reach of a Super$B$ facility, see Fig. 10.

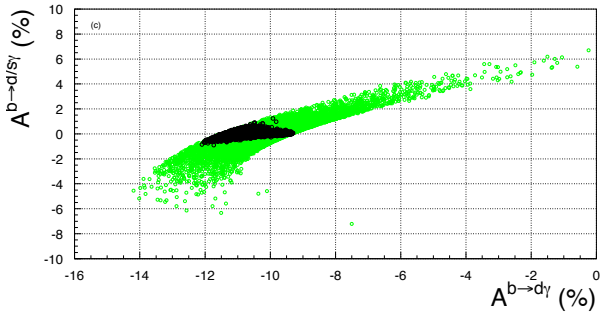

FIG. 10: Untagged rate asymmetry in MFV with flavour-blind phases with (black/dark) and without (green/light) neutron and electron EDM constraints imposed [113].

The inclusive rare decay $\bar{B} \to X_d\,\ell^+\ell^-$ offers, just as in the case of $b \to s$ transitions, a complementary test of the SM compared to $\bar{B} \to X_d\,\gamma$, since due to the three-body final state and the presence of the axial current the kinematic structure is richer. This results in three independent functions of the di-lepton invariant mass q^2, two of which are the differential branching ratio and the FBA [80]. Just as in the $b \to s$ case, one distinguishes several windows in q^2. The low-q^2 window $1 < q^2 < 6$ GeV^2 is dominated, due to the local OPE, by the quark-level decay and its perturbative corrections. The ρ, ω, and $\bar{c}c$ (J/ψ, ψ') resonances are cut out in this window, and the effect of their respective tails can be taken into account within the KS approach [119]. This way on-shell up-quark loops can

be avoided. A systematic analysis of power corrections would be desirable. The differential branching ratio integrated over the low-q^2 window is [109]

$$\mathcal{R}_{\rm quark} = \int_{0.05}^{0.25} d\hat{s}\, R_{\rm quark} = (4.75 \pm 0.25) \times 10^{-7}.$$

This number is without power corrections and without taking into account resonances. A very preliminary investigation of the feasibility of studying $\bar{B} \to X_d\, \ell^+\ell^-$ at Super$B$ looks promising.

The study of exclusive and inclusive rare semileptonic decays, $B \to X_{s,d}\ell^+\ell^-$, where $\ell^+\ell^-$ is either e^+e^- or $\mu^+\mu^-$, is an important task for a Super$B$ factory.

In the exclusive decays $B \to K\ell^+\ell^-$ and $B \to K^*\ell^+\ell^-$, both *BABAR* [120, 121] and Belle [122] measured branching fractions ($\mathcal{B}$), CP asymmetries ($\mathcal{A}_{CP}$), isospin asymmetries ($\mathcal{A}_I$), $\mu^+\mu^-/e^+e^-$ ratios ($\mathcal{R}_{K^{(*)}}$), the K^* longitudinal polarization ($\mathcal{F}_L$) and the lepton FBA ($\mathcal{A}_{FB}$) in several q^2 bins. *BABAR* [123] and Belle [124] also searched for $B \to \pi\ell^+\ell^-$ and $B \to \rho\ell^+\ell^-$. Both experiments measured partial branching fractions in the inclusive mode in several q^2 bins [96, 125], where $B \to X_s\ell^+\ell^-$ was approximated by a sum of 20 (36) exclusive final states in *BABAR* (Belle). *BABAR* is presently working on an update with the full data set using 28 final states. Here, the decay model uncertainty is reduced to 10%.

Another inclusive approach consists of reconstructing one B meson fully in an exclusive final state and looking for an $\ell^+\ell^-$ pair in the recoil. The advantage is that no assumptions have to be made on the $X_s\ell^+\ell^-$ final states, thus this is a true inclusive measurement. The disadvantage is that the B tagging reduces the total selection efficiency. Using both hadronic tags and semileptonic tags, the tagging efficiency can be up to 1.75%. The B reconstruction removes semileptonic backgrounds from the opposite B and from $D\bar{D}$. Additional requirements are necessary to remove backgrounds from B semileptonic cascade decays of the signal B. Residual semileptonic backgrounds can be subtracted bin-by-bin using an $e-\mu$ data sample. Furthermore, the $B \to X_d\ell^+\ell^-$ contribution also needs to be subtracted.

The best approach to $B \to K^*\ell^+\ell^-$ consists of a measurement of the full angular distribution in several q^2 bins. In the present $B \to K^*\ell^+\ell^-$ analyses, the one-dimensional angular distributions in $\cos\theta_K$ and $\cos\theta_\ell$ are used to extract $\mathcal{F}_L(q^2)$ and $\mathcal{A}_{FB}(q^2)$. In the SM $\mathcal{A}_{FB}$ crosses zero around 4.2 GeV^2/c^4 [103]. The ϕ distribution allows two additional asymmetries, $\mathcal{A}_{Im}(q^2)$ an interference between transverse and longitudinal components and $\mathcal{A}_T^{(2)}(q^2)$, an asymmetry between transverse and parallel components [126]. At Super$B$, we collect enough events to measure the full angular distribution and extract all its nine coefficients, which are functions of q^2 [126]. In addition, we have sufficient sensitivity to examine the $\cos\theta_\ell$ distribution for scalar and pseudoscalar contributions. In particular $B \to K\ell^+\ell^-$ is rather sensitive, since $\mathcal{A}_{FB}$ vanishes in the SM. In the inclusive analyses, we will explore the $\cos\theta_\ell$ angular distribution and determine the functions $H_T(q^2)$, $H_L(q^2)$ and $H_A(q^2)$ [80] in several q^2 bins.

Since the Super$B$ detector will be an improvement on *BABAR* detector, we focus on *BABAR* measurements and scale statistical errors to a luminosity of 75 ab^{-1} by $\sqrt{\mathcal{L}_{BABAR}/75\ ab^{-1}}$ in order to be conservative. For decay rates and rate asymmetries of exclusive modes, we use the *BABAR* publication [120]. For $\mathcal{F}_L(q^2)$ and $\mathcal{A}_{FB}(q^2)$ in $B \to K^*\ell^+\ell^-$, we use a recent study based on the total *BABAR* luminosity of $425 fb^{-1}$ assuming $\mathcal{B}(B \to K\ell^+\ell^-) = 0.48 \times 10^{-6}$ and $\mathcal{B}(B \to K^*\ell^+\ell^-) = 1.15 \times 10^{-6}$. The present statistical uncertainties of decay rates and rate asymmetries of the sum of exclusive decays are obtained from another recent *BABAR* study based on $425 fb^{-1}$ assuming $\mathcal{B}(B \to X_S\ell^+\ell^-) = 4.5 \times 10^{-6}$. The statistical uncertainty in the fully inclusive mode is obtained by scaling that in the sum of exclusive modes by the square root of the ratio of expected events in the two approaches. Since we have no studies on inclusive angular analyses yet, we base our estimates for $H_L(q^2)$ and $H_A(q^2)$ on the $\mathcal{F}_L(q^2)$ and $\mathcal{A}_{FB}(q^2)$ results measured in the $B \to K^*\ell^+\ell^-$ angular analysis.

Table VI shows event yields for the different decay channels at the *BABAR* luminosity of 425 fb^{-1} and extrapolations to 75 ab^{-1} for Super$B$. The statistical and systematic uncertainties of branching fractions, rate asymmetries and angular observables in different regions of q^2 for $B \to K\ell^+\ell^-$ and $B \to K^*\ell^+\ell^-$ at *BABAR* (425 fb^{-1}) and extrapolations at Super$B$ (75 ab^{-1}) are summarized in Table VII and Table VIII, respectively. Table IX shows estimates of statistical and systematic uncertainties of corresponding observables in the $B \to X_s\ell^+\ell^-$ analyses.

The systematic errors for observables in the exclusive modes are taken from the latest *BABAR* publications [120, 121], while the systematic error of the branching fraction in the sum of exclusive modes is estimated by adding in quadrature the individual contributions with updated values. For the cross feed, multivariate selection, and fitting systematics we assume 3%, 2% and 1.4%, respectively. These values are chosen after comparing systematic errors of the analysis of the sum of 20 exclusive modes [96] with those in the exclusive modes. This amounts to a total systematic error of 5.6% in the branching fraction. The systematic error of the total branching fraction of the fully inclusive mode is estimated by adding in quadrature

contributions from tagging, tracking, lepton identification, event selection, background parametrization, fitting, and total number of B mesons. For the present *BABAR* data set, we estimate a systematic error of 6%. The systematic errors of the partial branching fractions, rate asymmetries and angular observables are assumed to scale in a similar was as the total branching fraction in $B \to K^* \ell^+ \ell^-$.

At Super$B$, both exclusive and inclusive $b \to s\ell^+\ell^-$ modes will be measured with high precision. For example, for an integrated luminosity of 75 ab^{-1}, we expect to observe 8,200 selected $B \to K^* \ell^+ \ell^-$ signal events in the low q^2 region (< 8 GeV^2/c^4) and 5,500 selected signal events reconstructed fully inclusively with the recoil method. Thus, for both inclusive and exclusive decays we have sufficient statistics to measure the q^2 dependence of branching fractions and angular observables. For most observables, the statistical precision will be around one per cent or below. Thus, these measurements will be systematics limited. Reducing the q^2 region to 1 GeV^2/c^4 $< q^2 < 6$ GeV^2/c^4 yields an increase in the statistical uncertainty by a factor of 1.3 for rate asymmetries and by a factor of 1.38 for angular observables.

For $B \to \pi \ell^+ \ell^-$, we expect about 700 events in the entire q^2 region at 75 ab^{-1}. We find the same result whether we scale the results of a previous analysis or whether we adjust the $K\ell^+\ell^-$ results by $|V_{ts}/V_{td}|^2 = 0.206^2$ obtained from B_s and B_d mixing. Using the latter scaling for $K^*\ell^+\ell^-$ results, we expect about 800 $\rho\ell^+\ell^-$ signal events in the entire q^2 region at 75 ab^{-1}. Using the recoil method, we also expect a sizable sample for $B \to X_d \ell^+ \ell^-$ modes. From both exclusive and inclusive modes we can determine $|V_{td}/V_{ts}|$. Super$B$ should also be able to discover the exclusive modes $B \to K^+\tau^+\tau^-$and $B \to K^{*0}\tau^+\tau^-$. Thus, at Super$B$ there is a great potential to see NP at the order of $\mathcal{O}(0.1)$.

At the expected design luminosity of 2 fb^{-1} per year, the LHCb experiment expects to observe 4,000 $K^{*0}(\to K^+\pi^-)\mu^+\mu^-$ events with a background of 1,000 events in the q^2 region $4m_\mu^2 < q^2 <$ 9 GeV^2/c^4 [127]. This yields a large sample to perform a full angular analysis and determine the nine coefficients $I_i(q^2)$. In a recent study, LHCb focussed on the observables $\mathcal{A}_{FB}$, $\mathcal{F}_L$, $\mathcal{A}_{Im}$ and $\mathcal{A}_T^{(2)}$. For 10 fb^{-1}, integrated over the q^2 region 1 GeV^2/c^4 $< q^2 <$ 6 GeV^2/c^4, LHCb estimates statistical uncertainties of $\sigma_{\mathcal{A}_{FB}} = (+0.0047, -0.0050)$, $\sigma_{\mathcal{F}_L} = (0.0052, -0.0058)$, $\sigma_{\mathcal{A}_{Im}} = (+0.0060, -0.0057)$, and $\sigma_{\mathcal{A}^{(2)}{}_T} = (+0.095, -0.094)$, respectively. The zero crossing of $\mathcal{A}_{FB}$ is determined with a relative uncertainty of 4% at $q_0^2 = 4.33^{+0.18}_{-0.16}$ GeV^2/c^4. The LHCb errors are purely statistical. Systematic uncertainties have not been addressed and are expected to be larger than those in *BABAR*. In a toy study based on *BABAR* simulated events scaled to a luminosity to 75 ab^{-1}, we extract a relative statistical uncertainty of 9% for the zero crossing after fitting the q^2 dependence of $\mathcal{A}_{FB}(q^2)$ in the region of 2.75 GeV^2/c^4 to 5.75 GeV^2/c^4 with a linear shape. We think that further optimization of the angular fits is possible and that statistical errors may be further reduced.

CDF has presented a study of $B \to K^{*0}\mu^+\mu^-$ using 4.4 fb^{-1} of data [128]. For $q^2 < 8.68$ GeV^2/c^4 they observe 34.3 ± 6.7 events, yielding 780 events expected at 10 fb^{-1}, if the $b\bar{b}$ cross section at 14 TeV is a factor of ten higher than that at 2 TeV. For $\mathcal{A}_{FB}$ and $\mathcal{F}_L$ in the q^2 bin $q^2 < 4.3$ GeV^2/c^4, the statistical uncertainties of $(+0.31, -0.33)$ and $(+0.23, -0.24)$ at 4.4 fb^{-1} are reduced to ± 0.07 and ± 0.05, respectively at 10 fb^{-1}. The systematic errors at 4.4 fb^{-1} are 0.05 and 0.03, respectively. Thus, the extrapolated CDF yields are a factor of 5 lower than the LHCb simulation, while those in $\mathcal{A}_{FB}$ and $\mathcal{F}_L$ are factors of 14 and 8.3 higher, respectively.

4. $B \to X_{s/d}\ell^+\ell^-$ with a hadronic tag

It may be possible to study the process $B \to X_s\ell^+\ell^-$ (and maybe also $B \to X_d\ell^+\ell^-$, albeit with limited statistics) fully inclusively at Super$B$ using the hadronic tag reconstruction method. Although this technique has very low efficiency and hence can statistically limit the sensitivity of rare decay studies, it has a number of advantages. First, by selecting signal events using primarily information from the reconstructed B_{tag} and the di-lepton system, the X_s system can potentially be selected without substantial biases to the hadronic mass distribution. Even K_L modes are potentially accessible, regardless of whether the K_L interacts in the detector. Secondly, the tag reconstruction effectively eliminates the "irreducible" (in the un-tagged analysis) backgrounds from double-semileptonic $B\bar{B}$ decays and cascade $b \to c \to s$ semileptonic decays. The first of these is eliminated by the requirement of an exclusively reconstructed hadronic B meson accompanying the signal candidate, while the second is reduced based on missing energy considerations. Although this method still needs to be studied carefully with large background statistics in the context of the Super$B$ fast simulation, an initial study based on *BABAR* MC appears promising. Hadronic B decays are first reconstructed using the usual tag reconstruction method. These events are additionally required to possess a $\ell^+\ell^-$ ($\ell = e, \mu$) system, and all remaining detector activity in the event is defined to comprise the X_s hadronic system, and the combination of X_s with the di-lepton system is required to be kinematically consistent with a B meson recoiling against the reconstructed B_{tag}. Note that in

TABLE VI: Number of events for $B \to K\ell^+\ell^-$, $B \to K^*\ell^+\ell^-$, $B \to X_s\ell^+\ell^-$ via the sum of exclusive modes (SE) and $B \to X_s\ell^+\ell^-$ via the recoil method (RM) for luminosities of 425 fb^{-1} and 75 ab^{-1}. The signal yields are shown for the entire q^2 region, 0.1 GeV^2/c^4 $< q^2 <$ 7.84 GeV^2/c^4 and 1 GeV^2/c^4 $< q^2 <$ 6 GeV^2/c^4. Uncertainties in the yields are of the order of 20%.

	Number of events in 425 fb^{-1}			Expected number of events in 75 ab^{-1}		
Mode	all q^2	0.1–7.84	1–6	all q^2	0.1–7.84	1–6
$K\ell^+\ell^-$	90	42	26	15,900	7,340	4,600
$K^*\ell^+\ell^-$	110	46	24	19,400	8,200	4300
$X_s\ell^+\ell^-$ SL	270	171	101	47,500	30,000	17,900
$X_s\ell^+\ell^-$ RM	49	31	18	8,600	5,500	3250

TABLE VII: Present and extrapolated statistical and systematic uncertainties of the total branching fraction, partial branching fractions, *CP* asymmetries, isospin asymmetries, lepton flavor ratio for $B \to K\ell^+\ell^-$ after combining e^+e^- and $\mu^+\mu^-$ modes as well as K^+ and K^0_S modes.

		BABAR (425 fb^{-1})		Super$B$ (75 ab^{-1})	
Observable	q^2 region [GeV^2/c^4]	Stat.	Sys.	Stat.	Sys.
$\sigma\mathcal{B}/\mathcal{B}$	all	0.175	0.05	0.011	0.025-0.035
$\sigma\mathcal{B}/\mathcal{B}$	0.1–7.02	0.20	0.044	0.012	0.022-0.035
$\sigma\mathcal{B}/\mathcal{B}$	10.24–12.96 and $>$ 14.06	0.27	0.052	0.017	0.026-0.039
$\mathcal{R}_K$	all	0.34	0.05	0.021	0.025-0.038
$\mathcal{A}_{CP}$	all	0.18	0.01	0.012	0.008-0.01
$\mathcal{A}_I$	0.1–7.02	0.56	0.05	0.034	0.025-0.035

TABLE VIII: Present and extrapolated statistical and systematic uncertainties of the total branching fraction, partial branching fractions, *CP* asymmetries, isospin asymmetries, lepton flavor ratio, longitudinal polarization and lepton FBA for $B \to K^*\ell^+\ell^-$ after combining e^+e^- and $\mu^+\mu^-$ modes as well as K^{*+} and K^{*0} modes.

		BABAR (425 fb^{-1})		Super$B$ (75 ab^{-1})	
Observable	q^2 region [GeV^2/c^4]	Stat.	Sys.	Stat.	Sys.
$\sigma\mathcal{B}/\mathcal{B}$	all	0.162	0.063	0.01	0.032-0.048
$\sigma\mathcal{B}/\mathcal{B}$	0.1–7.02	0.23	0.070	0.014	0.035-0.053
$\sigma\mathcal{B}/\mathcal{B}$	10.24–12.96 and $>$ 14.06	0.24	0.071	0.015	0.036-0.054
$\mathcal{R}_{K*}$	all	0.34	0.07	0.02	0.035-0.048
$\mathcal{A}_{CP}$	all	0.15	0.01	0.009	0.008-0.01
$\mathcal{A}_I$	0.1–7.02	0.17	0.03	0.01	0.015-0.023
$\mathcal{F}_L$	0.1–4	0.15	0.04	0.011	0.02-0.03
$\mathcal{F}_L$	4–7.84	0.14	0.04	0.011	0.02-0.03
$\mathcal{A}_{FB}$	0.1–4	0.14	0.05	0.011	0.025-0.038
$\mathcal{A}_{FB}$	4–7.84	0.14	0.05	0.011	0.025-0.038

this case we have not only the usual ΔE and m_{ES} variables at our disposal, but also the angle between the 3-momenta of the reconstructed tag and signal B candidates. Vetoes are imposed on the $\ell^+\ell^-$ invariant mass to remove long distance contributions from J/Ψ and $\Psi(2S)$, and the mass of the hadronic system X_s is computed directly from the combination of the B_{tag} 4-vector and the $\ell^+\ell^-$ 4-vector (i.e. without any direct reconstruction of the hadronic system itself). Fig. 11 (top) shows the reconstructed hadronic mass for exclusive $B^+ \to K^+\mu^+\mu^-$ (low mass region) and inclusive $B^+ \to X_s\mu^+\mu^-$ (region above $m_{X_s} = 1$GeV) signal MC. The expected background is shown in the lower plot. Both signal and background plots are normalized

TABLE IX: Present and extrapolated statistical and systematic uncertainties of the total branching fraction, partial branching fractions, *CP* asymmetries, isospin asymmetries, lepton flavor ratio, and angular observables for $B \to X_s \ell^+ \ell^-$. The first two columns show the results for the sum of exclusive modes (SE), the second two columns those for the recoil method (RM), respectively. The sum of exclusive modes including 28 final states has an additional uncertainty of $\sim 10\%$ from the decay model.

		BABAR (425 fb^{-1})				Super$B$ (75 ab^{-1})			
Observable	q^2 region [GeV^2/c^4]	Stat. SE	Sys. SE	Stat. RM	Sys. RM	Stat. SE	Sys. SE	Stat. RM	Sys. RM
$\sigma\mathcal{B}/\mathcal{B}$	all	0.11	0.056	0.26	0.06	0.008	0.03-0.05	0.019	0.03-0.05
$\sigma\mathcal{B}/\mathcal{B}$	0.1–1	0.29	0.07	0.69	0.07	0.022	0.04-0.06	0.052	0.04-0.06
$\sigma\mathcal{B}/\mathcal{B}$	1–4	0.23	0.06	0.53	0.06	0.017	0.03-0.05	0.040	0.03-0.05
$\sigma\mathcal{B}/\mathcal{B}$	4–7.84	0.18	0.06	0.43	0.06	0.014	0.03-0.05	0.032	0.03-0.05
$\sigma\mathcal{B}/\mathcal{B}$	10.24–12.96	0.31	0.07	0.73	0.07	0.024	0.04-0.06	0.055	0.04-0.06
$\sigma\mathcal{B}/\mathcal{B}$	>14.06	0.29	0.07	0.69	0.07	0.022	0.04-0.06	0.052	0.04-0.06
$\mathcal{R}_{X_s}$	all	0.21	0.06	0.50	0.06	0.016	0.03-0.05	0.038	0.03-0.05
$\mathcal{R}_{X_s}$	0.1–7.84	0.25	0.06	0.58	0.06	0.019	0.03-0.05	0.044	0.03-0.05
$\mathcal{A}_{CP}$	all	0.06	0.01	0.14	0.01	0.004	0.005-0.008	0.011	0.005-0.008
$\mathcal{A}_{CP}$	0.1–7,84	0.07	0.01	0.16	0.01	0.005	0.005-0.008	0.012	0.005-0.008
$\mathcal{A}_I$	all	0.05	0.06	0.12	0.06	0.004	0.03-0.05	0.009	0.03-0.05
$\mathcal{A}_I$	0.1–7.84	0.06	0.06	0.14	0.06	0.005	0.03-0.05	0.011	0.03-0.05
$\mathcal{H}_L$	0.1–1	0.17	0.04	0.40	0.04	0.013	0.02-0.03	0.030	0.02-0.03
$\mathcal{H}_L$	1–4	0.17	0.04	0.40	0.04	0.013	0.02-0.03	0.030	0.02-0.03
$\mathcal{H}_L$	4–7.84	0.13	0.04	0.27	0.04	0.009	0.02-0.03	0.021	0.02-0.03
$\mathcal{H}_A$	0.1–1	0.22	0.06	0.51	0.06	0.016	0.03-0.05	0.039	0.03-0.05
$\mathcal{H}_A$	1–4	0.22	0.06	0.51	0.06	0.016	0.03-0.05	0.039	0.03-0.05
$\mathcal{H}_A$	4–7.84	0.15	0.06	0.35	0.06	0.011	0.03-0.05	0.026	0.03-0.05

to 75 ab^{-1}, however the background statistics represent only about 1 ab^{-1}. The low mass region is essentially background free, while in the higher mass region the background is predominantly from B^+B^- events in which the two muon candidates originate from the same B. This remaining background can then be further reduced through an appropriate choice of muon PID (and vertexing, in the case of the corresponding e^+e^- modes), and more stringent missing energy requirements on the signal B candidate. More detailed studies within the Super$B$ simulation framework are needed to establish an expected signal significance, but the method shows promise for a fully inclusive determination of $B \to X_s \ell^+ \ell^-$ branching fractions and angular asymmetries. This method can also in principle be extended to include $B \to X_d \ell^+ \ell^-$ simply by applying a kaon tag/veto to the hadronic system.

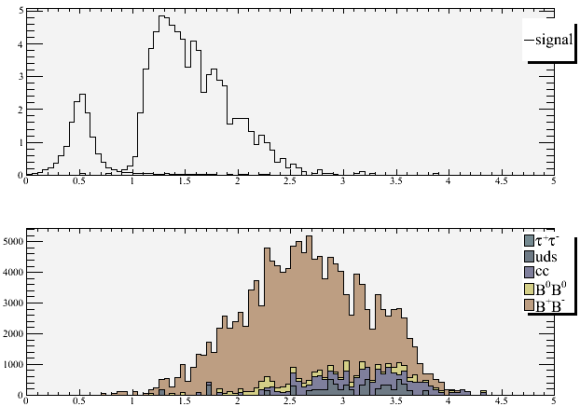

FIG. 11: The (top) reconstructed hadronic mass for exclusive $B^+ \to K^+ \mu^+ \mu^-$ (low mass region) and inclusive $B^+ \to X_s \mu^+ \mu^-$ (region above $m_{X_s} = 1$GeV) signal MC. The expected background is shown in the bottom plot.

C. Radiative penguins

1. *Inclusive $b \to s\gamma$*

In the B factory era, $\bar{B} \to X_s\gamma$ has been an extremely important channel for searching for NP and for constraining new models that go beyond the SM. The inclusive branching fraction for this decay is not small ($\sim 3 \times 10^{-4}$) and several measurements have been made at *BABAR* and Belle during the B-factory era [129–132]. Currently the experimental world-average [133] has a total uncertainty of 7%:

$$B(\bar{B} \to X_s\gamma) = (3.52 \pm 0.23 \pm 0.09) \times 10^{-4}. \quad (24)$$

This branching fraction is for $E_\gamma > 1.6$ GeV, where theoretical models have been used to extrapolate from the experimental photon energy cut, typically ~ 1.9 GeV, down to 1.6 GeV. The uncertainties quoted are experimental (statistical plus systematic) and model uncertainty inherent in the extrapolation.

At the same time, theorists have carried the calculation of the branching fraction to NNLO, resulting in a quite precise theoretical calculation of $B(\bar{B} \to X_s\gamma)$ within the SM [63]:

$$B(\bar{B} \to X_s\gamma) = (3.15 \pm 0.23) \times 10^{-4}, \quad (25)$$

which also has a total error of 7%. The experimental and theoretical values are in reasonable agreement.

Part of the experimental challenge has been to make the most inclusive measurements possible, in order to compare them to the inclusive theoretical calculation without introducing excessive model dependence. The earliest measurements used the "sum of exclusive modes" technique, whereby a large number of individual exclusive decay channels are fully reconstructed. This approach is easier experimentally, but the large systematic uncertainties associated with the unseen modes will make this technique obsolete at the Super$B$.

The alternative approach is the fully inclusive method, which attempts to make no requirements whatsoever on the X_s system, thereby making the branching fraction measurement fully inclusive. The one exception is making a cut on photon energy (which is equivalent to selecting on $m(X_s)$), although much effort is devoted to keeping the photon minimum energy as low as possible.

The fully inclusive approach can adopt the recoil tagging technique to identify the "other" B in the event *i.e.* the B_{tag} from the $\Upsilon(4S)$ (as described above) in order to reduce the large continuum background. At the B-factories, the lepton tagging method, which has an efficiency of roughly ten times the hadronic tag efficiency, has proved more useful. However, at the Super$B$ factory, where there will be a very large number of reconstructed hadronic tags, this method will make an important contribution to the measurement of $B(\bar{B} \to X_s\gamma)$.

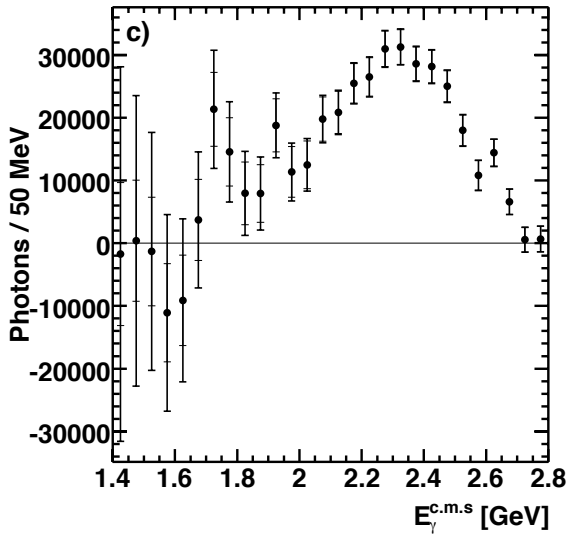

FIG. 12: Efficiency-corrected photon spectrum for $\bar{B} \to X_s\gamma$ decays. Taken from reference [129].

Figure 12 shows the efficiency-corrected photon spectrum from Belle's recent measurement. This fully inclusive analysis is based on combining a lepton-tagged sample and an untagged sample. The large uncertainties visible at lower energies are caused by the systematic uncertainty in the $B\bar{B}$ background subtraction.

At the Super$B$ the uncertainty on the branching fraction measurement will be dominated by the systematic error — we estimate that a systematic error of 3% will be achievable at Super$B$.

NP can also modify the direct CP asymmetries of $\bar{B} \to X_s\gamma$ decays and these asymmetries have been measured at the B-factories, although with still large statistical errors. The increased statistics available at the Super$B$ factory will make these CP asymmetries important tools in the search for NP. Experimentally, different analysis approaches measure different asymmetries.

The fully inclusive analyses do not distinguish the Cabibbo-suppressed process $\bar{B} \to X_d\gamma$ from $\bar{B} \to X_s\gamma$, and so measures the asymmetry of the sum: $A_{CP}(\bar{B} \to X_{s+d}\gamma)$. The sum of exclusive-modes analysis does measure $A_{CP}(\bar{B} \to X_s\gamma)$ and with good precision, since many of the systematic effects cancel in the asymmetry ratio. However, since this measurement is not truly inclusive (typically about 50% of the inclusive rate is reconstructed), there may be problems interpreting the result and comparing to the SM theoretical calculation for the inclusive process. The most precise

TABLE X: Selected experimental results on A_{CP} from the B-factories. The first uncertainty listed is statistical, the second systematic.

Quantity	Result
$A_{CP}(\bar{B} \to X_s\gamma)$	$-0.011 \pm 0.030 \pm 0.014$ [134]
	$0.002 \pm 0.050 \pm 0.030$ [135]
$A_{CP}(B \to X_{s+d}\gamma)$	$-0.11 \pm 0.12 \pm 0.02$ [131]
	$0.10 \pm 0.18 \pm 0.05$ [132]
$A_{CP}(B \to K^*\gamma)$	$-0.003 \pm 0.017 \pm 0.007$ [136]

A_{CP} measurements to date have been made with the exclusive channel $B \to K^*\gamma$.

Selected experimental results for these asymmetry measurements are reported in Table X. The SM predictions for each of these quantities is quite close to zero, so any measurement of a substantial asymmetry would be an indication of NP [113, 137, 138]. We note that currently the experimental measurements have small systematic errors, making them very attractive for the high-statistics environment of Super$B$.

Another quantity related to the $b \to s\gamma$ channel is the time-dependent CP asymmetry in the decay $B^0 \to K_s\pi^0\gamma$. In the SM the photon is this decay has, to order $\sim m_s/m_b$, definite helicity: $b \to s\gamma_L$ and $\bar{b} \to \bar{s}\gamma_R$. This results in quite small CP-violation in this decay, with the SM expectation being $S_{K_s\pi^0\gamma} \approx 0.02$ [139, 140]. A larger observed value would be an indication of NP. The latest *BABAR* measurements has found $S_{K_s\pi^0\gamma} = -0.03 \pm 0.29 \pm 0.03$ [141]. Again, we remark that at Super$B$ we can expect a reduction in the statistical error of roughly a factor of 10, making this measurement, with its small systematic uncertainty, a powerful probe of physics beyond the SM at the Super$B$ factory.

It is interesting to compare what LHCb will be doing with the $b \to s\gamma$ channel in the next few years. Most LHCb studies on radiative penguin decays thus far have focused on the related channel $B \to K^{(*)}\mu^+\mu^-$. They will not be able to perform an inclusive measurement, and so have focused on a few exclusive analyses such as time-dependent CP asymmetries in $B \to K^*\gamma$ and its B_s analog, $B_s \to \phi\gamma$. This last is of particular interest since it cannot be done at Super$B$ (assuming that only a relatively small number of B_s mesons will be produced there). An LHCb MC based study reports that with an integrated luminosity of 2 fb^{-1}, some 11,000 $B_s \to \phi\gamma$ will be reconstructed. With this sample, a precision of 0.2 on $\mathcal{A}^\Delta$, the relevant CP-violating parameter for this mode, is expected [142].

In summary, the radiative penguin process $\bar{B} \to X_s\gamma$ has played a crucial role in searching for physics beyond the SM at the B factories. This channel will continue to be important at the Super$B$ factory, where the increased statistics will quickly yield a branching fraction measurement with a total uncertainty close to 3%. Furthermore, the large Super$B$ data sample will make possible precision measurements of direct CP-violating asymmetries for inclusive $\bar{B} \to X_s\gamma$, as well as time-dependent CP-violation in the exclusive mode $B \to K_s\pi^0\gamma$.

2. *Exclusive $b \to s\gamma$*

3. $b \to d\gamma$

4. $B_d \to \gamma\gamma$

5. *Triple product asymmetries with $B \to K^{**}\gamma$*

D. CKM Side Measurements

1. Inclusive Determination of $|V_{ub}|$

The precise determination of $|V_{ub}|$ is an essential ingredient in the determination of the CKM matrix parameters. As the precise study of inclusive decays is a unique feature of Super$B$, it will be important to make maximal use of the data to extract $|V_{ub}|$ with small but robust uncertainties. The main experimental and theoretical challenge in the inclusive $|V_{ub}|$ determination is the background from $B \to X_c \ell \bar{\nu}$ decays which is roughly 50 times larger than the signal. At Super$B$ the experimental uncertainties will be reduced compared to the existing measurements at the B factories. In addition to reduced statistical uncertainties, the much larger statistics will also lead to reduced systematic uncertainties by allowing for cleaner data samples and a better understanding of the $\bar{B} \to X_c \ell \bar{\nu}$ background. For the theoretical uncertainties, one must distinguish between uncertainties due to higher-order perturbative and power corrections and parametric uncertainties due to input parameters. Currently, the dominant theoretical uncertainties are parametric due to m_b and the leading B-meson shape function, and these can be reduced by more precise measurements as explained below. The current approaches [143–145] heavily rely on modeling the shape function, and as a result the present uncertainty in the inclusive $|V_{ub}|$ determination [146] has been the subject of intense debate.

Measurements near the phase space boundary are experimentally cleaner with less contamination from $\bar{B} \to X_c \ell \bar{\nu}$, thus allowing for reduced systematic uncertainties, but are more sensitive to m_b and shape-function effects, leading to increased theoretical uncertainties. Hence, the choice of kinematic cuts is a trade-off between experimental and theoretical uncertainties, and so there is no unique optimal region of phase space from which to extract $|V_{ub}|$. Even if the kinematic cuts can be relaxed, at the expense of increased systematic uncertainties, to the point where there is no shape-function sensitivity in the theory, the most sensitivity to $|V_{ub}|$ in the data still comes from the shape-function region near the endpoint. In addition, one should recall that the Monte Carlo (MC) signal model requires the knowledge of the shape function as well.

Ultimately, the best determination of $|V_{ub}|$ with the smallest uncertainty might be achieved by performing a combined fit to all available measurements that simultaneously determines $|V_{ub}|$ and the required inputs, such as m_b and the leading shape function, as proposed in Ref. [147]. This follows the same strategy successfully employed in the inclusive determination of $|V_{cb}|$. It allows for the combination of different measurements with a consistent treatment of correlated uncertainties in measurements and input parameters. Moreover, it is straightforward to consistently include additional constraints on m_b (*e.g.*from the $\bar{B} \to X_c \ell \bar{\nu}$ fits) and the shape function, *e.g.*from the measured $\bar{B} \to X_s \gamma$ photon energy spectrum. Finally, the goodness of the fit itself provides an important test of the underlying theory.

Experimentally this strategy requires measurements of $\bar{B} \to X_u \ell \bar{\nu}$ decay spectra, which are already possible with the current data sets [148–150], and will be possible with increased precision at Super$B$. In the fit, the normalization of the spectra determines the value of $|V_{ub}|$, while their shape determines m_b and the shape function. Hence, in this way the increased statistics at Super$B$ is effectively utilized to also reduce the dominant theoretical uncertainties. Theoretically, the implementation of such a fit is complicated by the fact that one is fitting a function (rather than a few numbers as is the case for $|V_{cb}|$). To obtain small but reliable shape function uncertainties, it is desirable to include as much perturbative information on the shape function as possible, but at the same time have a model-independent treatment of its nonperturbative content. This can be achieved for instance using the approach of Ref. [147] which we now briefly outline.

First, the shape function $S(\omega, \mu)$ is factorized as

$$S(\omega, \mu_\Lambda) = \int dk \, \widehat{C}(\omega - k, \mu_\Lambda) \widehat{F}(k) \,, \qquad (26)$$

where $\widehat{C}$ is computed in perturbation theory and is known at the two loop level [151, 152], while $\widehat{F}(k)$ is a purely non-perturbative function to be extracted from data. Given $\widehat{F}(k)$, the shape function can be obtained from Eq. (26) order by order in perturbation theory and the perturbative uncertainty can be estimated by varying the scale μ, as illustrated in Fig. 13.

Next, to extract $\widehat{F}(k)$ from data in a model-independent way, it is expanded in a complete set of basis functions $\{f_n(k)\}$ that are designed to converge quickly for functions consistent with confinement,

$$\widehat{F}(k) = \left| \sum_{n=0}^{\infty} c_n f_n(k) \right|^2 . \qquad (27)$$

Here, the basis coefficients c_n are the unknown fit parameters. In practice, the series has to be truncated after a certain number of terms depending on the precision of the data. This results in a small residual model uncertainty, which can be studied systematically, *e.g.*by varying the number of coefficients, and decreases with increasing experimental precision.

Given Eq. (27), the i^{th} experimentally measured bin, Γ^i, is calculated as

$$\Gamma^i = |V_{ub}|^2 \sum_{m,n} c_m \, c_n \, \Gamma^i_{mn} \,, \qquad (28)$$

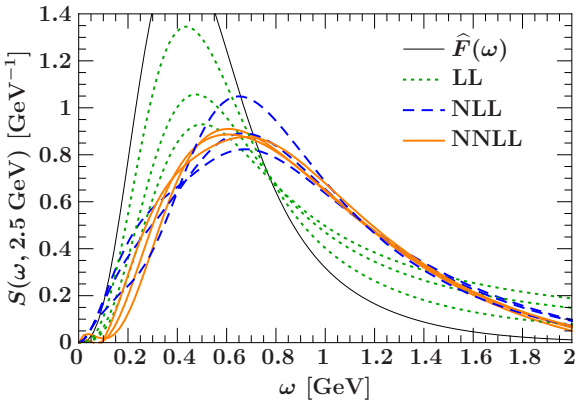

FIG. 13: The shape function $S(\omega,\mu)$ obtained by evaluating Eq. (26) at a low scale μ_Λ and RG evolving the result to the common scale $\mu = 2.5\,\mathrm{GeV}$. The three curves at each order correspond to the three values $\mu_\Lambda = \{1.1, 1.3, 1.8\}\,\mathrm{GeV}$. The solid black curve shows the assumed input function $\widehat{F}(k)$.

where Γ^i_{mn} is the contribution to Γ^i from the product of basis functions $f_m(k)f_n(k)$ in Eq. (27), which can be computed in advance. Hence, one simply has to fit polynomials of the basis coefficients c_n to the experimental measurements. Measurements of the $\bar{B} \to X_s\gamma$ photon energy spectrum are included in an analogous way. In addition, known constraints on the moments of $\widehat{F}(k)$ are included as additional constraints on the basis coefficients. For example the 0th and 1st moments are

$$1 = \sum_n c_n^2\,, \text{ and } m_B - \widehat{m}_b = \sum_{m,n} M^1_{mn} c_m c_n\,, \qquad (29)$$

where M^1_{mn} is the first moment of $f_m(k)f_n(k)$. In this way, existing information on $\widehat{m}_b$ can be included in the fit (the hat indicates a suitable short-distance scheme). The above combined fit approach will be key to push the precision of the inclusive $|V_{ub}|$ determination at Super$B$ below the 5% level. It makes maximal use of the increased data set by providing a rigorous treatment of uncertainties, provides tests for the theory, and yields an improved determination of m_b and the leading shape function. With sufficient data and measurements of different spectra, the same methods can also be used to reduce uncertainties due to subleading shape functions. A precise knowledge of leading and subleading shape functions is also crucial for a clean theoretical interpretation of measurements of the inclusive radiative decays $\bar{B} \to X_s\gamma$ and $\bar{B} \to X_s\ell^+\ell^-$.

2. *Inclusive Determination of $|V_{cb}|$*

The determination of $|V_{cb}|$ from inclusive semi-leptonic $b \to c$ transitions relies on the heavy quark expansion (HQE), resulting in an expansion in inverse powers of m_b and m_c. In the meantime, the methodology is in a very mature state, leading finally to a theoretical uncertainty as low as 1% in V_{cb} [153]. At Super$B$ this will be the limiting factor, since the large number of available events will reduce the experimental uncertainty to a negligible level.

The extraction of $|V_{cb}|$ relies on the HQE for the total rate, which takes the schematic form

$$\Gamma = \frac{G_F^2 m_b^5}{192\pi^3}|V_{cb}|^2 \qquad (30)$$
$$\left[f_0 + \left(\frac{\Lambda_{\rm QCD}}{m_b}\right)^2 f_2 + \left(\frac{\Lambda_{\rm QCD}}{m_b}\right)^3 f_3 + \left(\frac{\Lambda_{\rm QCD}}{m_b}\right)^4 f_4\right.$$
$$+ f_5\left(a_0\left(\frac{\Lambda_{\rm QCD}}{m_b}\right)^5 + a_2\left(\frac{\Lambda_{\rm QCD}}{m_b}\right)^3\left(\frac{\Lambda_{\rm QCD}}{m_c}\right)^2\right)$$
$$\left. + \ldots + f_7\left(\frac{\Lambda_{\rm QCD}}{m_b}\right)^3\left(\frac{\Lambda_{\rm QCD}}{m_c}\right)^4 \cdots\right],$$

where the f_i and a_i are functions of m_b/m_c which are - aside from logarithms $\ln(m_b/m_c)$ - regular as $m_c \to 0$.

In order to obtain a precise determination of $|V_{cb}|$ one has to control the following inputs:

1. On the first sight there is a strong dependence on the b quark mass due to the m_b^5 factor. However, the real dependence is weaker due to the presence of the charm mass m_c. In fact, the semi-leptonic decays depend roughly only on $m_b - 0.6\,m_c$, where this difference can be determined from the moments of the decay spectra of $b \to c$ semi-leptonic transitions with a sufficient accuracy.

2. QCD radiative corrections are taken into account up to and including α_s^2 terms [154, 155]. These corrections are under reasonable control provided a suitable scheme for the quark masses is used, in which the bulk part of the radiative corrections has been absorbed into the quark masses. Mainly used are the "kinetic scheme" [156] and the "1S scheme" [157], both of which yield comparably small uncertainties.

3. The non-perturbative inputs are given by local forward matrix elements of operators, which are calculated from the HQE. The quantity f_0 does not have any hadronic matrix element and is simply the result of the parton model calculation; f_0 is calculated including the complete α_s corrections. The current fits include f_2 and f_3, where

f_2 depends on

$$2M_b\mu_\pi^2 = \langle B|\bar{b}(i\vec{D})^2 b|B\rangle, \quad (31)$$
$$2M_b\mu_G^2 = \langle B|\bar{b}(\vec{\sigma}\cdot\vec{B})b|B\rangle, \quad (32)$$

where $\vec{B}$ denotes the chromomagnetic field inside the B meson, while f_3 depends on

$$2M_b\rho_D^3 = \langle B|\bar{b}\vec{D}\cdot\vec{E}b|B\rangle, \quad (33)$$
$$2M_b\rho_{LS}^3 = \langle B|\bar{b}(\vec{\sigma}\cdot(\vec{D}\times\vec{E}))b|B\rangle. \quad (34)$$

These matrix elements have to be fitted from the data. In particular, suitably chosen moments of the lepton energy, the hadronic energy and the hadronic mass spectra are sensitive to these matrix elements [133, 158].

4. QCD corrections to the subleading terms f_2, f_3, ... are only partially known. Up to now only corrections of order $\alpha_s\mu_\pi^2/m_b^2$ are calculated [159] and not yet included in the fit.

The perspectives for a further theoretical improvement are quite limited and depend on the following points

- Currently the leading element missing in the theoretical analysis is the calculation of the corrections of order $\alpha_s\mu_G^2/m_b^2$, which would complete our knowledge of the α_s/m_b^2 terms.
- A detailed consideration of the various quark mass determinations has to be performed in order to improve the control over the uncertainties related to the quark-mass input. Currently the quark masses are taken from B decays, which turn out to be consistent with determinations from e^+e^- threshold data. However, the uncertainties have to be scrutinized carefully.
- The number of non-perturbative parameters proliferates drastically, i.e. f_4 already depends on 9, f_5 on 18 and f_6 on 72 unknown matrix elements. The ability to extract this information from data remains limited even at Super$B$, in which case a calculation of these matrix elements would be needed; however, the perspectives to get a reliable calculation is also very limited.

In conclusion, with the current theoretical technology a relative theoretical uncertainty of 1% may be reached in this determination on $|V_{cb}|$. The current total uncertainty is roughly twice as large due to the experimental error; at a Super$B$ the experimental error will shrink considerably, but from todays perspective there is a brick wall at the level of 1%.

3. $|V_{td}|/|V_{ts}|$

TO COMPLETE ...

E. *CP* Violation

1. Introduction/Formalism

TO COMPLETE ...: intention is to review the formalism for a time-dependent analysis, and to include in general $\Delta\Gamma \neq 0$ as a serious issue to be addressed from day one.

2. Theoretical uncertainties

F. Theoretical uncertainties in the prediction of CP Asymmetries

The interpretation of the precise data on the time-dependent CP asymmetries in terms of the CKM parameters requires a reasonable control over the hadronic matrix elements. In particular, the ratio of the penguin versus the tree contribution has to be known from the theoretical side in order to turn the measurements of CP asymmetries into a test of the standard model. In the following we shall discuss this issue using the "golden mode" $B \to J/\psi K_s$ as an example.

Explicitly, the typical amplitude for a non-leptonic two-body decay can be written as

$$A(B^0 \to f) = \mathcal{A}\left[1 + r_f\, e^{i\delta_f}\, e^{i\theta_f}\right] \quad (35)$$

where usually $\mathcal{A}$ is the tree amplitude and r_f denotes the modulus of the penguin-over-tree ratio, which has a strong phase θ_f. The weak phase δ_f is in the cases at hand the CKM angle γ, while the modulus of the CKM factors is absorbed into r_f. The observables C^f and S^f can be expressed as

$$C^f = -2r_f \sin\theta_f \sin\delta_f \quad (36)$$
$$S^f = \sin\phi + 2r_f\cos\theta_f \sin(\phi+\delta_f) + r_f^2 \sin(\phi+2\delta_f) \quad (37)$$

where ϕ is the mixing phase stemming from the $\Delta B = 2$ interaction.

The key issue in the theoretical understanding of CP asymmetries is the ratio r_f, which of the "gold-plated modes" is heavily CKM supressed. However, at the precision of a Super-Flavour Factory even a small r_f will be observable and hence relevant for the analysis. In the following we give a short overview over the relevant theoretical approaches.

1. Partonic Calculation

The suggestion to estimate r_f is in fact quite old; it has been proposed originally by Bander, Silverman and Soni [160] and has been applied more recently to $B \to J/\psi K_s$ in [161].

Aside from the corrections to r_f one has also a contribution to the $\Delta B = 2$ interaction coming from internal up and charm quarks. Due to the GIM mechanism these contributions are suppressed by a factor m_c^2/M_W^2, but contain large logarithm $\ln\left(m_c^2/M_W^2\right)$. The total contribution from this source can be calculated reliably and turns out to be very small

$$\Delta\phi_d \approx -2\,\frac{m_c^2}{m_t^2}\,\ln\left(\frac{m_c^2}{M_W^2}\right) \approx -4\times 10^{-4}\,. \qquad (38)$$

A more severe problem is the estimate of the penguin contribution r_f. According to [160] we calculate the diagrams shown in fig. 14 which yields a contribution to the "effective interaction" of the form

$$\mathcal{H}_{\rm eff}^{\rm Peng.}(b\to c\bar{c}s) = -\frac{G_F}{\sqrt{2}}\left\{\frac{\alpha}{3\pi}\,(\bar{s}b)_{V-A}\,(\bar{c}c)_V \qquad (39)\right.$$
$$\left.+\frac{\alpha_s(k^2)}{3\pi}\,(\bar{s}T^a b)_{V-A}\,(\bar{c}T^a c)_V\right\}\left(\frac{5}{3}-\ln\left(\frac{k^2}{\mu^2}\right)+i\pi\right)$$

The matrix elements that appear in this expression can be estimated from the rate for $B \to J/\psi K_s$; in particular, the color-octet matrix element can be obtained from the non-factorizable contribution to this decay.

FIG. 14: Diagrams for the perturbative estimate of r_f.

The problem with expression (39) is that two parameters appear which have to be fixed. On one hand there is the scale k^2 of α_s the natural value of which is $k^2 = M_{J/\psi}^2$ on the other hand there is a dependence on the renormalization point μ, which we set to $\mu = m_b$. These choices are ambiguous, reflecting the fact that there are substantial uncertainties in this approach.

Inserting the numbers and taking into account the date from the rate of $B \to J/\psi K_s$, the authors of [161] obtain ($\phi = 2\beta$ in the standard model)

$$S(J/\psi\,K_S) = (\sin 2\beta)_0 - (2.16\pm 2.23)\times 10^{-4} \qquad (40)$$
$$C(J/\psi\,K_S) = (5.0\pm 3.8)\times 10^{-4} \qquad (41)$$

where the uncertainties are only the ones due to the extraction of the matrix elements from the rate of $B \to J/\psi K_s$.

Although this estimate suffers from substantial uncertainties, the conclusion form this calculation is that the standard contribution to r_f in case of $B \to J/\psi K_s$ is too small to matter even at the precision level of a super-flavour factory. However, in many other circumstances (such as e.g. perturbative calculations of form factors) it is observed that the perturbative approach tends to underestimate the true effects, sometimes even dramatically.

2. Hadronic Calculation

A different ansatz to estimate r_f has been proposed by Gronau and Rosner [162]. Here the backscattering of the quarks $\bar{u}u \to \bar{c}c$ is estimated by inserting hadronic intermediate states. Denoting the T-matrix for he weak interactions with T and the strong scattering with S_0, one obtains to leading order in the weak interactions

$$T = S_0 T S_0 \qquad (42)$$

This yields for the $\bar{u}u \to \bar{c}c$ backscattering

$$\langle J/\psi K^0|T^u|B\rangle = \sum_f \langle J/\psi K^0|S_0|f\rangle\langle f|T^u|B\rangle \qquad (43)$$

by inserting a complete set of states. Here T^u is the $b \to s\bar{u}u$ penguin contribution, and we now need an estimate of $\langle f|T^u|B\rangle$ for $f = K^*\pi, K^{**}\pi, ...$

This estimate is obtained by applying the same reasoning to the T^c piece of T, which corresponds to the tree contribution $b \to s\bar{c}c$.

$$\langle f|T^c|B\rangle = \sum_k \langle f|S_0|k\rangle\langle k|T^c|B\rangle \qquad (44)$$

where we inserted again a complete set of states.

If we saturate the sum by a single state, one may set up the inequality

$$|\langle f|T|B\rangle| \geq |\langle f|S_0|D^*D_s\rangle|\,|\langle D^*D_s|T|B\rangle| \qquad (45)$$

which leads to [162]

$$\xi_f \equiv \frac{|\langle J/\psi K^0|S_0|f\rangle\langle f|T^u|B\rangle|}{|\langle J/\psi K^0|T|B\rangle|} \qquad (46)$$
$$\leq \frac{1}{3}\frac{|\langle f|T^u|B\rangle|}{|\langle f|T^c|B\rangle|}\left(\frac{|\langle f|T|B\rangle|}{\langle J/\psi K^0|T|B\rangle|}\right)^2$$

which is the contribution to the penguin-over-tree ratio from the intermediate state f This relation may thus serve to bound the $\bar{u}u \to \bar{c}c$ backscattering contributions from each individual intermediate state f.

The right-hand side of this inequality can be estimated by using data on charmless two-body decays into a pseudoscalar and a vector meson. The authors of [162] estimate the contributions of the channels $K^*\pi$, ρK, ωK and $K\eta$ to be less than $\xi_f \leq 8\times 10^{-4}\cdots 8\times 10^{-5}$, depending on the channel. Since the individual contributions are all of order 10^{-3} or less, the authors of [162] end up with the conclusion that the full re-scattering, obtained from summing over all intermediate states, is less than 10^{-2}.

3. Approaches based on Data

As an alternative, one may try to obtain information on the penguin contributions by relating the matrix elements appearing in $B \to J/\psi K_s$ to the matrix elements of other decays, which are e.g related by flavour symmetries. This idea has been exploited extensively, for an application to the golden modes see e.g. [163].

Here we shall discuss the results of a recent fit from [164]. Here the golden mode $B \to J/\psi K$ is compared to the situation in the decay $B \to J/\psi\pi$. For the charged modes, these tow decays are U-spin partners, while this is not the case for the neutral B mesons, see e.g.. [165]. Nevertheless we shall use the size of the r_f ratio obtained from $B_d \to J/\psi\pi^0$ as an estimate of the size of the corresponding ratio in $B_d \to J/\psi K_s$.

We shall express our results in terms of the shift $\Delta\phi_d$ of the observed mixing angle induced by the penguin contribution. We obtain [164]

$$\tan\Delta\phi_d = \frac{2r_f\cos\theta\sin\gamma + r_f^2\sin 2\gamma}{1+2r_f\cos\theta\cos\gamma + r_f^2\cos 2\gamma} \qquad (47)$$

where γ is the weak (CKM) phase and θ is the strong phase.

We may determine a value for r_f from the data of $B_d \to J/\psi\pi^0$, where the CKM suppression of the penguin contributions is much less severe than in the golden mode. The time-dependent CP asymmetry $A_{\rm CP}(t; J/\psi\pi^0)$ was recently measured by the BaBar (SLAC) [**?**] and Belle (KEK) [**?**] collaborations, yielding the following averages [**?**]:

$$C(J/\psi\pi^0) = -0.10 \pm 0.13, \qquad (48)$$
$$S(J/\psi\pi^0) = -0.93 \pm 0.15\,. \qquad (49)$$

Note that the error of $S(J/\psi\pi^0)$ is that of the HFAG, which is not inflated due to the inconsistency of the data.

In addition to the CP asymmetries we will also use the data on the CP averaged branching ratios. We introduce

$$H \equiv \frac{2}{\epsilon}\left[\frac{\mathrm{BR}(B_d\to J/\psi\pi^0)}{\mathrm{BR}(B_d\to J/\psi K^0)}\right]\left|\frac{\mathcal{A}}{\mathcal{A}'}\right|^2\frac{\Phi_{J/\psi K^0}}{\Phi_{J/\psi\pi^0}} = \frac{1-2r_\pi\cos\theta'\cos\gamma+r_\pi^2}{1+2r_K\cos\theta\cos\gamma+r_K^2} \qquad (50)$$

where $\epsilon = \lambda^2/(1-\lambda^2) = 0.053$ is a CKM factor and Φ_f are phases space factors. The ratio of the amplitudes $|\mathcal{A}/\mathcal{A}'|$ takes into account flavour-symmetry breaking corrections. Furthermore, have expressed H in terms of the weak phase γ, the strong phase θ' and the ratio r_π for the penguin in $B_d \to J/\psi\pi^0$ and the strong phase θ and the ratio r_K for the penguin in $B_d \to J/\psi K_s$.

As discussed above, we shall make the assumption that the hadronic matrix elements and the strong phases are roughly the same in the to decays $B_d \to J/\psi K_s$ and $B_d \to J/\psi\pi^0$. To this end we shall assume

$$\theta = \theta' \quad r_K = \epsilon r_\pi \qquad (51)$$

and leave generous margin for a possible violation of these relations.

In the flavour symmetry limit, we would also have $|\mathcal{A}/\mathcal{A}'| = 1$. However, we shall include some of the breaking effects by assuming that the breaking behaves like the form factor ratio of the $B \to \pi$ and $B \to K$ form factors, the values of which are taken from a QCD sum rule calculation. Clearly this is debatable assumption, since non-factorizable contributions are known to be dominant in $B_d \to J/\psi K_s$.

Fig. 15 shows the resulting fit. In the left plot we show the constraints coming from the data on the decay $B \to J/\psi\pi^0$. From this we conclude that the preferred values, indicated by the yellow region, of $r_\pi \in [0.15, 0.67]$ and $\theta' \in [174, 213]^\circ$ at the one sigma level. Making use of relation (51), we end up with the right plot, which gives the shift $\Delta\phi_d$ and the value of the strong phase θ. We see that a negative value of $\Delta\phi_d$ emerges; the global fit to all observables yields $\Delta\phi_d \in [-3.9, -0.8]^\circ$, mainly due to the constraints from H and $C(J/\psi\pi^0)$.

The impact of violations of (51) is rather mild. Varying $r_K = \xi r_\pi$ and with $\xi \in [0.5, 1.5]$ and leaving θ and θ' completely uncorrelated in the region $\theta, \theta' \in [90, 270]^\circ$ the fit still prefers negative values of $\Delta\phi_d$; the global fit yields $\Delta\phi_d \in [-6.7, 0.0]^\circ$.

It is remarkable that the data seem to prefer sizable penguin contributions. The ratio r_f which are obtained by this fits is of the order of $r_f \sim 0.1...0.7$ which is considerably larger than what is obtained by the purely theoretical approaches discussed above.

The experimental precision at a future Super Flavour Factory will further constrain the hadronic

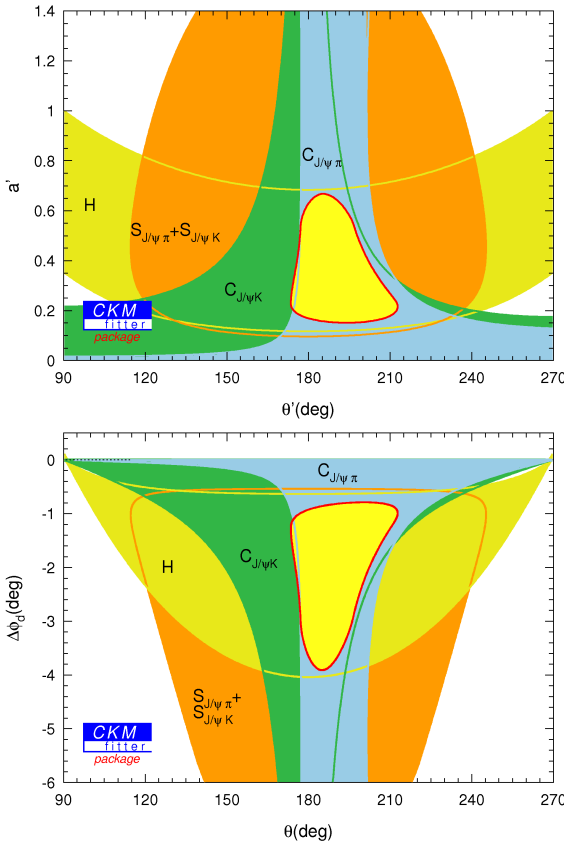

FIG. 15: Left: The $1\,\sigma$ ranges in the θ'–a' plane with current data ($a' = r_\pi$). Right: $\Delta\phi_d$ for the constraints shown in the left plot.

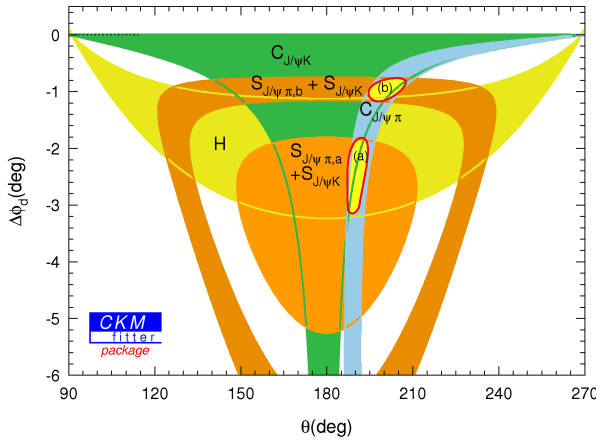

FIG. 16: Future benchmark scenarios, as discussed in the text.

parameters. However, the final reach for a NP contribution to the B^0_d–$\bar{B}^0_d$ mixing phase will strongly depend on the measured values of the CP asymmetries of $B^0 \to J/\psi\pi^0$, which are challenging for LHCb because of the neutral pions (here a similar analysis could be performed with $B^0_s \to J/\psi K_S$ [**?**]), but can be measured at future super-B factories.

We illustrate this through two benchmark scenarios, assuming a reduction of the experimental uncertainties of the CP asymmetries of $B^0 \to J/\psi K^0$ by a factor of 2, and errors of the branching ratios and γ that are five-times smaller; the scenarios agree in $C(J/\psi\pi^0) = -0.10 \pm 0.03$, but differ in $S(J/\psi\pi^0)$. In the high-S scenario (a), we assume $S = -0.98 \pm 0.03$. As can be seen in Fig. 16, $\Delta\phi_d \in [-3.1, -1.8]^\circ$ (with $a' \sim 0.42$, $\theta' \sim 191^\circ$) will then come from the lower value of S and H, which we assume as $H = 1.53 \pm 0.03 \pm 0.27$. In the low-$S$ scenario (b), we assume $S = -0.85 \pm 0.03$. In this case, $\Delta\phi_d \in [-1.2, -0.8]^\circ$ (with $a' \sim 0.18$, $\theta' \sim 201^\circ$) would be determined by S and C alone, while H would only be used to rule out the second solution. By the time the accuracies of these benchmark scenarios can be achived, we will also have a much better picture of $SU(3)$-breaking effects through data about $B_{s,d,u}$ decays.

Since the experimental uncertainty of $(\phi_d)_{J/\psi K^0}$ could be reduced to $\sim 0.3^\circ$ at an upgrade of LHCb and an e^+e^- super-B factory, these corrections will be essential. It is interesting to note that the quality of the data will soon reach a level in the era of precision flavour physics where subleading effects, i.e. doubly Cabibbo-suppressed penguin contributions, have to be taken into account. In particular, in the analyses of CP violation in the golden $B^0 \to J/\psi K_{S,L}$ modes this is mandatory in order to fully exploit the physics potential for NP searches.

4. Tree level time-dependent measurements: β

5. Tree level time-dependent measurements: α

6. Penguin dominated time-dependent measurements: β

7. New physics searches

8. ΔS measurements

It is possible to use time-dependent CP (TDCP) asymmetry measurements to search for signs of new physics (NP) in the form of heavy particles contributing to loop topologies and additional contributions from NP for tree level processes. In order for such a search to have a reasonable chance of seeing NP one has to study a mode, or set of modes, that are loop (or penguin) dominated. The golden channels for this type of measurement fall into the categories of penguin-dominated TDCP measurements of $b \to s$ transitions and tree level $b \to c\bar{c}s$ transitions. These measurements can trigger the observation of NP if the value of $S^f = \sin 2\beta_{\rm eff}$ measured in one of these decays devi-

ates significantly from that measured in the tree dominated $c\bar{c}s$ decays like $J/\psi K^0$ ($S = \sin 2\beta$), or from that predicted by the Standard Model (S^{SM}). The current level of such deviations $\Delta S^{tree} = S^{SM} - S$ and $\Delta S^{penguin} = S^f - S_{SM}$ from the theoretically clean penguin (tree) modes are 2.7σ (2.1σ) from the SM prediction [166, 167], and the deviation $\Delta S^f = S^f - S$ is small using current data. Such tantalizing hints of a deviation beckons us to study this area further to see if these deviations are indications of NP, or if these effects are merely statistical fluctuations.

The interpretation of the precise data on the TDCP asymmetries in terms of the CKM parameters requires a reasonable control over the hadronic matrix elements. In particular, the ratio of the penguin versus the tree contribution has to be known from the theoretical side in order to turn the measurements of CP asymmetries into a test of the Standard Model (SM).

Explicitly, the typical amplitude for a non-leptonic two-body decay can be written as:

$$A(B^0 \to f) = \mathcal{A}\left[1 + r_f\, e^{i\delta_f}\, e^{i\theta_f}\right], \qquad (52)$$

where usually $\mathcal{A}$ is the tree amplitude and r_f denotes the modulus of the penguin-over-tree ratio, which has a strong phase θ_f. The weak phase δ_f is in the cases at hand the CKM angle γ, while the modulus of the CKM factors is absorbed into r_f. The observables C^f and S^f can be expressed as:

$$C^f = -2r_f \sin\theta_f \sin\delta_f, \qquad (53)$$

$$S^f = \sin\phi + 2r_f \cos\theta_f \sin(\phi + \delta_f) + r_f^2 \sin(\phi + 2\delta_f), \qquad (54)$$

where ϕ is the mixing phase stemming from the $\Delta B = 2$ interaction.

The key issue in the theoretical understanding of CP asymmetries is the ratio r_f, which for the "gold-plated modes" is doubly Cabibbo suppressed. However, at the precision of a Super Flavour Factory even a small r_f will be observable and hence relevant for the analysis.

There are basically two ways to assess the ratio r_f. From the theoretical side one may compute r_f with a non-perturbative method, namely a variant of factorization (when applicable) [168–170] or try a phenomenological estimates otherwise [161, 162]. The second possibility is to rely more on data, making use of approximate flavour symmetry relations between matrix elements [163–165, 171] [3].

[3] In practice, these two ways are not well separated: theoretical approaches often use phenomenological constraints and data-drive approaches relies also on theory to some extent.

Theoretical calculations of $\Delta S^f = S^f - \sin\phi$ typically produce results in the range $\Delta S^f \sim 10^{-3}$ up to few$\times 10^{-2}$. Based on data there are indications that r_f in fact can be sizable [163]. As an example, based on the data of $B \to J/\psi\pi^0$ one extracts values for r_f which can be as large as 0.8, yielding shifts as large as $\Delta S^f \sim -7\%$ [164]. In fact the data on $B \to J/\psi\pi^0$ indicate a negative shift, which would soften the currently existing tension between $\sin 2\beta$ and V_{ub}.

Table XI summarizes the precision of current measurements [133] and Super$B$ extrapolations, together with a reference set of theoretical predictions for ΔS^f [168, 172, 173] in the SM. The NP discovery potential deviations required at a Super$B$ factory to observe NP are also shown. Where appropriate, reducible systematic uncertainties, and data driven bounds on the SM uncertainties have been scaled by luminosity from current measurements in making these extrapolations.

With the theoretical predictions for ΔS^f used in Table XI, the golden $b \to s$ penguin modes for this NP search are $B^0 \to \eta' K^0$ and $B^0 \to K_S^0 K_S^0 K_S^0$, together with $B^0 \to f_0^0 K_S^0$ for which the calculation of the SM uncertainty is however less accurate. Some interesting three-body modes, notably $B^0 \to \phi K_S^0 \pi^0$ and $B^0 \to \pi^0\pi^0 K_S^0$, presently lack an assessment of the theoretical uncertainty.

One can see from the table that it is possible to discover NP if there is a deviation of 0.02 from SM expectations of $\sin 2\beta$ as measured in tree decays. It is possible to observe a deviation of 5σ or more of about 0.1 in $\sin 2\beta_{\rm eff}$ from $b \to s$ transitions in the golden modes. It is worth noting however that these conclusions may change depending on the models used for computing ΔS^f. Indeed not all sources of theoretical error are under control in these estimates and in some case even the sign of the correction can be model dependent. On the other hand, theoretical estimates not explicitly data-driven also rely on experimental information to some extent and and could benefit from the Super$B$ large data set. This improvement has not be taken into account in Table XI. Clearly, if Super$B$ will find significant deviations in these measurements, further theoretical and phenomenological work will be required to pin down the SM value of ΔS^f and firmly establish the presence of NP. In the absence a theoretical leap in the understanding of non-leptonic decays, data-driven methods are expected to play a prominent role. In this respect, the opportunity of measuring several modes with different theoretical uncertainties, but possibly correlated NP contributions, is a unique advantage of Super$B$.

The golden $b \to d$ process is $B^0 \to J/\psi\pi^0$ from an experimental perspective. Yet current theoretical understanding indicates that the measurements of S^f for $b \to d$ modes are theoretically limited.

TABLE XI: Current experimental precision of S^f [133], and that expected at a Super$B$ experiment with $75\,\mathrm{ab}^{-1}$ of data. The 5σ discovery limit deviations at $75\,\mathrm{ab}^{-1}$ are also listed. The first entry in the table corresponds to the tree level calibration mode, and the next two sections of the table refer to $b \to s$ and $b \to d$ transitions. Theoretical estimates of ΔS^f are taken from Refs. [168, 172, 173]. A long dash '$-$'denotes that there is no theoretical estimate of ΔS^f computed yet for a given mode, thus the corresponding discovery limits are not evaluated.

Mode	Current Precision			Predicted Precision ($75\,\mathrm{ab}^{-1}$)			Discovery Potential	
	Stat.	Syst.	ΔS^f(Th.)	Stat.	Syst.	ΔS^f(Th.)	3σ	5σ
$J/\psi K^0_S$	0.022	0.010	0 ± 0.01	0.002	0.005	0 ± 0.001	0.02	0.03
$\eta' K^0_S$	0.08	0.02	0.015 ± 0.015	0.006	0.005	0.015 ± 0.015	0.05	0.08
$\phi K^0_S \pi^0$	0.28	0.01	–	0.020	0.010	–	–	–
$f_0 K^0_S$	0.18	0.04	0 ± 0.02	0.012	0.003	0 ± 0.02	0.07	0.12
$K^0_S K^0_S K^0_S$	0.19	0.03	0.02 ± 0.01	0.015	0.020	0.02 ± 0.01	0.08	0.14
ϕK^0_S	0.26	0.03	0.03 ± 0.02	0.020	0.005	0.03 ± 0.02	0.09	0.14
$\pi^0 K^0_S$	0.20	0.03	0.09 ± 0.07	0.015	0.015	0.09 ± 0.07	0.21	0.34
ωK^0_S	0.28	0.02	0.1 ± 0.1	0.020	0.005	0.1 ± 0.1	0.31	0.51
$K^+K^-K^0_S$	0.08	0.03	0.05 ± 0.05	0.006	0.005	0.05 ± 0.05	0.15	0.26
$\pi^0\pi^0 K^0_S$	0.71	0.08	–	0.038	0.045	–	–	–
ρK^0_S	0.28	0.07	-0.13 ± 0.16	0.020	0.017	-0.13 ± 0.16	0.41	0.69
$J/\psi \pi^0$	0.21	0.04	–	0.016	0.005	–	–	–
$D^{*+}D^{*-}$	0.16	0.03	–	0.012	0.017	–	–	–
D^+D^-	0.36	0.05	–	0.027	0.008	–	–	–

9. *Precision measurement of γ*

The measurement of the unitarity triangle angle γ is a standard candle measurement that can be used to perform precision tests of the SM. In this section we discuss why it is important to measure γ precisely, whether such a measurement is "safe" from NP, and also how we can perform such a measurement.

The main idea behind the measurement of γ dates back to almost two decades ago, and in retrospect this is a straight forward concept. One uses the interference between $b \to c\bar{u}s$ and $b \to u\bar{c}s$ [174, 175] transitions. The sensitivity to the weak phase γ comes from the interference between $B^- \to DK^-$ decay followed by $D \to f$ and the $B^- \to \bar{D}K^-$ decay followed by $\bar{D} \to f$, where f can be any common final state of D and $\bar{D}$.

Depending on the choice of the final state f in D decay there have been many variations of this central idea proposed in the literature. With f for instance taken to be a CP odd (-1) eigenstate ($e.g. K_S\pi^0$) [174, 175], a flavor state ($e.g. K^+\pi^-$) [176, 177], singly Cabibbo suppressed ($e.g. K^{*+}K^-$) [178], and many-body final state ($e.g. K_S\pi^+\pi^-$) [179, 180]. Other extensions include many-body B final states $B^+ \to DK^+\pi^0, K_S\pi^+$, $B^0 \to D\pi^-K^+$ [181–184], where D^{0*} is used in addition to D^0 [185], the use of self tagging D^{0**}, D_2^{*-} [182, 186] as well as neutral B and B_s decays (time dependent [187–191], time-integrated [192, 193], and self-tagging [194]).

For N_B different B decay channels and N_D different D decay channels one has $3N_B + N_D$ unknowns that are fit from data (in addition to γ, which is common to all the decays). On the other hand, one has $\sim 4N_BN_D$ observables – different branching ratios and CP asymmetries. It then immediately follows that the best strategy is to combine as many channels as possible in order to perform a precision measurement of γ.

An interesting question is whether the weak phase γ measured from $B \to DK$ decays is the SM weak phase. In other words – to what extent is $B \to DK$ a SM reference point for the value of γ? One would expect that since $B \to DK$ decays are mediated exclusively by tree diagrams, the contributions from NP are negligible. Schematically we have

$$A(B^- \to DK^-) \sim \underbrace{V_{cb}}_{\lambda^2}\underbrace{V_{us}}_{\lambda} T, \quad \underbrace{V_{ub}}_{\lambda^3}\underbrace{V_{cs}}_{1} C, \quad (55)$$

where we have also denoted explicitly the CKM scaling in the Wolfenstein parameterization. How could this amplitude be modified by NP? If it is modified due to non-SM charged currents then the effect of NP would be likely to show up elsewhere, $e.g.$in semi-leptonic B decays (if NP is leptophobic, this may be harder to see, though). If the modification is due to non-SM neutral currents then two insertions of NP flavor violation (FV) are needed, $e.g.$to generate a correction to $(\bar{c}u)(\bar{s}b)$ operator. In this case the NP effects are doubly suppressed. Compare this scenario with for

instance the decay $B \to \pi\pi$, where one can have a single NP FV insertion, *e.g.*to generate a correction to $(\bar{u}u)(\bar{d}b)$ operator. Thus, if we have TeV NP, then FV is small and the effect is suppressed in $B \to DK$. If, however we have general FV at high scale then the deviation is as likely to show in either of the two, $B \to DK$ and $B \to \pi\pi$ (but in this case the effect is also going to be very small given constraints from the $\bar{K}-K$ mixing).

Another interesting question is why measure the SM weak phase γ from $B \to DK$ and not from $B \to \rho\rho$, $\rho\pi$, $\pi\pi$ decays, which are also tree dominated. Schematically we have

$$A(B \to \rho\rho, \rho\pi, \pi\pi) \sim \underbrace{V_{ub}}_{\lambda^3}\underbrace{V_{ud}}_{1} T, \quad \underbrace{V_{cb}}_{\lambda^2}\underbrace{V_{cd}}_{\lambda} P. \quad (56)$$

The weak phase γ ($\alpha = \pi - \beta - \gamma$) determined from these decays is the SM one unless one has isospin breaking NP. This means that the γ measured would be the SM one even if there is NP in $B-\bar{B}$ mixing or in QCD penguins. NP in electro-weak penguins would, however, shift the measured value of γ from the SM one. Still, the NP has to compete with the tree transitions!

The extraction of γ from $B \to DK$ has one major advantage over extraction from $B \to \rho\rho$, $\rho\pi$, $\pi\pi$. In the latter case there are irreducible theoretical errors in extraction of γ (via α): due to (i) isospin breaking, which is hard to estimate to better than factors of few (i.e. that it is at a few percent level [195]) and (ii) due to the uncertainties in resonance shapes that are used in the extraction from $B \to \rho\pi$ [196]. There are no such errors in extraction of γ from $B \to DK$. Isospin is not used at any point, while reference to resonance parameterization can be avoided even in the case of multi-body D decays [179]. The remaining theoretical errors are much smaller and negligible at the precision level achievable at a Super Flavour Factory as we will see in more details below.

Charm factories (CLEO-c or BES-III) can have a big impact by measuring strong phases in D decays. Then only parameters of the B system need to be measured in B decays. Let us take as an example: $B^\pm \to [K_S\pi^+\pi^-]_D K^\pm$ where the D decay amplitude varies over the Dalitz plot

$$\begin{aligned} A_D(s_{12}, s_{13}) &\equiv A_{12,13}\, e^{i\delta_{12,13}}, \quad (57) \\ &\equiv A(D^0 \to K_S(p_1)\pi^-(p_2)\pi^+(p_3)), \end{aligned}$$

where $s_{12(13)} = (p_1 - p_{2(3)})^2$. The variation of the strong phase $\delta_{12,13}$ over the Dalitz plot can be measured by fitting the data with a resonance model, which leads to a hard to reduce $\sim 10^\circ$ systematic error on γ. A model independent treatment is possible using input from the CLEO-c and BES-III experiments as discussed in Ref. [179].

In the model independent method one partitions the Dalitz plot in bins [179] and introduces the sine and cosine of the strong phase differences averaged over the bins as new variables

$$\begin{aligned} c_i &\equiv \int_i dp\, A_{12,13}\, A_{13,12} \cos(\delta_{12,13} - \delta_{13,12}), \\ s_i &\equiv \int_i dp\, A_{12,13}\, A_{13,12} \sin(\delta_{12,13} - \delta_{13,12}). \quad (58) \end{aligned}$$

Since D decays do not violate CP one can relate c_i and s_i in i^{th} bin with the CP conjugated one, $\bar{i}$, hence $c_{\bar{i}} = c_i$, and $s_{\bar{i}} = -s_i$. A MC based feasibility study showed that the optimal strategy using this model independent approach is statistically only 30% worse than the model dependent method [197, 198]. The prior measurement of c_i, and s_i at charm factory (or at Super$B$ via running at charm threshold) is a crucial ingredient to measure γ in this way. The measurement of c_i, and s_i is possible because in the $\Psi(3770) \to D\bar{D}$ mesons in the final state are entangled. Let us assume that the D meson flying to the right decays to bin i of $K_S\pi^+\pi^-$ final state. Then by choosing different decay channels of the D meson flying to the left, one has enough information to measure both the phase and the amplitude of the $D \to K_S\pi^+\pi^-$ decay [179].

This was done by CLEO-c [199]. Using optimal binning with the least variation in strong phase difference across a bin $\Delta\delta_f$ [197, 198] for $D \to K_{S/L}\pi^+\pi^-$ decays and using entangled decays of $\Psi(3770) \to D\bar{D}$ with D's decaying into flavor tagged, CP-tagged and $D \to K_{S/L}\pi^+\pi^-$ decay modes the collaboration estimates that the decay model uncertainty on γ is reduced to 1.7° (from toy MC based studies with $\gamma = 60^\circ$, $\delta_B = 130^\circ$ and $r_B = 0.1$). D Decays involving more than three final-state particles can also be used to measure γ. In this case, it is simpler and in some modes sufficient to measure the total $B \to DK$ decay rates rather than to analyze the full phase-space distribution [200, 201]. This is also the case for some three-body modes [202].

There are several ways that would improve constraints on γ: include as many D decay modes as possible and include more B decay modes. To include $B^\pm \to D^* K^{*\pm}$ would be very hard, since one would need to perform an angular analysis of the decay. It is much easier to include neutral modes $B^0 \to DK_S$, $B_s^0 \to D\phi, D\eta^{(\prime)}$. At first glance neutral B decays are less attractive since in this case both $b \to us\bar{c}$ and $b \to cs\bar{u}$ are color suppressed, while in charged B decays $b \to cs\bar{u}$ is color allowed. The neutral decays therefore have smaller decay rates ($A_n \sim \frac{1}{3}A_c$). However, the statistical error on γ scales roughly as the smallest of the two interfering amplitudes, which both in B^+ and B^0 decays are color suppressed. Furthermore, using isospin (and neglecting annihilation) one

gains an extra constraint [192]

$$A(B^+ \to D^0 K^+) \simeq \sqrt{2} A(B^0 \to D^0 K_S), \qquad (59)$$

which reduces the number of independent unknowns to be determined. Time dependent measurements of B^0 decays contain full information [175, 203], but already time integrated B^0 rates (untagged rates) alone suffice to determine γ [192, 193]. The analysis can also be simplified by the use of self-tagging modes: $B^0 \to DK^{*0} \to D\pi^- K^+$ [194].

In the above discussion we have neglected $D - \bar{D}$ mixing, direct CP violation in $D \to f$ decays and $\Delta\Gamma$ in B_d and B_s time integrated decays. We now move to the estimate of the related theory errors.

The $D - \bar{D}$ mixing parameters $x_D = \frac{\Delta m_D}{\Gamma_D}, y_D = \frac{\Delta\Gamma_D}{2\Gamma_D}$ are both measured to be $O(10^{-2})$. Furthermore in the SM, $D - \bar{D}$ mixing is CP conserving to a very good approximation, with the mixing phase $\theta \sim O(10^{-4})$. For CP conserving $D - \bar{D}$ mixing the only important change in equations used to extract γ from $B \to DK$ are in the interference terms, where one changes the relative strong phase δ_f with a time averaged one, $\langle\delta_f\rangle$. $D - \bar{D}$ mixing also dilutes the interference so that it gets multiplied by $e^{-\epsilon_f}$. The effect on γ is small and is of second order in small parameters $\epsilon_f \sim O(x_D^2, y_D^2)$ [204]. These terms can still be enhanced, if the suppressed term is multiplied by a large amplitude, which happens for doubly Cabibbo suppressed D decays. Even in this case, however, the shift is small, $\Delta\gamma \lesssim 1^\circ$, while otherwise it is much smaller [204].

To recapitulate, the effect of CP conserving $D - \bar{D}$ mixing on the measurement of γ is small. It can also be included for precisely measured x_D and y_D. For the model independent analysis the news are even better – the way the model-independent analysis is set up, the inclusion of $D - \bar{D}$ mixing actually does not require any change in the analysis. Since both the average of the sine and of the cosine of the strong phase are measured independently from experiment, this means that the dilution due to time averaging is already determined experimentally [204]. The last approximation we used was neglecting $\Delta\Gamma_{d,s}$. The inclusion of $\Delta\Gamma_s$ dependence is important only in untagged $B_s \to D\phi$ so that $\Delta\Gamma_s$ needs to be well measured and kept in the analysis [193]. Once all these reducible theoretical errors are taken into account the theory error would come from higher electroweak corrections and CP violation in D decays. The resulting theoretical error is conservatively $\Delta\gamma < 10^{-5}$, so the measurement will be statistics dominated for a long time.

We conclude that measurement of γ from $B \to DK$ decays is the theoretically cleanest measurement of the SM weak phase and thus represents a standard candle with which to test the SM. This can for instance be contrasted with the measurements of α that may start to become theory limited at a Super Flavour Factory due to poorly known isospin breaking effects (for example see Ref. [40]). Under quite general assumptions the measurement of γ is also safe from NP contamination. An important input is provided by charm factories that can measure the strong phase differences in the D decays from entangled $\Psi(3770)$ decays. The estimated systematic uncertainty on γ is below 2° and can be reduced with increased statistics. This is true also of other systematic uncertainties in the present analyses, including the neglect of $D - \bar{D}$ mixing and $\Delta\Gamma$. They stem from simplifications made for convenience when analyzing currently available data. While in the future more complicated analyses will be required that incorporate these effects directly. Thus the irreducible theoretical error on γ is well below Super Flavour Factory sensitivities.

10. Direct CP violation

G. Lifetimes and Mixing

1. Measurement of Δm_d

The measurement of the mixing frequency Δm_d at Super$B$ is of interest as this physics parameter will come to be a significant systematic uncertainty in many of the time-dependent *CP* asymmetry studies and other NP searches. The current precision on this parameter is dominated by early measurements of the B-Factories, so there is the potential to improve knowledge of this parameter sufficiently so that it no longer plays an important role in error evaluation of other more important observables. It is anticipated that one will be able to measure Δm_d with a precision of better than ± 0.006 at Super$B$ and will be systematically limited. This level of precision is comparable with the current PDG average value [205].

With the discoveries of *CP* violation in decay and indirect *CP* violation at the B-Factories, it is natural to continue to search for *CP* violation in mixing. The test for this phenomenon is a part of generic time-dependent *CP* violation measurements where one searches for $|\lambda| = q/p \neq 0$, where q/p. The cosine coefficient measured at the same time as the ΔS parameters discussed previously are related to $|\lambda|$, and the Charmonium decays are a good place to search for CP violation in mixing where Super$B$ will be able to achieve a precision on $C = (1 - |\lambda|^2)/(1 + |\lambda|^2)$ of 0.005 with $J/\psi K^0$. It is possible to perform a precision measurement of $|q/p|$ using di-lepton events with a precision of a few per mille as discussed in Section 4 H.

2. Measurement of $\Delta\Gamma$

3. New Physics in mixing

It is possible to search for signs of NP in mixing in a model independent way. This is done, starting from a tree level determination of the apex of the unitarity triangle $(\overline{\rho},\overline{\eta})$, and searching for any perturbation from the SM solution using a generic parameterization of NP with an amplitude and phase, in addition to the SM contribution. The ratio of NP and SM amplitudes can be parameterized simply in terms of an amplitude ratio C_d and phase difference ϕ_{B_d}:

$$\begin{aligned} C_d e^{2i\phi_{B_d}} &= \frac{\langle B_d|\mathcal{H}_{eff}^{NP+SM}|\overline{B}_d\rangle}{\langle B_d|\mathcal{H}_{eff}^{SM}|\overline{B}_d\rangle} \\ &= \frac{A_d^{SM}e^{2i\phi_d^{SM}} + A_d^{NP}e^{2i(\phi_d^{SM}+\phi_d^{NP})}}{A_d^{SM}e^{2i\phi_d^{SM}}} \end{aligned}$$

where the SM phase for B_d mixing $\phi_d^{SM} = \beta$. The corresponding constraints on the NP phase and amplitude ratios are given in Fig. 17. Current data is consistent with small values of the amplitude for NP, and a large NP phase. Using data from Super$B$ we would be able to make a precision search for NP in B_d mixing.

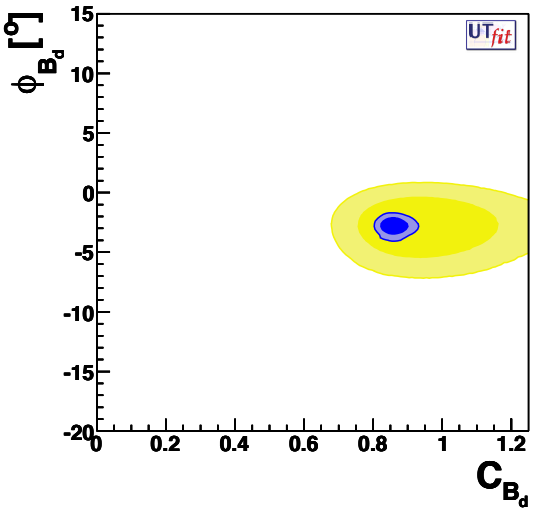

FIG. 17: Current constraints on possible NP amplitude and phase contributions to B_d mixing [206]. The SM solution is $(\phi_{B_d}, C_{B_d}) = (0, 1)$, and any deviation would be the result of NP. The light shaded regions correspond to the current 68, 95 and 99% CL constraints on C_{B_d} and ϕ_{B_d}, while the dark shaded regions correspond to the expected result from Super$B$.

H. Tests of *CPT*

The combined symmetry of C, P, and T otherwise written as CPT is conserved in locally gauge invariant quantum field theory. The role of CPT in our understanding of physics is described in more detail in Refs. [207–210] and an observation of CPT violation would be a sign of new physics. CPT violation could be manifest in neutral meson mixing, so a Super Flavour Factory is well suited to test this symmetry. The text-book description of neutral meson mixing in terms of the complex parameters p and q can be extended to allow for possible CPT violation. On doing so the heavy and light mass eigenstates of the B_z meson $B_{\rm H}$ and $B_{\rm L}$ become

$$|B_{\rm L,H}\rangle = p\sqrt{1\mp z}|B_z\rangle \pm q\sqrt{1\pm z}|\overline{B}^0\rangle,$$

where B_z and $\overline{B}^0$ are the strong eigenstates of the neutral B meson. The CPT conserving solution is recovered when $z = 0$ and if CP and CPT are conserved in mixing then $|q|^2 + |p|^2 = 1$.

There are two types of CPT test that have been performed at the current B-factories. The more powerful of these methods is the analysis of di-lepton events where both B mesons in an event decay into an $X^{\mp}\ell^{\pm}\nu$ final state. Di-lepton events can be categorized by lepton charge into three types: $++$, $+-$ and $--$ where the numbers of such events N^{++}, N^{+-} and N^{--} are related to $\Delta\Gamma$ and z as a function of Δt as described in Ref. [211]. Using these distributions one can construct two asymmetries: the first is a T/CP asymmetry:

$$\begin{aligned} \mathcal{A}_{T/CP} &= \frac{P(\overline{B}^0\to B_z) - P(B_z\to\overline{B}^0)}{P(\overline{B}^0\to B_z) + P(B_z\to\overline{B}^0)} \\ &= \frac{N^{++}-N^{--}}{N^{++}-N^{--}} \\ &= \frac{1-\left|\frac{q}{p}\right|^4}{1+\left|\frac{q}{p}\right|^4}, \end{aligned}$$

and the second is a CPT asymmetry:

$$\begin{aligned} \mathcal{A}_{CPT}(\Delta t) &= \frac{N^{+-}(\Delta t>0) - N^{+-}(\Delta t<0)}{N^{+-}(\Delta t>0) + N^{+-}(\Delta t<0)} \\ &\simeq 2\frac{{\rm Im}z\sin(\Delta m_d\Delta t) - {\rm Re}z\sinh\left(\frac{\Delta\Gamma\Delta t}{2}\right)}{\cosh\left(\frac{\Delta\Gamma\Delta t}{2}\right)+\cos(\Delta m_d\Delta t)}, \end{aligned}$$

where $\mathcal{A}_{CPT}(\Delta t)$ is sensitive to $\Delta\Gamma\times{\rm Re}z$. In the SM $\mathcal{A}_{T/CP}\sim 10^{-3}$ and $\mathcal{A}_{CPT} = 0$ [212–214]. *BABAR* measures [215]:

$$\begin{aligned} \left|\frac{q}{p}\right| - 1 &= (-0.8\pm 2.7({\rm stat})\pm 1.9({\rm syst}))\times 10^{-3}, \\ {\rm Im}z &= (-13.9\pm 7.3({\rm stat})\pm 3.2({\rm syst}))\times 10^{-3}, \\ \Delta\Gamma\times{\rm Re}z &= (-7.1\pm 3.9({\rm stat})\pm 2.0({\rm syst}))\times 10^{-3}, \end{aligned}$$

which is compatible with no *CP* violation in $B_z - \overline{B}^0$ mixing and *CPT* conservation. It is possible to study variations as a function of sidereal time, where 1 sidereal day is approximately 0.99727 solar days [216] where z depends on the four momentum of the B candidate. *BABAR* re-analyzed their data and find that it is consistent with $z = 0$ at 2.8 standard deviations [211]. With data from the first few years of operation at Super$B$ it would be possible to perform a more precise test of *CPT* than performed by the current experiments and on doing so continue the search for *CPT* violation. These measurements would become limited by systematic uncertainties after the first few years of running at Super$B$. The precision on *CPT* violating observables that could be reached with Super$B$ is:

$$\begin{aligned} \sigma(\mathrm{Im})z &= 0.6 \times 10^{-3}, \\ \sigma(\Delta\Gamma \times \mathrm{Re}z) &= 0.3 \times 10^{-3}, \end{aligned}$$

However with such a measurement it would be possible to test if the 2.8σ hint for *CPT* violation were a real effect or the result of a statistical fluctuation.

I. Charmless hadronic B decays

Charmless hadronic B decays can be used to test the SM and CKM theory in detail. In principle, such decays can be used to measure all of the angles of the unitarity triangle, however SM uncertainties are a concern for all such measurements as existing calculations are either computing the hadronic amplitudes using factorization, or invoking flavour SU(2) or SU(3) symmetries in order to achieve their goals. Without further improvements in the theoretical tools available, in many cases the potential of using charmless hadronic B data, both branching fractions and direct *CP* asymmetries, to test the CKM picture will be limited by theoretical uncertainties, coming either by unknown power-suppressed terms or by flavour symmetry breaking. On the other hand, a Super Flavour Factory provides a full set of high precision data to test and possibly improve the theoretical tools developed so far to describe these hadronic B decays.

J. Section summary

The section summary should provide a succinct recap of the main points discussed within the section, including (if relevant) summary tables of sensitivitites.

1. New physics searches

2. Precision CKM

By the time Super$B$ starts to take data it is expected that the knowledge of the CKM matrix parameters (sides and angles) will be dominated by a combination of measurements from the B-factories and LHCb. These will include measurements of β and γ with a precision of the order of 1°, and a measurement of α with a precision of $5 - 6^\circ$. LHCb will not be able to improve upon the existing measurements of $|V_{ub}|$ and $|V_{cb}|$, which have uncertainties of 8% and 2%, respectively. Super$B$ will be able to perform precision measurements of the angles of the unitarity triangle as well as $|V_{ub}|$ and $|V_{cb}|$. The anticipated precision attainable for these observables is given in Table XII. Together with hadronic parameters computed mainly using lattice QCD (see Section 10), this set of information will play a vital role in defining a model-independent determination of quark mixing in the Standard Model, thus providing a precision test of the CKM anzatz. Precision knowledge of the CKM matrix itself facilitates several NP search opportunities available to Super$B$ and other experiments.

TABLE XII: The expected precision on CKM observables from Super$B$. The third column indicates if the measurement is theoretically clean, or dominated by theory uncertainties.

CKM observable	Precision ($75\,\mathrm{ab}^{-1}$)	Theory uncertainty
β ($c\bar{c}s$)	0.1°	clean
α	$1 - 2^\circ$	dominant
γ	$1 - 2^\circ$	clean
$\lvert V_{cb}\rvert$ (inclusive)	1.0%	dominant
$\lvert V_{cb}\rvert$ (exclusive)	1.0%	dominant
$\lvert V_{ub}\rvert$ (inclusive)	2.0%	dominant
$\lvert V_{ub}\rvert$ (exclusive)	3.0%	dominant

5. B Physics at the $\Upsilon(5S)$

Measurement of CKM- and New Physics-related quantities in the B_s sector is a natural extension of the traditional B Factory program. In some cases, studies of B_s mesons allow the extraction of the same fundamental quantities accessible at a B Factory operating at the Υ(4S) resonance, but with reduced theoretical uncertainty. Experiments running at hadronic machines are expected to be the main source of B_s-related measurements. In particular, in the near future, the increased dataset of the Tevatron experiments and the start of the LHCb, ATLAS, and CMS programs will surely yield important new results.

It is worth noting, however, that despite the rapid $B_s\overline{B}_s$ oscillation frequency, it is feasible to carry out B_s studies in the very clean environment of e^+e^- annihilation machines by running at the $\Upsilon(5S)$ resonance, where it is possible to perform measurements involving neutral particles (*e.g.*, π^0, η and η' mesons, radiative photons, *etc.*). CLEO [217–219] and Belle [220, 221] have had short runs at the $\Upsilon(5S)$, measuring the main features of this resonance. The results clearly indicate the potential for an e^+e^- machine to contribute to this area of B physics, and have inspired the work in this section, and elsewhere [222–224]. Note that, in contrast to much of the remainder of this chapter, there are no experimental analyses for many of the measurements of interest, and therefore our studies are based on Monte Carlo simulations.

A detailed study of the physics capability of Super$B$ at the $\Upsilon(5S)$ can be found in the Conceptual Design Report [40]. The main conclusions of that study are summarized here.

The production of B_s mesons at the $\Upsilon(5S)$ allows comprehensive studies of the decay rates of the B_s with a completeness and accuracy comparable to that currently available for B_d and B_u mesons, thereby improving our understanding of B physics and helping to reduce the theoretical uncertainties related to New Physics-sensitive B_d quantities. Moreover, B_s physics provides additional methods and observables to probe New Physics effects in $b \to s$ transitions. In the following, we concentrate on this second point, providing examples of some of the highlight measurements that could be performed by Super$B$ operating at the $\Upsilon(5S)$ resonance.

The $\Upsilon(5S)$ resonance is a $J^{PC} = 1^{--}$ state of a $b\bar{b}$ quark pair with an invariant mass of $m_{\Upsilon(5S)} = (10.865 \pm 0.008)$ GeV/c^2 [225–227]. The cross section $\sigma(e^+e^- \to \Upsilon(5S))$ is $0.301 \pm 0.002 \pm 0.039$ nb [228], which is about three times smaller than $\sigma(e^+e^- \to \Upsilon(4S))$. Unlike the $\Upsilon(4S)$ state, this resonance is sufficiently massive to decay into several B meson states: vector-vector ($B^*\bar{B}^*$), pseudoscalar-vector ($B\bar{B}^*$), and pseudoscalar-pseudoscalar (BB) combinations of charged B mesons, as well as neutral B_d and B_s mesons, as well as into $B^{(*)}\bar{B}^{(*)}\pi$ states. The B pair production rates at the $\Upsilon(5S)$ resonance are summarized in Ref. [40]. As with reconstructing B decays at the $\Upsilon(4S)$, one can use the precisely determined initial state kinematics to compute the usual discriminating variables $m_{\rm ES}$ and ΔE. There is a small complication that the different B pairs produced occupy slightly different regions in the $m_{\rm ES} - \Delta E$ plane and this can be used to study fine details of the decay properties of these B mesons. With the small beam energy spread of Super$B$, the resolution of $m_{\rm ES}$ will be comparable to that of the current B Factories, resulting in almost negligible crossover between $B_s\overline{B}_s$ and $B\overline{B}\pi$ states.

A. Rare decays

It is possible to search for possible NP effects by comparing measurements of $\Delta B = 1$ $b \to s$ transitions, measurements of $|V_{td}/V_{ts}|$, and Δm_s. Super$B$ will be able to perform a precision measurement of $|V_{td}/V_{ts}|$ using the ratio $R = \mathcal{B}(B^0_d \to \rho^0\gamma)/\mathcal{B}(B_d \to K^{*0}\gamma)$ to a precision that is expected to be ultimately limited by the presence of a power-suppressed correction term. The ratio $R_s = \mathcal{B}(B^0_s \to K^{*0}\gamma)/\mathcal{B}(B^0_d \to K^{*0}\gamma)$ has the advantage that there is no W exchange diagram contribution to hinder interpretation of results. Assuming that $\mathcal{B}(B^0_s \to K^{*0}\gamma) = 1.54 \times 10^{-6}$, and taking reasonable estimates from lattice QCD for the form factor ratio ξ to extract $|V_{td}/V_{ts}|$ with a precision of a few percent with a multi- ab^{-1} sample of data, as shown in Table XIV.

1. $B_s \to \gamma\gamma$

In analogy with the B_d decay $b \to s\gamma$, the decay $B_s \to \gamma\gamma$ is considered a promising golden channel to search for new physics at Super$B$. The final state contains both *CP*-odd and *CP*-even components, allowing for the study of *CP*-violating effects with B Factory tagging techniques. The Standard Model expectation for the branching ratio is $\mathcal{B}(B_s \to \gamma\gamma) \sim (2-8) \times 10^{-7}$ [229]. New Physics effects are expected to give sizable contributions to the decay rate in certain scenarios [230, 231]. For instance, in R-parity-violating SUSY models, neutralino exchange can enhance the branching ratio up to $\mathcal{B}(B_s \to \gamma\gamma) \simeq 5 \times 10^{-6}$ [232]. On the other hand, in R-parity-conserving SUSY models, in particular in

softly broken supersymmetry, $\mathcal{B}(B_s \to \gamma\gamma)$ is found to be highly correlated with $\mathcal{B}(b \to s\gamma)$ [233].

Experimentally the measurement of $B_s \to \gamma\gamma$ will be much less demanding at Super$B$ than the well established measurement of final states such as $B^0_d \to \pi^0\pi^0$. The presence of two high-energy photons in the final state is a clear signature for the signal, particularly with a recoil technique. Both *BABAR* [234] and Belle [235] have published results of searches for $B^0_d \to \gamma\gamma$, setting the current experiment upper limit at $\mathcal{B}(B_d \to \gamma\gamma) < 6.2 \times 10^{-7}$ which is a proof of principle that one can measure the corresponding B_s decay at Super$B$. We anticipate that it will be possible to observe 14 signal events and 20 background events in a sample of 1 ab^{-1} assuming a Standard Model branching fraction. With 30 ab^{-1}, one can achieve a statistical error of 7% and a systematic error smaller than 5% from a straight forward analysis. It would be possible to improve upon this precision using tagging information, which would also facilitate the measurement of a direct CP asymmetry in this mode.

B. Correlated production: quantum correlated decays, Time integrated studies/time dependent studies.

1. A^s_{SL}

In analogy with the B_d system, the absolute value and the phase of the $B_s\overline{B}_s$ mixing amplitude can be used to test for the presence of New Physics in $\Delta B = 2$ $b \to s$ transitions. These measurements can be made at hadronic colliders [236]. The recent measurement of Δm_s [237–239] provides the first milestone in this physics program. Similar tests for New Physics effects can be made by measuring quantities such as $\Delta\Gamma_s$ and the *CP* asymmetry in semi-leptonic decays $A^s_{\rm SL}$. These observables can be measured using the large statistics, and high reconstruction efficiency available in the clean environment of Super$B$. It is not necessary to resolve B_s oscillations to make these measurements.

In a generic New Physics scenario, the effect of $\Delta B = 2$ New Physics contributions can be parameterized in terms of an amplitude and phase, C_{B_s} and ϕ_{B_s}, (in analogy with Section 4 G 3). In the absence of New Physics effects, $C_{B_s} = 1$ and $\phi_{B_s} = 0$. The measured values of Δm_s and $\sin 2\beta_s$ are related to Standard Model quantities through the relations :

$$\Delta m_s^{\rm exp} = C_{B_s} \cdot \Delta m_s^{\rm SM}, \quad (60)$$

$$\sin 2\beta_s^{\rm exp} = \sin(2\beta_s^{\rm SM} + 2\phi_{B_s}). \quad (61)$$

The semi-leptonic *CP* asymmetry [240] is very sensitive to New Physics contributions, while and the value of $\Delta\Gamma_s/\Gamma_s$ [241] may also be sensitive when constraining new physics, but non perturbative effects on interpreting $\Delta\Gamma_s$ could degrade this. Both of these observables can be used to constrain NP in the $\Delta B = 2$ effective Hamiltonian, and can be expressed in terms of the parameters C_{B_s} and ϕ_{B_s}.

Different experimental methods have been proposed to extract the lifetime difference $\Delta\Gamma_s$ [242]. For instance, $\Delta\Gamma_s$ can be obtained from the angular distribution of untagged $B_s \to J/\psi\phi$ decays. This angular analysis allows separation of the *CP* odd and *CP* even components of the final state, which have a distinct time evolution, given by different combinations of the two exponential factors $e^{-\Gamma_{L,H}t}$. This allows the extraction of the two parameters $\Gamma_{L,H}$ or, equivalently, Γ_s and $\Delta\Gamma_s$. The weak phase of the mixing amplitude, β_s, also appears in this parameterization, and a constraint on this phase can be extracted along with the other two parameters (see Eq. 63 below). Measurements of $\Delta\Gamma_s$ and β_s have been performed by CDF [243] and DØ [244]. With a few ab^{-1} of data at the $\Upsilon(5S)$ Super$B$ will be able to improve upon the current experimental precision, and provide a useful second measurement to cross check any results from LHCb in this area.

We have also studied the performance of two different experimental techniques that can be used to to extract the semi-leptonic asymmetry $A^s_{\rm SL}$, defined as:

$$A^s_{\rm SL} = \frac{1 - |q/p|^4}{1 + |q/p|^4}. \quad (62)$$

The first technique consists of exclusively reconstructing one of the two B mesons into a self-tagging hadronic final state (such as $B_s \to D_s^{(*)}\pi$) and looking for the signature of a semi-leptonic decay (high momentum lepton) in the rest of the event. The second approach is more inclusive, using all events with two high momentum leptons. In this case, contributions from B_s and B_d decays cannot be separated, and a combined asymmetry, $A_{\rm CH}$ is measured. Results from this type of analysis are available from DØ [245]. We expect to be able to reach precisions of 0.006 and 0.004 on $A^s_{\rm SL}$ and $A_{\rm CH}$, respectively, with 1 ab^{-1} of data. These measurements quickly become systematically limited at Super$B$, however the achievable precision would be a clear improvement over the current experimental situation. The cleaner experimental environment at Super$B$ suggests that this experiment is better suited at making precision measurements of the semi-leptonic asymmetries than experiments at a hadron collider. For example, the measurement of $A^s_{\rm SL}$ (and, to a lesser extent, also to $A^d_{\rm SL}$), can be used to test the Littlest Higgs Model with T-parity as discussed in Ref. [40].

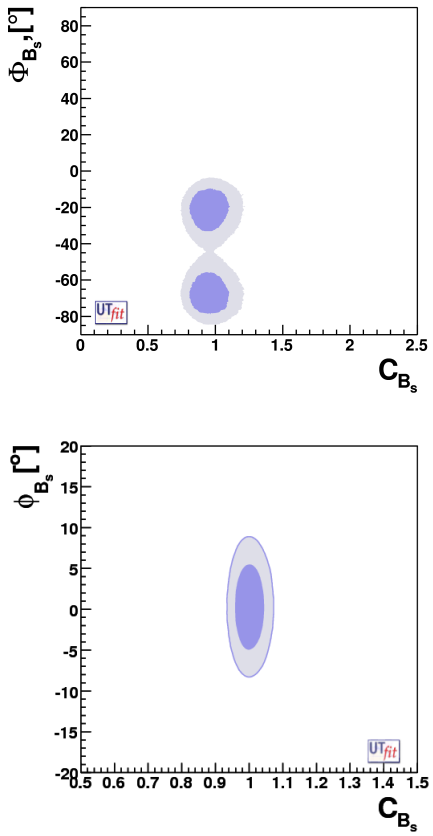

FIG. 18: Allowed regions in the C_{B_s}–ϕ_{B_s} plane given by the current data (top) and at the time of Super$B$ (bottom). Note that the scales for the axes are different in the two cases. See Table XIII for the corresponding values anticipated for these measurements.

2. *Phenomenological Implications*

The experimental measurements of $\Delta\Gamma$, $A_{\rm SL}^s$, $A_{\rm CH}$ and *CP* violation parameters described in the previous sections can be used to determined the $\Delta B = 2$ New Physics contributions in the B_s sector. The knowledge of $\overline{\rho}$ and $\overline{\eta}$ is assumed to come from studies at the $\Upsilon(4S)$.

To illustrate the impact of the measurement at Super$B$ at the $\Upsilon(5S)$, we show in Fig. 18 selected regions in the ϕ_{B_s}–C_{B_s} plane (right), compared to the current situation (left). Corresponding numerical results are given in Table XIII.

It is important to note that the uncertainty on the parameter C_{B_s} is dominated by the uncertainty on f_{B_s} and bag parameters. The error on ϕ_{B_s} is not limited by systematics and theory, and can be improved to 1–2° with a longer dedicated run at the $\Upsilon(5S)$. LHCb will also measure the New Physics phase ϕ_{B_s} and is expected to achieve a comparable sensitivity with full statistics (~ 10 fb^{-1}) of $\sim 1°$.

TABLE XIII: Uncertainty of New Physics parameters ϕ_{B_s} and C_{B_s} using the experimental and theoretical information available at the time of Super$B$ and given in Tables XIV (30 ab^{-1}) and XX. These uncertainties are compared to the present determination.

Parameter	Today	At Super$B$ (30 ab^{-1})
ϕ_{B_s}	$(-3 \pm 19)° \cup (94 \pm 19)°$	$\pm 1.9°$
C_{B_s}	1.15 ± 0.36	± 0.026

C. Section summary

The recently reported evidence from the D0 collaboration for a di-muon asymmetry $A_{\rm CH}$ that is incompatible with the Standard Model [246, 247] (also see references therein) has been followed by theoretical attempts to interpret the result, for example [248–253], where the SM expectation can be found in Ref. [214]. If this effect is confirmed, then we can expect to observe new physics in meson decays in the B and D sector. One prime example of an observable that would be expected to manifest new physics in B_s decays is the semi-leptonic asymmetry $A_{\rm SL}^s$. In some models the phases postulated to be responsible for large semi-leptonic asymmetries are flavour blind, and thus we would expect effects to also be manifest in other meson decays as well as in the B_s sector. Other models have postulated a richer texture of new physics that may be related to this D0 result. In both cases, and even if the D0 result turns out to be a statistical fluctuation rather than evidence for new physics, Super$B$ will be able to test a variety of new physics scenarios using a wide array of measurements as outlined in Section 11.

The results presented in this section section are summarized in Table XIV for two scenarios (i) a short (1 ab^{-1}) and (ii) a long (30 ab^{-1}) run at the $\Upsilon(5S)$ resonance. Collecting 1 ab^{-1} will take less than one month at the Super$B$ design luminosity of 10^{36} cm^{-2} sec^{-1}.

While it is clear that Super$B$ cannot compete with hadronic experiments on modes such as $B_s \to \mu^+\mu^-$ and $B_s \to J/\psi\phi$, it is also evident that many important channels that are not easily accessible at hadronic experiments such as LHCb will be measurable at Super$B$. Besides the flagship measurement of the semi-leptonic asymmetry $A_{\rm SL}^s$, the channels $B_s \to \gamma\gamma$ and $B_s \to K^0\bar{K}^0$ will also be measurable at Super$B$. Therefore Super$B$ will complement the results from

TABLE XIV: Summary of the expected precision of some of the most important measurements that can be performed at Super$B$ operating at the $\Upsilon(5S)$ resonance, with an integrated luminosity of 1 ab^{-1} and 30 ab^{-1}.

Observable	1 ab^{-1}	30 ab^{-1}
$\Delta\Gamma$	0.16 ps^{-1}	0.03 ps^{-1}
Γ	0.07 ps^{-1}	0.01 ps^{-1}
$A^s_{\rm SL}$	0.006	0.004
$A_{\rm CH}$	0.004	0.004
$\mathcal{B}(B_s \to \mu^+\mu^-)$	-	$< 8 \times 10^{-9}$
$\lvert V_{td}/V_{ts}\rvert$	0.08	0.017
$\mathcal{B}(B_s \to \gamma\gamma)$	38%	7%
β_s (angular analysis)	20°	8°
β_s ($J/\psi\phi$)	10°	3°
β_s ($K^0\bar{K}^0$)	24°	11°

LHCb and enrich the search for new physics in flavour decays by accumulating several ab^{-1} of data at the $\Upsilon(5S)$ resonance [224].

Measuring an absolute branching fraction in a hadronic environment is limited by ones determination of luminosity and the production mechanisms at play. So in addition to being able to study these B_s golden modes, it is anticipated that there will be benefits to the field when interpreting some LHCb analyses if one can obtain precision measurement of at least one absolute branching fraction from Super$B$. In order to measure an absolute branching fraction with precision it will be necessary to study a number of B_s decays at the $\Upsilon(5S)$. In time and with an understanding of the performance of LHCb, it will be possible to identify a full list of useful branching fractions to measure at Super$B$ and thus understand better how much data to record at the $\Upsilon(5S)$ resonance.

D. White paper contribution on B_s physics

This may fit in to the TDR, but should be revisited and re-written

1. *Time Dependent CP Asymmetries at the $\Upsilon(5S)$*

Let us consider a B_s pair produced at the $\Upsilon(5S)$ resonance, through a $B_s^* \overline{B}_s^*$ state. If one of the two B_s mesons decays into a CP eigenstate f and the other to a flavour-tagging final state, the untagged time-dependent decay rate $R(\Delta t)$ as a function of the proper time difference Δt can be written in terms of the parameter $\lambda_f = \frac{q}{p}\frac{\bar{A}_f}{A_f}$ as [241]:

$$R(\Delta t) = \mathcal{N}\frac{e^{-|\Delta t|/\tau(B_s)}}{2\tau(B_s)}\Big[\cosh(\frac{\Delta\Gamma_s\Delta t}{2}) - \frac{2\,\Re(\lambda_f)}{1+|\lambda_f|^2}\sinh(\frac{\Delta\Gamma_s\Delta t}{2})\Big], \quad (63)$$

where the normalization factor $\mathcal{N}$ is fixed to $1-(\frac{\Delta\Gamma_s}{2\Gamma_s})^2$. Here we have neglected CP violation in mixing.

It is not possible to perform a a similar time-dependent analysis to that for the case of $B_d \to J/\psi K^0$ decays, at Super$B$ as the detector would be unable to resolve the very fast B_s oscillations. However, since $\Delta\Gamma_s \neq 0$, the untagged time-dependent decay rate also allows λ_f to be probed, through the $\Re(\lambda_f)$-dependence of the coefficient of the Δt-odd $\sinh(\frac{\Delta\Gamma_s\Delta t}{2})$ term. Such an analysis has been performed by DØ [254, 255]. A "two-bin" time-dependent analysis using this approach is possible at Super$B$.

If one considers the decay $B_s \to J/\psi\phi$ decay, and for simplicity assumes that this is a pure CP-even eigenstate (more generally a full angular analysis can be used to isolate CP-even and CP-odd contributions), it is possible to measure the weak phase of B_s mixing $2\beta_s$. A precision of $\sim 10°$ and $\sim 3°$ can be achieved on β_s, with 1 ab^{-1} and 30 ab^{-1} of integrated luminosity, respectively. There is a two-fold ambiguity resulting from the sign of β_s that can produce almost twice the resolution in the measurement, when β_s has a value close to zero as in the SM. Such a measurement as this is not limited by systematics and the precision can be improved by collecting more data.

While LHCb is expected to achieve a better precision on the measurement of β_s using a tagged analysis of $B_s \to J/\psi\phi$, the strength of Super$B$ lies in the ability to make measurements that are not possible in a hadronic environment, in analogy with the ΔS measurements discussed for B_d decays (Section **??**) there is an effective β_s (denoted $\beta_{s,\rm eff}$) that will form a secondary basis for new physics searches. As with the B_d case it will be necessary to compare the SM expectations of β_s with the measurements from tree decays and with $\beta_{s,\rm eff}$ from penguin-dominated rare decays. Among the interesting final states Super$B$ can study are $B_s \to J/\psi\eta$, $B_s \to J/\psi\eta'$, $B_s \to D_s^{(*)+}D_s^{(*)-}$, $B_s \to D^{(*)}K_S^0$, $B_s \to D^{(*)}\phi$, and $B_s \to \phi\eta'$. Studies on the measurement of the effective β_s using the pure $b \to s$ penguin transition $B_s \to K^0\bar{K}^0$, indicate that Super$B$ will be able to measure this phase with a precision of 11° given 30 ab^{-1} of data.

6. Charm physics

The SM projects a rather mundane weak phenomenology for charm transitions; yet as has been stated since the early discussions about a Tau-Charm Factory in the late 1980's, this fact can be turned to our advantage: detailed studies in particular of CP invariance in charm decays can act as (almost) zero-background searches for physics beyond the SM. While no clear signal for the intervention of NP has been uncovered yet in charm transitions, the situation has changed qualitatively in the last two years:

- $D^0 - \bar{D}^0$ oscillations have been resolved experimentally with x_D, $y_D \sim 0.5 - 1\%$.
- This breakthrough has lead to 'new thinking' among theorists. They have begun to realize that scenarios of NP motivated by considerations *outside* of flavour dynamics can produce an observable footprint in charm decays; i.e., one is no longer forced to invoke the old 'stand-by' of NP scenarios, namely SUSY models with *broken R* parity, to produce observable effects in an ad-hoc fashion. There is every reason to think that this emerging renaissance of creative thinking about charm dynamics will continue and bear novel fruits.

The Super Flavour Factory allows comprehensive charm studies in two different environments:

1. One has the large production rate of charm mesons and baryons at (or close to) the $\Upsilon(4S)$ and can benefit greatly from the Lorentz boost imparted onto the charm hadrons.
2. The Super Flavour Factory design discussed here allows running at the charm threshold region, where one can make use of quantum correlations. With data collected at charm threshold one will also be able to use a D recoil technique to search for rare decays that may be otherwise background dominated. Such recoil analyses in B decays provide useful constraints on scenarios of physics beyond the SM, and the D analogues of these will, in general, also be interesting. The anticipated ultra-high luminosity is again crucial, since high statistics can be achieved with relatively limited running. This will provide a raw sample of 1.8×10^9 D^0 $\overline{D}^0$ and 1.5×10^9 D^+ D^- pairs. We will demonstrate that valuable information relevant to interpretation of the role of NP in charm decays can be made from a sample of ~ 500 fb^{-1} obtained from a Super$B$ run at the $\psi(3770)$. This could be accumulated in a few months' running.

A. On the Uniqueness of Charm

In general NP will induce flavour changing neutral currents (FCNC). The SM had to be crafted judiciously to have them greatly suppressed for strangeness; the weight of FCNC is then even more reduced for the up-type quarks u, c and t. Yet NP scenarios could exhibit a very different pattern with FCNC being significantly more relevant for up-type quarks.

Among those it is only the charm quark that allows the full range of probes for FCNC in general and for CP violation in particular [256]. For top quarks do not hadronize [257] thus eliminating the occurrence of $T^0 - \bar{T}^0$ oscillations. Neutral pions etc. cannot oscillate, since they are their own antiparticles; furthermore CPT constraints are such that they rule out most CP asymmetries.

In general, particles and couplings that enhance FCNC in charm above the SM expectation are distinct from those that contributed to FCNC in the B and K sectors. Thus, charm sector provides a unique window to observe or constrain BSM physics.

B. CPV: Mixing and CPV in mixing, Tools for CPV in mixing/decay

1. Experimental Status

While the existence of $D^0 - \bar{D}^0$ oscillations is considered as established - $(x_D, y_D) \neq (0, 0)$ - the size of x_D, y_D and even their relative strengths are not known with sufficient accuracy to know if *CPV* is manifest in mixing. Their accurate values will hardly shed light on their theoretical interpretation; yet having them is not merely a 'noble goal' (G. Wilkinson), but a practical one: for knowing their values with some accuracy will help validate measurements of the presumably small CP asymmetries, as discussed later.

So far, almost all the information on mixing parameters has come from decays where the final state f is accessible to either D^0 or $\overline{D}^0$. In such cases, deviations from exponential behavior in the number of D^0 ($\overline{D}^0$)'s, $N(\bar{N})$, at time t have been exploited. To second order

in x and y,

$$\begin{aligned} N(t) &= N(0)e^{-\Gamma t} \times [1 + \frac{x^2+y^2}{4}|\lambda_f|^2(\Gamma t)^2 \\ &+ |\lambda_f|(y\cos\overline{\delta_f+\phi_f} - x\sin\overline{\delta_f+\phi_f})(\Gamma t)], \\ \bar{N}(t) &= \bar{N}(0)e^{-\Gamma t} \times [1 + \frac{x^2+y^2}{4}|\lambda_f|^{-2}(\Gamma t)^2 \\ &+ |\lambda_f|^{-1}(y\cos\overline{\delta_f-\phi_f} - x\sin\overline{\delta_f-\phi_f})(\Gamma t)], \end{aligned} \quad (64)$$

where $\lambda_f = \left(q\bar{\mathcal{A}}_f\right)/\left(p\mathcal{A}_f\right)$, $\phi_f = \psi_f + \phi_m$, and $\phi_m = \arg q_D/p_D$. The first and second terms in Eq. (64) correspond, respectively, to direct decay ($D^0 \to f$) [4], and to decay after mixing ($D^0 \to \overline{D}^0 \to f$). The third term, linear in t, is due to the interference between these two.

The decay amplitudes $\mathcal{A}_f$ and $\bar{\mathcal{A}}_f$ describe, respectively, the processes $D^0 \to f$ and $\overline{D}^0 \to f$ with relative strong (weak) phases δ_f (ψ_f). This phase is generally unknown, and this limits the measurability of x_D and y_D to quantities rotated by δ_f. However, in decays to self-conjugate multi-body states (the "golden channels") such as $K^0_S h^+h^-$, $h = \pi$ or K, where f is expressible as a combination of *CP* odd and even eigenstates, δ_f is zero (or π), making it possible to measure x_D, y_D, (and $|q_D/p_D|$ and ϕ_m) directly, with a time-dependent Dalitz plot (TDDP) analysis of the final, 3-body system.

Three kinds of successful mixing parameter measurements have exploited the linear dependence of the interference term in Eq. (64) on x_D and y_D (both $\ll 1$): Wrong-Sign (WS) decays $D^0 \to K^+\pi^-$; decays to *CP* eigen-states h^-h^+ ($h = K$ and $h = \pi$); and decays to 3-body states ($K^+\pi^-\pi^0$, $K^0_S\pi^+\pi^-$ and $K^0_S K^+K^-$).

WS semi-leptonic decays $D^0 \to X^+\ell^-\bar{\nu}_\ell$ have also been examined for mixing. Such decays can only arise from mixing ($D^0 \to \overline{D}^0$) followed by decay, so their time-dependence is described by the second term alone in Eq. (64). The rates, proportional to $(x^2+y^2)/4 \sim 5\times10^{-5}$, are very small, however, and only upper limits have been found so far.

Evidence for $D^0\overline{D}^0$ oscillations was found by *BABAR* [258] and confirmed by CDF [259] from WS decays $D^0 \to K^+\pi^-$ by comparing their time-dependence with that for decays to the Right-Sign (RS) final state, $f = K^-\pi^+$. In the WS case, direct decays are doubly Cabibbo-suppressed (DCS), so $|\lambda_f| \gg 1$ and deviations from exponential are quite large. By contrast, such deviations for RS decays are negligible. Even assuming *CP* conservation ($\phi_m = \phi_f = 0$), the strong phase difference $\delta_{K\pi}$ between D^0 and $\overline{D}^0$ decays to $K^+\pi^-$ is virtually unknown, making it possible only to measure x'^2 and y', where x', and y' are (x_D, y_D), rotated by angle $\delta_{K\pi}$

$$\begin{aligned} x' &= x_D\cos\delta_{K\pi} + y_D\sin\delta_{K\pi} \\ y' &= y_D\cos\delta_{K\pi} - x_D\sin\delta_{K\pi} \end{aligned} \quad (65)$$

and not x and y directly.

Mean lifetimes, τ_{hh}, of decays to *CP*-even states $f = h^+h^-$ (where $h = \pi$ or K) are related to y_{CP}, the value of y_D if *CP* is conserved. With *CP* conservation, y_{CP} is given by

$$y_{CP} \approx \frac{\tau_{K^-\pi^+}}{\tau_{hh}} - 1, \quad (66)$$

where $\tau_{K^-\pi^+}$ is the lifetime for the mixed-*CP* state $f = K^-\pi^+$.

Measurements of y_{CP} by Belle [260] and *BABAR* [261, 262] show evidence for mixing ($y_{CP} \neq 0$) at a level of at least 3σ in each case, and are in good agreement. The world average for all measurements is $1.107 \pm 0.217\%$ [263].

WS decays to three-body final states $K^+\pi^-\pi^0$ have been studied by *BABAR* [264]. In these decays, the final state f is specified by its position (s_1, s_2) in the Dalitz plot (DP) representing the phase space available to the three-body system. The coordinates are two of the three squared invariant masses. Eq. (64) applies for each point in the DP so, with a model for the variation of strong phase $\delta(s_1, s_2)$ over the DP due to final state interactions, both x_D and y_D are measurable through the interference term in which they are linear. However, since there is an unknown, strong phase $\delta_{K\pi\pi}$, arising from the decay, only x'' and y'' (x_D and y_D, respectively, rotated by the $\delta_{K\pi\pi}$) are measurable. However, unlike the 2-body decay to $K^+\pi^-$, these rotated parameters are both linear, not quadratic as in WS $K^+\pi^-$ decays - a distinct advantage.

Golden channel decays (to 3-body self-conjugate states) do not suffer from the unknown strong decay phase, so measurement of x_D and y_D are, possible. Measurements of the $K^0_S\pi^+\pi^-$ final state carried out by Belle [265] and *BABAR* [266] have uncertainties in x_D and y_D of $\sim 3\times10^{-3}$. In each case, uncertainties in the assumptions made in the decay models used to describe the strong phase variations in the DP introduce irreducible systematic uncertainties of $\sim 1 \times 10^{-3}$.

2. Combination of measurements and CPV

Asymmetries between D^0 and $\overline{D}^0$ event samples have also been measured, providing information on the *CP* mixing parameters $|q_D/p_D|$ and $\arg(q_D/p_D)$. In 3-body decays to self-conjugate final states, these parameters can be determined directly from time-dependent effects on the Dalitz plot population. Asymmetries in

[4] Charge-conjugate modes are implicitly included unless noted otherwise.

direct decay rates (either allowing $\mathcal{A}_{\bar{f}} \neq \bar{\mathcal{A}}_f$ or not) have also provided information on direct *CPV*. However, all these asymmetries are, so far, consistent with zero.

In all, 28 mixing observables have been measured. The Heavy Flavor Averaging Group (HFAG) has included these, with their covariances, in a χ^2 fit to obtain mixing parameter values [263], both allowing for *CPV* and requiring *CP* conservation. The values obtained from this *CPV* fit are

$$\begin{aligned} x &= (0.98^{+0.24}_{-0.26})\ \% & y &= (0.83 \pm 0.16)\ \% \\ |q_D/p_D| &= 0.87^{+0.17}_{-0.15} & \phi_M &= (-8.5^{+7.4}_{-7.0})^\circ \\ \delta_{K\pi} &= (26.4^{+9.6}_{-9.9})^\circ & \delta_{K\pi\pi} &= (14.8^{+20.2}_{-22.1})^\circ \end{aligned}$$

To summarize, mixing has clearly been established, but so far there is no evidence for *CPV* in charm decays. As shown later, measurements of x_D depend heavily on the golden channels, and of y_D on the y_{CP} results. Uncertainties in x_D and y_D are of order 2×10^{-3}, too large to detect *CPV* differences between D^0 and $\bar{D}^0$.

C. Rare decays (FCNC)

1. $D^0 \to \mu^+\mu^-,\ \gamma\gamma$

$D^0 \to \mu^+\mu^-$ has, potentially, the cleanest experimental signature if seen at rates greater than $D^0 \to \gamma\gamma$. However, its rate suffers greatly from helicity suppression and the need for weak annihilation – two effects that are basically model independent. In the SM the rate is estimated to be greatly dominated by long-distance dynamics – yet on a very tiny level [267]:

$$\begin{aligned} \mathrm{BR}(D^0 \to \mu^+\mu^-)_{\mathrm{SM}} &\simeq \mathrm{BR}(D^0 \to \mu^+\mu^-)_{\mathrm{LD}} \\ &\simeq 3 \cdot 10^{-5} \times \mathrm{BR}(D^0 \to \gamma\gamma)_{\mathrm{SM}}. \end{aligned} \tag{67}$$

With the SM contribution to $D^0 \to \gamma\gamma$ again being dominated by long-distance forces [267]

$$\mathrm{BR}(D^0 \to \gamma\gamma)_{\mathrm{SM}} \simeq \mathrm{BR}(D^0 \to \gamma\gamma)_{\mathrm{LD}} \sim (1 \pm 0.5) \cdot 10^{-8}\ , \tag{68}$$

one infers

$$\mathrm{BR}(D^0 \to \mu^+\mu^-)_{\mathrm{SM}} \sim 3 \cdot 10^{-13}, \tag{69}$$

to be compared with the present bounds

$$\mathrm{BR}(D^0 \to \mu^+\mu^-)_{exp} \leq 5.3 \cdot 10^{-7}, \tag{70}$$

$$\mathrm{BR}(D^0 \to \gamma\gamma)_{exp} \leq 2.7 \cdot 10^{-5}. \tag{71}$$

The bound of Eq.(71) implies a bound of 10^{-9} in Eq.(70) – i.e., a much tighter one. In either case there is a rather wide window of opportunity for discovering NP in $D^0 \to \mu^+\mu^-$. As pointed out in [268] in several NP models there is actually a relatively tight connection between the NP contributions to $\mathrm{BR}(D^0 \to \mu^+\mu^-)$ and x_D.

Specifically, LHT makes short-distance contributions to $D^0 \to \mu^+\mu^-$ and $D^0 \to \gamma\gamma$ that can be calculated in a straightforward way as a function of viable LHT parameters. Their size is under active study now [269]. No matter what drives $D^0 \to \gamma\gamma$ - whether it is from short or long distance dynamics – it provides a long distance contribution to $D^0 \to \mu^+\mu^-$. For a proper interpretation of these rare D decays it is thus important to search for $D^0 \to \gamma\gamma$ with as high a sensitivity as possible.

2. $D \to l^+l^-X$

It has been suggested that studying $D \to \gamma X$ etc. is very unlikely to allow establishing the presence of NP because of uncertainties due to long distance dynamics [267]. The same strong caveat probably applies also to $D \to l^+l^-X$, unless a CP asymmetry is observed there, in particular in the lepton spectra. However, BaBar's experimental limits on the $D^+ \to \pi^+l^+l^-$ branching fractions [270], obtained with 288 fb^{-1}, are about an order of magnitude above the theoretical calculations based on long-distance effects [271]. Therefore, the high SuperB luminosity should enable probing of these effects, as well as provide hadronic-mode measurements needed to improve the calculations. For many $D^0 \to Xl^+l^-$ decays, the only existing upper limits are from searches by CLEO [272], performed with 3.85 fb^{-1}. There is clearly much room for improvement in these modes.

D. Experimental possibilities for rare decay searches at Super$B$

The scale for rare decay rates at Super$B$ is set by the numbers of D mesons that will be produced. From a 75 ab^{-1} sample at $\Upsilon(4S) \sim 7.5 \times 10^{10}$ are expected. A 500 fb^{-1} sample at $\psi(3770)$ produces $\sim 2 \times 10^9$. A special advantage in rare decay searches from the use of events at threshold is that backgrounds are extremely low, in most instances.

The Super$B$ reach can be estimated for the $D^0 \to \mu^+\mu^-$ rate from current measurements from *BABAR* (and Belle). The best published limit on the $D^0 \to \mu^+\mu^-$ rate so far is from *BABAR* (13×10^{-7}) [273]. Lower, unpublished limits are also available now: 4.3×10^{-7} from CDF [274] (360 pb^{-1}, unpublished) and 1.4×10^{-7} from the Belle collaboration [275]. A further, similar result from *BABAR* is also imminent.

Results from neither of these experiments are yet limited by systematic uncertainty. The major source

of background in each case is from $D^0 \to \pi^+\pi^-$ decays, where the π's either decay in flight to μ or are mis-identified by the PID devices. This background peaks at a mass below, but has a significant tail in the $\mu^+\mu^-$ invariant mass signal region. There is also a flat, combinatorial background from semi-leptonic B decays that is hard to eliminate. These two sources account for 90% of the background.

In the significantly larger Super$B$ samples from $\Upsilon(4S)$ running, these backgrounds should be relatively simple to parameterize, and the major limiting factor should be the uncertainty in their shapes. It is reasonable to assume that limits in the lower 10^{-8} level should be achievable. For comparison, the LHCb experiment can also reach a level of about $2,5 \times 10^{-8}$ before reaching a systematic limit.

Prospects for searches for these decays in a Super$B$ run at threshold could provide an interesting opportunity in the search for NP. Further study is, however, still required and is ongoing. BES III estimates are for a limit of 1.7×10^{-6} per fb^{-1}, but this estimate cannot be easily scaled up to the 500 fb^{-1} anticipated at Super$B$.

At the $\psi(3770)$, there will be no background from B decays of course, but the most serious background will come from $D^0 \to \pi^+\pi^-$ decays. The D^0's are produced with virtually no transverse momentum so, in this view, the muons have equal and opposite momenta - an excellent kinematic signature that should help reduce the number of $\pi^\pm \to \mu^\pm\nu_\mu$ decays in flight, which confuse PID selectors. The muons from $D^0 \to \mu^+\mu^-$ decays will have laboratory momenta of $\sim 0.9 - 1.0$ GeV/c, a range where none of the *BABAR* PID devices would work well in separating them from pions. Super$B$ PID systems, however, should perform significantly better. Many of the muons will hit the end-caps where a TOF device, one of the Super$B$ options being considered, should perform well. The focusing DIRC option for the barrel PID system should also perform significantly better in distinguishing μ from π than the *BABAR* DIRC in this momentum range. Kinematic separation of $\pi^+\pi^-$ and $\mu^+\mu^-$ modes is also attainable, making use of the beam energy constraints used in many CLEO-c analyses. These issues are under simulation study at this time. It is conceivable that running at charm threshold will open up the low 10^{-8} or high 10^{-9} range of sensitivity, a very interesting range for this important branching fraction.

Decays of $D^0 \to e^+e^-$ and (LFV) $D^0 \to e^\mp\mu^\pm$ should also be accessible at rates that can be estimated from current *BABAR* and Belle results. The first of these decays is predicted to be $\sim 10^{-18}$, by the SM. The LFV modes can occur in the SM at a rate $\sim 10^{-14}$. Observation of these modes at Super$B$ would require explanation beyond the SM.

The best rates so far, $\mathcal{B}(D^0 \to e^+e^-) < 7.9 \times 10^{-8}$ and $\mathcal{B}(D^0 \to e^\pm\mu^\mp) < 2.6 \times 10^{-7}$ are preliminary from Belle [275]. In the modes with electrons, more background will exist from γ conversions, but PID would be more reliable than for the $\mu^+\mu^-$ mode. Super$B$ should be able to achieve rates an order of magnitude lower than this.

Upper limits on the $D^0 \to \gamma\gamma$ decay rate, of importance in estimating long range effects in SM calculations of rare decay modes such as $D^0 \to \mu^+\mu^-$, have been published. The best so far ($< 2.9 \times 10^{-5}$) comes from CLEO [276] using a 13.8 fb^{-1} sample taken at $\Upsilon(4S)$. *BABAR* should publish a limit in the region of 2.5×10^{-6} in the near future using 481 fb^{-1}. Extending this to Super$B$, it is possible to reach the mid to low 10^{-7} range at the $\Upsilon(4S)$.

Prospects for a measurement of the $D^0 \to \gamma\gamma$ decay rate at threshold are good. A recent CLEO-c thesis [277] demonstrates an efficiency for this mode at 5.2%, with no background events detected in a 818 pb^{-1} sample at $\psi(3770)$. A reasonable projection from this is that a limit of a few times 10^{-7} can be achieved, a very useful clarification of the SM and of the true $D^0 \to \mu^+\mu^-$ rate.

1. $D \to l^+l^-X$

The Super$B$ reach can be estimated from limits in these modes obtained by the *BABAR* collaboration [270] using a 288 fb^{-1} sample. These are a few parts per million for D^+ modes and a factor three larger for D_s. Best limits for D^0 modes are in the 10^{-3} to 10^{-4} range [272] from a 3.85 fb^{-1} sample. One of the largest backgrounds in all cases again comes from semi-leptonic B decays. With a 75 ab^{-1} sample, this can be modeled quite well from data sidebands - more precisely than in *BABAR*. It is reasonable to expect that rates an order of magnitude lower can be achieved, pushing several rates within the range of SM predictions [267, 271] from long range effects. At charm threshold, CLEO-c can probe rates for decays of D^+ and for D_s in the few times 10^{-6} range [278], comparable to rates from *BABAR*. The projection to a run of 500 fb^{-1} at threshold, therefore, Super$B$ could outperform results from the $\Upsilon(4S)$ by a factor ~ 2.

Better estimates for the reach achievable in the modes discussed will require more simulation, mostly because PID devices are an important component of each result. Super$B$ PID should, in all cases, be superior to *BABAR*, so these limits may err on the conservative side. More information from CLEO-c data, as yet unpublished, should also be forthcoming. This can be used to improve on estimates of the expected performance from data at charm threshold.

E. At the psi(3770)

If taken sufficiently early in the Super$B$ run plan, the data sample at $\psi(3770)$ could lead to significant discoveries in a much shorter period than would be possible without it. One example is the search for $D^0 \to \mu^+\mu^-$ decay. If this occurs at a rate of a few times 10^{-8}, a sure sign of NP, a signal could be seen in $\Upsilon(4S)$ data only after the full 75 ab^{-1} sample is analyzed. Meanwhile, the LHCb experiment will have already seen this signal too. The same signal could be seen in the $\psi(3770)$ data that could be taken in a few months' running at reduced luminosity [5]. Were this data taken early in the Super$B$ schedule, a more competitive, and complementary discovery would be possible much sooner.

There are many good reasons to collect events at (or near) charm threshold. For such events, tagging those in which one D meson is identified, the other D can be studied with very small background contamination. These can, therefore, be used to search for rare decays and, potentially, asymmetries that are especially sensitive to backgrounds.

In several charm studies, particularly those involving leptonic or SL decays of charm particles, the CLEO-c collaboration has shown that data with an integrated luminosity of 818 pb^{-1} of data taken at the $\psi(3770)$ can provide measurements that are competitive with, or superior to, those from approximately three orders more data from *BABAR* and Belle at the $\Upsilon(4S)$. The proposed 500 fb^{-1} data sample at $\psi(3770)$, almost 1% of the integrated luminosity anticipated at $\Upsilon(4S)$, and the availability of time-dependent information in the decays from the (albeit modest) boost, represent an even richer prospect for discovery.

Running at charm threshold also provides an essential check on any new discovery in $\Upsilon(4S)$ data. A confirmation and possible clarification of the result can made more easily in a different charm production scenario than in a repetitive study with a significantly enhanced sample at $4S$.

Quantum correlations in decays of D pairs from $\psi(3770)$ can lead to measurements of their relative strong phases. It is conceivable that, with the Super$B$ boost, any weak phase could, in principal, also be studied, though the precision achievable requires further study.

In addition to the aforementioned studies, one could test for possible *CPT* violation in $D^0\overline{D}^0$ decays, which could be manifest through Lorentz violation (For example see Refs. [279–281]) or decoherence effects (For example see Ref. [282] and references therein) of the correlated wave-function of the neutral mesons. This is an interesting area that needs to be studied, as *CPT* could be violated in different ways in K, D, and B meson states.

Below, we summarize a few specific areas where $\psi(3770)$ data have already been noted to add to the physics reach from that achievable with $\Upsilon(4S)$ data.

- *Search for $D^0 \to \mu^+\mu^-$*

  These rare decays are a clean signal for new physics, if seen. At $\Upsilon(4S)$, our upper limit should be in the low to mid 10^{-8} range when PID efficiency (for mis-identification) will limit our reach. At $\psi(3770)$, we would rely on kinematic separation in addition to PID, so a lower limit is conceivable, provided that kinematic resolution is sufficiently good. This needs further study, but we can expect to achieve a limit similar to that from $\Upsilon(4S)$ data.

- *Improved precision in mixing parameters x_D and y_D*

  Running at $D\bar{D}$ threshold allows independent measurements of strong phases $\delta_{K\pi}$, $\delta_{K\pi\pi}$, etc.. for channels that we will use for mixing measurements at the $\Upsilon(4S)$. In Table XV and Figs. 19(c) and (d), results that might be expected from inclusion of such measurements of $\delta_{K\pi}$ from the 10 fb^{-1} threshold sample expected to come from BES III and also what we would expect from a 500 fb^{-1} at Super$B$ are indicated. As can be seen, running at threshold brings a factor 2 in precision of the measurements of x_D and y_D.

  A large part of this improvement comes from a model independent strong phase measurement over the $K^0_S h^+h^-$ Dalitz plots. This improvement will also apply to measurements of CKM γ that are limited by these models. The improvement should be a factor 3 or more than that which will be available from BES III data from $\psi(3770)$.

- *Measurement of a_{SL}*

  This parameter cannot be measured well at $\Upsilon(4S)$. We expect a precision of only about ± 0.8 from the small sample of WS SL decays. Prospects are somewhat better at the $\psi(3770)$, using WS $K\pi$ decays to obtain a precision of about 20%. This situation could improve to a more useful level if, following studies with CLEO-c data yet to be made, we find that we are able to use events in which both D^0's decay to SL modes.

[5] A re-configuration of the final focus is required for such a run. The machine is designed to make this possible in a period of order one month. It is unlikely that the $\psi(3770)$ run could require as much as a whole year to complete.

- *Time-Dependent Measurements*

  A study needs to be made to see if time-dependent correlations in D decays from $\psi(3770)$ can provide any information on weak phases in the charm sector, a signal for NP.

- *Impact on the measurement of γ*

  Measurements of D decays at charm threshold can be used to reduce model uncertainties on the extraction of γ, not only for Super$B$, but also LHCb. See Section 4 F 9 for more details.

1. Time-dependent CP violation

TO COMPLETE ...

2. Quantum correlations and strong phase measurement at threshold.

3. Measurements of strong phases

Data taken at the $\psi(3770)$ ($D\bar{D}$ threshold), allow independent determination of the strong phases δ_f [283, 284]. Using the coherence of D^0 and $\overline{D}^0$ pairs from $\psi(3770)$ decays, values of the strong phases δ_f have been obtained by the CLEO-c collaboration [201, 285]. An 818 pb^{-1} sample of such decays for $\delta_{K\pi} = (50^{+38}_{-28})^\circ$ (for $D^0 \to K^+\pi^-$) and $\delta_{K\pi\pi} = (59^{+32}_{-28})^\circ$ (for $D^0 \to K^+\pi^-\pi^0$) [6]. We note that the overall phase for $K^+\pi^-\pi^0$ decays is not quite what is required to convert x'' and y'' to x_D and y_D since the population of the quantum-correlated DP's for events from the 818 pb^{-1} sample is not quite the same as that observed in freely decaying D^0's. A re-averaging process would be required. In the projections presented here, however, we simply shift the central values as outlined to agree with the *BABAR* central values for x_D and y_D.

These results are less precise than the indirectly determined values from the HFAG averages. More $\psi(3770)$ data is forthcoming, however, from BES III which should improve this estimate by a factor ~ 6. A 500 fb^{-1} Super$B$ run (approximately the same integrated luminosity as that accumulated by the *BABAR* experiment) at threshold would improve on the CLEO measurement by a factor ~ 25, so should add much to the precision of the mixing parameters. We examine this possibility in Section 6 H 1.

[6] We take the results from the fit made without input from other mixing measurements, and adjust for a 180° difference in phase definition used in this paper.

More interestingly, threshold data also provides a measurement of point to point variations in strong phase over the $K^+\pi^-\pi^0$ and $K^0_S\,h^+h^-$ Dalitz plots that is independent of any model. The precision and granularity required of such measurements, *per se*, is hard to assess without detailed simulation, but it should add a valuable reality check to any of the decay amplitude models presently in use. Such information will clearly, therefore, reduce the model uncertainties inherent in both TDDP mixing measurements as well as in those of CKM γ that also requires such phase information [197].

4. Theoretical Interpretation

Most authors have concluded that effects even as 'high' as $x_D \simeq 1\% \simeq y_D$ could conceivably be generated by SM dynamics alone (see, e.g., [256, 286**?** –288]). Some, however, think that x_D in particular might contain a sizable or even large contribution from NP [256]. Short of a breakthrough in our computational powers – one that lattice QCD seems unlikely to achieve – this issue cannot be decided by theoretical means.

The current world average value of x_D, appears to lie at the tantalizingly high end of SM expectations. The new TDDP analysis by the *BABAR* collaboration [266] of the golden channels, however, indicates a value that is consistent with zero. This will reduce the average considerably, to little more than 3σ from zero. To make progress in understanding what role (if any) new physics beyond the SM plays in the charm sector, we not only need to know how large x_D is, but also to understand at what level *CPV* occurs in either mixing or in decay. Such effects will show up in asymmetries in effective values for x_D (or y_D) obtained from separated samples of D^0 and $\overline{D}^0$ decays. To answer either of these questions will require measurements of x_D with a precision at least of the order of 10^{-4}.

5. Rare Decays

TO COMPLETE ...

F. Semileptonic D, D_s decays

TO COMPLETE ...

G. Leptonic decays and f_{D_s}

TO COMPLETE ...

H. Measuring x_D and y_D at Super$B$ using $\Upsilon(4S)$ and $\psi(3770)$ data

At Super$B$, we will address this situation in several ways. First, sample sizes at the $\Upsilon(4S)$ will be much larger, thereby improving statistical precision on all current measurements by a factor ~ 12. Simulation studies have shown that Super$B$ also provides improved D^0 decay time resolution that effectively enhances this statistical significance by a further factor ~ 1.5 in event yield [289] though, to be conservative, we do not include this in our estimates.

Secondly, in addition to x_D and y_D, TDDP analyses of golden decays can provide direct measurement of the *CPV* parameters $|q_D/p_D|$ and ϕ_m that should now approach a level where *CPV* could be identified.

Super$B$ will use data from $\psi(3770)$, anticipated to come on the Super$B$ time-scale from BES III, to overcome the limitation imposed by uncertainty in the models used to define the strong phase structure in the golden channel DP's. Such data can also add information on δ_f required for mixing measurements in other channels.

Further improvements would also come from Super$B$ data from a dedicated 500 fb^{-1} run at the $\psi(3770)$. We estimate that this should improve precision in x_D (and y_D) by a factor two and to come close to the goal of $\sim 10^{-4}$ [7].

1. *Projections for mixing measurements at SuperB*

Realistic estimates for the Super$B$ mixing reach can be made on the basis of what has been achieved with *BABAR*'s accumulation of 482 fb^{-1} running at the $\Upsilon(4S)$. Also, by projecting results already obtained by CLEO-c, we can estimate the gain we might expect from the measurement of strong phases from $D\bar{D}$ threshold data either from BES III, or from a 500 fb^{-1} Super$B$ sample [8].

In Fig. 19(a) the four main mixing results from *BABAR* are shown combined into average values for (x_D, y_D). To compute this average we used a χ^2 minimization technique, similar to that employed by HFAG [263], which includes effects from correlations between the measured observables, (x'^2, y') from WS $D^0 \to K^+\pi^-$ decays [258], (x'', y'') from TDDP analysis of $K^+\pi^-\pi^0$ [264], y_{CP} from both tagged [261] and untagged [262] samples of $D^0 \to h^-h^+$ decays and (x_D, y_D) from the combined $K^0_S\, h^+h^-$ golden channel samples [290] ($h = \pi, K$). In each case, results are based upon the assumption of no *CPV*

We are omitting other mixing results anticipated to come from *BABAR* data that should also be projected to Super$B$. These include three further golden channels - $D^0 \to h^+h^-\pi^0$, $D^0 \to K^+K^-\pi^+\pi^-$, $D^0 \to K^0_S\pi^+\pi^-\pi^0$. A joint analysis of the channels $D^0 \to K^0_S K^\mp\pi^\pm$ is also anticipated.

The averages obtained are reported in Table XV. The figure indicates the 68.3% confidence region that each of these measurements covers in the (x_D,y_D) plane. It is evident that the most precise information on x_D comes from the golden channels (black ellipse) and, for y_D, from the y_{CP} results (horizontal band).

TABLE XV: Mixing parameters (x_D,y_D) and strong phases $\delta_{K\pi}$ and $\delta_{K^+\pi^-\pi^0}$ obtained from χ^2 fits to observables obtained either from *BABAR* or from their projections to Super$B$. Fit a) is for 482 fb^{-1} from *BABAR* alone and this is scaled up in b) to 75 ab^{-1} at $\Upsilon(4S)$ for Super$B$. In each case, no input from measurements of strong phase is included. Fit c) includes strong phase information projected to come from a BES III run at $D\bar{D}$ threshold, and d) is what would be possible from a 500 fb^{-1} $D\bar{D}$ threshold run at Super$B$. For each of these scenarios, the uncertainties due to statistical limitation alone are entered, in parentheses, on the line below the results for the corresponding fit. In all but fit a) (*BABAR* results) the central values have no meaning.

Fit	$x \times 10^3$	$y \times 10^3$	$\delta^\circ_{K^+\pi^-}$	$\delta^\circ_{K^+\pi^-\pi^0}$
(a)	$3.01^{+3.12}_{-3.39}$	$10.10^{+1.69}_{-1.72}$	$41.3^{+22.0}_{-24.0}$	43.8 ± 26.4
Stat.	(2.76)	(1.36)	(18.8)	(22.4)
(b)	$xxx^{+0.72}_{-0.75}$	$xxx \pm 0.19$	$xxx^{+3.7}_{-3.4}$	$xxx^{+4.6}_{-4.5}$
Stat.	(0.18)	(0.11)	(1.3)	(2.9)
(c)	$xxx \pm 0.42$	$xxx \pm 0.17$	$xxx \pm 2.2$	$xxx^{+3.3}_{-3.4}$
Stat.	(0.18)	(0.11)	(1.3)	(2.7)
(d)	$xxx \pm 0.20$	$xxx \pm 0.12$	$xxx \pm 1.0$	$xxx \pm 1.1$
Stat.	(0.17)	(0.10)	(0.9)	(1.1)

This fit procedure is repeated on projections to various Super$B$ scenarios. The first of these, in Fig. 19(b), shows expectations of measurements solely from a 75 ab^{-1} run at the $\Upsilon(4S)$. To compare with *BABAR* results, the various observables are shifted to correspond to values expected for the x_D and y_D averages for *BABAR*, and are then smeared with correlated uncertainties based on those reported by *BABAR*, and projected to the Super$B$ sample.

[7] We might also speculate on possibilities for time-dependent measurements at threshold utilizing the boost unique to Super$B$, but these studies still have to be made.

[8] In using BES III results, we ignore some differences wrt CLEO-c. BES III has no RICH which will affect the precision of measurements of channels ($D^0 \to K\pi$, for example) where K/π separation is important. We also observe that systematic uncertainties in BES III may take some time to be as well understood as those in CLEO-c.

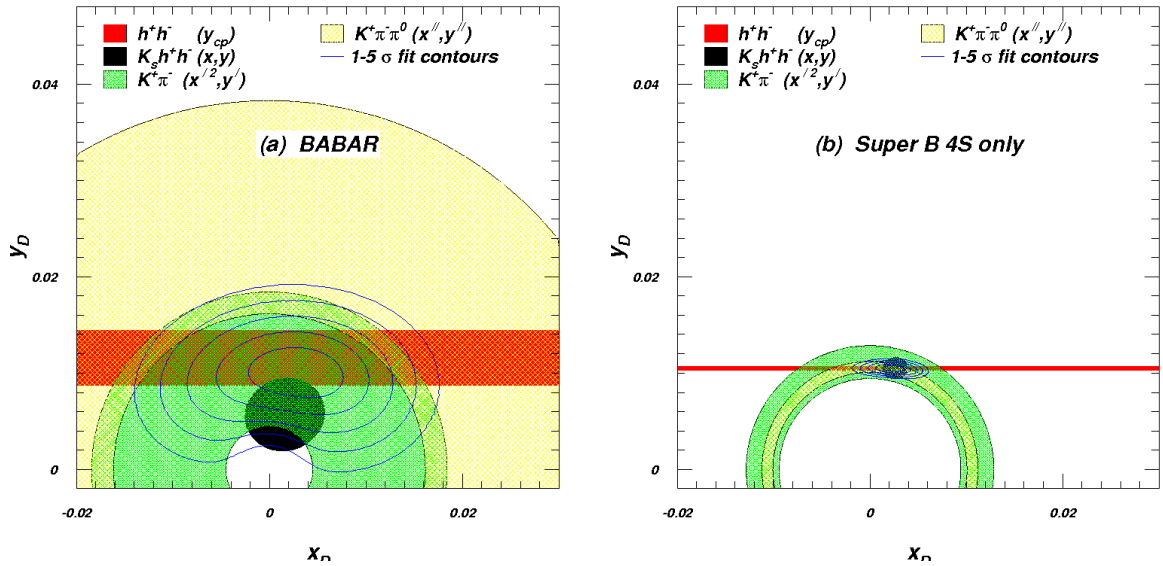

FIG. 19: Mixing observables projected into the (x_D,y_D) plane. Shaded areas indicate the coverage of measured observables lying within their 68.3% confidence region. Contours enclosing 68.3% (1σ), 95.45% (2σ), 99.73% (3σ), 99.994% (4σ) and $1 - 5.7 \times 10^{-7}$ two-dimensional confidence regions from the χ^2 fit to these results are drawn as solid lines. (a) Shows current results from *BABAR* alone. (The $K^+\pi^-\pi^0$ projection is omitted since it obscures much of the area shown); (b) includes results anticipated from a 75 ab^{-1} Super$B$ run at the $\Upsilon(4S)$ only (no data from $\psi(3770)$ running.

In making this projection, it is assumed that statistical and systematic uncertainties will shrink in accordance with the square root of the luminosities - a reasonable assumption since major systematic uncertainties are estimated from data and simulated studies that should scale in this way. The Dalitz plot amplitude model uncertainty in the TDDP of the golden channels is, however, left unchanged. While a better understanding of such models could develop on the Super$B$ time-scale, our conservative assumption is that it will not reduce this uncertainty.

This assumption is treated differently in the three Super$B$ scenarios illustrated in Figs. 20(a)-(c). In these, measurement of strong phases from data taken at $D\bar{D}$ threshold by CLEO-c [201], from data anticipated to come from BES III, and from a dedicated 500 fb^{-1} run at $\psi(3770)$ by Super$B$, are examined. In Fig. 20(a), no such data are included (in fact, CLEO-c results make little difference). BES III measurements are included in Fig. 20(b) and the putative Super$B$ measurements in Fig. 20(c).

Our assumption is that such measurements will not only provide the average strong phases to be used in various channels, but will also improve our DP model. Without detailed modeling of ways to include this, we estimate, a factor 3 improvement in DP model uncertainty for BES III data and a factor 10 for the Super$B$ threshold run.

Averages that result from these assumptions for all scenarios are reported in Table XV.

The most precise localization of x_D and y_D is seen to come from the golden channels, and it is clear that uncertainties in the DP amplitude models represent a limiting factor in this precision. It is also noteworthy that the TDDP measurements for $K^+\pi^-\pi^0$ decays, with linear dependence on x'', provide a better localization of x_D and y_D than do those from the WS $K^+\pi^-$ mode, with dependence only on x'^2.

The most dramatic improvements in precision of x_D and y_D result from a better understanding of DP amplitude models.

LHCb has projected the statistical uncertainties expected in D^0 mixing observables corresponding to a 10 fb^{-1} run [291]. In Table XVI, we compare these projections with the same observables measured in *BABAR* and also with their projections to a 75 fb^{-1} Super$B$ sample at $\Upsilon(4S)$.

Table XV indicates the statistical uncertainties in the values of x_D and y_D expected in the various averaging scenarios. The LHCb collaboration also plans to use 3-body golden channels and decays to the 4-body, self-conjugate state $K^+K^-\pi^+\pi^-$. These channels will, we can assume, benefit from BES III results from $\psi(3770)$ in a way similar to that discussed above. No projections for these modes are yet available, nor are systematic uncertainties.

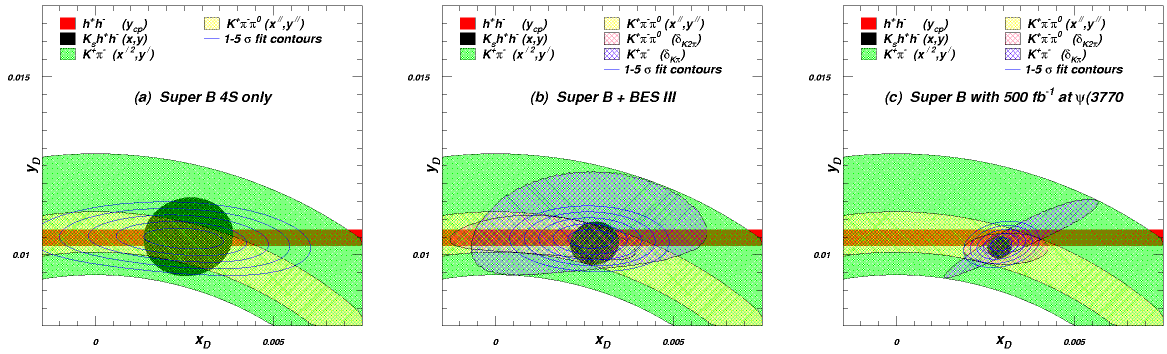

FIG. 20: Mixing observables projected into the (x_D,y_D) plane. Shaded areas indicate the coverage of measured observables lying within their 68.3% confidence region. In (b) and (c), the projections of $\delta_{K\pi}$ and $\delta_{K\pi\pi}$ measurements are also shown. Contours enclosing 68.3% (1σ), 95.45% (2σ), 99.73% (3σ), 99.994% (4σ) and $1-5.7\times10^{-7}$ two-dimensional confidence regions from the χ^2 fit to these results are drawn as solid lines. (a) includes results anticipated from a 75 ab^{-1} Super$B$ run at the $\Upsilon(4S)$ only (no data from $\psi(3770)$ running. In (b) a 10 fb^{-1} threshold run by BES III is estimated to provide a factor three improvement in the uncertainties arising from the Dalitz plot amplitude model, and a factor six in the measurement of the strong phase for $D^0\to K^+\pi^-$ and $K^+\pi^-\pi^0$ decays. In (c) a 75 ab^{-1} Super$B$ run at the $\Upsilon(4S)$ is combined with a 500 fb^{-1} run at the $\psi(3770)$, assumed to reduce DP model uncertainty by a factor 10 and in the strong phases by factor given by the ratio of luminosities wrt CLEO-c. Note that the figures use the SAME vertical and horizontal scales.

TABLE XVI: Event yields and projected statistical uncertainties for various observables for the final *BABAR* sample, a projected 10 fb^{-1} (approximately five year) LHCb run and for a 75 ab^{-1} Super$B$ run at $\Upsilon(4S)$. For *BABAR*, the yields for published mixing results using both D^*-tagged and untagged K^-K^+ and for WS $K^+\pi^-$ events are scaled up from published results to the final integrated luminosity of 482 fb^{-1}. LHCb estimates come from Ref. [291].

Decay Mode	*BABAR*	Super$B$	LHCB
K^+K^- (D^*-tag):			
N (Events)	88×10^3	13.7×10^6	8×10^6
Δy_{CP} (stat)	$\pm3.9\times10^{-3}$	0.28×10^{-3}	0.5×10^{-3}
K^+K^- (no tag):			
N (Events)	330×10^3	51.4×10^6	–
Δy_{CP} (stat)	$\pm2.3\times10^{-3}$	0.19×10^{-3}	–
$K^+\pi^-$ (WS):			
N (Events)	5.1×10^3	0.79×10^6	0.23×10^6
$\Delta y'$ (stat)	$\pm4.4\times10^{-3}$	0.31×10^{-3}	0.87×10^{-3}
$\Delta x'^2$ (stat)	$\pm3.0\times10^{-4}$	0.21×10^{-4}	0.64×10^{-4}

In summarizing these projections, it is clear that interesting levels of sensitivity in mixing measurements in the precision range of 10^{-4}, are achievable both by Super$B$ and LHCb, though Super$B$ can be expected to do better. It is observed that uncertainties in x_D are typically twice those of y_D. This is probably due to the precise y_{CP} measurements. It is also clear that the TDDP analyses for golden channels are most important, and that the main limiting factor for all experiments is the DP model uncertainty. This can be largely mitigated using BES III $\psi(3770)$ data. A further factor two improvement is also possible with a 500 fb^{-1} $\psi(3770)$ run of Super$B$.

2. *Estimated sensitivity to CPV from mixing measurements*

CPV in mixing, or in its interference with decay can reveal information on the underlying parameters in the mass matrix [292], and would have an important bearing on the role of NP. A simple strategy for studying *CPV* is to measure asymmetries in *effective* values (x_D^+,y_D^+) for D^0 and (x_D^-,y_D^-) for $\overline{D}^0$. Systematic uncertainties will be almost identical for D^0 as for $\overline{D}^0$, so their contribution to uncertainties in these differences can be neglected. Statistical uncertainties are listed in Table XV and it is seen that Super$B$ will be sensitive, at the 3σ level, to a difference $x_D^+-x_D^-$ ($y_D^+-y_D^-$) of $5(3)\times10^{-4}$ in the average $x(y)$ values.

If observed, and if they were due to *CPV* in mixing, they would provide a measurement of $|q_D/p_D|$. Neglecting direct *CPV*, $x_D^+\simeq|q_D/p_D|x_D$ and $x_D^-\simeq|p/q|x_D$, with similar relations for y_D^+ and y_D^-. Asymmetries are, therefore, given by

$$a_z=\frac{z^+-z^-}{z^++z^-}\approx\frac{1-\left|\frac{q}{p}\right|^2}{1+\left|\frac{q}{p}\right|^2}, \qquad (72)$$

where z can be $x_D, y_D, y_{CP}, y', x''$ or y''.

This test can be made in different decay modes. If *CPV* originates in the decay, rather than in mixing, then the asymmetries will depend on the mode.

These asymmetries are largely independent of systematic uncertainty. Statistical uncertainties for various *BABAR* analyses are projected to Super$B$ to obtain the precisions in $|q_D/p_D|$ listed in Table XVII. If *CPV* originates in mixing, these asymmetries should be the same in all modes.

For the golden channels, a direct measurement of *CPV* parameters $|q_D/p_D|$ and ϕ_M, is possible. *BABAR* has yet to make this measurement, so the statistical and systematic uncertainties obtained from the Belle analysis [265] are projected, in Table XVII to the Super$B$ luminosity at $\Upsilon(4S)$. Uncertainties arising from the Dalitz plot model will be important, and a Super$B$ run at threshold will increase the *CPV* reach, as indicated in the Table.

A third metric for *CPV* also comes from measurement of the asymmetry:

$$a_{SL} = \frac{\Gamma_{\ell^-} - \bar{\Gamma}_{\ell^+}}{\Gamma_{\ell^-} + \bar{\Gamma}_{\ell^+}} = \frac{|q|^4 - |p|^4}{|q|^4 + |p|^4}, \qquad (73)$$

where Γ_{ℓ^-} ($\bar{\Gamma}_{\ell^+}$) are decay rates for "wrong-sign" semi-leptonic (SL) D ($\bar{D}$) decays. Such decays can only occur, without NP contributions, through mixing, and have a time-dependence $\propto t^2 e^{-\Gamma t}$. Though difficult to measure, this asymmetry can be large. For the current world average value for $|q_D/p_D|$ [263], it is in the 90% confidence range $a_{SL} \in \{+0.3, -0.75\}$. If its measured value is not zero, then it is clear evidence for *CPV* in mixing and, therefore, for NP.

Measurement of a_{SL} using $\Upsilon(4S)$ data can only come from WS, SL decays, so far unseen by any experiment. The precision achievable, $\sigma(a_{SL} \sim \pm\sqrt{S+B}/S$, is limited by the number of background events, B, beneath a WS signal of S events in the sample (of both polarities combined) selected for the measurement.

An estimate of S at Super$B$ can be obtained from RS signals that have been observed by *BABAR*, using the reasonably well-known mixing rate $R_M \simeq 5\times10^{-5}$. Background B under a WS signal can be expected at roughly the same level as under the corresponding RS signal.

With these assumptions, we can estimate $S(B)$ from two *BABAR* observations. The first, a conventional, singly-tagged RS $D^{*+} \to D^0\pi_s^+$ ($D^0 \to K^-e^+\nu_e$ sample Ref. [293] predicts $S(B) \sim 2140(\sim\ 3M)$ events at Super$B$, resulting in an uncertainty, $\sigma(a_{SL}) \sim 0.8$ that is not useful. The second, a double-tagged sample [294], with a reconstructed D or D^* of known flavour on the recoil side is much cleaner and, when projected to Super$B$, predicts a WS signal of $S = 50 \pm 16$ events on a background $B = 195$ leading to $\sigma(a_{SL}) \simeq 0.3$. Improvements in the selection of the latter signal are known, in retrospect, to be possible and can lead to a precision of $\sigma(a_{SL}) \simeq 0.20$. This would result in a measurement of $|q_D/p_D|$ with precision 0.10, listed in Table XVII.

This asymmetry can also be measured in $\psi(3770) \to D^0\overline{D}^0$ decays from the 500 fb^{-1} sample. In this case, three types of event can be used:

$$\begin{aligned} D^0 &\to K\pi \quad ; \ \overline{D}^0 \to K\pi, \\ D^0 &\to X\ell\nu_\ell \ ; \ \overline{D}^0 \to X\ell\nu_\ell, \\ D^0 &\to X\ell\nu_\ell \ ; \ \overline{D}^0 \to K\pi, \end{aligned}$$

in which both D^0 and $\overline{D}^0$ decay to the $K^\pm\pi^\mp$ mode with the same sign K mesons, where both D^0 and $\overline{D}^0$ decay semi-leptonically with leptons of the same sign, or where one of the D's decays semi-leptonically and the other to $K\pi$ where the lepton on one side has the same sign as the K meson on the other. In the first case, Bose symmetry prevents DCS decays to a WS $K\pi$ state so that mixing has to occur in either the D^0 or the $\overline{D}^0$ decay.

CLEO-c has published data with 630 events with a (RS-RS) $K\pi$ on each side, with virtually no background events from their 280 pb^{-1} $\psi(3770)$ sample. Guessing that the background for a (RS-WS) combination (not published) is 0.1 events, then this projects to 56 signal and 178 background events in our putative 500 fb^{-1} sample. This would allow a precision of approximately 26% in a_{SL} (13% in $|q_D/p_D|$). No data on the second mode are published, though studies are underway.

The third mode has, however, been observed by CLEO-c [278] and the electron events are virtually background free. In these cases, however, an ambiguity arises over which decay is WS. The probability for the $K\pi$ decay to be DCS is $\sim 3\times10^{-3}$ and for the SL decay to have been preceded by mixing the probability is $\sim 5\times10^{-5}$. It is possible that the different (and coherent) time-dependencies can be used to distinguish these, but a simulation study must be made to estimate how well this could work.

We can, perhaps, imagine a combined result from all three modes with $\sigma(a_{SL} \sim$ 20% (10% uncertainty in $|q_D/p_D|$). This estimate, with other estimates for *CPV* reach, are included in Table XVII. Asymmetries in other mixing parameters come closer to challenging SM estimates than do those from a_{SL} measurements.

I. CP Violation

1. Generalities

On the phenomenological level one differentiates between two classes of CP violation, namely *indirect* CP

TABLE XVII: Estimates for uncertainties in *CPV* mixing parameters $|q_D/p_D|$ and ϕ_M obtainable at Super$B$ using various methods. Asymmetries a_z and a_{SL} are as defined in the text, and are determined for the observables and channels indicated. Time-dependent Dalitz plot (TDDP) analyses, allowing *CPV*, include scenarios where uncertainties from the decay model are reduced from Belle estimates [265] by either a factor 3 ("BES III DP model") or a factor 10 ("Super$B$ DP model").

Strategy	**Decay**	$\boldsymbol{\sigma(\lvert q_D/p_D\rvert)\times 10^2}$	$\boldsymbol{\sigma(\phi_M)^\circ}$
HFAG (direct *CPV* allowed):			
Global χ^2 fit	<All modes>	± 18	± 9
Asymmetries a_z:			
x_D	<All modes>	± 1.8	–
y_D	<All modes>	± 1.1	–
y_{CP}	K^+K^-	± 3.8	–
y'	$K^+\pi^-$	± 4.9	–
x'^2	$K^+\pi^-$	± 4.9	–
x''	$K^+\pi^-\pi^0$	± 5.4	–
y''	$K^+\pi^-\pi^0$	± 5.0	–
TDDP (*CPV* allowed):			
Model-dependent	$K^0_S h^+h^-$	± 8.4	± 3.3
BES III DP model	$K^0_S h^+h^-$	± 3.7	± 1.9
Super$B$ DP model	$K^0_S h^+h^-$	± 2.7	± 1.4
SL Asymmetries a_{SL}:			
75 ab^{-1} at $\Upsilon(4S)$	$X\ell\nu_\ell$	± 10	
500 fb^{-1} at $\psi(3770)$	$K\pi$	± 10	
500 fb^{-1} at $\psi(3770)$	$X\ell\nu_\ell$	TBD	

violation residing in $\Delta C = 2$ dynamics driving oscillations and *direct* CP violation affecting $\Delta C = 1$ decays. These two sources can produce three classes of effects [295]:

1. 'CP violation *in* $D^0 - \bar{D}^0$ oscillations': due to the SM's selection rules this is most cleanly expressed through a difference in the transitions to 'wrong-sign' leptons:

$$a_{SL}(D^0) \equiv \frac{\Gamma(D^0(t)\to \ell^-\bar{\nu}K^+) - \Gamma(\bar{D}^0\to \ell^+\nu K^-)}{\Gamma(D^0(t)\to \ell^-\bar{\nu}K^+) + \Gamma(\bar{D}^0\to \ell^+\nu K^-)}, = \frac{|q_D|^4 - |p_D|^4}{|q_D|^4 + |p_D|^4}\,. \quad (74)$$

   While the fraction of wrong-sign leptons oscillates with the time of decay, the fractional asymmetry does not. Data tell us that the production rate of 'wrong-sign' leptons in D decays is very low. Yet as illustrated below their CP asymmetry could be rather large.

   It should be noted that also non-leptonic modes of neutral D mesons depend on the quantity $|q_D/p_D|$, see Eq. (76).

2. 'CP violation *involving* $D^0 - \bar{D}^0$ oscillations': it can emerge in non-leptonic final states common to D^0 and $\bar{D}^0$ decays in qualitative, though of course not quantitative analogy to $B_d \to \psi K_S$. Relevant channels are $D^0 \to K_S\phi/\eta$, $K^+K^-/\pi^+\pi^-$, $K^+\pi^-$ on the Cabibbo allowed, once and twice forbidden levels, respectively. CP asymmetries are driven by $|q_D/p_D| \neq 1$ as well as $\mathrm{Im}\frac{q_D}{p_D}\bar{\rho}(f) \neq 0$ with $\bar{\rho}(f) = T(\bar{D}^0 \to f)/T(D^0 \to f)$ denoting the ratio of decay amplitudes. Such asymmetries depend on the time of decay in a characteristic way, which can be well approximated by a linear dependence due to x_D, $y_D \ll 1$:

$$\frac{\Gamma(D^0(t)\to f) - \Gamma(\bar{D}^0(t)\to f)}{\Gamma(D^0(t)\to f) + \Gamma(\bar{D}^0(t)\to f)} \equiv S_f \frac{t}{2\bar{\tau}}, \quad (75)$$

   with

$$S_f = -\eta_f y_D \left(\left|\frac{q_D}{p_D}\right| - \left|\frac{p_D}{q_D}\right|\right)\cos 2\varphi + -\eta_f x_D \left(\left|\frac{q_D}{p_D}\right| + \left|\frac{p_D}{q_D}\right|\right)\sin 2\varphi, \quad (76)$$

   in the *absence* of *direct* CP violation. In that case one has a useful connection between the two

asymmetries listed so far [296, 297]:

$$S_f = -\eta_f \frac{x_D^2 + y_D^2}{y_D} a_{\rm SL}(D^0). \quad (77)$$

3. 'Direct CP violation' characterized by a difference in the moduli of the decay amplitudes describing CP conjugate transitions:

$$|T(D \to f)| \neq |T(\bar{D} \to \bar{f})|. \quad (78)$$

For two-body final states it requires the presence of two coherent amplitudes differing in both their weak as well as strong phases.

Three-body final states with their much richer dynamical structure can provide us with more detailed information about the operators driving these decays [298]. Accordingly they require a more involved analysis. Fortunately a great deal of experience exists on how to deal with it through Dalitz plot studies. A Super Flavour Factory provides a particularly suitable environment, since it allows one to study not only all charged particle final states like $D^\pm \to \pi^\pm\pi^+\pi^-$ but also ones with neutrals like $D^0 \to \pi^+\pi^-\pi^0$ and $D^\pm \to \pi^\pm\pi^0\pi^0$. Comparing transitions with different charge combinations provides insight into the impact of the strong interactions. A working group of theorists and experimentalists has been formed under the name 'Les Nabis' [299] to refine the theoretical tools for Dalitz plot studies to a degree that the huge statistics anticipated from a Super Flavour Factory can be exploited. While a full Dalitz plot description has to be the ultimate goal, achieving it represents a long term task. A model independent method has been proposed in Ref.[298] as an intermediate step at least.

2. SM Expectations

As far as *direct* CP violation in the SM is concerned, it can occur only in singly Cabibbo suppressed channels, but not in Cabibbo allowed and doubly suppressed ones, where one has only a single weak amplitude. Thus any observation of a CP asymmetry in the latter establishes the intervention of NP – except for final states containing K_S mesons, where the CP odd component in the K_S wave function induces an asymmetry [295]. Cabibbo suppressed modes like $D^0 \to K^+K^-$, $\pi^+\pi^-$ are expected to show direct CP violation within the SM, yet only on the $\mathcal{O}(10^{-4})$ level.

While $D^0 - \bar{D}^0$ oscillations are dominated by long distance dynamics within the SM, CP violation can arise there through $|q_D/p_D| \neq 1$ via a deficit in weak universality, albeit only on less than the 10^{-3} level [288]. Time dependent CP asymmetries involving oscillations can arise also in the SM. Since, however, they are driven by terms of the form x_D or $y_D \times {\rm Im}\frac{q_D}{p_D}\bar{\rho}(f)$, they cannot exceed the 10^{-5} level.

In summary: Due to the impact of non-perturbative dynamics that are beyond firm theoretical control one cannot make accurate predictions on SM CP asymmetries in charm decays. Nevertheless one can make highly non-trivial ones, as sketched above, namely that they are at best tiny. One can*not count* on NP creating large CP asymmetries in D transitions, but its manifestations might be clearer here than in B decays; for the SM creates much smaller "backgrounds"; i.e., SM *CP* effects are much larger in B decays than in D decays, thus:

$$\left[\frac{\text{exp. NP signal}}{\text{SM CP "backgr."}}\right]_{\mathbf{D}} > \left[\frac{\text{exp. NP signal}}{\text{SM CP "backgr."}}\right]_{\mathbf{B}}. \quad (79)$$

3. Experimental Landscape

While it is an experimental fact that no evidence for CP violation has emerged in charm transitions so far, one should not over-interpret this statement. In particular, CP asymmetries involving oscillations depend on expressions of the form x_D or $y_D \times$ weak phases and with x_D and $y_D \leq 1\%$ one can hardly exceed the 1% level. To put it differently: only recently has one entered a regime where NP has a chance to induce an observable asymmetry, yet now any improvement in experimental sensitivity could reveal an effect.

CPV in a decay $D \to f$ results in a time-integrated asymmetry

$$A_f = \frac{\Gamma - \bar{\Gamma}}{\Gamma + \bar{\Gamma}}, \quad (80)$$

where Γ is the decay rate, and $\bar{\Gamma}$ is that for the conjugate decay $\bar{D} \to \bar{f}$. For charged D or D_s any asymmetry would arise from direct *CPV*, while for D^0, it could also result from *CPV* in the mixing or the interference between mixing and decay (indirect *CPV*). In this case, for a small asymmetry,

$$A_f = a_d + a_m + a_i, \quad (81)$$

where a_d, a_m and a_i are, respectively, asymmetries resulting from direct CPV in the decay, mixing and from the interference between these.

Until recently, measurements of A_f were limited to a precision of a few times 10^{-2} by two experimental uncertainties. The first arose from an asymmetry of order 10^{-2} in detection and reconstruction efficiency between positively and negatively charged particles that used to be measured using samples of events generated in simulations. These simulations are always limited in the precision with which they can mimic differences in interactions between positive and negative particles and the various detector components. The second

uncertainty arose from the poorly-known production asymmetry inherent in $e^+e^- \to c\bar{c}$ interactions resulting from $Z^0 - \gamma$ interference, and from higher order effects (ISR, FSR, box diagram, etc.) Together with the built-in forward-backward asymmetry in detector efficiency, this led to an unknown apparent asymmetry, also of order 10^{-2}.

A way to overcome these uncertainties has recently been found by the *BABAR* collaboration [300] in their measurement of $A_{K^+K^-}$ from D^*-tagged $D^* \to D^0(\to K^+K^-)\pi_s$ decays. They use data rather than simulations to estimate the charge asymmetry in efficiency for the π_s's, measuring the ratios of π_s to the corresponding $D^0 \to K^-\pi^+$ decay for each charge separately. These ratios should be the same, assuming only that these Cabibbo favored decays exhibit no *CPV*. The uncertainty in the charge asymmetry, once a subject of simulation-limited systematic uncertainty, is thereby limited only by the data sample size. They also eliminated the effect of the production asymmetry simply by evaluating A_f in slices of production angle.

With these innovations, a precision in $A_f^{K^+K^-}$ of 3.6×10^{-3} (upper limit of $\sim$ 1%) was obtained. A_f for $D^0 \to \pi^+\pi^-$ and for $D^0 \to \pi^+\pi^-\pi^0$ modes were also measured with precisions in the range $4 - 5 \times 10^{-3}$ [300, 301].

The Belle collaboration [302] used these technique to obtain a similar precision in the K^+K^- mode, and have recently adapted it to decays of charged mesons in the modes $D^+_{(s)} \to K^0_S\pi^+$ and $D^+_{(s)} \to K^0_S K^+$ [303], obtaining comparable precisions in the few times 10^{-3} range. These decays are expected to have an asymmetry, induced by the *CP*-odd component in K^0_S, of $-2\mathrm{Re}\{\epsilon_K\} \simeq -3.3 \times 10^{-3}$ [304].

Since systematic uncertainties can now be estimated from data, they should scale in the same way as statistical uncertainties. Super$B$, therefore, should be able to achieve a precision of a few parts in 10^{-4} in similar measurements. For these singly Cabibbo-suppressed decays, this is close to SM expectations. Furthermore, the SM limit for $D^+_{(s)} \to K^0_S\pi^+$ and $D^+_{(s)} \to K^0_S K^+$ decays of $\simeq -3.3 \times 10^{-3}$ can be confronted with a truly precise measurement at Super$B$. It is conceivable, therefore, that effects from NP should be observable!

The effects of *CPV* in multi-body final states such as $D^0 \to h^+h^-\pi^0$ will ultimately be more likely to appear in the sub processes of which it is made. For instance, A_f may be expected to be different for $D^0 \to \rho^0\pi^0$ from that for $D^0 \to f_0(980)\pi^0$. Asymmetry in the total $h^+h^-\pi^0$ system would, therefore, probably be diluted. *BABAR* examined this possibility in several ways for these channels [301]. Differences in the (normalized) D^0 and $\overline{D}^0$ Dalitz plot distributions, and their Legendre polynomial moments in each of the three channels were examined for structure. None was found, to a precision of a few parts in 10^{-2}.

Such model-independent tests are virtually free from PID and other experimental asymmetries, since rates are normalized to the total number of events in D^0 and $\overline{D}^0$ Dalitz plots. A 75 fb^{-1} at the $\Upsilon(4S)$ sample from Super$B$ should, therefore, be capable of observing a *CPV* effect, for instance, in $D^0 \to \rho^0\pi^0$ at a few parts per 10^{-3}.

Other tests of *CPV* can also be projected to Super$B$ performance levels. Measurements of the "T-odd" quantity [304]

$$C_T = \vec{p}_{K^+} \cdot (\vec{p}_{\pi^+} \times \vec{p}_{\pi^-}) \,, \tag{82}$$

can provide a sensitive test for $D^0 \to K^+K^-\pi^+\pi^-$ decays. In practice, it is necessary, to eliminate the effects of final state interactions, to measure the difference in asymmetries $A_T - \bar{A}_T$, where

$$A_T = \frac{\Gamma(D^0, C_T > 0) - \Gamma(D^0, C_T < 0)}{\Gamma(D^0, C_T > 0) + \Gamma(D^0, C_T < 0)}, \tag{83}$$

and $\bar{A}_T$ is the corresponding quantity for $\overline{D}^0$ decays. This has recently been measured by the *BABAR* collaboration [305] who find a value $(1.0 \pm 6.7) \times 10^{-3}$. The systematic uncertainty includes a contribution of 3.5×10^{-3} from PID. Improvements in PID are contemplated at Super$B$, so the limiting precision could be somewhat better than this - perhaps 2×10^{-3}.

4. Littlest Higgs Models with T Parity – A Viable Non-ad-hoc Scenario

What has changed over the last two years – and is likely to produce further 'fruits' in the future – is that theorists have developed *non*-ad-hoc scenarios for NP – i.e. ones *not* motivated by considerations of flavour dynamics – that are *not* minimal flavour violating [296, 297].

'Little Higgs' models are motivated by the desire to 'delay the day of reckoning'; i.e., to reconcile the *non*-observation of NP effects in the electroweak parameters even on the quantum level with the possibility to discover NP quanta via their direct production in LHC collisions. A sub-class of them – Little Higgs models with T parity – are *not* minimal flavour violating in general and in particular can generate observable CP violation in charm decays [296]. Since they are relatively 'frugal' in introducing extra parameters, observing their quanta in high p_t collisions would allow one to significantly tighten predictions of their impact on K, D and B decays.

While these models are hard pressed to generate values for $|q_D/p_D|$ *out*side its present experimental range of $0.86^{+0.17}_{-0.15}$, they can well induce it *in*side it;

i.e., they could move $|q_D/p_D|$ much further away from unity than the less than 10^{-3} amount expected for the SM. Likewise they could produce CP asymmetries in $D^0 \to K_S\phi$, K^+K^-, $\pi^+\pi^-$ up to the 1% level; i.e., much larger than the 10^{-5} SM expectation. It should also be noted that in some parts of the parameter space of these models their impact could not be identified in B decays: in particular the CP asymmetry in $B_s \to \psi\phi$ would still remain below 5% as predicted in the SM. Their strongest correlation exists with the branching ratio for the ultra-rare mode $K_L \to \pi^0\nu\bar{\nu}$ [296].

J. Section summary

The section summary should provide a succinct recap of the main points discussed within the section, including (if relevant) summary tables of sensitivitites.

7. Electroweak measurements

A. Introduction

B. $\sin^2\theta_W^e\, ff$ measurements for leptons, charm and beauty from A_{LR}

The combination of high luminosity and polarized electrons at Super$B$ provides a unique opportunity to measure a number of electroweak neutral current parameters with precisions comparable to those obtained at SLC and LEP but at a Q^2 of $(10.58\ \mathrm{GeV})^2$. The cross-sections for $e^+e^- \to \mu^+\mu^-$, as for the other final-state fermions, are sensitive to the beam polarization almost entirely through $Z-\gamma$ interference. Although the asymmetries are small, the Super$B$ sample size will be sufficiently large to yield very interesting physics. This physics program includes precision $\sin^2\theta_W$ measurements with $\mu^+\mu^-$, $\tau^+\tau^-$ and $c\bar{c}$ events as well as measurements of the neutral current vector coupling of the b. Such measurements are sensitive to a Z' and can probe neutral current universality at high precision.

With polarization, Super$B$ will make a relatively straightforward measurement of the left-right asymmetry of $e^+e^- \to \mu^+\mu^-$ in a manner identical to that performed by the SLC collaboration [306, 307] which operated at the Z-pole. SLC measured $\sin^2\theta_W = 0.23098 \pm 0.00026$ where the error includes a systematic uncertainty component of ± 0.00013 dominated by the polarization uncertainty of 0.5%. The ZFITTER software has been used to estimate the level of sensitivity that might be reached at Super$B$ where the left-right asymmetry is be approximately -0.0005. A $e^+e^- \to \mu^+\mu^-(\gamma)$ selection using *BABAR* data had a selection efficiency of 53% for a 99.6% purity. Such a selection will provide a sample of 46 billion μ-pair events at Super$B$ for an integrated luminosity of 75 ab^{-1}. Assuming 80% polarization can be achieved, the statistical error on the left-right asymmetry will be approximately 5×10^{-6} which corresponds to a relative error of $\mathcal{O}(1\%)$. If the polarimeter systematic errors can be kept below this level, the uncertainty on $\sin^2\theta_W$ will be ~ 0.0002, which is competitive with the SLC measurement but at a much lower Q^2. Similar measurements can be made with $e^+e^- \to \tau^+\tau^-(\gamma)$ and with charm, although one would expect the statistical errors to be larger owing to a lower selection efficiency. Nonetheless, those measurements will provide the most stringent tests of neutral current universality.

These precision measurements are sensitive to the same new physics scenarios, such as a Z', being probed by the QWeak experiment at the Jefferson Laboratory, which will measure $\sin^2\theta_W$ to approximately 0.3% at $Q^2 = (0.16\,\mathrm{GeV})^2$. Figure 21 shows the current and planned measurements of $\sin^2\theta_W$.

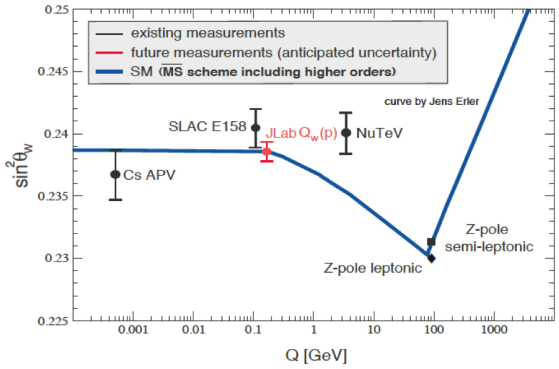

FIG. 21: Summary of experiments that have measured or are proposing to measure $\sin^2\theta_W$ as compiled in [308]. The standard model running of $\sin^2\theta_W$ is overlaid on the data points. Super$B$ will provide a point at $Q = 10.58$ GeV with an error comparable to that of the measurement at the Z-pole.

C. Precision probes of neutral current vector coupling universality

As Super$B$ will be running on the $\Upsilon(4S)$, the left-right asymmetry for B-mesons will be sensitive to the product of the electron neutral current axial coupling and b-quark neutral current vector coupling g_V^b, as described in a proposal for measuring the g_V^s at a ϕ-factory [309]. With one billion reconstructed $B\bar{B}$ events from $\Upsilon(4S)$ decays with an 80% polarized beam, Super$B$ will provide a measurement of g_V^b that is competitive with the measurement from LEP and SLC, $g_V^b = -0.3220 \pm 0.0077$[**?**] but at a lower Q^2. In addition to probing new physics, this measurement will shed light on the long-standing 3σ difference between the measurements of $\sin^2\theta_W$ obtained from the forward-backward asymmetry of b-quarks and those obtained using leptons.

We note that other asymmetry measurements at Super$B$, such as the forward-backward left-right asymmetry can provide additional information about neutral current couplings.

D. Requirements on polarisation measurement precision

E. Neutral current measurements with un-polarised beams

F. Constraints on new physics

G. Precision measurement of α_S ?

H. Section summary

TO COMPLETE ...

The section summary should provide a succinct recap of the main points discussed within the section, including (if relevant) summary tables of sensitivitites.

8. Spectroscopy

A. Introduction

Although the Standard Model is well-established, QCD, the fundamental theory of strong interactions, provides a quantitative comprehension of phenomena at very high energy scales, where perturbation theory is effective due to asymptotic freedom. The description of hadron dynamics below the QCD dimensional transmutation scale, in spite of the success obtained with numerical simulations on the lattice, is not under full theoretical control.

Systems that include heavy quark-antiquark pairs (quarkonia) are a unique and, in fact, ideal laboratory for probing both the high energy regimes of QCD, where an expansion in terms of the coupling constant is possible, and the low energy regimes, where non-perturbative effects dominate. For this reason, quarkonia have been studied for decades in great detail. The detailed level of understanding of the quarkonia mass spectra is such that a particle mimicking quarkonium properties, but not fitting any quarkonium level, is most likely to be considered to be of a different nature.

In particular, in the past few years the B Factories and the Tevatron have provided evidence for states that do not admit the conventional mesonic interpretation and that instead could be made of a larger number of constituents. While this possibility has been considered since the beginning of the quark model [310], the actual identification of such states would represent a major revolution in our understanding of elementary particles. It would also imply the existence of a large number of additional states that have not yet been observed.

Finally, the study of the strong bound states could be of relevance to understanding the Higgs boson, if it turns out to be itself a bound state, as predicted by several technicolor models (with or without extra dimensions) [311, 312].

The most likely possible states beyond the mesons and the baryons are:

- **hybrids:** bound states of a quark-antiquark pair and a number of constituent gluons. The lowest-lying state is expected to have quantum numbers $J^{PC} = 0^{+-}$. Since a quarkonium state cannot have these quantum numbers (see below), this is a unique signature for hybrids. An additional signature is the preference for a hybrid to decay into quarkonium and a state that can be produced by the excited gluons (*e.g.* $\pi^+\pi^-$ pairs); see *e.g.* Ref. [313, 314].

- **molecules:** bound states of two mesons, usually represented as $[Q\bar{q}][q'\bar{Q}]$, where Q is the heavy quark. The system would be stable if the binding energy were to set the mass of the states below the sum of the two meson masses. While this could be the case for when $Q = b$, this does not apply for $Q = c$, the case for which most of the current experimental data exist. In this case, the two mesons can be bound by pion exchange. This means that only states decaying strongly into pions can bind with other mesons (*e.g.* there could be D^*D states), but that the bound state could decay into its constituents [315–322].

- **tetraquarks:** a bound quark pair, neutralizing its color with a bound antiquark pair, usually represented as $[Qq][\bar{q}'\bar{Q}]$. A full nonet of states is predicted for each spin-parity, *i.e.*, a large number of states are expected. There is no need for these states to be close to any threshold [323].

In addition, before the panorama of states is fully clarified, there is always the lurking possibility that some of the observed states are misinterpretations of threshold effects: a given amplitude might be enhanced when new hadronic final states become energetically possible, even in the absence of resonances.

While there are now several good experimental candidates for unconventional states, the overall picture is not complete and needs confirmation, as well as discrimination between the alternative explanations. A much larger dataset than is currently available is needed, at several energies, to pursue this program; this capability is uniquely within the reach of Super$B$.

B. Light Mesons

The problem of the interpretation of the light scalar mesons, namely f_0, a_0, κ, and σ, is one of the oldest problems in hadron physics [324]. For many years the question about the existence of the σ meson as a real resonance in $\pi\pi$ scattering has been debated [325]; only recently has a thorough analysis of $\pi\pi$ scattering amplitudes shown that the $\sigma(500)$ and $\kappa(800)$ can be considered as proper resonances [326, 327].

Reconsideration of the σ was triggered by the E791 analysis of $D \to 3\pi$ data [328]; a number of papers have commented on those results, *e.g.* Ref. [329–332]. The role of the scalar mesons in several exclusive B decays could be rather relevant: for example, in the perspective of a high precision measurement of the α angle at the Super$B$ factory, the hadronic contributions, like the one of the isoscalar σ in $B \to \rho\pi$, must be properly

controlled [333–335]. Also several studies on light and heavy scalar mesons could be performed analyzing the Dalitz plots of exclusive decays like $B \to KKK$ and $B \to K\pi\pi$. In this respect, having sufficient statistics to clearly assess the presence of a scalar $\kappa(800)$ resonance, would certainly be a major result for hadron spectroscopy.

Beyond the "taxonomic" interest in the classification of scalar mesons, the idea that these mesons could play a key role in our understanding of aspects of non-perturbative QCD has been raised several times; see for example Ref. [336].

In what follows we would like to underscore the latter point by observing that:

- Light scalar mesons are most likely the lightest particles with an *exotic* structure, *i.e.*, they cannot be classified as $q\bar{q}$ mesons.
- Their dynamics is tightly connected with instanton physics. Recent discussions have shown that instanton effects make possible a consistent model for the description of light scalar meson dynamics, under the hypothesis that these particles are diquark-antidiquark mesons.

Therefore, new modes of aggregation of quark matter could be established by the experimental/theoretical investigation of these particles, further expanding the role of instantons in hadron physics.

The idea of four-quark mesons dates back to the pioneering papers by Jaffe [337–339], while the discussion of exotic mesons and hadrons in terms of diquarks was introduced in Ref. [340] and then extended in Ref. [341] to the scalar meson sector.

We will assume that the scalar mesons below 1 GeV are indeed bound states of a spin 0 diquark and an anti-diquark (we will often call this a tetraquark). A spin 0 diquark field is a color antitriplet $\mathfrak{q} = qq$ bound state (same color of an antiquark).

As in a standard $q\bar{q}$ meson, the color is neutralized between a diquark and an antidiquark $\mathfrak{q}^{\alpha}\bar{\mathfrak{q}}_{\alpha}$. Since a spin zero diquark is in a $\bar{\mathbf{3}}$-flavor representation because of Fermi statistics, flavor nonets of $\mathfrak{q}\bar{\mathfrak{q}}$ states are allowed, the so called 'crypto-exotic' multiplets. We believe that the sub-GeV scalar mesons most likely represent the lowest tetraquark nonet.

The $\mathfrak{q}\bar{\mathfrak{q}}$ model of light-scalars is very effective at explaining the most striking feature of these particles, namely their inverted pattern, with respect to that of ordinary $q\bar{q}$ mesons, in the mass-versus-I_3 diagram [337–339], as shown in Fig. 22.

Such a pattern cannot be explained in a $q\bar{q}$ model where, for example, the $f_0(980)$ would be an $s\bar{s}$ state [329–332] while the $I = 1$, $a_0(980)$, would be a $u\bar{u} + d\bar{d}$ state. If this were the case, the degeneracy of the two particles would be rather unnatural.

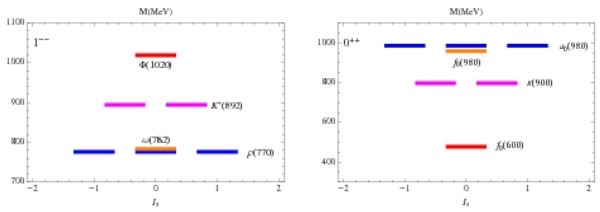

FIG. 22: Vector mesons ($q\bar{q}$ states) and the sub-GeV scalar mesons in the $I_3 - m$ plane.

Besides a correct description of the mass-I_3 pattern, the tetraquark model offers the possibility of explaining the decay rates of scalars at a level never reached by standard $q\bar{q}$ descriptions. The effective decay Lagrangian into two pseudoscalar mesons, *e.g.* $\sigma \to \pi\pi$, is written as:

$$\mathcal{L}_1 = c_1 S^i_j \epsilon^{jtu} \epsilon_{irs} \partial_\mu \Pi^r_t \partial^\mu \Pi^s_u, \tag{84}$$

where i, j are the flavor labels of $\mathfrak{q}^i$ and $\bar{\mathfrak{q}}^j$, while r, s, t, u are the flavor labels of the quarks $\bar{q}^t, \bar{q}^u$ and q^r, q^s. c_1 is an effective coupling and S, Π are the scalar and pseudoscalar matrices of meson fields. Observe for example how $\pi^+\pi^-$ are produced by a $[ud][\bar{u}\bar{d}]$ tetraquark by setting the right flavor indices in Eq. (84).

This Lagrangian describes the quark exchange amplitude for the quarks to tunnel out of their diquark shells in S to form ordinary pseudoscalar mesons Π [341]. The antisymmetrization in the flavor indices of quarks ($\bar{\mathbf{3}}-$flavor representation) is guaranteed by the ϵ tensors.

Such a mechanism is the straightforward alternative to the most natural color string breaking $\mathfrak{q}\,\overbrace{\ \ q\bar{q}\ \ }\,\bar{\mathfrak{q}} \to B\bar{B}$, *i.e.*, a baryon-anti-baryon decay, which happens to be phase-space forbidden to sub-GeV scalar mesons. For a discussion about baryonia see [342].

The problem with Eq. (84) is simply that it is not able to describe the observed decay $f_0 \to \pi\pi$, since $f_0 \sim [qs][\bar{q}\bar{s}]$, with $q = u, d$. To form a $\pi^+\pi^-$ pair of mesons in the final state one should require to: *i*) break the diquarks binding to annihilate the s and the $\bar{s}$ quarks *ii*) create a $q\bar{q}$ pair from the vacuum. Alternatively one could annihilate the diquark and the antidiquark directly into a $q\bar{q}$ pair via a six-fermion interaction, not paying the price of breaking the diquark shells, and hadronize the two light quarks produced into two pions via a quark pair creation. This possibility is provided by six-fermion, instanton induced low energy vertices [343]. Such vertices contain a term of the form $\mathcal{I} = \sum_{i,j} \bar{\mathfrak{q}}_i \mathfrak{q}_j \bar{q}_j q_i$, i, j being flavor indices and $\mathfrak{q}_{i\alpha} = \epsilon_{ijk}\epsilon_{\alpha\beta\gamma}\bar{q}^{j\beta}_C \gamma_5 q^{k\gamma}$ being a spin zero diquark.

Alternatively, one can go through a mixing between the two isoscalars f_0 and σ. However, as discussed

in [343], such mixing is expected to be too small, $< 5^\circ$, to account for the structure of the inverted mass pattern (a precise determination of the κ mass would be crucial to fix this point).

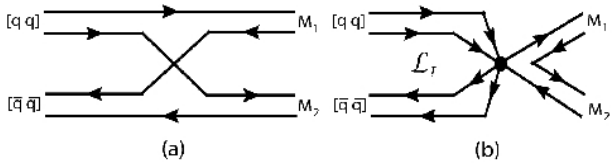

FIG. 23: Decay of a tetraquark scalar meson S in two $q\bar{q}$ mesons M_1M_2: (a) quark rearrangement (b) instanton-induced process.

Thus in addition to the quark-exchange diagrams, described at the effective theory level by the Lagrangian of Eq. (84), (see Fig. 23 (a)), we a have six-fermion microscopic interaction of the form $\mathcal{I}$ (see Fig. 23 (b) [9]) which contributes to the following effective Lagrangian term:

$$\mathcal{L}_2 = c_2 \mathrm{Tr}(\mathbf{S}(\partial\mathbf{\Pi})^2), \tag{85}$$

(roughly, introduce a $\bar{q}_k q_k$ in $\mathcal{I}$ and call $S^i_j \sim \bar{\mathfrak{q}}_j \mathfrak{q}^i$, $\Pi^i_j \sim \bar{q}_j q^i$ respectively). c_2 is an effective coupling expected to be rather smaller than c_1 in Eq. (84). Observe that this term is also contained in Eq. (84) which actually corresponds to the combination $2\mathrm{Tr}(\mathbf{S}(\partial\mathbf{\Pi})^{\mathbf{2}}) - \mathrm{Tr}\mathbf{S}\mathrm{Tr}(\partial\mathbf{\Pi})^2$, barring the contribution from the singlet pseudoscalar. The latter term could be described by an 'annihilation' diagram at the meson level.

If on the other hand we assume that the lowest scalar nonet is made up of standard $\bar{q}q$ mesons, there are no diquarks around, and we expect the instanton contributions to enter only in operators of the kind $\mathrm{Tr}\mathbf{S}\mathrm{Tr}(\partial\mathbf{\Pi})^2$. Thus the decay Lagrangians to be used to fit data in the $4q$ and $2q$ hypotheses are:

$$\mathcal{L}^{(4q)} = \mathcal{L}_1(c_1) + \mathcal{L}_2(c_2),$$
$$\mathcal{L}^{(2q)} = \mathcal{L}_1(c_2') + \mathcal{L}_2(c_1'),$$

with evident notation. It is expected $|c_1^{(\prime)}| \gg |c_2^{(\prime)}|$.

With such a description of the dynamics one can determine numerical results for the decay amplitudes as reported in Table XVIII (four-quark fit $|c_1| \simeq 0.02, |c_2| \simeq 0.002$). Such a good description of decays is possible *only* if the assumption is made that sub-GeV light scalars are diquark-antidiquark mesons (see Table XVIII). In the $q\bar{q}$ hypothesis, the agreement of $a_0 \to \pi^0\eta$ with data appears very poor.

TABLE XVIII: Numerical results for amplitudes in GeV. Second and third columns: results obtained with a decay Lagrangian including or not including instanton effects, respectively (Labels I and no-I mean that we add or do not add the instanton contribution). No $f_0 - \sigma$ mixing is assumed in this table. Fourth column: best fit, see text, with instanton effects included. Fifth column: predictions for a $q\bar{q}$ picture of the light scalars. The $\eta - \eta'$ singlet-octet mixing angle assumed: $\phi_{PS} = -22^\circ$ [344, 345]. Data for σ and κ decays are from [326, 327], the reported amplitudes correspond to: $\Gamma_{\rm tot}(\sigma) = 272 \pm 6$, $\Gamma_{\rm tot}(\kappa) = 557 \pm 24$.

Proc.	$\mathcal{A}_{\rm th}([qq][\bar{q}\bar{q}])$			$\mathcal{A}_{\rm th}(q\bar{q})$	$\mathcal{A}_{\rm expt}$
	I	no-I	best fit	I	
$\sigma(\pi^+\pi^-)$	input	input	1.7	input	2.27(0.03)
$\kappa^+(K^0\pi^+)$	5.0	5.5	3.6	4.4	5.2(0.1)
$f_0(\pi^+\pi^-)$	input	**0**	1.6	input	1.4(0.6)
$f_0(K^+K^-)$	4.8	4.5	3.8	4.4	3.8(1.1)
$a_0(\pi^0\eta)$	4.5	5.4	3.0	8.9	2.8(0.1)
$a_0(K^+K^-)$	3.4	3.7	2.4	3.0	2.16(0.04)

A relative of the lowest lying scalar mesons may have been found very recently by *BABAR*: the $Y(2175)$, a particle first observed in the decay $Y \to \phi f_0(980)$ [346]. For a discussion see Ref. [347].

C. Charmonium

In the past few years the B Factories have observed several states with clear $c\bar{c}$ content, which do not behave like standard mesons, and that are therefore an indication of new spectroscopy.

The $X(3872)$ was the first state found not to easily fit into charmonium spectroscopy. It was initially observed decaying into $J/\psi\pi^+\pi^-$ with a mass just beyond the open charm threshold [348]. The $\pi^+\pi^-$ invariant mass distribution, the observation of the $X \to J/\psi\gamma$ and the full angular analysis by CDF [349] and Belle [350], along with the evidence for the $X \to \psi(2S)\gamma$ decay found by *BABAR* [351], favor the assignment of $J^{PC} = 1^{++}$ for this state, and of $X \to J/\psi\rho$ as its dominant decay. There are several indications that this is not a (pure) charmonium state: the mass assignment does not match any prediction of long-verified potential models (see Fig. 24); the dominant decay would be isospin-violating; and the state is narrow (less than a few MeV), despite its mass lying above threshold for the production of two charmed mesons. At the same time the relative rates to $\psi(2S)\gamma$ and $J/\psi\gamma$ are more easily explained in terms of conventional charmonium decays. The closeness to the D^0D^{*0} threshold suggests also the hypothesis that it

[9] The six-fermion interaction expands to terms of the form: $(\bar{u}^\alpha(1-\gamma_5)u_\alpha)(\bar{d}^\alpha(1-\gamma_5)d_\alpha)(\bar{s}^\alpha(1-\gamma_5)s_\alpha)$. Upon appropriate Fierz rearrangement of, *e.g.*, $(\bar{d}^\alpha(1-\gamma_5)d_\alpha)(\bar{s}^\alpha(1-\gamma_5)s_\alpha)$, one obtains: $C \times (\bar{u}^\alpha(1-\gamma_5)u_\alpha)\mathfrak{q}^{1\gamma}\bar{\mathfrak{q}}_{1\gamma}$, C being a constant factor.

may be a molecule composed of these two mesons or a threshold effect.

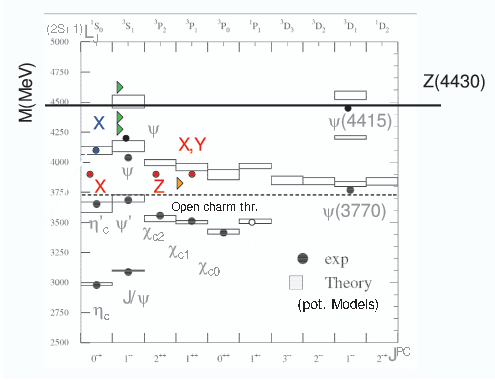

FIG. 24: Measured masses of the newly observed states, positioned in the spectroscopy according to their most likely quantum numbers. The charged state ($Z(4430)$) clearly has no C quantum number.

Another aspect of interest is the measurement of the mass of the $X(3872)$ in the $D^{*0}D^0$ decay mode [352, 353], which could differ from the value measured in the $J/\psi\pi\pi$ decay. The mass difference and the difference in the line-shape in the two modes could help in discriminating between the many models [354, 355]. If the mass difference is confirmed, it is possible that there are indeed two different states, one decaying to $D^{*0}D^0$ and the other decaying to $J/\psi\pi\pi$: the di-quarks with a heavy meson are effectively flavor-triplets, and di-quark pairs would show the same nonet structure as ordinary mesons, so that it would be natural to expect two states with $S = I_3 = 0$ very close in mass [323].

A data sample of $\mathcal{O}(50\,ab^{-1})$ would yield several (3 to 11) thousand fully reconstructed $B \to X(3872)K$ decays in each of the above-mentioned modes. This would allow a detailed study of the $X(3872)$ decay dynamics and line-shape, crucial to enlighten possible evidence for non-$q\bar{q}$ composition.

The B Factories have also found a number of new states with $J^{PC} = 1^{--}$ by looking for events where the initial state radiation brings the e^+e^- center-of-mass energy down to the particle's mass. It was expected that above the open charm threshold all states would be seen in $R = \sigma_{had}/\sigma_{\mu\mu}$ scans. When the high luminosity at B Factories allowed one to study exclusive final states containing a J/ψ or a $\psi(2S)$, at least three new unusual particles were discovered: the $Y(4260)$ decaying to $J/\psi\pi^+\pi^-$ [356], the $Y(4350)$ [357] and the $Y(4660)$ [358] decaying to $\psi(2S)\pi^+\pi^-$.

The $\pi^+\pi^-$ invariant mass is a critical observable in discerning the nature of these particles, which are unlikely to belong to charmonium since there are already other 1^{--} known charmonium states, their masses are above the open-charm threshold, yet they are relatively narrow and are not observed to decay into two charmed mesons (the most stringent limit being $\mathcal{B}(Y(4260) \to D\bar{D})/\mathcal{B}(Y(4260) \to J/\psi\pi^+\pi^-) < 1.0$ at 90% CL) Ref. [359]. Another puzzling feature of these states is the ratio of the partial widths $\Gamma(J/\psi\pi^+\pi^-)/\Gamma(\psi(2S)\pi^+\pi^-)$, that is small for the $Y(4260)$ and large for the $Y(4350)$ and $Y(4260)$. The current statistics does not allow one to measure these ratios.

Figure 25 shows the dipion invariant mass spectra for all regions in which new resonances have been observed. Only the $Y(4660)$ seems to show a well-defined intermediate state (most likely an f_0), while others have a more complex structure.

The $Y(4260)$ is currently considered a good hybrid candidate, while the $Y(4350)$ and $Y(4660)$ are good candidates for $[cd][\bar{c}\bar{d}]$ and $[cs][\bar{c}\bar{s}]$ tetraquarks, respectively. The latter would prefer to decay to f_0, while the mass difference is consistent with the hypothesis that the two belong to the same nonet.

An experiment with 50 ab^{-1} of integrated luminosity, yielding samples of 30 K $Y(4260) \to J/\psi\pi^+\pi^-$ and $\approx$ 3 K events each for $Y(4350), Y(4660) \to \psi(2S)\pi^+\pi^-$, would allow a detailed study of the line-shape, a measurement of $\Gamma(J/\psi\pi^+\pi^-)/\Gamma(\psi(2S)\pi^+\pi^-)$, and a study of the $\pi^+\pi^-$ invariant mass spectra, as well as of the angular distributions. Furthermore it will be possible to search for other exclusive decays to Charmonia such as $J/\psi\eta/\pi^0$, $\psi(2S)\eta/\pi^0$, $\chi_{cJ}\pi^+\pi^-$, $\gamma J/\psi$, and $\gamma\psi(2S)$.

The turning point in the query for states beyond charmonium has been the observation by the Belle Collaboration of a charged state decaying into $\psi(2S)\pi^\pm$ [360, 361] soon followed by two more charged states, the $Z_1^+(4050)$ and the $Z_2^+(4430)$, decaying to $\chi_{c1}\pi^+$[362]. Figure 26 shows the fit to the $\psi(2S)\pi$ invariant mass distribution in $B \to \psi(2S)\pi K$ decays, returning a mass $M = 4433 \pm 4(\text{stat.}) \pm 2(\text{syst.})$ MeV/c^2 and a width $\Gamma = 44^{+18}_{-13}(\text{stat.})^{+30}_{-13}(\text{syst.})$ MeV.

Such states must contain a c and a $\bar{c}$, but according to their charge they must also contain at least an u and a $\bar{d}$. The only possibilities for explaining these state are the tetraquark or the molecule composition, or the presence of some threshold effects. The latter two options are viable for the $Z^+(4430)$ due to the closeness of the D_1D^* threshold.

The analysis is highly complicated by the presence of K^* resonances in the $B \to (c\bar{c})\pi^+K$ final state and by the $c\bar{c}$ polarization. The analysis of the full *BABAR* data sample did not confirm nor exclude the observation of the $Z^+(4430)$ [363]. No result has yet been presented on the search for the $Z_1^+(4050)$ and $Z_2^+(4430)$.

It is critical to confirm the existence of these states, and if confirmed to find the corresponding neutral states and/or to observe them in other decay modes.

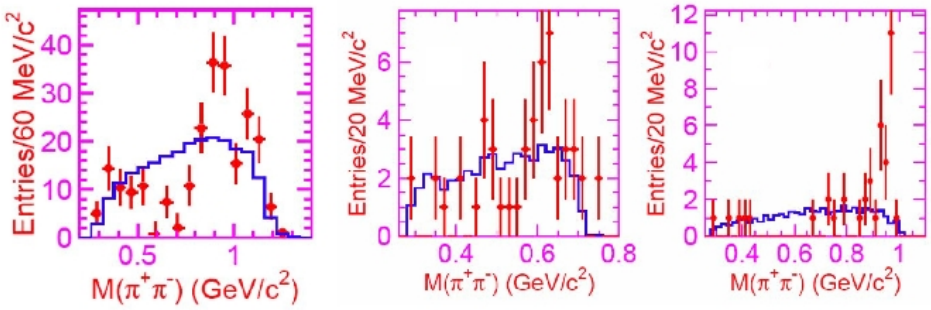

FIG. 25: Di-pion invariant mass distribution in $Y(4260) \to J/\psi\pi^+\pi^-$ (left), $Y(4350) \to \psi(2S)\pi^+\pi^-$ (center), and $Y(4660) \to \psi(2S)\pi^+\pi^-$ (right) decays.

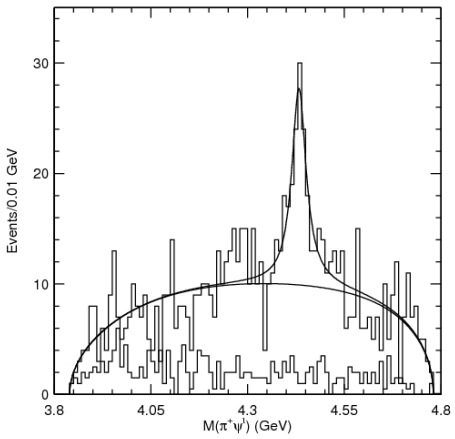

FIG. 26: The $\psi(2S)\pi$ invariant mass distribution in $B \to \psi(2S)\pi K$ decays.

With an integrated luminosity of 50 ab^{-1} we can expect to collect samples of 100 K to 1.5 M fully reconstructed $B \to J/\psi\pi^+K$, $B \to \psi(2S)\pi^+K$ and $B \to \chi_{cJ}\pi^+K$ events that will allow one to establish unambiguously the existence of these states and to determine their properties.

In summary, there are several reasons why a run at fifty to a hundred times the existing integrated luminosity is decisive to convert these hints into a solid picture:

- All the new states, apart from the $X(3872)$, have been observed in only a single decay channel, each with a significance barely above 5σ. A hundredfold increase in statistics would allow searches in several other modes. In particular, it is important to observe both the decay to charmonium and to D-meson pairs and/or D_s meson pairs. Since the branching fractions of observable final states for the D and especially for the D_s mesons are particularly small, current experiments do not have the sensitivity to observe all the decays.

- Most models predict several other states, such as the neutral partners of the $Z(4430)$ and the nonet partners, for instance $[cd][\bar{c}\bar{s}]$ candidates decaying into a charmonium state and a kaon, at a significantly lower rate (see *e.g.* Ref. [364]) than the observed modes. Furthermore, several of these states decay into particles (in particular neutral pions and kaons) that have a low detection efficiency.

In order to achieve high luminosities the event rate and the machine backgrounds will increase significantly. It is therefore important to estimate the impact of the changes in the detector and of this background on the search potentiality. As a first step it has been tested with a fast simulation of the $e^+e^- \to Y(4260)\gamma_{ISR}, Y(4260) \to J/\psi\pi\pi$ signal that the detector changes do not affect significantly the efficiency. A more comprehensive study is on the way.

D. Bottomonium

In comparison to charmonium, our knowledge of bottomonium below flavor threshold is far from complete: in particular, as shown in Fig. 27, almost all the spectrum of spin singlet states (parabottomonia) is still *terra incognita*. Moreover, in the bottomonium system, four narrow D wave states are expected in the region around 10.16 GeV, and their study [365], started by CLEO-III, is currently under way in the

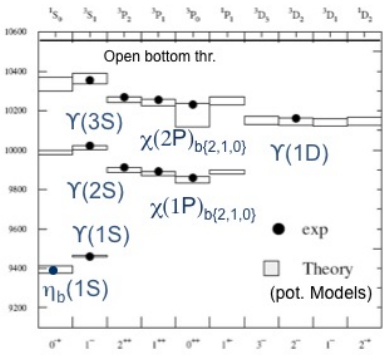

FIG. 27: Measured masses of the bottomonia, positioned in the spectroscopy according to their most likely quantum numbers.

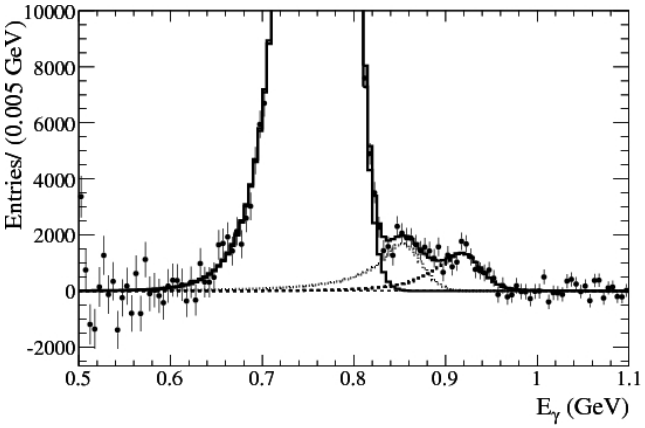

FIG. 28: The inclusive photon spectrum at 3S from *BABAR*, after continuum subtraction: the peaks from $\chi_{b1,2} \to \Upsilon(1S)$, ISR production of $\Upsilon(1S)$ and $\Upsilon(3S) \to \eta_b$ are visible, left to right in the plot.

present generation of B-factories. In total, the current generation of B-factories have integrated (1.2, 2.6, 1.3)*10^8 Υ(1, 2, 3S) decays on resonance peak, as shown in table XIX.

TABLE XIX: $\Upsilon(nS, n \neq 4)$ datasets after the year 2000 at the B-factories.

Expt.	$\Upsilon(1S)$	$\Upsilon(2S)$	$\Upsilon(3S)$	$\Upsilon(5-6S)$
CLEO	20M	9M	6M	0.5 fb^{-1}
Belle	98M	160M	11M	133 fb^{-1}
BABAR	-	100M	122M	3.3 fb^{-1}

Moreover, up to 133 fb^{-1} were accumulated in the Υ(5S) region, and have started yielding interesting results about transitions to narrow states through the open beauty threshold, defying naïve expectations. The analysis of this data is in progress and will probably lead to new discoveries in the near future, but it is clear that ten to a hundred times the statistics are needed to find all the pieces of the bottomonium puzzle.

1. *Regular bottomonium*

Only recently, the ground state η_b(1S) has been discovered by *BABAR* [366, 367], as shown in Fig.28, but all other parabottomonia are still missing and surely two of them will hardly be within reach of the current generation of B-factories. Besides the hyperfine splitting, other η_b decay properties can be predicted with relatively small errors in the NRQCD approximation and deserve experimental verification: the total width and the partial width to two photons.

The total width of η_b should be measurable by *BABAR* and Belle, at least as an upper limit, from the inclusive photon spectra of suppressed transitions. A precise measurement (i.e. better than 10% error) of the η_b total width requires much higher statistics, which will be available only at a Super Flavour Factory. Given the large photon background in the low energy part of the spectrum (i.e. below 100 MeV), the experimentalists are challenged to detect all the η_b decay products on one or more specific channels and try an exclusive reconstruction. At present date, only few exclusive decay modes have been observed by CLEO [368], with significances above 5σ, for the χ_b states, which can be reached from Υ(2, 3S) peaks via transitions which have branching ratios at the 10% level. As ratios for direct M1 transitions to η_b are expected in the 10^{-4} range, at least two orders of magnitude increase in statistics is needed.

In the long term the most important measurement to perform is that of the two-photon width, as theory predictions on the ratio $\Gamma_{\gamma\gamma}(\eta_b)/\Gamma_{l+l-}(\Upsilon)$ are quite insensitive to the renormalization scale [369], and yield $\Gamma_{\gamma\gamma}(\eta_b) = 0.66 \pm 0.09$ keV. If $\Gamma_{tot}(\eta_b) < 10$ MeV this would imply a branching ratio at the level of 10^{-4}, and a cross section $\sigma(\Upsilon(2,3S) \to \gamma\eta_b \to \gamma\gamma\gamma) \sim 0.2$ fb, which is by far smaller than the cross section for the continuum process $\sigma(e^+e^- \to \gamma_{ISR} \to \gamma\gamma\gamma)$. The ISR background can actually be avoided by running on the Υ3S resonance peak and using the dipion pair to tag the Υ2S decay, and then select exclusive $\pi\pi\gamma\gamma\gamma$ events, from the process $\Upsilon(3S) \to \pi\pi\Upsilon(2S) \to \pi\pi\gamma\eta_b(1S)$. In this case, experimentalists are challenged to maximize the efficiency on detection and tracking of low momentum dipion pairs.

The discovery of one or more exclusive decay modes of η_b(1S) will also be useful for the search of the analogous direct M1 transitions between vector and pseu-

doscalar 2S and 3S excitations. For the time being, the current record sample of $\Upsilon(3S)$ decays can allow *BABAR* to discover the $\eta_b(2S)$ in the inclusive photon spectrum, and the $h_b(1P)$ either via the cascade process $\Upsilon(3S) \to \pi^0 h_b(1P) \to \pi^0\gamma\eta_b(1S)$, as done by CLEO to find the $h_c(1P)$ state in the charmonium system, or via $\Upsilon(3S) \to \pi\pi h_b(1P) \to \pi\pi\gamma\eta_b(1S)$, as suggested in Ref. [370, 371].

In order to discover the states $h_b(2P)$ and $\eta_b(3S)$ we probably need a Super Flavour Factory. While $\eta_b(3S)$ detection should depend crucially on exclusive reconstruction of some decay channel, and it is almost certainly reachable from the $\Upsilon(3S)$, it is not yet clear which transition will allow us to reach $h_b(2P)$: as the expected mass difference $M(\Upsilon(3S)) - M(h_b(2P)) < M(\pi^0)$, detection of $h_b(2P)$ cannot benefit from running on narrow bottomonia.

The recent discovery of unexpectedly large widths for the transitions $\Upsilon(4S) \to \eta\Upsilon(1S)$ [372] and $\Upsilon(5S) \to \pi\pi\Upsilon(1S)$ [373] may suggest that hadronic transitions to other narrow bottomonia can open new pathways to these states, *e.g.* $\Upsilon(5S) \to \eta h_b(2P)$. In the next section, we elaborate on the large physics potential of running above the $B_s\bar{B}_s$ threshold, also for hadron spectroscopy.

2. *Exotic bottomonium*

This section discussed recent *BABAR* and Belle scans and the future prospects for high energy scans at Super$B$.

Exotic states with two bottom quarks, analogous to those with two charm quarks, could also exist. In this respect, bottomonium spectroscopy is a very good test-bench for speculations advanced to explain the charmonium states. As a down side, searching for new bottomonium states is more challenging, since they tend to be broader and there are more possible decay channels than the charmonium situation. This explains why there are still eight unobserved states with masses below open bottomonium threshold.

Among the known states, there is already one with unusual behavior: there has been a recent observation [373] of an anomalous enhancement, by two orders of magnitude, of the rate of $\Upsilon(5S)$ decays to the $\Upsilon(1S)$ or a $\Upsilon(2S)$ and two pions. This indicates that either the $\Upsilon(5S)$ itself or a state very close by in mass has a decay mechanism that enhances the amplitudes for these processes.

In order to understand whether the exotic state coincides with the $\Upsilon(5S)$ or not, a high luminosity (at least 20 fb^{-1} per point to have a 10% error) scan of the resonance region is needed.

In any case, the presence of two decay channels to other bottomonium states excludes the possibility of this state being a molecular aggregate, but all other models are possible, and would predict a large variety of not yet observed states.

As an example, one can estimate possible resonant states with the tetraquark model, by assuming that the masses of states with two b quarks can be obtained from one with two c quarks by adding the mass difference between the $\Upsilon(1S)$ and the J/ψ. Under this assumption, which works approximately for the known bottomonium states, we could expect three nonets that could be produced by the $\Upsilon(3S)$ and decaying into $\Upsilon(1S)$ and pions. Assuming that the production and decay rates of these new states are comparable to the charmonium states, and assuming a data sample of $\Upsilon(3S)$ events comparable in size to the current $\Upsilon(4S)$ sample is needed to clarify the picture, we would need about 10^9 $\Upsilon(3S)$ mesons, corresponding to an integrated luminosity of 0.3 ab^{-1}.

As already mentioned, searching for bottomonium-like states would require higher statistics than the corresponding charmonium ones; this therefore represents an even stronger case for Super$B$.

E. $\gamma\gamma$ physics

TO COMPLETE ...

F. Interplay with other experiments

Super$B$ is not the only next generation experiment capable of investigating heavy quark spectroscopy.

The LHCb experiment is starting to investigate its potentialities in the field. The complementarity of these studies with Super$B$ are evident, considering the present interplay between B-Factories and the Tevatron: the larger number of mesons produced allows detailed studies of the decay modes with final states made of charged particles. All other modes are best investigated by e^+e^- machines.

The only other next generation experiment at an e^+e^- machine is BES-III, but their current plan is to run below the energies of interest, at the $\psi(3770)$ [374], where they expect to collect 5 fb^{-1} per year. Even if a plan to run at the energies of the exotic states were developed, given the lower luminosity the complementarity of Super$B$ and BES-III would be the same as the B-Factories and CLEO-c.

A separate mention is deserved by the PANDA experiment at FAIR [375], a proton-antiproton collider which could produce the exotic resonances at threshold (i.e. $e^+e^- \to X, Y$). This innovative production mechanism allows for copious production without the hindrance of fragmentation products. Considering the expected characteristics of the antiproton beam and

an integrated luminosity of 2 fb^{-1} per year, running at the J/ψ mass would yield 3.5 10^9 J/ψ mesons per year. Considering that $\Gamma_{ee}[Y(4260)] * \mathcal{B}(Y(4260) \rightarrow p\bar{p}) < 0.05\Gamma_{ee}[J/\psi] * \mathcal{B}(J/\psi \rightarrow p\bar{p})$@90% C.L. [376] and assuming $\Gamma_{ee}[Y(4260)] = \Gamma_{ee}[J/\psi]$, we could expect as many as 30K $Y(4260) \rightarrow J/\psi\pi\pi$ with a J/ψ decaying leptonically per year. Besides the large uncertainty on the assumption, this estimate can be compared with the 60K events in the same decay chain produced in a year at Super$B$ via ISR. The complementarity of the two experiments is guaranteed by the fact that the final states that can be studied by the two experiments are different and that the PANDA experiment can more easily access the narrow states while Super$B$ can study in detail larger states if the production mechanism is favorable. Furthermore, in case the center-of-mass-energy of Super$B$ is changed to the $Y(4260)$ mass, assuming a factor 10 loss in luminosity with respect to running at the $\Upsilon(4S)$, the number of events produced in the decay chain used as example would raise to 700K per year: a few weeks scan would then be equivalent to the PANDA dataset. Finally, PANDA can only reach center-of-mass energies as high as 5 GeV and therefore has no access to bottomonium spectroscopy.

G. Section summary

TO COMPLETE ...

The section summary should provide a succinct recap of the main points discussed within the section, including (if relevant) summary tables of sensitivitites.

9. Direct Searches

Bottomonium decays also allow direct searches for physics beyond the SM in regions of the parameters space that have not been reached by LEP [377]: the possibility of a rather light non-standard Higgs boson has not been ruled out in several scenarios beyond the SM [378–380], due to the fact that a new scalar may be uncharged under the gauge symmetries, similar to a sterile neutrino in the fermion case. These studies indicate that its mass could be less than twice the b mass, placing it within the reach of Super$B$. Moreover, the LHC might not be able to unravel a signal from a light Higgs boson whose mass is below $B\bar{B}$ threshold, since it will be difficult for the soft decay products to pass the LHC triggers. Dark matter may also be light, evading LEP searches if it does not couple strongly to the Z^0 [381–384]. Finally, the new field of Dark Forces (see Sec. 9 C) predicts low interacting light particles that couple mostly to photons that can therefore be produced at a Flavour Factory and that would require a large luminosity to study.

Super$B$ will be required in most of these cases to precisely determine the masses and couplings of any light non-SM particles, and thus will play an important discovery role.

A. Light Higgs

A Higgs h with $M_h < M_\Upsilon$ can be produced in $\Upsilon(nS)$ decays via the Wilczek mechanism [385] with a branching ratio, at leading-order,

$$\frac{\Gamma(\Upsilon(nS) \to \gamma h)}{\Gamma(\Upsilon(nS) \to \mu\mu)} = \frac{\sqrt{2} G_F m_b^2}{\alpha\pi M_{\Upsilon(nS)}} E_\gamma X_d^2,$$

where X_d is a model-dependent quantity containing the coupling of the Higgs to bottom quarks, m_b is the bottom quark mass, α and G_F are the electroweak parameters, and E_γ is the photon energy.

From a theoretical viewpoint, the existence of a light pseudoscalar Higgs is not unexpected in many extensions of the SM. As an example, the Next-to-Minimal Supersymmetric Standard Model (NMSSM) has a gauge singlet added to the MSSM two-doublet Higgs sector [386] leading to seven physical Higgs bosons, five of them neutral, including two pseudoscalars. In the limit of either slightly broken R or Peccei-Quinn (PQ) symmetries, the lightest CP-odd Higgs boson (denoted by A_1) can be much lighter than the other Higgs bosons, providing unique signatures at a Super Flavour Factory as discussed in the following.

The A_1 coupling to down-type fermions turns out to be proportional to $X_d = \cos\theta_A \tan\beta$, where $\tan\beta$ denotes the ratio of the vacuum expectation values of the up- and down-type Higgs bosons and θ_A is the mixing angle of the singlet and non-singlet components that constitute the physical A_1 state [387]. If $\cos\theta_A \sim 0.1 - 0.5$, present LEP and B physics bounds can be simultaneously satisfied [388], while a light Higgs could still show up in Υ radiative decays into tauonic pairs: $\Upsilon(nS) \to \gamma A_1(\to \tau^+\tau^-)$; $\quad n = 1, 2, 3$.

As this light Higgs acquires its couplings to SM fermions via mixing with the SM Higgs, it therefore couples to mass, and will decay to the heaviest available SM fermion. In the region $M_{A_1} > 2M_\tau$, there are two measurements which have sensitivity: lepton universality of Υ decays, and searches for a monochromatic photon peak in tauonic Υ decays.

The measurement of lepton universality compares the branching ratios of Υ to e^+e^-, $\mu^+\mu^-$ and $\tau^+\tau^-$ [389, 390], which should all have identical couplings in the SM, and differ only by factors given by phase-space differences. This inclusive measurement is relevant especially when the monochromatic photon signal is buried under backgrounds. Under reasonable sets of the NMSSM parameters that satisfy all current LEP and B physics bounds, it has been shown [380, 391] that A_1 bosons with masses between 9 to 10.5 GeV can give sizeable deviations from the SM if $5 \lesssim \tan\beta \lesssim 20$.

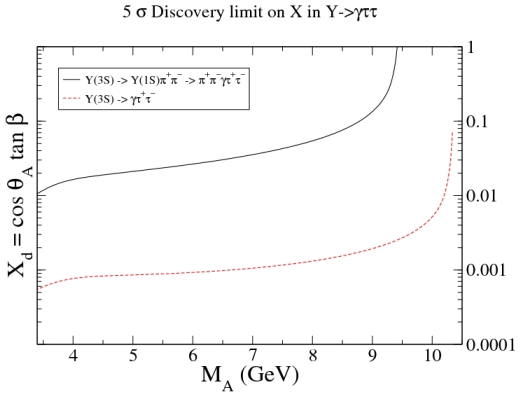

FIG. 29: Five σ discovery potential of Super$B$ with $\Upsilon(3S)$ data, in the mode $\Upsilon(3S) \to \pi^+\pi^-\Upsilon(1S) \to \pi^+\pi^-\tau^+\tau^-\gamma$ (solid) and $\Upsilon(3S) \to \tau^+\tau^-\gamma$ (dashed). An integrated luminosity of 1 ab^{-1} has been assumed for this projection.

Unfortunately recent measurements of these branching fractions are limited by systematics and it is hard to conceive of a dramatic improvement below the level of 1% precision at Super$B$. Alternatively, once can consider the search for monochromatic photons [379] where the first relevant decay mode is $\Upsilon(3S) \to \Upsilon(1S)\pi^+\pi^-$, which is followed by the decay $\Upsilon(1S) \to \gamma\tau^+\tau^-$. This only has a 4.5% branching fraction, but it also has a low background. The second

decay mode is $\Upsilon(3S) \to \gamma\tau^+\tau^-$, which suffers from a larger background arising from $e^+e^- \to \tau^+\tau^-\gamma$ events, but also has a rate that is more than a factor of ten higher than $\Upsilon(3S) \to \Upsilon(1S)\pi^+\pi^-$. The corresponding exclusion plots expected at Super$B$ are shown in Fig. 29.

Let us finally point out another possible signal for detection of a light CP-odd Higgs boson related to bottomonium spectroscopy. As studied in [392], significant $A_1 - \eta_b(nS)$ mixing should significantly alter the hyperfine splitting $M(\Upsilon(nS)) - M(\eta_b(nS))$ compared to SM expectations. This kind of search has a great advantage with respect to the radiative decays of Υ resonances since it is free of theoretical uncertainties coming from QCD and relativistic corrections plaguing the Wilczek formula. Moreover, from an experimental point of view, the mixing could spoil a straight forward search for narrow peaks in the photon spectrum while the measurement of hyperfine splittings could still yield unexpected results hinting at the existence of a light pseudoscalar Higgs [392].

B. Invisible decays and Dark Matter

Finally, if Dark Matter is lighter than 5 GeV, it will require a Super Flavour Factory to determine its properties. Generally, in this mass region one needs two particles, the dark matter particle χ, and a boson that couples it to the SM U . The most promising searches are in invisible and radiative decays of the Υ, which can be measured in the mode $\Upsilon(3S) \to \pi^+\pi^- invisible$, which is sensitive to a vector U [382]. The current best sensitivity to this process has been achieved by the *BABAR* Experiment [393]; however, this result is still an order of magnitude above the SM prediction. The sensitivity is limited by the amount of background that needs to be subtracted, primarily due to undetected leptons from $\Upsilon(1S) \to \ell^+\ell^-$ in the final state. Studies of this background suggest that the only way to further improve the measurement to the level of the SM is to employ both far-backward and far-forward tagging into the design of the detector. Achieving a $3-5\sigma$ sensitivity to the SM will require active background tagging down to 5-10 degrees above the beam-line in both the forward and backward directions.

The second most promising signature is radiative decays $\Upsilon(1S) \to \gamma + invisible$. This is probably the most favored mode theoretically, and is sensitive to a scalar or pseudoscalar U. The mediator coupling the SM particles to final state χ's can be a pseudoscalar Higgs, $U = A_1$, which can be naturally light, and would appear in this mode [38]. In such models the Dark Matter can be naturally be a bino-like neutralino. Extended detector coverage in the forward and backward directions is important to reducing the radiative QED backgrounds which dominate this final state.

It is expected that improving detector coverage with active coverage for tagging low-angle or missing-particle backgrounds will also improve the sensitivity in flagship measurements of Super$B$, including $B \to K\nu\bar{\nu}$ and $B \to \ell\nu$.

C. Dark Forces

Recent cosmic ray measurements of the electron and positron flux from ATIC [394], FERMI [395], and PAMELA [396] have spectra which are not well described by galactic cosmic ray models such as GALPROP [397]. For instance, PAMELA shows an increase in the positron/electron fraction with increasing energy. No corresponding increase in the antiproton spectrum is observed. There have been two main approaches attempting to explain these features: astrophysical sources (particularly from undetected, nearby pulsars) [398] and annihilating or decaying dark matter.

Arkani-Hamed *et al.* [399] and Pospelov *et al.* [400] have introduced a class of theories containing a new "dark force" and a light, hidden sector. In this model, the ATIC and PAMELA signals are due to dark matter particles with mass $\sim 400 - 800\,\mathrm{GeV}/c^2$ annihilating into the gauge boson force carrier with mass $\sim 1\,\mathrm{GeV}/c^2$, dubbed the A', which subsequently decays to SM particles. If the A' mass is below twice the proton mass, decays to $p\overline{p}$ are kinematically forbidden allowing only decays to states like e^+e^-, $\mu^+\mu^-$, and $\pi\pi$. If the dark force is non-Abelian, this theory can also accommodate the 511 keV signal found by the INTEGRAL satellite [401] and the DAMA modulation data [402].

The dark sector couples to the SM through kinetic mixing with the photon (hence we call the A' the "dark photon") with a mixing strength ϵ. The current limits on ϵ from various experiments are shown on Figure 30. Low-energy, high luminosity e^+e^- experiments like the B-Factories are in excellent position to probe these theories, as pointed out in papers by Batell *et al.* [403] and Essig *et al.* [404]. Broadly speaking, there are three categories for dark force searches at Super$B$: direct production, rare B-decays, and rare decays of other mesons.

The most general searches for dark forces are in direct e^+e^- production. The primary model independent signature is $e^+e^- \to \gamma A' \to \gamma l^+l^-$. While these channels are the cleanest theoretically, they suffer from large irreducible QED backgrounds. Searches for narrow resonances in $e^+e^- \to \gamma\mu\mu$ and $e^+e^- \to \gamma\tau\tau$ have been carried out by CLEO [405] and *BABAR* [406]. The limit on ϵ obtained from the *BABAR* $e^+e^- \to \gamma\mu\mu$ anal-

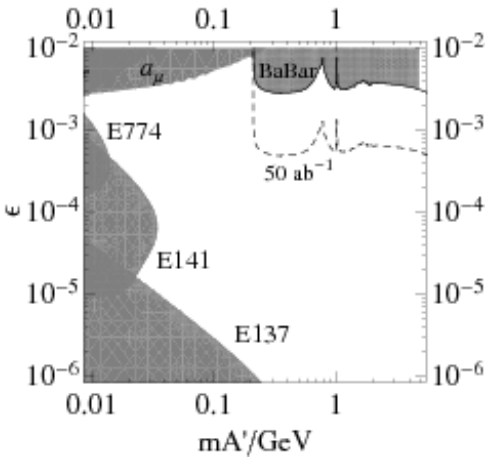

FIG. 30: Shaded: The current constraints on the kinetic mixing parameter ϵ as a function of dark photon mass. Dashed line: the expected constraint from Super$B$ with $50ab^{-1}$ of data.

ysis using $32fb^{-1}$ is shown on Figure 30. With the increased luminosity, Super$B$ should be sensitive to values of ϵ down to 5×10^{-4}. Since the gauge symmetry of the dark sector is by construction broken, there is also at least one "dark Higgs" (h') in the model. Therefore there can also be interactions like $e^+e^- \to A'h' \to 3(l^+l^-)$. While this channel is suppressed with respect to $e^+e^- \to \gamma A'$, the final state of 6-leptons (with possibly all three pairs giving a narrow resonance) should be much cleaner with a small irreducible QED background. There are a number of other, more model dependent searches we can do at Super$B$. For instance, if the dark force is non-Abelian there can be final states with 4-,8-, or even 12- or more leptons with many pairs forming a narrow resonance. While these final states are harder to use to extract ϵ limits, any evidence of a narrow resonance in them would be evidence for new physics.

Searches can also be performed in very rare decays of the B meson. Generally speaking, and decay involving a photon can be used to search for a dark photon. We can search in the l^+l^- mass spectrum in modes such as $B \to Kl^+l^-$ for a narrow resonance, although there will be a large background from the normal SM process. In addition, loop dominated modes such as $B^0 \to l^+l^-l^+l^-$ or $B \to Kl^+l^-l^+l^-$ can enhanced by a "Higgs′-strahlung' from the top quark in the loop [407]. If these modes are observed, We can look in the di-lepton mass spectrum for a resonance.

Finally, we can search for dark forces in rare meson decays [408]. The Super$B$ experiment will not be just a B meson factory, it will also produce huge samples of other mesons such as π^0, η, K, ϕ, and $J\psi$. For instance, there are roughly $10^{10}\pi^0/ab^{-1}$ and $10^9\eta/ab^{-1}$ produced which can be used to search for the channel $\pi^0/\eta \to \gamma A' \to \gamma l^+l^-$. Searching the huge meson samples for rare decays such as these should give limits on ϵ that are competitive to other measurements.

D. Section summary

TO COMPLETE ...

The section summary should provide a succinct recap of the main points discussed within the section, including (if relevant) summary tables of sensitivitites.

10. Role of Lattice QCD

This section describes the role of lattice QCD in the physics case of Super$B$.

While there are some flavour observables, like the angles of unitarity triangle, which can be determined with rather small or even negligible theoretical uncertainties, in other cases the extraction of physical results also relies on theoretical inputs, mainly on lattice QCD calculations. This is the case, for example, of several among the constraints entering the unitarity triangle analysis, for which an extrapolation at the Super$B$ is illustrated in Fig. 31 [40]. In this analysis,

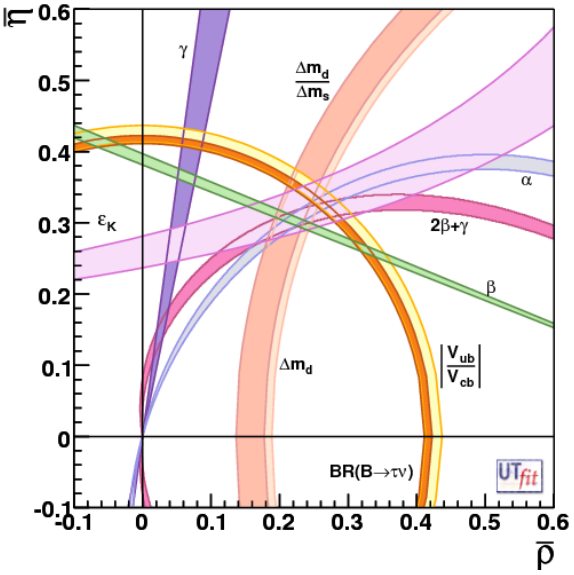

FIG. 31: Unitarity triangle fit within the SM extrapolated using expected results at Super$B$ and future lattice QCD calculations [40]. Central values of the constraints are chosen from the present UT fit. The bands show the 95% probability regions selected by the single constraints.

in order to convert into constraints in the $(\bar{\rho},\bar{\eta})$-plane the measurements of leptonic $(B \to \tau\nu)$ and semileptonic $(B \to \pi(\rho)l\nu / B \to D(D^*)l\nu)$ B decay rates and of $K^0 - \bar{K}^0$ and $B^0_{d/s} - \bar{B}^0_{d/s}$ mixing amplitudes (ε_K, Δm_d and $\Delta m_d/\Delta m_s$), a determination of the corresponding hadronic matrix elements is required. These matrix elements are expressed in terms of decay constants (f_B), form factors ($\mathcal{F}^{B\to D/D^*}$, $f_+^{B\pi}, \ldots$) and bag parameters ($f_{Bs}\sqrt{B_{B_s}}$, ξ).

For the physics case of Super$B$, in order to exploit the full power of flavour physics for NP searches and, even more, NP characterization, improved theoretical predictions are essential. Hadronic uncertainties in particular need to be controlled with an unprecedented accuracy, comparable to the one achieved by the experimental measurements. For most of the hadronic parameters, the precision necessary to fulfill such a requirement is at the level of few percent or better.

Lattice QCD is the theoretical tool of choice to compute hadronic quantities. Being only based on first principles, it does not introduce additional free parameters besides the fundamental couplings of QCD, namely the strong coupling constant and the quark masses. In addition, all systematic uncertainties affecting the results of lattice calculations can be systematically reduced in time, with the continuously increasing availability of computing power. The development of new algorithms and of new theoretical techniques further speeds up the process of improving precision.

The important issue of whether the precision of lattice QCD calculations will succeed in competing with the experimental one at the time when a Super$B$ factory could be running has been addressed in a dedicated study [409] reported in the Super$B$ CDR [40]. The result of this study was promising: in order to reach the few percent accuracy required in the determination of the most relevant hadronic parameters, supercomputers performing in the 1-10 PFlops range are required. This computing power is just in the ball park of what is expected to be available to lattice QCD collaborations in $\sim$ 2015, when a Super$B$ factory could be running and producing results.

In the study of Ref. [40], the estimate of the precision expected to be reached by lattice QCD calculations covered a temporal extension of about 10 years (2006-2015). Such an estimate is unavoidably affected by some uncertainties. The dominant sources of errors in lattice QCD calculations have systematic origin, so that the accuracy of the lattice results does not improve in time by following simple scaling laws (at variance with the computing power, which increases instead according to a rather predictable exponential behavior). Therefore, predictions in this context are necessarily based also on educated guesses, and their reliability decreases the more we attempt to go further in time.

After three years from the presentation of Ref. [40], we are now in the position of start verifying whether the improvements predicted for lattice QCD calculations were accurate. This is already a non-trivial check. Indeed, while for many years lattice calculations have been plagued by the use of the quenched approximation, so that the typical lattice uncertainties at the time of Ref. [40] were at the level of 10-15%, in the last few years extensive unquenched lattice QCD simulations have been performed, by various lattice collaborations and using different approaches (i.e. different lattice actions, renormalization techniques, etc.). For

TABLE XX: Prediction of the accuracy on the lattice QCD determinations of various hadronic parameters from Ref. [40]. The 5^{th} column has been added for the present work.

Measurement	Hadronic Parameter	Status End 2006	6 TFlops (Year 2009)	**Status End 2009**	60 TFlops (Year 2011)	1-10 PFlops (Year 2015)
$K \to \pi\, l\, \nu$	$f_+^{K\pi}(0)$	0.9 %	0.7 %	0.5 %	0.4 %	< 0.1 %
ε_K	$\hat{B}_K$	11 %	5 %	5 %	3 %	1 %
$B \to l\, \nu$	f_B	14 %	3.5-4.5 %	5 %	2.5-4.0 %	1.0-1.5 %
Δm_d	$f_{Bs}\sqrt{B_{B_s}}$	13 %	4-5 %	5 %	3-4 %	1-1.5 %
$\Delta m_d/\Delta m_s$	ξ	5 %	3 %	2 %	1.5-2 %	0.5-0.8 %
$B \to D/D^*\, l\, \nu$	$\mathcal{F}^{B\to D/D^*}$	4 %	2 %	2 %	1.2 %	0.5 %
$B \to \pi/\rho\, l\, \nu$	$f_+^{B\pi}, \ldots$	11 %	5.5-6.5 %	11 %	4-5 %	2-3 %
$B \to K^*/\rho(\gamma, l^+l^-)$	$T_1^{B\to K^*/\rho}$	13 %	——	13 %	——	3-4 %

this reason, for several hadronic parameters, the typical uncertainties are now significantly reduced with respect to three years ago, by a factor 2 or 3.

A summary of lattice uncertainties and predictions for the future is presented in Table XX, which is reported from Ref. [40] except for the 5^{th} column, which is new. A representative set of measurements relevant for flavour physics and corresponding hadronic parameters is listed in the Table. The corresponding lattice uncertainty, as it was quoted at the end of 2006, is given in the 3rd column. In the 4^{th}, 6^{th} and 7^{th} columns, the accuracy predicted for the future is presented, assuming the availability of a computing power of about 6 TFlops, 60 TFlops and 1-10 PFlops respectively. These performances are those expected for supercomputers typically available to lattice QCD collaborations in the years 2009, 2011 and 2015 respectively. Thus, the last column of the Table predicts in particular the accuracy that is expected to be reached by lattice QCD calculations at the time of the Super$B$. This prediction indicates that, for most of the relevant quantities, a precision at the level of 1% should be reached.

In Table XXI we collect a set of current lattice averages for the same hadronic parameters listed in Table XX. Central values and errors are quoted from Ref. [410] for the kaon observables ($f_+^{K\pi}(0)$ and $\hat{B}_K$), Ref. [411] for the B physics parameters (f_B, $f_{Bs}\sqrt{B_{B_s}}$, ξ) and Ref. [412] for the semi-leptonic form factors ($\mathcal{F}^{B\to D^*}$, $\mathcal{G}^{B\to D}$ and $f_+^{B\pi}$). On the basis of these results we have compiled the new (5^{th}) column of Table XX summarizing the status of lattice calculations at the end of 2009.

The main conclusion which can be drawn from this analysis is that there is quite a good agreement between the predictions for the year 2009 (4th column of Table XX) and the accuracy actually reached by lattice calculations (5^{th} column of Table XX). Even though the prediction was made only 3 years ago, thus a relatively short time with respect to the whole time interval of about 10 years considered in Table XX, it should be also noted that we have witnessed significant changes in the last 3 years. Realistic unquenched lattice simulations have been performed, and for most of the hadronic quantities listed in Table XX the achieved accuracy has improved by a factor two or more (compare the 3^{rd} and 5^{th} columns of the Table). This improvement has been quite precisely predicted, at a quantitative level, by the dedicated studies of Refs. [40, 409].

There is one notable exception to the previous conclusion. It is represented by the lattice determination of the form factor controlling the exclusive $B \to \pi\, l\, \nu$ semi-leptonic decays. The relative uncertainty on this form factor was about 11% at the end of 2006. It was predicted to decrease by approximately a factor 2 within by the end of 2009, but it is actually unchanged with respect to three years ago. One possible reason for that is the following: at variance with the

TABLE XXI: Lattice averages for various hadronic parameters. The result for the semi-leptonic form factor $f_+^{B\pi}$ has been already converted into the corresponding exclusive determination of $|V_{ub}|$.

Hadronic Parameter	Lattice average	Ref.
$f_+^{K\pi}(0)$	0.962(3)(4)	[410]
$\hat{B}_K$	0.731(7)(35)	[410]
f_B (MeV)	192.8(9.9)	[411]
$f_{Bs}\sqrt{\hat{B}_{B_s}}$ (MeV)	275(13)	[411]
ξ	1.243(28)	[411]
$\mathcal{F}^{B\to D^*}(1)$	0.924(22)	[412]
$\mathcal{G}^{B\to D}(1)$	1.060(35)	[412]
$\lvert V_{ub}\rvert_{excl.}$	$35(4)\,10^{-4}$	[412]

other quantities listed in Table XX, only two modern lattice studies [413, 414] of the exclusive $B \to \pi\, l\, \nu$ decays have been performed so far (both based on the same staggered gauge configurations generated by the MILC collaboration). The results of these studies are in agreement within each other and also with older quenched results, see Fig. 32. The accuracy on the de-

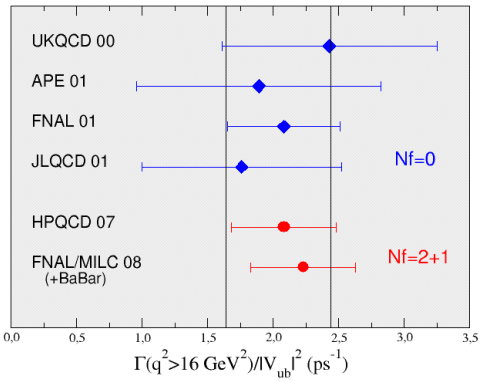

FIG. 32: Lattice QCD results for $\Gamma(B \to \pi\, l\, \nu; q^2 > 16\ GeV^2)/|V_{ub}|^2$. The estimated average is shown by the vertical band. The plot is an update from Ref. [412].

termination of the relevant form factor, $f_+^{B\pi}(q^2)$, in the two modern calculations, however, is still at the level of 10%, which is the uncertainty quoted in Tables XX and XXI. Thus, a larger number of (possibly) more accurate lattice studies of $B \to \pi\, l\, \nu$ decays would be welcome in order to improve the theoretical prediction also in this case.

For all other quantities listed in Table XX, the agreement between the prediction of Refs. [40, 409] and the accuracy actually reached at present by lattice calculations is encouraging. It shows that lattice calculations are rapidly improving in the last few years, and to expectations. It also supports the prediction for the time in which a Super$B$ factory could be running, indicating that the percent accuracy could be actually reached by lattice QCD. If this will be the case, then the next generation of flavour physics experiments will not be limited by the hadronic uncertainties, and the theoretical accuracy will succeed in competing with the experimental one.

A. Section summary

The section summary should provide a succinct recap of the main points discussed within the section, including (if relevant) summary tables of sensitivitites.

11. Interplay between measurements

Numerous studies of flavour and *CP* violating observables in New Physics models have been performed over the past years. In the following we give a brief summary of the results obtained within the MSSM with various realizations of flavour, in the SM with a 4th generation of quarks and leptons (SM4), in Randall-Sundrum models with bulk fields, both with the SM bulk gauge group (minimal RS) and with a protective custodial symmetry (RSc), and in the Littlest Higgs model with T-parity (LHT model). Clearly our focus lies on those observables that can be measured at a Super Flavour Factory with high precision and thus provide a powerful tool to discriminate among various scenarios.

A. MSSM

MSSM contains large numbers of new parameters which can potentially produce the flavour and *CP* violating phenomena beyond SM. The search for SUSY via flavour physics is particularly important since many of the parameters mentioned above are related to the SUSY breaking mechanism, which occurs at higher energies than that accessible at the energy frontier experiments. For this reason, various scenarios to search for signals of MSSM at Super$B$ have been devised.

Since the SUSY breaking term contains a huge number of free parameters, how to interpret the New Physics signal in the framework of MSSM is non trivial. With regard to this aspect, the large number of observables measurable at Super$B$ is advantageous as the correlations of those different observables play a central role in constraining the SUSY parameters. In the following we will illustrate different kinds of "interplay" (correlation among the observables) between observables measurable at Super$B$.

1. *Minimal flavour model: interplay to the LHC direct search*

Even if we assume the SUSY breaking is flavour blind (no additional flavour violation beyond that introduced via the CKM matrix), there are still SUSY effects observable at Super$B$. The effects are expected for example when one chooses a large value for $\tan\beta$ and/or the split Higgs mass. Since most of the SUSY particle searches at LHC are aiming to investigate this class of models one can study the complementarity of Super$B$ and the energy frontier experiments such as ATLAS and CMS. Figure 33 (taken from Ref. [415]) shows the constraints that can be obtained for the charged Higgs mass for given value of $\tan\beta$ from different observables, which include the Super$B$ golden channels, $B \to \tau\nu$ and $B \to D\tau\nu$. We have superimposed the constraint expected to be achieved from direct searches at ATLAS [416] [10]. In Table XXII, we show the expected deviation from the SM for various Super$B$ observables for the so-called LHC benchmark points.

TABLE XXII: Predictions of flavor observables based on expected measurements from the LHC in mSUGRA at SPS1a, SPS4, SPS5 benchmark points. Quantities denoted $\mathcal{R}$ are the ratios of the branching fractions relative to their Standard Model values. Quoted uncertainties (when available) come from the errors on the measurement of the New Physics parameters at LHC. Uncertainties on the Standard Model predictions of flavor observables are not included. For the SPS4 benchmark point the sensitivity study at LHC are not available. The SPS parameters are as follows (see [62] for more details). SPS 1a: (m_0 = 100 GeV, $m_{1/2}$ = 250 GeV, $A_0 = -100$ GeV, $\tan\beta = 10$, $\mu > 0$), SPS 4: (m_0 = 400 GeV, $m_{1/2}$ = 300 GeV, $A_0 = 0$, $\tan\beta = 50$, $\mu > 0$), and SPS 5: (m_0 = 150 GeV, $m_{1/2} = 300$ GeV, $A_0 = -1000$, $\tan\beta = 5$, $\mu > 0$).

	SPS1a	SPS4	SPS5
$\mathcal{R}(B \to X_s\gamma)$	0.919 ± 0.038	0.248	0.848 ± 0.081
$\mathcal{R}(B \to \tau\nu)$	0.968 ± 0.007	0.436	0.997 ± 0.003
$\mathcal{R}(B \to X_s l^+ l^-)$	0.916 ± 0.004	0.917	0.995 ± 0.002
$\mathcal{R}(B \to K\nu\overline{\nu})$	0.967 ± 0.001	0.972	0.994 ± 0.001
$\mathcal{B}(B_d \to \mu^+\mu^-)/10^{-10}$	1.631 ± 0.038	16.9	1.979 ± 0.012
$\mathcal{R}(\Delta m_s)$	1.050 ± 0.001	1.029	1.029 ± 0.001
$\mathcal{B}(B_s \to \mu^+\mu^-)/10^{-9}$	2.824 ± 0.063	29.3	3.427 ± 0.018
$\mathcal{R}(K \to \pi^0\nu\overline{\nu})$	0.973 ± 0.001	0.977	0.994 ± 0.001

2. *Model independent analysis: interplay among the similar flavour transitions*

Contrary to the previous type of study, one can also consider the SUSY breaking parameters as free and use the Super$B$ observables to constrain them. Such study has been intensively carried out in the Super$B$ framework using the so-called Mass Insertion Approximation (MIA) (see e.g. [40]). In this approximation, a certain level of degeneracy in the squark mass is assumed in order to guarantee the suppression of the un-

[10] Additional constraints on these parameters are expected to come from the measurement of $\mathcal{B}(B_s \to \mu^+\mu^-)$ at LHCb.

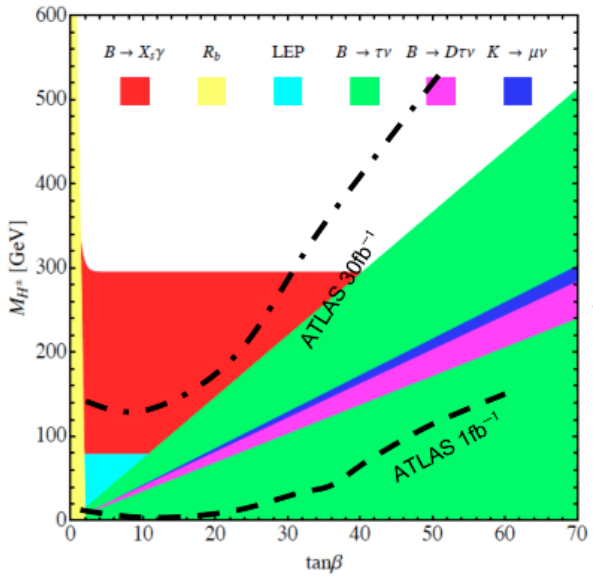

FIG. 33: The excluded region at 95% confidence level for the charged Higgs mass versus $\tan\beta$ from Ref. [415]. The branching ratio of $B \to \tau\nu$ as well as $B \to D\tau\nu$ will be significantly improved at Super$B$. The ATLAS potential expected for the excluded region obtained using 1 and 30 fb^{-1} of running at a center of mass energy of 14 TeV is also shown.

wanted large flavour violation effects (i.e. Super GIM mechanism) to the previously observed flavour phenomena, which are in good agreement with the SM predictions. Since the mass insertion parameters are defined at the electroweak scale, the relation between the SUSY parameters and the observables are quite simple. As a result, one can readily study the effect of the same mass insertion contribution to the different Super$B$ observables (e.g. mass insertion $(\delta^d)_{13/23}$ to various type of $b \to d/s$ transitions) as shown in Fig. 34. Such interplay is extremely useful to distinguish between different types of SUSY.

3. *Model dependent analysis: interplay among different type of flavour observables*

Another approach to tackle the large number of SUSY parameters is to use a theoretically motivated flavour symmetry for the SUSY parameters at a high energy (at the SUSY breaking scale, GUT scale etc.). There have been various attractive proposals for such symmetry. One such example is a Grand Unification Theory (GUT) in which the quark and the lepton sectors are unified at the GUT scale. In this class of approach, non-trivial correlations can appear. One of such examples contains an apparent relation between

TABLE XXIII: "DNA" of flavour physics effects for the most interesting observables in a selection of SUSY models from Ref. [419]. ★★★ signals large effects, ★★ visible but small effects and ★ implies that the given model does not predict sizable effects in that observable.

	AC	RVV2	AKM	δLL	FBMSSM
$D^0 - \bar{D}^0$	★★★	★	★	★	★
$S_{\psi\phi}$	★★★	★★★	★★★	★	★
$S_{\phi K_S}$	★★★	★★	★	★★★	★★★
$A_{\rm CP}\,(B \to X_s\gamma)$	★	★	★	★★★	★★★
$A_{7,8}(B \to K^*\mu^+\mu^-)$	★	★	★	★★★	★★★
$A_9(B \to K^*\mu^+\mu^-)$	★	★	★	★	★
$B \to K^{(*)}\nu\bar{\nu}$	★	★	★	★	★
$B_s \to \mu^+\mu^-$	★★★	★★★	★★★	★★★	★★★
$\tau \to \mu\gamma$	★★★	★★★	★	★★★	★★★

the the $2-3$ generation transition of quark and lepton sectors (such as $b \to s$ transitions and $\tau \to \mu$ transition) in SUSY-GUT models. Some examples are shown in Fig. 35 from Ref. [417].

In Ref. [419], various kinds of flavour models are studied. A brief summary of their results are shown in Table XXIII, which indicates the possible size of effects in various B physics observables, in $D^0 - \bar{D}^0$ mixing and in the $\tau \to \mu\gamma$ decay. Finding for instance large NP effects in the latter decay or in the CP asymmetry $S_{\phi K_S}$ would rule out the AKM model [420] while favoring the other models analyzed. Similarly observing significant CP violating effects in $D - \bar{D}$ mixing would disfavor all models analyzed except the AC [421] model [422].

In the same article, it is also pointed out that even the flavour blind MSSM (FBMSSM) analyzed in [423] can account for large effects in various B physics observables. Of particular interest in this case are CP violating observables like $A_{\rm CP}^{b\to s\gamma}$ and $S_{\phi K_S}$ which, due to the minimal flavour structure of the model, are highly correlated with electric dipole moments (EDMs). In Fig. 36 we show $A_{\rm CP}^{b\to s\gamma}$ as a function of $S_{\phi K_S}$. Due to the strong correlation between these two asymmetries, the aim to address the present tension in $S_{\phi K_S}$ unambiguously predicts large NP effects in the CP asymmetry in $b \to s\gamma$, which even changes sign with respect to the SM prediction.

B. Fourth generation of quarks and leptons

Recently the implications on flavour physics observables from extending the SM by adding a fourth generation of quarks and leptons (SM4) have received a

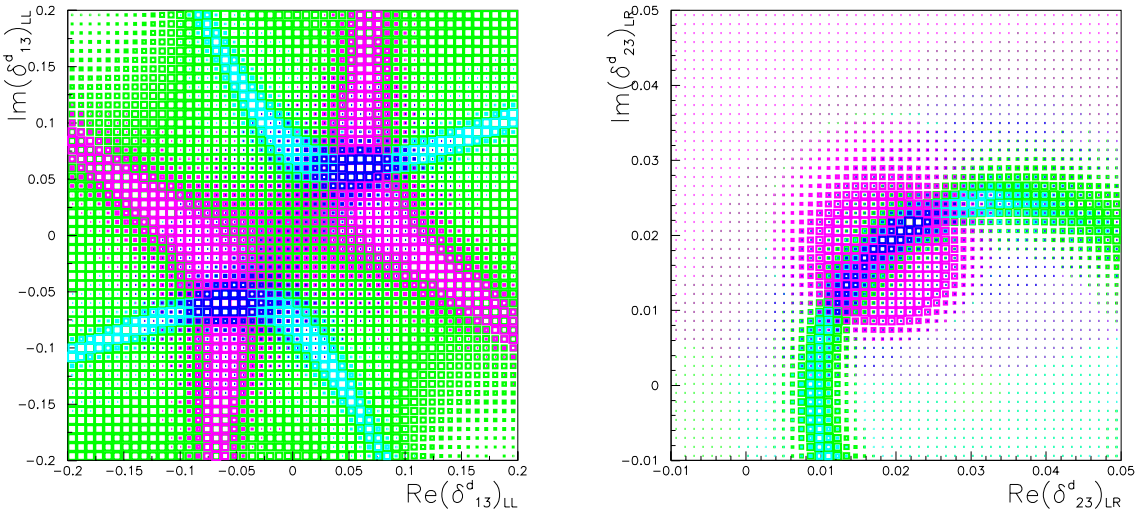

FIG. 34: Left: Density plot of the selected region in the $Re(\delta^d_{13})_{LL} - Im(\delta^d_{13})_{LL}$ for $m_{\tilde{q}} = m_{\tilde{g}} = 1$ TeV and $(\delta^d_{13})_{LL} = 0.085e^{i\pi/4}$ using Super$B$ measurements (namely, 1-3 generation transitions). Different colors correspond to different constraints: $A^d_{\rm SL}$ (green), β (cyan), Δm_d (magenta), all together (blue). Right: Density plot of the selected region in the $Re(\delta^d_{23})_{LR} - Im(\delta^d_{23})_{LR}$ for $m_{\tilde{q}} = m_{\tilde{g}} = 1$ TeV and $(\delta^d_{23})_{LR} = 0.028e^{i\pi/4}$ using Super$B$ measurements (namely, 2-3 generation transitions). Different colors correspond to different constraints: $\mathcal{B}(B \to X_s\gamma)$ (green), $\mathcal{B}(B \to X_s l^+ l^-)$ (cyan), $A_{CP}(B \to X_s\gamma)$ (magenta), all together (blue).

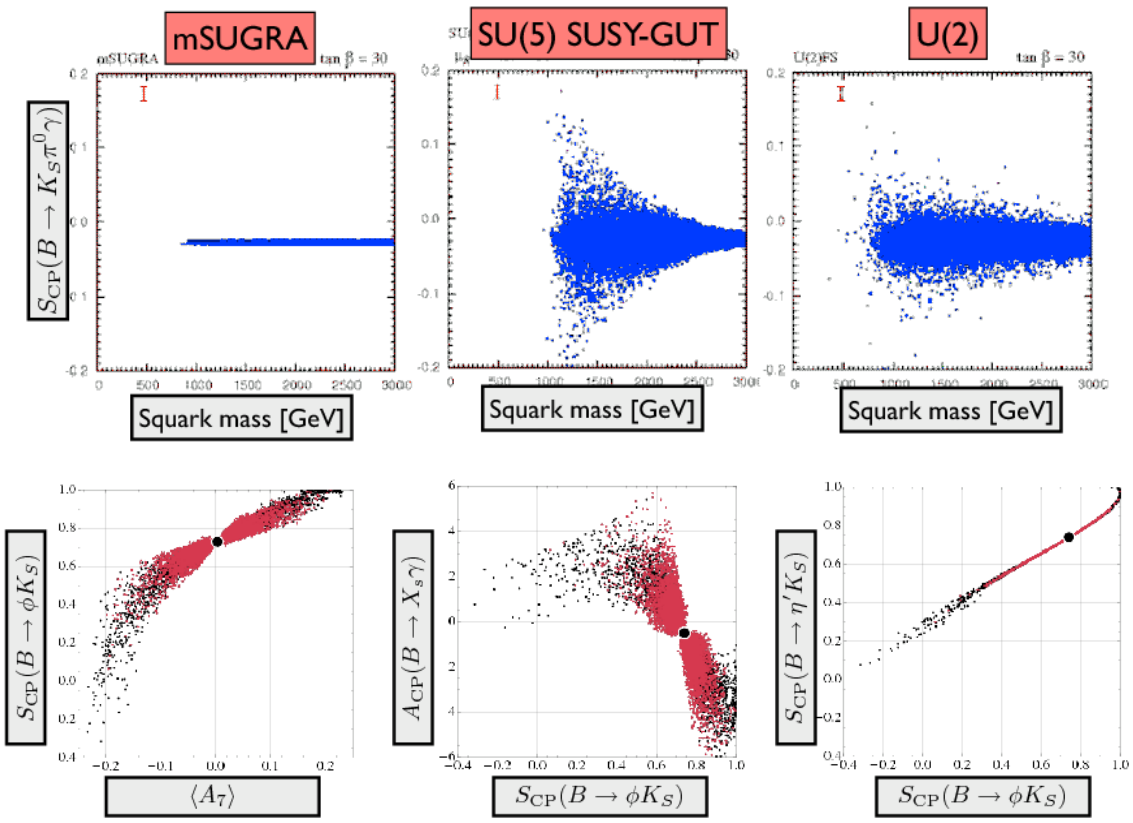

FIG. 35: The top figures are scatter plots of the time-dependent *CP* asymmetry for $B \to K_S\pi^0\gamma$ in terms of the averaged squark mass. The varied parameters are those given in the specific flavour models, mSUGRA (top-left), SU(5) SUSY-GUT (top-middle), U(2) (top-right) (see [417] for more details). The bottom figures are the result for the various observables for the so-called δLL mass insertion model [418]. Large correlations can be observed between various Super$B$ observables (see [419] for more details).

lot of attention, see e. g. [222, 248, 424–430]. The guidelines of how to extract the new parameters of the CKM4 matrix from future data has been presented in [430] and will not be repeated here. Instead we show in Figs. 37 and 38 the *CP* asymmetries $S_{\phi K_S}$ and $A_{\rm CP}^{b\to s\gamma}$, respectively, as functions of $S_{\psi\phi}$. In both cases a strong correlation can be observed. Therefore, if the present deviation from the SM prediction in $S_{\psi\phi}$ will be confirmed in the future more accurate experiments, the SM4 unambiguously predicts large effects in $S_{\phi K_S}$ and $A_{\rm CP}^{b\to s\gamma}$. Together with the possible direct observation of a 4th generation at the LHC, these effects can be used to tighten the allowed SM4 parameter space.

C. Minimal and custodially extended RS models

A theoretically appealing approach to the SM flavour puzzle is given by Randall-Sundrum models with bulk fermions [431]. In this scenario the observed hierarchies in quark masses and CKM mixings are naturally obtained from the different localization of fermions along the 5D bulk. Implications for low energy flavour violating observables have been studied extensively in the literature, see e. g. [432–434].

Interestingly the observed pattern of effects depends crucially on the realization of the model. In the minimal scenario with only the SM gauge group in the bulk, the NP contributions to rare decays are dominantly left-handed. Consequently large effects could be expected in both B and K decays [432–434]. As an example Fig. 39 shows the correlation between $Br(B_s \to \mu^+\mu^-)$ and $Br(B \to X_s\nu\bar{\nu})$ in the minimal RS model. The latter branching ratio can reach values larger than 10^{-4}, which necessarily coincide with large NP effects also in the former channel.

The situation is completely different in the case of a custodially extended bulk gauge symmetry [433]. Due to the suppression of left-handed flavour changing Z couplings, rare decays in this case are dominated by right-handed currents. Consequently, while large NP effects can appear in the kaon sector, the effects in rare B decays are predicted to be small and therefore difficult to disentangle from the SM. The situation is however different in the $\Delta F = 2$ sector, where a large

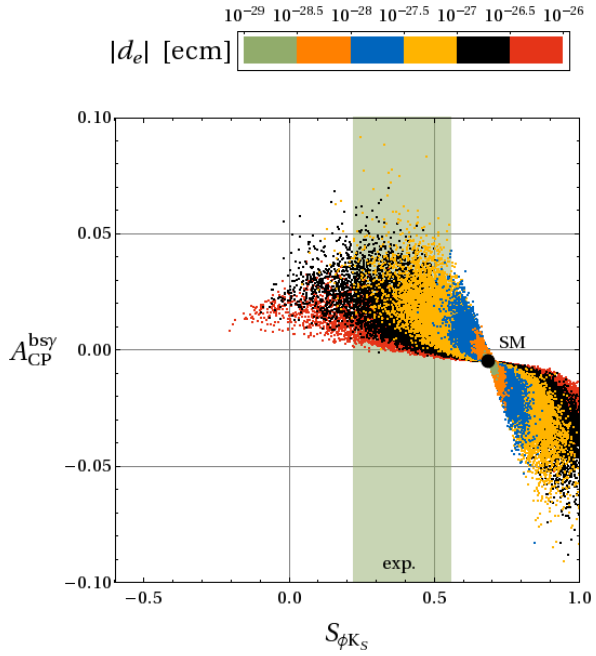

FIG. 36: Correlation between the CP asymmetries $A_{\rm CP}^{b\to s\gamma}$ and $S_{\phi K_S}$ in the FBMSSM [423]. The various colors indicate the predicted lower bound on the electron EDM.

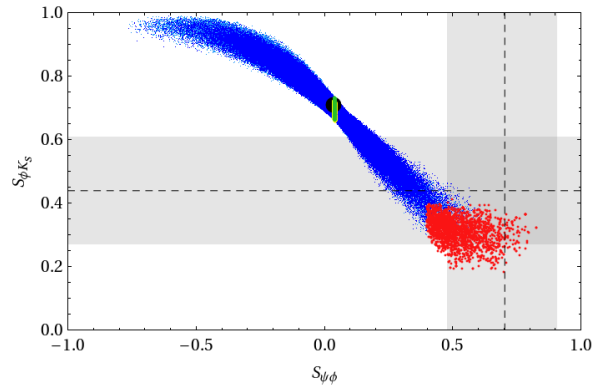

FIG. 37: Correlation between the *CP* asymmetries $S_{\phi K_S}$ and $S_{\psi\phi}$ in the SM4 [430].

new phase in $B_s - \bar{B}_s$ mixing can be generated (see Fig. 40).

D. Littlest Higgs model with T-parity

The detailed FCNC studies in the Littlest Higgs model with T-parity (LHT) performed in 2006–2007 [435] have recently been updated [436] in light of an additional LHT contribution to the Z penguin pointed out in [437] and of new input from experiments and lattice calculations. While the additional contribution

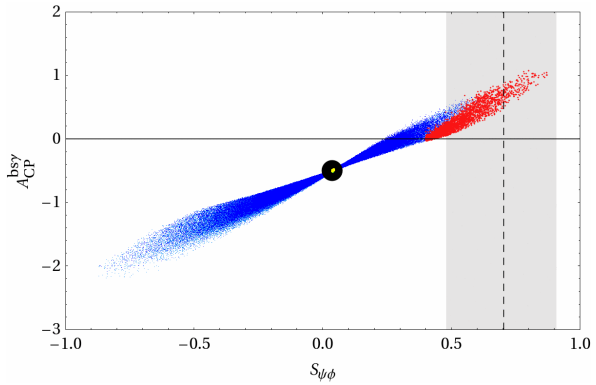

FIG. 38: Correlation between the *CP* asymmetries $A_{\rm CP}^{b\to s\gamma}$ and $S_{\psi\phi}$ in the SM4 [430].

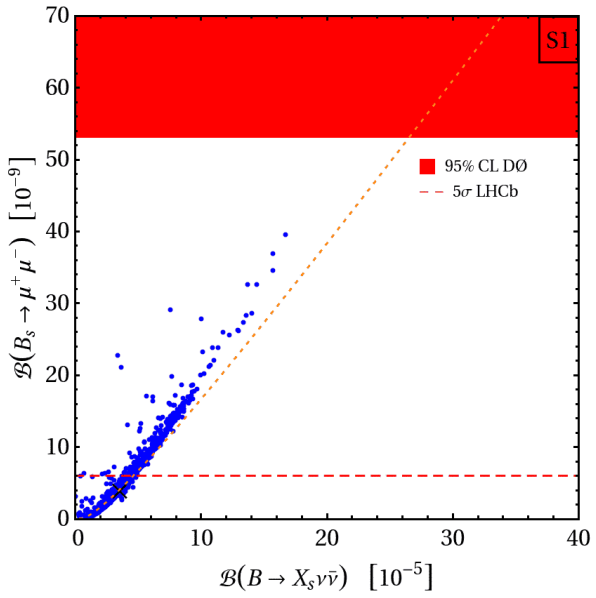

FIG. 39: Correlation between the branching ratios for $B_s \to \mu^+\mu^-$ and $B \to X_s\nu\bar{\nu}$ in the minimal RS model [434].

affected the size of some of the possible effects, the main conclusions from [435] remained intact:

- Large NP effects are possible in *CP* asymmetries related to $B_s - \bar{B}_s$ mixing and in rare K decays.
- The effects in rare B decays are small and therefore difficult to measure.
- Large effects can be expected in LFV μ and τ decays, as summarized in Table XXIV.
- Ratios of LFV branching ratios turn out to be very different from the MSSM predictions and can therefore serve as a clean tool to distinguish between these two models (see Table XXV).

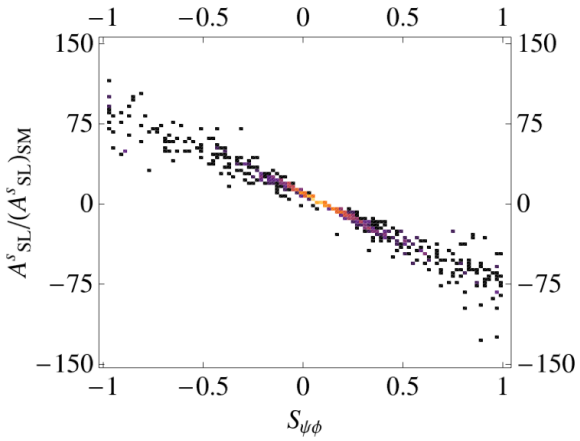

FIG. 40: Correlation between the *CP* asymmetries $A^s_{\rm SL}$ and $S_{\psi\phi}$ in the RSc model [433].

TABLE XXIV: Maximal values on LFV τ decay branching ratios in the LHT model, for two different values of the scale f, after imposing the constraints on $\mu \to e\gamma$ and $\mu^- \to e^-e^+e^-$ [436].

decay	$f = 1000\,\text{GeV}$	$f = 500\,\text{GeV}$	Super$B$ sensitivity
$\tau \to e\gamma$	$8 \cdot 10^{-10}$	$2 \cdot 10^{-8}$	$2 \cdot 10^{-9}$
$\tau \to \mu\gamma$	$8 \cdot 10^{-10}$	$2 \cdot 10^{-8}$	$2 \cdot 10^{-9}$
$\tau^- \to e^-e^+e^-$	$1 \cdot 10^{-10}$	$2 \cdot 10^{-8}$	$2 \cdot 10^{-10}$
$\tau^- \to \mu^-\mu^+\mu^-$	$1 \cdot 10^{-10}$	$2 \cdot 10^{-8}$	$2 \cdot 10^{-10}$
$\tau^- \to e^-\mu^+\mu^-$	$1 \cdot 10^{-10}$	$2 \cdot 10^{-8}$	
$\tau^- \to \mu^-e^+e^-$	$1 \cdot 10^{-10}$	$2 \cdot 10^{-8}$	
$\tau^- \to \mu^-e^+\mu^-$	$6 \cdot 10^{-14}$	$1 \cdot 10^{-13}$	
$\tau^- \to e^-\mu^+e^-$	$6 \cdot 10^{-14}$	$1 \cdot 10^{-13}$	
$\tau \to \mu\pi$	$4 \cdot 10^{-10}$	$5 \cdot 10^{-8}$	
$\tau \to e\pi$	$4 \cdot 10^{-10}$	$5 \cdot 10^{-8}$	
$\tau \to \mu\eta$	$2 \cdot 10^{-10}$	$2 \cdot 10^{-8}$	$4 \cdot 10^{-10}$
$\tau \to e\eta$	$2 \cdot 10^{-10}$	$2 \cdot 10^{-8}$	$6 \cdot 10^{-10}$
$\tau \to \mu\eta'$	$1 \cdot 10^{-10}$	$2 \cdot 10^{-8}$	
$\tau \to e\eta'$	$1 \cdot 10^{-10}$	$2 \cdot 10^{-8}$	

A detailed study of $D^0 - \bar{D}^0$ mixing in the LHT model has been performed in [439]. While in case of the *CP* conserving observables x and y a possible NP contribution is difficult to disentangle due to the poor knowledge of the SM long-distance contributions, an observation of *CP* violation in the D system would be an unambiguous sign of NP. Figure 41 shows the correlation between the semi-leptonic *CP* asymmetry $a_{\rm SL}$ and the asymmetry in $D \to K_S\phi$ decays. We observe that in both observables LHT physics can lead to spectacular deviations from the tiny SM prediction. A deviation from the correlation in Fig. 41 would be a clear sign of direct *CP* violation in the $D \to K_S\phi$ channel.

TABLE XXV: Comparison of various ratios of branching ratios in the LHT model ($f = 1\,\text{TeV}$) [436] and in the MSSM without [438] and with [12] significant Higgs contributions.

ratio	LHT	MSSM (dipole)	MSSM (Higgs)
$\frac{Br(\tau^- \to e^-e^+e^-)}{Br(\tau \to e\gamma)}$	$0.04 \ldots 0.4$	$\sim 1 \cdot 10^{-2}$	$\sim 1 \cdot 10^{-2}$
$\frac{Br(\tau^- \to \mu^-\mu^+\mu^-)}{Br(\tau \to \mu\gamma)}$	$0.04 \ldots 0.4$	$\sim 2 \cdot 10^{-3}$	$0.06 \ldots 0.1$
$\frac{Br(\tau^- \to e^-\mu^+\mu^-)}{Br(\tau \to e\gamma)}$	$0.04 \ldots 0.3$	$\sim 2 \cdot 10^{-3}$	$0.02 \ldots 0.04$
$\frac{Br(\tau^- \to \mu^-e^+e^-)}{Br(\tau \to \mu\gamma)}$	$0.04 \ldots 0.3$	$\sim 1 \cdot 10^{-2}$	$\sim 1 \cdot 10^{-2}$
$\frac{Br(\tau^- \to e^-e^+e^-)}{Br(\tau^- \to e^-\mu^+\mu^-)}$	$0.8 \ldots 2.0$	~ 5	$0.3 \ldots 0.5$
$\frac{Br(\tau^- \to \mu^-\mu^+\mu^-)}{Br(\tau^- \to \mu^-e^+e^-)}$	$0.7 \ldots 1.6$	~ 0.2	$5 \ldots 10$

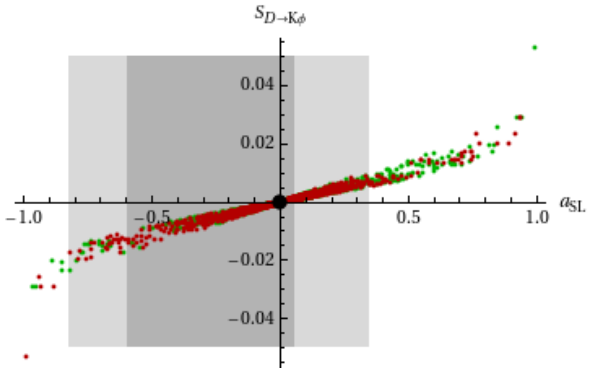

FIG. 41: Correlation between the *CP* asymmetries $a_{\rm SL}$ and $S_{K_S\phi}$ in the LHT model [439].

E. Precision CKM constraints.

The CKM ansatz has been tested at the 10% level by *BABAR* and Belle. One significant consequence of recording $75\,\text{ab}^{-1}$ of data at the $\Upsilon(4S)$ is that it will be possible to push the precision of this global CKM test down to the percent level. It is worth recalling that there are direct (i.e. measurements of the angles of the unitarity triangle) and indirect ways to test the CKM mechanism. One advantage of a Super Flavour Factory compared to other flavour experiments is that it will be able to perform a wide array of measurements of both the direct and indirect constraints. The consequence of this is that Super$B$ will be able to perform a self-consistent over-constraint of the description of quark mixing in the SM, and as is shown in Figure 31, if one extrapolates measurements from today, to the era of Super$B$ we could find the dream scenario where

constraints do not converge on a single point indicating that new physics modifies our understanding of quark mixing. The alternative so-called nightmare scenario would be that once again the SM description is a good enough description of the experimental picture of nature that we have built up since the pivotal work of Cabibbo from 1963 on quark mixing [440].

The nightmare scenario is by no means the end of the road. In fact in many situations, this would signify the beginning of a number of new physics searches, some of which would be possible at Super$B$, but there would also be a number of new physics searches possible at other experiments. One example is that of the measurement of the the $K \to \pi\nu\overline{\nu}$ branching fraction. The theoretical uncertainty on the branching fraction of the charged and neutral modes is dominated by knowledge of the CKM matrix. In the case of $K^+ \to \pi^+\nu\overline{\nu}$ this is 33%, and for $K_L^0 \to \pi^0\nu\overline{\nu}$ this is 52% [441]. With the current knowledge of the CKM mechanism a measurement of either of these modes would provide another constraint on the SM, however with a precision over-constraint of the CKM mechanism from Super$B$, then these kaon branching fractions would be sensitive probes of new physics via loop amplitudes in analogy with the discussions in Section 4 for the study of rare B decays. Thus the role of Super$B$ in elucidating flavour physics and searching for new physics, transcends the limitations of measurements possible at a Super Flavour Factory and has potentially important consequences for the interpretation of the results from other proposed or existing flavour physics experiments.

F. Summary

The section summary should provide a succinct recap of the main points discussed within the section, including (if relevant) summary tables of sensitivitites.

TABLE XXVI: Golden matrix of observables/modes that can be measured at SuperB. The effect of a given model is indicated by the number of stars: ⋆⋆⋆, ⋆⋆, ⋆. The more stars the larger the effect. Additional notes: CKM indicates precision CKM required. Lattice QCD improvements are required at the predicted level (See CDR/White paper for details). The information here is taken from previous work done within superb and from arXiv:0909.1333.

Observable/mode	H^+ high $\tan\beta$	MFV	non-MFV	NP Z penguins	Right-handed currents	LTH	SUSY AC	SUSY RVV2	SUSY AKM	SUSY δLL	SUSY FBMSSM
$\tau \to \mu\gamma$						⋆	⋆	⋆	⋆	⋆	⋆
$\tau \to \ell\ell\ell$						⋆⋆	⋆⋆	⋆⋆		⋆⋆	⋆⋆
$B \to \tau\nu, \mu\nu$	⋆⋆⋆(CKM)					⋆	⋆	⋆			
$B \to K^{(*)+}\nu\overline{\nu}$			⋆	⋆⋆				⋆	⋆	⋆	⋆
S in $B \to K_S^0\pi^0\gamma$					⋆⋆⋆						
S in other penguin modes			⋆⋆⋆(CKM)		⋆⋆⋆		⋆⋆⋆	⋆⋆	⋆	⋆⋆⋆	⋆⋆⋆
$A_{CP}(B \to X_s\gamma)$			⋆⋆⋆		⋆⋆		⋆	⋆	⋆	⋆⋆⋆	⋆⋆⋆
$BR(B \to X_s\gamma)$		⋆⋆⋆	⋆		⋆						
$BR(B \to X_s\ell\ell)$			⋆	⋆	⋆						
$B \to K^{(*)}\ell\ell$ (FB Asym)							⋆	⋆	⋆	⋆⋆⋆	⋆⋆⋆
$B_s \to \mu\mu$							⋆⋆⋆	⋆⋆⋆	⋆⋆⋆	⋆⋆⋆	⋆⋆⋆
β_s from $B_s \to J/\psi\phi$							⋆⋆⋆	⋆⋆⋆	⋆⋆⋆	⋆	⋆
a_{sl}						⋆⋆⋆					
Charm mixing							⋆⋆	⋆	⋆	⋆	⋆
CPV in Charm	⋆⋆						⋆⋆			⋆⋆	

12. Tools

This section needs to be written from scratch

A. Monte Carlo simulation frameworks

1. *Fast Simulation*

2. *Full Simulation*

B. Analysis tools

C. Section summary

13. Conclusions

This should be a succinct summary of the global programme.

14. Appendices

A. Some detailed content ...

[1] B. C. Allanach et al., Eur. Phys. J. **C25**, 113 (2002), hep-ph/0202233.
[2] E. Arganda, M. J. Herrero, and J. Portoles, JHEP **06**, 079 (2008), 0803.2039.
[3] A. Masiero, S. K. Vempati, and O. Vives, Nucl. Phys. **B649**, 189 (2003), hep-ph/0209303.
[4] S. Antusch, E. Arganda, M. J. Herrero, and A. M. Teixeira, JHEP **11**, 090 (2006), hep-ph/0607263.
[5] E. Arganda and M. J. Herrero, Phys. Rev. **D73**, 055003 (2006), hep-ph/0510405.
[6] J. Hisano and Y. Shimizu, Phys. Lett. **B565**, 183 (2003), hep-ph/0303071.
[7] M. Ciuchini, A. Masiero, L. Silvestrini, S. K. Vempati, and O. Vives, Phys. Rev. Lett. **92**, 071801 (2004), hep-ph/0307191.
[8] J. K. Parry and H.-h. Zhang, Nucl. Phys. **B802**, 63 (2008), 0710.5443.
[9] M. Ciuchini et al., Nucl. Phys. **B783**, 112 (2007), hep-ph/0702144.
[10] L. Calibbi, J. Jones-Perez, and O. Vives, Phys. Rev. **D78**, 075007 (2008), 0804.4620.
[11] L. Calibbi et al. (2009), 0907.4069.
[12] P. Paradisi, JHEP **02**, 050 (2006), hep-ph/0508054.
[13] M. J. Herrero, J. Portoles, and A. M. Rodriguez-Sanchez, Phys. Rev. **D80**, 015023 (2009), 0903.5151.
[14] H. K. Dreiner, M. Kramer, and B. O'Leary, Phys. Rev. **D75**, 114016 (2007), hep-ph/0612278.
[15] M. Raidal et al. (2008), arXiv:0801.1826 [hep-ph].
[16] R. D. Cousins and V. L. Highland, Nucl. Instrum. Meth. **A320**, 331 (1992).
[17] S. Banerjee, B. Pietrzyk, J. M. Roney, and Z. Was, Phys. Rev. D (in press) (2007), arXiv:0706.3235 [hep-ph], arXiv:0706.3235 [hep-ph].
[18] B. Aubert et al. (BABAR), Phys. Rev. Lett. **104**, 021802 (2010), 0908.2381.
[19] A. Matsuzaki and A. I. Sanda, Phys. Rev. **D77**, 073003 (2008), 0711.0792.
[20] B. Oberhof, Master's thesis, University of Pisa, Italy (2009).
[21] J. Bernabeu, G. A. Gonzalez-Sprinberg, J. Papavassiliou, and J. Vidal, Nucl. Phys. **B790**, 160 (2008), 0707.2496.
[22] A. Pilaftsis and C. E. M. Wagner, Nucl. Phys. **B553**, 3 (1999), hep-ph/9902371.
[23] V. D. Barger, A. K. Das, and C. Kao, Phys. Rev. **D55**, 7099 (1997), hep-ph/9611344.
[24] G. A. Gonzalez-Sprinberg, J. Bernabeu, and J. Vidal (2007), 0707.1658.
[25] J. Bernabéu, G. A. Gonzalez-Sprinberg, and J. Vidal, Nucl. Phys. **B763**, 283 (2007), hep-ph/0610135.
[26] S. Schael et al. (ALEPH), Phys. Rept. **421**, 191 (2005), hep-ex/0506072.
[27] M. Davier (2007), private communication.
[28] S. Jadach, B. F. L. Ward, and Z. Was, Comput. Phys. Commun. **130**, 260 (2000), hep-ph/9912214.
[29] J. H. Kuhn, Phys. Rev. **D52**, 3128 (1995), hep-ph/9505303.
[30] K. Inami et al. (Belle), Phys. Lett. **B551**, 16 (2003), hep-ex/0210066.
[31] D. Delepine, G. Lopez Castro, and L. T. Lopez Lozano, Phys. Rev. **D72**, 033009 (2005), hep-ph/0503090.
[32] I. I. Bigi and A. I. Sanda, Phys. Lett. **B625**, 47 (2005), hep-ph/0506037.
[33] D. Delepine, G. Faisel, and S. Khalil, Phys. Rev. **D77**, 016003 (2008), 0710.1441.
[34] A. Datta, K. Kiers, D. London, P. J. O'Donnell, and A. Szynkman, Phys. Rev. **D75**, 074007 (2007), hep-ph/0610162.
[35] K. Kiers et al., Phys. Rev. **D78**, 113008 (2008), 0808.1707.
[36] D. Kimura, K. Y. Lee, T. Morozumi, and K. Nakagawa (2008), 0808.0674.
[37] G. Bonvicini et al. (CLEO Collaboration), Phys. Rev. Lett. **88**, 111803 (2002), hep-ex/0111095.
[38] P. Krawczyk and S. Pokorski, Phys. Rev. Lett. **60**, 182 (1988).
[39] A. Pich, Int. J. Mod. Phys. **A21**, 5652 (2006), hep-ph/0609138.
[40] M. Bona et al. (2007), 0709.0451.
[41] A. Lusiani, PoS **KAON**, 054 (2008), 0709.1599.
[42] S. Weinberg, Phys. Rev. **112**, 1375 (1958).
[43] S. Nussinov and A. Soffer, Phys. Rev. **D78**, 033006 (2008), 0806.3922.
[44] B. Aubert et al. (BaBar), Phys. Rev. **D77**, 112002 (2008), 0803.0772.
[45] S. Nussinov and A. Soffer, Phys. Rev. **D80**, 033010 (2009), 0907.3628.
[46] B. Aubert et al. (BABAR), Phys. Rev. Lett. **103**, 041802 (2009), 0904.3080.
[47] W. Altmannshofer, A. J. Buras, D. M. Straub, and M. Wick, JHEP **04**, 022 (2009), 0902.0160.
[48] J. F. Kamenik and C. Smith, Phys. Lett. **B680**, 471 (2009), 0908.1174.
[49] B. Aubert et al. (BABAR), Phys. Rev. **D78**, 072007 (2008), 0808.1338.
[50] M. Bartsch, M. Beylich, G. Buchalla, and D. N. Gao, JHEP **11**, 011 (2009), 0909.1512.
[51] K. F. Chen et al. (BELLE), Phys. Rev. Lett. **99**, 221802 (2007), 0707.0138.
[52] R. Barate et al. (ALEPH), Eur. Phys. J. **C19**, 213 (2001), hep-ex/0010022.
[53] G. Buchalla, G. Hiller, and G. Isidori, Phys. Rev. **D63**, 014015 (2000), hep-ph/0006136.
[54] Y. Yamada, Phys. Rev. **D77**, 014025 (2008), 0709.1022.
[55] C. Bird, P. Jackson, R. V. Kowalewski, and M. Pospelov, Phys. Rev. Lett. **93**, 201803 (2004), hep-ph/0401195.
[56] R. Adhikari and B. Mukhopadhyaya, Phys. Rev. **D52**, 3125 (1995), hep-ph/9411347.
[57] H. K. Dreiner et al., Phys. Rev. **D80**, 035018 (2009), 0905.2051.
[58] G. Hiller, Phys. Rev. **D70**, 034018 (2004), hep-ph/0404220.

[59] H. Davoudiasl and E. Ponton, Phys. Lett. **B680**, 247 (2009), 0903.3410.
[60] H. Georgi, Phys. Rev. Lett. **98**, 221601 (2007), hep-ph/0703260.
[61] T. M. Aliev, A. S. Cornell, and N. Gaur, JHEP **07**, 072 (2007), 0705.4542.
[62] D. G. Hitlin et al. (2008), 0810.1312.
[63] M. Misiak et al., Phys. Rev. Lett. **98**, 022002 (2007), hep-ph/0609232.
[64] T. Huber, T. Hurth, and E. Lunghi, Nucl. Phys. **B802**, 40 (2008), 0712.3009.
[65] T. Becher and M. Neubert, Phys. Rev. Lett. **98**, 022003 (2007), hep-ph/0610067.
[66] M. Misiak (2008), 0808.3134.
[67] M. Misiak and M. Steinhauser, Nucl. Phys. **B683**, 277 (2004), hep-ph/0401041.
[68] M. Gorbahn and U. Haisch, Nucl. Phys. **B713**, 291 (2005), hep-ph/0411071.
[69] M. Gorbahn, U. Haisch, and M. Misiak, Phys. Rev. Lett. **95**, 102004 (2005), hep-ph/0504194.
[70] M. Czakon, U. Haisch, and M. Misiak, JHEP **03**, 008 (2007), hep-ph/0612329.
[71] I. R. Blokland, A. Czarnecki, M. Misiak, M. Slusarczyk, and F. Tkachov, Phys. Rev. **D72**, 033014 (2005), hep-ph/0506055.
[72] K. Melnikov and A. Mitov, Phys. Lett. **B620**, 69 (2005), hep-ph/0505097.
[73] H. M. Asatrian et al., Nucl. Phys. **B749**, 325 (2006), hep-ph/0605009.
[74] H. M. Asatrian, T. Ewerth, A. Ferroglia, P. Gambino, and C. Greub, Nucl. Phys. **B762**, 212 (2007), hep-ph/0607316.
[75] M. Misiak and M. Steinhauser, Nucl. Phys. **B764**, 62 (2007), hep-ph/0609241.
[76] K. Bieri, C. Greub, and M. Steinhauser, Phys. Rev. **D67**, 114019 (2003), hep-ph/0302051.
[77] S. J. Lee, M. Neubert, and G. Paz, Phys. Rev. **D75**, 114005 (2007), hep-ph/0609224.
[78] M. Benzke, S. J. Lee, M. Neubert, and G. Paz (2010), 1003.5012.
[79] U. Haisch and A. Weiler, Phys. Rev. **D76**, 034014 (2007), hep-ph/0703064.
[80] K. S. M. Lee, Z. Ligeti, I. W. Stewart, and F. J. Tackmann, Phys. Rev. **D75**, 034016 (2007), hep-ph/0612156.
[81] C. Bobeth, M. Misiak, and J. Urban, Nucl. Phys. **B574**, 291 (2000), hep-ph/9910220.
[82] H. H. Asatryan, H. M. Asatrian, C. Greub, and M. Walker, Phys. Rev. **D65**, 074004 (2002), hep-ph/0109140.
[83] H. H. Asatryan, H. M. Asatrian, C. Greub, and M. Walker, Phys. Rev. **D66**, 034009 (2002), hep-ph/0204341.
[84] A. Ghinculov, T. Hurth, G. Isidori, and Y. P. Yao, Nucl. Phys. **B648**, 254 (2003), hep-ph/0208088.
[85] H. M. Asatrian, K. Bieri, C. Greub, and A. Hovhannisyan, Phys. Rev. **D66**, 094013 (2002), hep-ph/0209006.
[86] A. Ghinculov, T. Hurth, G. Isidori, and Y. P. Yao, Eur. Phys. J. **C33**, s288 (2004), hep-ph/0310187.
[87] A. Ghinculov, T. Hurth, G. Isidori, and Y. P. Yao, Nucl. Phys. **B685**, 351 (2004), hep-ph/0312128.
[88] C. Bobeth, P. Gambino, M. Gorbahn, and U. Haisch, JHEP **04**, 071 (2004), hep-ph/0312090.
[89] H. M. Asatrian, H. H. Asatryan, A. Hovhannisyan, and V. Poghosyan, Mod. Phys. Lett. **A19**, 603 (2004), hep-ph/0311187.
[90] F. Kruger and L. M. Sehgal, Phys. Lett. **B380**, 199 (1996), hep-ph/9603237.
[91] P. Gambino, U. Haisch, and M. Misiak, Phys. Rev. Lett. **94**, 061803 (2005), hep-ph/0410155.
[92] T. Huber, E. Lunghi, M. Misiak, and D. Wyler, Nucl. Phys. **B740**, 105 (2006), hep-ph/0512066.
[93] Z. Ligeti and F. J. Tackmann, Phys. Lett. **B653**, 404 (2007), 0707.1694.
[94] A. Ali, E. Lunghi, C. Greub, and G. Hiller, Phys. Rev. **D66**, 034002 (2002), hep-ph/0112300.
[95] T. Huber, T. Hurth, and E. Lunghi (2008), 0807.1940.
[96] B. Aubert et al. (*BABAR* Collaboration), Phys. Rev. Lett. **93**, 081802 (2004), hep-ex/0404006.
[97] M. Iwasaki et al. (Belle), Phys. Rev. **D72**, 092005 (2005), hep-ex/0503044.
[98] K. S. M. Lee and I. W. Stewart, Phys. Rev. **D74**, 014005 (2006), hep-ph/0511334.
[99] K. S. M. Lee, Z. Ligeti, I. W. Stewart, and F. J. Tackmann, Phys. Rev. **D74**, 011501 (2006), hep-ph/0512191.
[100] K. S. M. Lee and F. J. Tackmann, Phys. Rev. **D79**, 114021 (2009), 0812.0001.
[101] T. Hurth and M. Nakao (2010), 1005.1224.
[102] A. K. Alok et al., JHEP **02**, 053 (2010), 0912.1382.
[103] T. Feldmann and J. Matias, JHEP **01**, 074 (2003), hep-ph/0212158.
[104] F. Kruger and J. Matias, Phys. Rev. **D71**, 094009 (2005), hep-ph/0502060.
[105] E. Lunghi and J. Matias, JHEP **04**, 058 (2007), hep-ph/0612166.
[106] U. Egede, T. Hurth, J. Matias, M. Ramon, and W. Reece, JHEP **11**, 032 (2008), 0807.2589.
[107] U. Egede, T. Hurth, J. Matias, M. Ramon, and W. Reece, to appear.
[108] M. Beneke, T. Feldmann, and D. Seidel, Nucl. Phys. **B612**, 25 (2001), hep-ph/0106067.
[109] H. M. Asatrian, K. Bieri, C. Greub, and M. Walker, Phys. Rev. **D69**, 074007 (2004), hep-ph/0312063.
[110] D. Seidel, Phys. Rev. **D70**, 094038 (2004), hep-ph/0403185.
[111] G. Buchalla, G. Isidori, and S. J. Rey, Nucl. Phys. **B511**, 594 (1998), hep-ph/9705253.
[112] T. Hurth, E. Lunghi, and W. Porod, Eur. Phys. J. **C33**, 382 (2004), hep-ph/0310282.
[113] T. Hurth, E. Lunghi, and W. Porod, Nucl. Phys. **B704**, 56 (2005), hep-ph/0312260.
[114] A. Ali, H. Asatrian, and C. Greub, Phys. Lett. **B429**, 87 (1998), hep-ph/9803314.
[115] M. Battaglia et al. (2003), hep-ph/0304132.
[116] J. M. Soares, Nucl. Phys. **B367**, 575 (1991).
[117] T. Hurth and T. Mannel, Phys. Lett. **B511**, 196 (2001), hep-ph/0103331.
[118] T. Hurth and T. Mannel, AIP Conf. Proc. **602**, 212 (2001), hep-ph/0109041.
[119] F. Kruger and L. M. Sehgal, Phys. Rev. **D55**, 2799 (1997), hep-ph/9608361.
[120] B. Aubert et al. (BABAR), Phys. Rev. Lett. **102**, 091803 (2009), 0807.4119.
[121] B. Aubert et al. (BABAR), Phys. Rev. **D79**, 031102 (2009), 0804.4412.

[122] J. T. Wei et al. (BELLE), Phys. Rev. Lett. **103**, 171801 (2009), 0904.0770.

[123] B. Aubert et al. (BABAR), Phys. Rev. Lett. **99**, 051801 (2007), hep-ex/0703018.

[124] J. T. Wei et al. (Belle), Phys. Rev. **D78**, 011101 (2008), 0804.3656.

[125] T. Iijima, invited talk at 24th Int. Symp. on Lepton-Photon Interactions at High Energy (LP09), Hamburg, Germany, 17-22 Aug.

[126] F. Kruger, L. M. Sehgal, N. Sinha, and R. Sinha, Phys. Rev. **D61**, 114028 (2000), hep-ph/9907386, Erratum-ibid.D63,019901 (2001).

[127] W. Reece and U. Egede (LHCb collaboration) (2009), LHCb-2008-041.

[128] F. F. H. Miyake, S. Kim (CDF Collaboration) (2010), CDF note 10047.

[129] A. Limosani et al. (Belle), Phys. Rev. Lett. **103**, 241801 (2009), 0907.1384.

[130] B. Aubert et al. (*BABAR* Collaboration), Phys. Rev. **D72**, 052004 (2005), hep-ex/0508004.

[131] B. Aubert et al. (*BABAR* Collaboration), Phys. Rev. Lett. **97**, 171803 (2006), hep-ex/0607071.

[132] B. Aubert et al. (BABAR), Phys. Rev. **D77**, 051103 (2008), 0711.4889.

[133] Heavy Flavour Averaging Group *http://www.slac.stanford.edu/xorg/hfag/*.

[134] B. Aubert et al. (BABAR), Phys. Rev. Lett. **101**, 171804 (2008), 0805.4796.

[135] S. Nishida et al. (BELLE), Phys. Rev. Lett. **93**, 031803 (2004), hep-ex/0308038.

[136] B. Aubert et al. (BABAR), Phys. Rev. Lett. **103**, 211802 (2009), 0906.2177.

[137] A. L. Kagan and M. Neubert, Phys. Rev. **D58**, 094012 (1998), hep-ph/9803368.

[138] C. Greub et al., Nucl. Phys. B **434**, 39 (2005).

[139] D. Atwood, M. Gronau, and A. Soni, Phys. Rev. Lett. **79**, 185 (1997), hep-ph/9704272.

[140] B. Grinstein and D. Pirjol, Phys. Rev. **D73**, 014013 (2006), hep-ph/0510104.

[141] B. Aubert et al. (BABAR), Phys. Rev. **D78**, 071102 (2008), 0807.3103.

[142] LHCb Collaboration (2009), arXiv:0912.4179.

[143] B. O. Lange, M. Neubert, and G. Paz, Phys. Rev. **D72**, 073006 (2005), hep-ph/0504071.

[144] J. R. Andersen and E. Gardi, JHEP **01**, 097 (2006), hep-ph/0509360.

[145] P. Gambino, P. Giordano, G. Ossola, and N. Uraltsev, JHEP **10**, 058 (2007), 0707.2493.

[146] E. Barberio et al. (Heavy Flavor Averaging Group) (2008), 0808.1297.

[147] Z. Ligeti, I. W. Stewart, and F. J. Tackmann, Phys. Rev. **D78**, 114014 (2008), 0807.1926.

[148] I. Bizjak et al. (Belle), Phys. Rev. Lett. **95**, 241801 (2005), hep-ex/0505088.

[149] B. Aubert et al. (BABAR), Phys. Rev. Lett. **100**, 171802 (2008), 0708.3702.

[150] K. Tackmann (BABAR), Eur. Phys. J. **A38**, 137 (2008), 0801.2985.

[151] C. W. Bauer and A. V. Manohar, Phys. Rev. **D70**, 034024 (2004), hep-ph/0312109.

[152] T. Becher and M. Neubert, Phys. Lett. **B633**, 739 (2006), hep-ph/0512208.

[153] D. Benson, I. I. Bigi, T. Mannel, and N. Uraltsev, Nucl. Phys. **B665**, 367 (2003), hep-ph/0302262.

[154] A. Pak and A. Czarnecki, Phys. Rev. **D78**, 114015 (2008), 0808.3509.

[155] S. Biswas and K. Melnikov, JHEP **02**, 089 (2010), 0911.4142.

[156] I. I. Y. Bigi, M. A. Shifman, N. G. Uraltsev, and A. I. Vainshtein, Phys. Rev. **D52**, 196 (1995), hep-ph/9405410.

[157] A. H. Hoang, Z. Ligeti, and A. V. Manohar, Phys. Rev. **D59**, 074017 (1999), hep-ph/9811239.

[158] P. Gambino and N. Uraltsev, Eur. Phys. J. **C34**, 181 (2004), hep-ph/0401063.

[159] T. Becher, H. Boos, and E. Lunghi, JHEP **12**, 062 (2007), 0708.0855.

[160] M. Bander et al., Phys. Rev. Lett. **43**, 242 (1979).

[161] H. Boos, T. Mannel, and J. Reuter, Phys. Rev. **D70**, 036006 (2004), hep-ph/0403085.

[162] M. Gronau and J. L. Rosner, Phys. Lett. **B672**, 349 (2009), 0812.4796.

[163] M. Ciuchini, M. Pierini, and L. Silvestrini, Phys. Rev. Lett. **95**, 221804 (2005), hep-ph/0507290.

[164] S. Faller, M. Jung, R. Fleischer, and T. Mannel, Phys. Rev. **D79**, 014030 (2009), 0809.0842.

[165] M. Jung and T. Mannel, Phys. Rev. **D80**, 116002 (2009), 0907.0117.

[166] A. J. Buras and D. Guadagnoli, Phys. Rev. **D78**, 033005 (2008), 0805.3887.

[167] E. Lunghi and A. Soni, JHEP **08**, 051 (2009), 0903.5059.

[168] M. Beneke, Phys. Lett. **B620**, 143 (2005), hep-ph/0505075.

[169] H.-n. Li and S. Mishima, Phys. Rev. **D74**, 094020 (2006), hep-ph/0608277.

[170] A. R. Williamson and J. Zupan, Phys. Rev. **D74**, 014003 (2006), hep-ph/0601214.

[171] R. Fleischer, Eur. Phys. J. **C10**, 299 (1999), hep-ph/9903455.

[172] H.-Y. Cheng, C.-K. Chua, and A. Soni, Phys. Rev. **D72**, 014006 (2005), hep-ph/0502235.

[173] H.-Y. Cheng, C.-K. Chua, and A. Soni, Phys. Rev. **D72**, 094003 (2005), hep-ph/0506268.

[174] M. Gronau and D. Wyler, Phys. Lett. **B265**, 172 (1991).

[175] M. Gronau and D. London., Phys. Lett. **B253**, 483 (1991).

[176] D. Atwood, I. Dunietz, and A. Soni, Phys. Rev. Lett. **78**, 3257 (1997), hep-ph/9612433.

[177] D. Atwood, I. Dunietz, and A. Soni, Phys. Rev. **D63**, 036005 (2001), hep-ph/0008090.

[178] Y. Grossman, Z. Ligeti, and A. Soffer, Phys. Rev. **D67**, 071301 (2003), hep-ph/0210433.

[179] A. Giri, Y. Grossman, A. Soffer, and J. Zupan, Phys. Rev. **D68**, 054018 (2003), hep-ph/0303187.

[180] A. Poluektov et al. (Belle), Phys. Rev. **D70**, 072003 (2004), hep-ex/0406067.

[181] R. Aleksan, T. C. Petersen, and A. Soffer, Phys. Rev. **D67**, 096002 (2003), hep-ph/0209194.

[182] T. Gershon, Phys. Rev. **D79**, 051301 (2009), 0810.2706.

[183] T. Gershon and A. Poluektov, Phys. Rev. **D81**, 014025 (2010), 0910.5437.

[184] T. Gershon and M. Williams, Phys. Rev. **D80**, 092002 (2009), 0909.1495.

[185] A. Bondar and T. Gershon, Phys. Rev. **D70**, 091503 (2004), hep-ph/0409281.

[186] N. Sinha, Phys. Rev. **D70**, 097501 (2004), hep-ph/0405061.
[187] R. Aleksan et al., Z. Phys. C **54**, 653 (1992).
[188] I. Dunietz, Phys. Rev. **D52**, 3048 (1995), hep-ph/9501287.
[189] R. Fleischer and I. Dunietz, Phys. Lett. **B387**, 361 (1996), hep-ph/9605221.
[190] R. Fleischer, Nucl. Phys. **B659**, 321 (2003), hep-ph/0301256.
[191] R. Fleischer, Phys. Lett. **B562**, 234 (2003), hep-ph/0301255.
[192] M. Gronau, Y. Grossman, N. Shuhmaher, A. Soffer, and J. Zupan, Phys. Rev. **D69**, 113003 (2004), hep-ph/0402055.
[193] M. Gronau, Y. Grossman, Z. Surujon, and J. Zupan, Phys. Lett. **B649**, 61 (2007), hep-ph/0702011.
[194] I. Dunietz, Phys. Lett. B **270**, 75 (1991).
[195] M. Gronau and J. Zupan, Phys. Rev. **D71**, 074017 (2005), hep-ph/0502139.
[196] M. Gronau and J. Zupan, Phys. Rev. **D70**, 074031 (2004), hep-ph/0407002.
[197] A. Bondar and A. Poluektov, Eur. Phys. J. **C47**, 347 (2006), hep-ph/0510246.
[198] A. Bondar and A. Poluektov, Eur. Phys. J. **C55**, 51 (2008), 0801.0840.
[199] R. A. Briere et al. (CLEO), Phys. Rev. **D80**, 032002 (2009), 0903.1681.
[200] D. Atwood and A. Soni, Phys. Rev. **D68**, 033003 (2003), hep-ph/0304085.
[201] N. Lowrey et al. (CLEO), Phys. Rev. **D80**, 031105 (2009), 0903.4853.
[202] A. Soffer, W. Toki, and F. Winklmeier, Phys. Rev. **D79**, 014026 (2009), 0810.3490.
[203] B. Kayser and D. London, Phys. Rev. **D61**, 116013 (2000), hep-ph/9909561.
[204] Y. Grossman, A. Soffer, and J. Zupan, Phys. Rev. **D72**, 031501 (2005), hep-ph/0505270.
[205] C. A. *et al.* (Particle Data Group), Phys. Lett. B **667**, 1 (2008).
[206] M. Bona et al. (UTfit), JHEP **03**, 080 (2006), hep-ph/0509219, and updates online at `http://www.utfit.org/`.
[207] G. Lüders, Mat. Fys. Medd. **28**, 5 (1954).
[208] R. Jost, Helv. Phys. Acta **30**, 409 (1957).
[209] W. Pauli, Nuovo Cimento **6**, 204 (1957).
[210] F. Dyson, Phys. Rev. **110**, 579 (1958).
[211] B. Aubert et al. (BABAR), Phys. Rev. Lett. **100**, 131802 (2008), 0711.2713.
[212] M. Beneke et al., Phys. Lett. B **576**, 173 (2003).
[213] M. Ciuchini, E. Franco, V. Lubicz, F. Mescia, and C. Tarantino, JHEP **08**, 031 (2003), hep-ph/0308029.
[214] A. Lenz and U. Nierste, JHEP **06**, 072 (2007), hep-ph/0612167.
[215] B. Aubert et al. (*BABAR* Collaboration), Phys. Rev. Lett. **96**, 251802 (2006), hep-ex/0603053.
[216] V. A. Kostelecky, Phys. Rev. Lett. **80**, 1818 (1998), hep-ph/9809572.
[217] M. Artuso et al. (CLEO Collaboration), Phys. Rev. Lett. **95**, 261801 (2005), hep-ex/0508047.
[218] G. Bonvicini et al. (CLEO Collaboration), Phys. Rev. Lett. **96**, 022002 (2006), hep-ex/0510034.
[219] G. S. Huang et al. (CLEO Collaboration), Phys. Rev. **D75**, 012002 (2007), hep-ex/0610035.
[220] A. Drutskoy et al. (Belle), Phys. Rev. Lett. **98**, 052001 (2007), hep-ex/0608015.
[221] K. Abe et al. (Belle) (2006), hep-ex/0610003.
[222] W.-S. Hou, M. Nagashima, and A. Soddu, Phys. Rev. **D76**, 016004 (2007), hep-ph/0610385.
[223] W.-S. Hou and N. Mahajan, Phys. Rev. **D75**, 077501 (2007), hep-ph/0702163.
[224] E. Baracchini et al., JHEP **08**, 005 (2007), hep-ph/0703258.
[225] D. Besson et al. (CLEO Collaboration), Phys. Rev. Lett. **54**, 381 (1985).
[226] D. M. J. Lovelock et al., Phys. Rev. Lett. **54**, 377 (1985).
[227] W. M. Yao et al. (Particle Data Group), J. Phys. **G33**, 1 (2006).
[228] G. S. Huang et al. (CLEO Collaboration) (2006), hep-ex/0607080.
[229] L. Reina, G. Ricciardi, and A. Soni, Phys. Rev. **D56**, 5805 (1997), hep-ph/9706253.
[230] T. M. Aliev and G. Turan, Phys. Rev. **D48**, 1176 (1993).
[231] G. G. Devidze and G. R. Dzhibuti, Phys. Lett. **B429**, 48 (1998).
[232] A. Gemintern, S. Bar-Shalom, and G. Eilam, Phys. Rev. **D70**, 035008 (2004), hep-ph/0404152.
[233] S. Bertolini and J. Matias, Phys. Rev. **D57**, 4197 (1998), hep-ph/9709330.
[234] B. Aubert et al. (*BABAR* Collaboration), Phys. Rev. Lett. **87**, 241803 (2001), hep-ex/0107068.
[235] K. Abe et al. (Belle), Phys. Rev. **D73**, 051107 (2006), hep-ex/0507036.
[236] M. Bona et al. (UTfit), Phys. Rev. Lett. **97**, 151803 (2006), hep-ph/0605213.
[237] A. Abulencia et al. (CDF), Phys. Rev. Lett. **97**, 242003 (2006), hep-ex/0609040.
[238] A. Abulencia et al. (CDF - Run II), Phys. Rev. Lett. **97**, 062003 (2006), hep-ex/0606027.
[239] V. M. Abazov et al. (D0), Phys. Rev. Lett. **97**, 021802 (2006), hep-ex/0603029.
[240] S. Laplace, Z. Ligeti, Y. Nir, and G. Perez, Phys. Rev. **D65**, 094040 (2002), hep-ph/0202010.
[241] I. Dunietz, R. Fleischer, and U. Nierste, Phys. Rev. **D63**, 114015 (2001), hep-ph/0012219.
[242] A. S. Dighe, I. Dunietz, and R. Fleischer, Eur. Phys. J. **C6**, 647 (1999), hep-ph/9804253.
[243] T. Aaltonen et al. (CDF), Phys. Rev. Lett. **100**, 161802 (2008), 0712.2397.
[244] V. M. Abazov et al. (D0), Phys. Rev. Lett. **101**, 241801 (2008), 0802.2255.
[245] V. M. Abazov et al. (D0), Phys. Rev. Lett. **98**, 151801 (2007), hep-ex/0701007.
[246] V. M. Abazov et al. (The D0) (2010), 1005.2757.
[247] V. M. Abazov et al. (D0) (2010), 1007.0395.
[248] O. Eberhardt, A. Lenz, and J. Rohrwild (2010), 1005.3505.
[249] A. Dighe, A. Kundu, and S. Nandi (2010), 1005.4051.
[250] B. A. Dobrescu, P. J. Fox, and A. Martin (2010), 1005.4238.
[251] C.-H. Chen and G. Faisel (2010), 1005.4582.
[252] A. J. Buras, M. V. Carlucci, S. Gori, and G. Isidori (2010), 1005.5310.
[253] Z. Ligeti, M. Papucci, G. Perez, and J. Zupan (2010), 1006.0432.
[254] V. M. Abazov et al. (D0), Phys. Rev. Lett. **98**, 121801 (2007), hep-ex/0701012.

[255] V. M. Abazov et al. (D0), Phys. Rev. **D76**, 057101 (2007), hep-ex/0702030.

[256] S. Bianco, F. L. Fabbri, D. Benson, and I. Bigi, Riv. Nuovo Cim. **26N7**, 1 (2003), hep-ex/0309021.

[257] I. I. Y. Bigi, Y. L. Dokshitzer, V. A. Khoze, J. H. Kuhn, and P. M. Zerwas, Phys. Lett. **B181**, 157 (1986).

[258] B. Aubert et al. (BABAR), Phys. Rev. Lett. **98**, 211802 (2007), hep-ex/0703020.

[259] T. Aaltonen (CDF) (2007), arXiv:0712.1567 [hep-ex].

[260] M. Staric et al. (Belle), Phys. Rev. Lett. **98**, 211803 (2007), hep-ex/0703036.

[261] B. Aubert et al. (BABAR), Phys. Rev. **D78**, 011105 (2008), 0712.2249.

[262] B. Aubert et al. (BABAR), Phys. Rev. **D80**, 071103 (2009), 0908.0761.

[263] A. J. Schwartz (2009), 0911.1464.

[264] B. Aubert et al. (BABAR), Phys. Rev. Lett. **103**, 211801 (2009), 0807.4544.

[265] K. Abe et al. (BELLE), Phys. Rev. Lett. **99**, 131803 (2007), arXiv:0704.1000 [hep-ex].

[266] P. del Amo Sanchez et al. (The BABAR) (2010), 1004.5053.

[267] G. Burdman and I. Shipsey, Ann. Rev. Nucl. Part. Sci. **53**, 431 (2003), hep-ph/0310076.

[268] E. Golowich, J. Hewett, S. Pakvasa, and A. A. Petrov, Phys. Rev. **D79**, 114030 (2009), 0903.2830.

[269] I. Bigi, A. Paul, and S. Recksiegel (paper in preparation).

[270] B. Aubert et al. (BABAR) (2006), hep-ex/0607051.

[271] S. Fajfer, J. F. Kamenik, and S. Prelovsek (2007), hep-ph/0702172.

[272] A. Freyberger et al. (CLEO), Phys. Rev. Lett. **76**, 3065 (1996).

[273] B. Aubert et al. (BABAR), Phys. Rev. Lett. **93**, 191801 (2004), hep-ex/0408023.

[274] B. Aubert et al. (BABAR) (2008), URL `http://www.slac.stanford.edu/econf/C080527/casey-hcp2008.pdf%`.

[275] E. Won (BELLE) (2004), URL `http://belle.kek.jp/belle/talks/EPS09/won.pdf`.

[276] T. E. Coan et al. (CLEO), Phys. Rev. Lett. **90**, 101801 (2003), hep-ex/0212045.

[277] D. Asner (2010), private communication.

[278] D. Asner.

[279] V. A. Kostelecky and R. Potting, Phys. Rev. **D51**, 3923 (1995), hep-ph/9501341.

[280] D. Colladay and V. A. Kostelecky, Phys. Rev. **D52**, 6224 (1995), hep-ph/9510365.

[281] V. A. Kostelecky, Phys. Rev. **D64**, 076001 (2001), hep-ph/0104120.

[282] N. E. Mavromatos and S. Sarkar, Phys. Rev. **D79**, 104015 (2009), 0812.3952.

[283] D. M. Asner and W. M. Sun, Phys. Rev. **D73**, 034024 (2006), hep-ph/0507238.

[284] J. L. Rosner et al. (CLEO), Phys. Rev. Lett. **100**, 221801 (2008), 0802.2264.

[285] D. M. Asner et al. (CLEO), Phys. Rev. **D78**, 012001 (2008), 0802.2268.

[286] A. F. Falk, Y. Grossman, Z. Ligeti, and A. A. Petrov, Phys. Rev. **D65**, 054034 (2002), hep-ph/0110317.

[287] A. F. Falk, Y. Grossman, Z. Ligeti, Y. Nir, and A. A. Petrov, Phys. Rev. **D69**, 114021 (2004), hep-ph/0402204.

[288] I. I. Y. Bigi and N. G. Uraltsev, Nucl. Phys. **B592**, 92 (2001), hep-ph/0005089.

[289] R. Andreassen (BABAR), *Progress with Charm Mixing Measurements at the 4S* (2009), URL `http://www.slac.stanford.edu/~rolfa/meeting05Oct2009.pdf`.

[290] J. G. Ticó (BABAR), $D^0 - \bar{D}^0$ *mixing and charm CP violation* (2010), oral presentation at the "45th Rencontres de Moriond, Electroweak session, 6-13 March 2010, La Thuile", URL `http://indico.in2p3.fr/materialDisplay.py?contribId=123&sessionId=3&materialId=slides&confId=2065`.

[291] P. M. Spradlin (2007), see also CERN-lhcb-2007-049. For WS $K\pi$ we use the illustration with background/signal=2.56., 0711.1661.

[292] A. L. Kagan and M. D. Sokoloff, Phys. Rev. **D80**, 076008 (2009), 0907.3917.

[293] B. Aubert et al. (BABAR), Phys. Rev. **D70**, 091102 (2004), hep-ex/0408066.

[294] B. Aubert et al. (BABAR), Phys. Rev. **D76**, 014018 (2007), 0705.0704.

[295] I. I. Y. Bigi and A. I. Sanda, Camb. Monogr. Part. Phys. Nucl. Phys. Cosmol. **9**, 1 (2000).

[296] I. I. Bigi, M. Blanke, A. J. Buras, and S. Recksiegel, JHEP **07**, 097 (2009), 0904.1545.

[297] Y. Grossman, Y. Nir, and G. Perez, Phys. Rev. Lett. **103**, 071602 (2009), 0904.0305.

[298] I. Bediaga et al., Phys. Rev. **D80**, 096006 (2009), 0905.4233.

[299] I. Bigi, Phys. Rev. **D80**, 096006 (2009), 0905.4233.

[300] B. Aubert et al. (BaBar), Phys. Rev. Lett. **100**, 061803 (2008), 0709.2715.

[301] B. Aubert et al. (BABAR), Phys. Rev. **D78**, 051102 (2008), 0802.4035.

[302] M. Staric et al. (Belle), Phys. Lett. **B670**, 190 (2008), 0807.0148.

[303] B. R. Ko, E. Won, and f. t. B. collaboration (2010), 1001.3202.

[304] I. I. Bigi (2001), hep-ph/0107102.

[305] P. d. A. Sanchez (for BABAR) (2010), 1003.3397.

[306] K. Abe et al. (SLD), Phys. Rev. Lett. **73**, 25 (1994), hep-ex/9404001.

[307] S. Schael et al. (LEP Electroweak Working Group), Phys. Rept. **427**, 257 (2006), hep-ex/0509008.

[308] W. T. H. Van Oers et al. (Qweak), Experimental proposal for JLab E02-020 *http://qweak.jlab.org/DocDB/0007/000703/005/Qweak_Update_final2.pdf*.

[309] J. Bernabeu, F. J. Botella, and O. Vives, Nucl. Phys. **B472**, 659 (1996), hep-ph/9512424.

[310] M. Gell-Mann, Phys. Lett. **8**, 214 (1964).

[311] D. D. Dietrich, F. Sannino, and K. Tuominen, Phys. Rev. **D72**, 055001 (2005), hep-ph/0505059.

[312] R. Contino, T. Kramer, M. Son, and R. Sundrum, JHEP **05**, 074 (2007), hep-ph/0612180 *and references therein.*

[313] E. Kou and O. Pene, Phys. Lett. **B631**, 164 (2005), hep-ph/0507119.

[314] F. E. Close and P. R. Page, Phys. Lett. **B628**, 215 (2005), hep-ph/0507199.

[315] E. Braaten and M. Kusunoki, Phys. Rev. **D69**, 074005 (2004), hep-ph/0311147.

[316] F. E. Close and P. R. Page, Phys. Lett. **B578**, 119 (2004), hep-ph/0309253.

[317] N. A. Tornqvist, Phys. Lett. **B590**, 209 (2004), hep-ph/0402237.
[318] E. S. Swanson, Phys. Rept. **429**, 243 (2006), hep-ph/0601110.
[319] M. B. Voloshin (2006), hep-ph/0605063.
[320] S. Fleming, M. Kusunoki, T. Mehen, and U. van Kolck, Phys. Rev. **D76**, 034006 (2007), hep-ph/0703168.
[321] E. Braaten and M. Lu, Phys. Rev. **D76**, 094028 (2007), 0709.2697.
[322] E. Braaten and M. Lu, Phys. Rev. **D77**, 014029 (2008), 0710.5482.
[323] L. Maiani, F. Piccinini, A. D. Polosa, and V. Riquer, Phys. Rev. **D71**, 014028 (2005), hep-ph/0412098.
[324] M. Gell-Mann and M. Levy, Nuovo Cim. **16**, 705 (1960).
[325] N. A. Tornqvist and M. Roos, Phys. Rev. Lett. **76**, 1575 (1996), hep-ph/9511210.
[326] I. Caprini, G. Colangelo, and H. Leutwyler, Phys. Rev. Lett. **96**, 132001 (2006), hep-ph/0512364.
[327] S. Descotes-Genon and B. Moussallam, Eur. Phys. J. **C48**, 553 (2006), hep-ph/0607133.
[328] E. M. Aitala et al. (E791), Phys. Rev. Lett. **86**, 770 (2001), hep-ex/0007028.
[329] R. Gatto, G. Nardulli, A. D. Polosa, and N. A. Tornqvist, Phys. Lett. **B494**, 168 (2000), hep-ph/0007207.
[330] N. A. Tornqvist and A. D. Polosa, Frascati Phys. Ser. **20**, 385 (2000), hep-ph/0011107.
[331] N. A. Tornqvist and A. D. Polosa, Nucl. Phys. **A692**, 259 (2001), hep-ph/0011109.
[332] A. Deandrea, R. Gatto, G. Nardulli, A. D. Polosa, and N. A. Tornqvist, Phys. Lett. **B502**, 79 (2001), hep-ph/0012120.
[333] A. Deandrea and A. D. Polosa, Phys. Rev. Lett. **86**, 216 (2001), hep-ph/0008084.
[334] S. Gardner and U.-G. Meissner, Phys. Rev. **D65**, 094004 (2002), hep-ph/0112281.
[335] I. Bigi, L. Maiani, F. Piccinini, A. D. Polosa, and V. Riquer, Phys. Rev. **D72**, 114016 (2005), hep-ph/0510307.
[336] F. E. Close et al., Phys. Lett. B **319**, 291 (1993).
[337] R. L. Jaffe, Phys. Rev. D **15**, 267 (1977).
[338] R. L. Jaffe, Phys. Rev. D **15**, 281 (1977).
[339] R. L. Jaffe, Phys. Rept. **409**, 1 (2005), hep-ph/0409065.
[340] R. L. Jaffe and F. Wilczek, Phys. Rev. Lett. **91**, 232003 (2003), hep-ph/0307341.
[341] L. Maiani, F. Piccinini, A. D. Polosa, and V. Riquer, Phys. Rev. Lett. **93**, 212002 (2004), hep-ph/0407017.
[342] G. Cotugno, R. Faccini, A. D. Polosa, and C. Sabelli, Phys. Rev. Lett. **104**, 132005 (2010), 0911.2178.
[343] G. 't Hooft, G. Isidori, L. Maiani, A. D. Polosa, and V. Riquer, Phys. Lett. **B662**, 424 (2008), 0801.2288.
[344] R. Escribano and J.-M. Frere, JHEP **06**, 029 (2005), hep-ph/0501072.
[345] J. M. Gerard and E. Kou, Phys. Lett. **B616**, 85 (2005), hep-ph/0411292.
[346] B. Aubert et al. (*BABAR* Collaboration), Phys. Rev. **D74**, 091103 (2006), hep-ex/0610018.
[347] N. V. Drenska, R. Faccini, and A. D. Polosa, Phys. Lett. **B669**, 160 (2008), 0807.0593.
[348] S. K. Choi et al. (Belle), Phys. Rev. Lett. **91**, 262001 (2003), hep-ex/0309032.
[349] A. Abulencia et al. (CDF), Phys. Rev. Lett. **98**, 132002 (2007), hep-ex/0612053.
[350] K. Abe et al. (Belle) (2005), hep-ex/0505038.
[351] B. Aubert et al. (BABAR), Phys. Rev. Lett. **102**, 132001 (2009), 0809.0042.
[352] B. Aubert et al. (BABAR), Phys. Rev. **D77**, 011102 (2008), 0708.1565.
[353] I. Adachi et al. (Belle) (2008), 0810.0358.
[354] E. Braaten and J. Stapleton, Phys. Rev. **D81**, 014019 (2010), 0907.3167.
[355] W. Dunwoodie and V. Ziegler, Phys. Rev. Lett. **100**, 062006 (2008), 0710.5191.
[356] B. Aubert et al. (*BABAR* Collaboration), Phys. Rev. Lett. **95**, 142001 (2005), hep-ex/0506081.
[357] B. Aubert et al. (*BABAR* Collaboration), Phys. Rev. Lett. **98**, 212001 (2007), hep-ex/0610057.
[358] X. L. Wang et al. (Belle), Phys. Rev. Lett. **99**, 142002 (2007), 0707.3699.
[359] B. Aubert et al. (BaBar), Phys. Rev. Lett. **99**, 071801 (2007), 0705.1190.
[360] S. K. Choi et al. (BELLE), Phys. Rev. Lett. **100**, 142001 (2008), 0708.1790.
[361] R. Mizuk et al. (BELLE), Phys. Rev. **D80**, 031104 (2009), 0905.2869.
[362] R. Mizuk et al. (Belle), Phys. Rev. **D78**, 072004 (2008), 0806.4098.
[363] B. Aubert et al. (BABAR), Phys. Rev. **D79**, 112001 (2009), 0811.0564.
[364] L. Maiani, A. D. Polosa, and V. Riquer, Phys. Rev. Lett. **99**, 182003 (2007), 0707.3354.
[365] G. Bonvicini et al. (CLEO), Phys. Rev. **D70**, 032001 (2004), hep-ex/0404021.
[366] B. Aubert et al. (BABAR), Phys. Rev. Lett. **101**, 071801 (2008), 0807.1086 [Erratum-ibid. **102**, 029901 (2009)].
[367] B. Aubert et al. (BABAR), Phys. Rev. Lett. **103**, 161801 (2009), 0903.1124.
[368] D. M. Asner et al. (CLEO), Phys. Rev. **D78**, 091103 (2008), 0808.0933.
[369] A. A. Penin, A. Pineda, V. A. Smirnov, and M. Steinhauser, Nucl. Phys. **B699**, 183 (2004), hep-ph/0406175.
[370] M. B. Voloshin, Sov. J. Nucl. Phys. **43**, 1011 (1986), [Yad. Fiz. **43**, 1571 (1986)].
[371] Y.-P. Kuang, Front. Phys. China **1**, 19 (2006), hep-ph/0601044.
[372] B. Aubert et al. (BABAR), Phys. Rev. **D78**, 112002 (2008), 0807.2014.
[373] K. F. Chen et al. (Belle), Phys. Rev. Lett. **100**, 112001 (2008), 0710.2577.
[374] D. M. Asner et al. (2008), 0809.1869.
[375] M. F. M. Lutz, B. Pire, O. Scholten, and R. Timmermans (The PANDA) (2009), 0903.3905.
[376] B. Aubert et al. (*BABAR* Collaboration), Phys. Rev. **D73**, 012005 (2006), hep-ex/0512023.
[377] S. Schael et al. (ALEPH), Eur. Phys. J. **C47**, 547 (2006), hep-ex/0602042.
[378] R. Dermisek and J. F. Gunion, Phys. Rev. **D73**, 111701 (2006), hep-ph/0510322.
[379] R. Dermisek, J. F. Gunion, and B. McElrath, Phys. Rev. **D76**, 051105 (2007), hep-ph/0612031.
[380] M.-A. Sanchis-Lozano (2007), 0709.3647.
[381] J. F. Gunion, D. Hooper, and B. McElrath, Phys. Rev. **D73**, 015011 (2006), hep-ph/0509024.

[382] B. McElrath, Phys. Rev. **D72**, 103508 (2005), hep-ph/0506151.
[383] P. Fayet, Phys. Rev. **D75**, 115017 (2007), hep-ph/0702176.
[384] C. Bird, R. V. Kowalewski, and M. Pospelov, Mod. Phys. Lett. **A21**, 457 (2006), hep-ph/0601090.
[385] F. Wilczek, Phys. Rev. Lett. **39**, 1304 (1977).
[386] U. Ellwanger, C. Hugonie, and A. M. Teixeira (2009), 0910.1785.
[387] E. Fullana and M.-A. Sanchis-Lozano, Phys. Lett. **B653**, 67 (2007), hep-ph/0702190.
[388] F. Domingo and U. Ellwanger, JHEP **12**, 090 (2007), 0710.3714.
[389] M. A. Sanchis-Lozano, Int. J. Mod. Phys. **A19**, 2183 (2004), hep-ph/0307313.
[390] M.-A. Sanchis-Lozano, J. Phys. Soc. Jap. **76**, 044101 (2007), hep-ph/0610046.
[391] F. Domingo, U. Ellwanger, E. Fullana, C. Hugonie, and M.-A. Sanchis-Lozano, JHEP **01**, 061 (2009), 0810.4736.
[392] F. Domingo, U. Ellwanger, and M.-A. Sanchis-Lozano, Phys. Rev. Lett. **103**, 111802 (2009), 0907.0348.
[393] B. Aubert et al. (BABAR), Phys. Rev. Lett. **103**, 251801 (2009), 0908.2840.
[394] A. Chang et al. (ATIC), Nature **456**, 362 (2008).
[395] A. A. Abdo et al. (The Fermi LAT), Phys. Rev. Lett. **102**, 181101 (2009), 0905.0025.
[396] O. Adriani et al. (PAMELA), Nature **458**, 607 (2009), 0810.4995.
[397] I. V. Moskalenko and A. W. Strong, AIP Conf. Proc. **801**, 57 (2005), astro-ph/0509414.
[398] D. Hooper, P. Blasi, and P. D. Serpico, JCAP **0901**, 025 (2009), 0810.1527.
[399] N. Arkani-Hamed, D. P. Finkbeiner, T. R. Slatyer, and N. Weiner, Phys. Rev. **D79**, 015014 (2009), 0810.0713.
[400] M. Pospelov and A. Ritz, Phys. Lett. **B671**, 391 (2009), 0810.1502.
[401] P. Jean et al., Astron. Astrophys. **407**, L55 (2003), astro-ph/0309484.
[402] R. Bernabei et al. (DAMA), Eur. Phys. J. **C56**, 333 (2008), 0804.2741.
[403] B. Batell, M. Pospelov, and A. Ritz, Phys. Rev. **D79**, 115008 (2009), 0903.0363.
[404] R. Essig, P. Schuster, and N. Toro, Phys. Rev. **D80**, 015003 (2009), 0903.3941.
[405] W. Love et al. (CLEO), Phys. Rev. Lett. **101**, 151802 (2008), 0807.1427.
[406] B. Aubert et al. (BABAR), Phys. Rev. Lett. **103**, 081803 (2009), 0905.4539.
[407] B. Batell, M. Pospelov, and A. Ritz (2009), 0911.4938.
[408] M. Reece and L.-T. Wang, JHEP **07**, 051 (2009), 0904.1743.
[409] V. Lubicz, talk given at the 4th Workshop on Super B Factory `http://www.infn.it/csn1/conference/superb`.
[410] V. Lubicz, plenary talk given at Lattice 2009 `http://rchep.pku.edu.cn/workshop/lattice09/index.xml`.
[411] J. Laiho, E. Lunghi, and R. S. Van de Water, Phys. Rev. **D81**, 034503 (2010), 0910.2928.
[412] V. Lubicz and C. Tarantino, Nuovo Cim. **123B**, 674 (2008), 0807.4605.
[413] E. Dalgic et al., Phys. Rev. **D73**, 074502 (2006), hep-lat/0601021.
[414] J. A. Bailey et al., Phys. Rev. **D79**, 054507 (2009), 0811.3640.
[415] U. Haisch (2008), 0805.2141.
[416] G. Aad et al. (The ATLAS) (2009), 0901.0512.
[417] T. Goto, Y. Okada, T. Shindou, and M. Tanaka, Phys. Rev. **D77**, 095010 (2008), 0711.2935.
[418] L. J. Hall and H. Murayama, Phys. Rev. Lett. **75**, 3985 (1995), hep-ph/9508296.
[419] W. Altmannshofer, A. J. Buras, S. Gori, P. Paradisi, and D. M. Straub, Nucl. Phys. **B830**, 17 (2010), 0909.1333.
[420] S. Antusch, S. F. King, and M. Malinsky (2007), arXiv:0708.1282 [hep-ph].
[421] K. Agashe and C. D. Carone, Phys. Rev. **D68**, 035017 (2003), hep-ph/0304229.
[422] W. Altmannshofer, A. J. Buras, and P. Paradisi, Phys. Lett. **B688**, 202 (2010), 1001.3835.
[423] W. Altmannshofer, A. J. Buras, and P. Paradisi, Phys. Lett. **B669**, 239 (2008), 0808.0707.
[424] W.-S. Hou, M. Nagashima, and A. Soddu, Phys. Rev. **D72**, 115007 (2005), hep-ph/0508237.
[425] G. D. Kribs, T. Plehn, M. Spannowsky, and T. M. P. Tait, Phys. Rev. **D76**, 075016 (2007), 0706.3718.
[426] J. A. Herrera, R. H. Benavides, and W. A. Ponce, Phys. Rev. **D78**, 073008 (2008), 0810.3871.
[427] M. Bobrowski, A. Lenz, J. Riedl, and J. Rohrwild, Phys. Rev. **D79**, 113006 (2009), 0902.4883.
[428] M. S. Chanowitz, Phys. Rev. **D79**, 113008 (2009), 0904.3570.
[429] A. Soni, A. K. Alok, A. Giri, R. Mohanta, and S. Nandi (2010), 1002.0595.
[430] A. J. Buras et al. (2010), 1002.2126.
[431] L. Randall and R. Sundrum, Phys. Rev. Lett. **83**, 3370 (1999), hep-ph/9905221.
[432] K. Agashe, G. Perez, and A. Soni, Phys. Rev. Lett. **93**, 201804 (2004), hep-ph/0406101.
[433] M. Blanke, A. J. Buras, B. Duling, S. Gori, and A. Weiler, JHEP **03**, 001 (2009), 0809.1073.
[434] M. Bauer, S. Casagrande, U. Haisch, and M. Neubert (2009), 0912.1625.
[435] M. Blanke et al., JHEP **12**, 003 (2006), hep-ph/0605214.
[436] M. Blanke, A. J. Buras, B. Duling, S. Recksiegel, and C. Tarantino, Acta Phys. Polon. **B41**, 657 (2010), 0906.5454.
[437] T. Goto, Y. Okada, and Y. Yamamoto, Phys. Lett. **B670**, 378 (2009), 0809.4753.
[438] J. R. Ellis, J. Hisano, M. Raidal, and Y. Shimizu, Phys. Rev. **D66**, 115013 (2002), hep-ph/0206110.
[439] I. I. Bigi, M. Blanke, A. J. Buras, and S. Recksiegel, JHEP **07**, 097 (2009), 0904.1545.
[440] N. Cabibbo, Phys. Rev. Lett **10** (1963).
[441] U. Haisch, PoS **KAON**, 056 (2008), 0707.3098.